Evaluations of the environmental effects of controlled tile drainage on watershed and river using the improved SWAT and the QUAL2Kw under current and future climate regimes

by

Que, Zhenyang

Thesis submitted to the University of Ottawa

in partial fulfillment of the requirements for a Ph.D. degree

in Environmental Engineering

Department of Civil Engineering

Faculty of Engineering

University of Ottawa

Supervisor: Dr. Ousmane Seidou
Co-supervisor: Dr. David R Lapen

ABSTRACT

In agriculture-dominated areas, water pollution resulting from nutrients migrating from farms to water bodies is a major concern. The migration is further exacerbated by traditional tile drain known as Uncontrolled Tile Drainage (UCTD), which removes excess water from areas to keep the water table low enough for crops to grow. UCTD, commonly used in Ontario, Canada, is believed to contribute to water quality issues, whereas Controlled Tile Drainage (CTD) is an alternative technique in which a structure controls the outlets of the drains so that water only leaves a field when the water table level exceeds a desired threshold. Considered as a Best Management Practice (BMP), CTD has been documented as an efficient practice preventing nutrients from migrating out of agricultural fields. This thesis aims to improve our understanding of the environmental benefits of replacing UCTD with CTD. Three significant contributions were achieved.

The first contribution of the thesis is the improvements of the algorithm for calculating nitrates in tile flows in the Soil and Water Assessment Tool (SWAT) model. Researchers have simulated CTD by dynamically changing tile depth to mimic the operation of outlet structure gates, but it has been demonstrated that doing so results in inaccuracies, and so the algorithm in the model has been improved subsequently. The current author proposed and tested a new algorithm for calculating nitrates in tile flows that better represents the dynamics of water and nutrients in soil layers for the SWAT model. A model for the South Nation watershed, located in Ontario, Canada, was then developed and successfully calibrated using the improved SWAT model.

The second contribution was the extension of the SWAT model to simulate riverine hydraulic and water quality processes by coupling it with the QUAL2Kw model. In this

thesis, a procedure is developed to couple the SWAT model and the QUAL2Kw model to enable continuous simulations of 13 water quality parameters in the South Nation River system. The coupled model was calibrated and verified at various observed locations along the river during the five seasons of growth from 2006 to 2010. The simulation results suggested that CTD also improved the water quality of the river by lowering biologically available N levels of NO_2^--N, and NO_3^--N, thereby impeding phytoplankton growth in the river.

The third contribution is the verification of the benefits of replacing UCTD with CTD in the future climates. The confirmation was done using the SWAT model alone, and then the coupled SWAT/QUAL2K models, using a matrix of climate change experiments performed with several Global Climate Models (GCMs) and Regional Climate Models (RCMs). The results suggest that nutrient loading from the watershed will increase in the 2021–2050 period compared to the 1985–2006 period. Thus, pollution from agricultural fields will worsen with the current UCTD approach, while the results also show that CTD would perform effectively and stably in future climate scenarios and could counterbalance the effects of climate change on water quality.

To the author's knowledge, this study is the first attempt to date to assess the environmental effects of CTD on a watershed and river by coupling the SWAT and QUAL2Kw models. The findings expand the current scope of knowledge on the environmental effects of CTD on watersheds and rivers under current and future climate change regimes. Long periods of continuous simulation and a matrix of climate change scenarios also make this study stand out from other studies. It laid a foundation for future investigations.

ACKNOWLEDGMENTS

I would like to thank my supervisor Prof. Ousmane Seidou for his support and guidance during the long journey of this study. Prof. Seidou continuously encouraged me and was always willing and enthusiastic to assist me throughout the study. This study would not have been possible without him.

I would like to thank the committee members, specially Dr. Sarah Dorner, Dr. Paul H. Simms, and Dr. Abdolmajid Mohammadian. Their encouraging words and thoughtful, and detailed feedbacks have been very important to me.

I would like to extend my thanks to my colleagues at Agriculture and Agri-Food Canada, Mark Sunohara, Emilia Craiovan, Graham Wilkes, Jason Vanrobaeys, Steve Sager, and Dr. Yefang Jiang for their help and support at the beginning and during the study and work.

Also, I would like to thank the University of Ottawa for the scholarship supporting me carry out this study.

Last, but not least, my warm and heartfelt thanks go to my kindly grandma Yulian Yang, father Jushan, and mother Zhenrong for their raising and inspiring me to be the kind of person I am today. Special thanks go to my wife Peihong, son Jinghang, and lovely daughters Lucia and Sophie for their tremendous support and motivation they had given to me.

Contents

List of Figures

LIST OF TABLES

List of Abbreviations and Acronyms

AAFC	Agriculture and Agri-Food Canada
AGNPS	Agricultural Non-Point Source Pollution
AnnAGNPS	Annualized Agricultural Non-Point Source
ANSWERS	Areal Nonpoint Source Watershed Environmental Response Simulation
ARS	Agricultural Research Service
BMPs	Beneficial Management Practices
BOD	Biochemical Oxygen Demand
Can85	CanESM2_RCA4_85
CanESM2	The second-generation Canadian Earth System Model
CanRCM	Canadian Centre for Climate Modelling and Analysis Regional Climate Model
CBOD	Carbonaceous Biochemical Oxygen Demand
CFSR	Climate Forecast System Reanalysis
CN	Curve Number
CORDEX	Coordinated Regional Climate Downscaling Experiment
CREAMS	Chemicals, Runoff and Erosion from Agricultural Management Systems
CTD	Controlled Tile Drainage
CWEEDS	Canadian Weather Energy and Engineering Datasets

DEM	Digital Elevation Model
DHI	Danish Hydraulic Institute
DO	Dissolved Oxygen
DRP	Dissolved Reactive Phosphorus
EC	Electrical Conductivity
EC45	EC-EARTH_RCA4_45
EC-EARTH	European Community Earth-System Model
ECS	Equilibrium Climate Sensitivity
EFDC	Environment Fluid Dynamics Code
EPIC	Erosion-Productivity Impact Calculator
ESMs	Earth System Models
GCMs	Global Climate Models
GFDL	Geophysical Fluid Dynamics Laboratory
GFDL-ESM2M	Geophysical Fluid Dynamics Laboratory Earth System Model version 2M
GLEAMS	Groundwater Loading Effects on Agricultural Management Systems
GLUE	Generalized Likelihood Uncertainty Estimation
GLVHT	Generalized Longitudinal-Vertical Hydrodynamics and Transport Model
HadGEM2	Hadley Centre Global Environment Model version 2
HIRHAM	High Resolution Limited Area Model

H-K	Hooghoudt and Kirkham
HRU	Hydrological Respond Unit
HSPF	Hydrological Simulation Program – FORTRAN
ICID	International Commission on Irrigation and Drainage
IPCC	Intergovernmental Panel on Climate Change
IROWC-N	Indicator of The Risk of Water Contamination by Nitrogen
IROWC-P	Indicator of The Risk of Water Contamination by Phosphorus
LARM	Laterally Averaged Reservoir Model
MCMC	Markov Chain Monte Carlo
MPI-ESM-LR	The Max Planck Institute for Meteorology Earth System Model at Low Resolution
MUSLE	Modified Universal Soil Loss Equation
N	Nitrogen
NA-CORDEX	North American CORDEX Program
NH_3-N	Ammonia As N
NH_4^+	Ammonium
NO_2^-	Nitrite
NO_2^--N	Nitrite As N
NO_3^-	Nitrate
NO_3^--N	Nitrate As N
NSE	Nash–Sutcliffe Efficiency

Org-N	Organic Nitrogen As N
Org-P	Organic Phosphorus As P
P	Phosphorus
Parasol	Parameter Solution
PBIAS	Percent Bias
PSO	Particle Swarm Optimization
RCA	The Rossby Centre Regional Climate Model
RCMs	Regional Climate Models
RCPs	Representative Concentration Pathways
RCA4	Rossby Centre of Atmospheric model version 4
RegCM	Regional Climate Model
RMSE	Root Mean Square Error
RRMSE	Relative RMSE
RSN	The Residual Soil Nitrogen Indicator
RSR	RMSE-Observations Standard Deviation Ratio
SCS	Soil Conservation Service
Sol P	Dissolved Phosphorus As P
SNRW	South Nation River watershed
SUFI2	Sequential Uncertainty Fitting Ver. 2
SWAT	Soil and Water Assessment Tool
SWAT-CUP	SWAT Calibration and Uncertainty Procedures

SWRRB	Simulator For Water Resources in Rural Basins
T	Temperature
TMDL	Total Maximum Daily Load
TN	Total N
TP	Total P
UCTD	Uncontrolled Tile Drainage
UNICEF	United Nations International Children's Emergency Fund
USBR	US Bureau of Reclamation
USGS	US Geological Survey
USLE	Universal Soil Loss Equation
VBA	Visual Basic for Applications
WASP	Water Quality Analysis Simulation Program
WEBs	Evaluation of Beneficial Management Practices
WHO	World Health Organization
WRF	Weather Research and Forecasting
WWAP	World Water Assessment Program

LIST OF APPENDICES

1 INTRODUCTION

1.1 Background

Water pollution is on the rise globally, and nearly 80% of the world's population lives in areas facing either incipient water insecurity or biodiversity threats, with the highest threats occurring in regions of intensive agriculture and dense settlement (Vörösmarty et al., 2010; WHO and UNICEF, 2015; WWAP, 2012; WWAP, 2015; WWAP, 2016). Agricultural nonpoint pollution, a leading pollution source, is a significant contributor to water contamination, especially in watersheds dominated by agriculture (European Environment Agency, 2005; Hamilton and Miller, 2002; James et al., 2007; Rabalais et al., 2002; USEPA, 1984; USGAO, 1990; Zhang et al., 2004).

Nutrients carried in agricultural runoff, mainly related N and phosphorus (P) compounds, are likely to trigger algal growth in rivers and lakes, and consequently degrade water quality (Anderson et al., 2002; Beman et al., 2005; Smith et al., 2006; Withers et al., 2014). Canada, a water-rich country, has naturally abundant water resources. World Band (2013) estimated that Canada had 6.6% of all renewable freshwater on earth, corresponding to 81,061 m^3 per capita, while the world average is 6,013 m^3 per capita. In Canada, the gross N balance increased by 80% between 1990–1992 and 2002–2004 (Parris, 2011). Eutrophication resulting from excessive nutrients from agricultural sources has been reported from coast to coast. Examples include the St. Lawrence estuary in Quebec, the Great Lakes in Ontario, Lake Winnipeg in Manitoba, and the Lower Fraser River in British Columbia (Bunting et al., 2011; Chambers et al., 2001; Environment Canada, 2001; Environment Canada and Manitoba Water Stewardship, 2011; Environment Canada and the USEPA, 2014; Michalak et al., 2013; Working Group on the State of the St. Lawrence Monitoring, 2014). Three agri-environmental indicators were developed by Agriculture and Agri-Food Canada (AAFC) to monitor the status of water and soil in Canada, which are 1) the Indicator of the Risk of Water Contamination by Nitrogen (IROWC-N), 2) the Residual Soil Nitrogen Indicator (RSN), and 3) the Indicator of the Risk of Water Contamination by Phosphorus (IROWC-P). Clearwater et al. (2016) reported that these indicators increased between 1981 and 2011. They also reported that although 75% of the farmland remained at very low risk of N contamination nationally, both the RSN and IROWC-N increased gradually over that period. IROWC-P was found to have been declining in 50% of the 280 agricultural watersheds studied by Clearwater et al. (2016), suggesting an increase of P application into agricultural lands or its transport to surface water bodies. This situation is most likely due to the increased use of mineral fertilizers and a greater concentration of livestock production.

From 2004 to 2013, AAFC, in collaboration with over 70 other governments, academics, and local watershed authorities, carried out the Watershed Evaluation of Beneficial Management Practices (WEBs) program which was aimed at making careful decisions regarding land use both at the farm and landscape levels. Nine watersheds were selected across Canada to assess the economic and water quality impact of selected agricultural BMPs, such as manure management, small reservoirs, CTD, etc. The WEBs team in Ontario focused on understanding the benefits of CTD. It has been demonstrated in the literature that CTD could mitigate pollution resulting from nutrients migrating from agricultural fields (Evans et al., 1992; Lalonde et al., 1996). Besides studies at field level, the benefits of CTD at watershed level have also been assessed using hydrological and water quality models (Ale et al., 2012; Borah et al., 2006; Eman et al., 2020; Luo et al., 2010; Ng et al., 2002; Que et al., 2015; Santhi et al., 2006; Sunohara et al., 2014; Tan et al., 1999; Thorp et al., 2008; Wesström and Messing, 2007; Youssef et al., 2018; Yuan et al., 2006 and 2011).

The impacts of CTD on water quality were assessed within the WEBs program using the paired experimental micro-watersheds located in the South Nation River watershed in eastern Ontario, Canada. Based on the field observations, Sunohara et al. (2015) discovered that measured daily fluxes were significantly different between the micro-watershed under CTD and another micro-watershed under UCTD in the seasons of growth from May to October. Que et al. (2015) showed that direct runoff, total N (TN), and dissolved N would be reduced by an average of 6.6%, 3.5%, and 13.7% respectively if all suitable crop fields in the watershed were converted to CTD. The thesis aims to expand the work of Sunohara et al. (2015) and Que et al. (2015) by looking at the environmental effects of CTD on the water quality of the South Nation watershed and river under current and future climate regimes.

1.2 Problem statement and objectives

1.2.1 Problem statement

Studies at multiple locations and scales worldwide have shown that CTD effectively reduces nutrient effluence from agricultural fields. However, little is known about the environmental effects of CTD on watershed and river system together. More importantly, most CTD studies have focused on how much pollutants can migrate at either the field or watershed level but have not further evaluate the ecological impact of CTD on a river system. This study intends to simulate CTD and then evaluate the environmental and ecological benefits of CTD on watershed and river. Since the performance of CTD is linked to the climate regime, the impacts of climate change on its benefits will be further investigated.

1.2.2 Research objectives

The general objective of this study is to evaluate the environmental effects of CTD on the South Nation watershed and the South Nation River under the current and future climate regimes using the SWAT and the QUAL2Kw models.

Therefore, the specific objectives are to:

1. Critically assess the SWAT model's ability to simulate CTD and propose a new CTD routine for the SWAT model
2. Verify the ability of the improved model to simulate CTD
3. Evaluate the environmental effects of CTD on the watershed using the improved SWAT model for current and future climates
4. Couple the SWAT and QUAL2Kw models, calibrate, and verify the QUAL2Kw model for the South Nation River
5. Assess the ecological impacts of CTD on the river system using the coupled SWAT/QUAL2Kw model for current and future climates

The improved watershed water quality model, SWAT, and the river water quality model, QUAL2Kw, will be coupled together to achieve the objectives of this study. A preliminary analysis of how the nitrate in tile flow is calculated in the original SWAT model led to the discovery of the inability of the original algorithm of calculating nitrate concentration in tile flow when the tile drain depth was changed. The source codes of the SWAT model were analyzed and improved to better reflect the reality of tile drainage in fields. The improved SWAT model is applied to the WEBs sites to validate the new CTD routine (Objective One). A SWAT model of the South Nation watershed was built and fine-tuned (Objective Two). The model was then used to simulate and evaluate the CTD and UCTD scenarios in the South Nation watershed for current climate and a matrix of climate scenarios (Objective Three). Coupled with the improved SWAT model, a QUAL2Kw model was built, calibrated, and verified using field observations collected from the river (Objective Four). The calibrated QUAL2Kw was used to assess the ecological impacts of CTD on the river system in the current climate and climate change scenarios (Objective Five).

1.3 Contributions to current knowledge

The environmental effects of CTD on the water quality of watershed and river system were evaluated by coupling the watershed water quality model SWAT with the stream water quality model QUAL2Kw. Although previous researchers have investigated the effects of CTD on water quality at either a field level or watershed level at different locations, no investigation proceeded further by assessing river water quality. Therefore, the current scope of knowledge on the environmental effects of CTD for watershed and river systems remains unknown, and so this thesis contributes to the current scope of knowledge in both theoretical and methodological ways.

1.3.1 Theoretical contributions

Although several researchers used the SWAT model to simulate CTD by artificially moving depths of the tiles to simulate control structure operations, the tile drainage algorithm available in the SWAT model has been shown to be inadequate, as it was demonstrated that doing so leads to incorrect calculations for NO_3^--N in tile flows. This aspect is critical to CTD evaluations as the NO_3^--N in tiles ends up in the river system. A new algorithm was proposed that does not have that limitation, effectively improving the ability of the SWAT model to simulate CTD. Given that SWAT is a very popular model used worldwide, the improvement on the model is likely to be significant.

1.3.2 Methodological contributions

The methodological contributions of the thesis are listed below:

- The thesis leads to a better understanding of the impact of climate change on water quantity and quality in the South Nation watershed under both CTD and UCTD.
- It is the first study to successfully evaluate the environmental effects of CTD on the watershed using the improved SWAT model.
- This study developed an innovative approach to retrieve necessary inputs required by the QUAL2Kw model from the outputs of the SWAT model.
- It is the first study to continuously assess the ecological impacts of CTD on river water quality using the QUAL2Kw model coupled with the SWAT model over five continuous seasons of growth.
- Using various climate change datasets combined with GCM and RCM configurations, the improved SWAT model and the QUAL2Kw model were tested on climate changes.

1.4 Outline of the thesis

This thesis consists of eight chapters. Chapter One is the introduction to the study, which covers the perspectives, objectives, and technical paths of the study.

Chapter Two is a literature review covering previous research on CTD, water quality models for a watershed and river, and climate change. Sections 2.1, 2.2, and 2.3 describe the study area and surveys the literatures related to CTD covering both experiments and numerical assessments of that BMP. Section 2.4 is a comprehensive review of available water quality models that could be used to assess the environmental and biological impact of CTD on both watersheds and rivers. Sections 2.5 and 2.6 present the theories and approaches of the QUAL2Kw model and SWAT model, respectively. Section 2.7 reviews the climate models and downscaling methods.

Chapter Three presents the development and verification of an improved routine for the SWAT model. Firstly, the limitations of the original SWAT model in simulating CTD are thoroughly presented and discussed, and then a modification is proposed to simulate CTD properly. Finally, the modified SWAT model was applied to the WEBs experimental sites to verify its capabilities.

Chapter Four focuses on modeling the environmental effects of CTD on the watershed by using the improved SWAT model. The model was satisfactorily calibrated and validated to simulate flow, sediment, NO_3^--N, TN, and TP under the South Nation watershed conditions. Over the five periods of growth from 2006 to 2010, the scenarios for CTD and UCTD were evaluated using the calibrated model, and the performances of the CTD scenarios were examined under a matrix of climate change scenarios.

Chapter Five presents the modeling of the ecological impact of CTD on river water quality by using the river water quality model QUAL2Kw. This chapter describes the approach to retrieve and prepare necessary inputs for the QUAL2Kw model from the outputs of the SWAT model. The model was calibrated and verified using the observed data along the river, and the model agreed well with the water quantity and quality observations during the calibration and validation periods. Two CTD scenarios were assessed by analyzing the simulated loads of 13 water quality parameters: flow, DO, pH, EC, bottom algae net growth, phytoplankton level, Org-N, NH_4^+-N, NO_2^--N+NO_3^--N, TN, Org-P, Min-P, and TP, and then the simulation results for CTD and UCTD were discussed and summarized. The calibrated QUAL2Kw model was used to investigate further the biological impacts of the CTD scenarios on river water quality under the projected 2056-2060 climates.

Chapter Six draws the conclusions of the study.

The last two chapters comprise the references and appendices, respectively.

2 BACKGROUND AND LITERATURE REVIEW

2.1 Study area

The South Nation River, a tributary flowing into the Ottawa River near Plantagenet, Ontario, Canada, rises in northern Brockville, located in eastern Ontario (Figure 2.1). It travels about 175 km from southwest to northeast draining approximately 3900 km^2. The riverbanks compose of Champlain Sea clays cause large- and small-scale landslides. Major tributaries include the North Branch South Nation River, Sandy Creek, Payne River, Castor River, Moose Creek, Bear Brook, Scotch River, and Caledonia Creek. There are seven communities located in the watershed: Spencerville, South Mountain, Chesterville, Crysler, St. Albert, Casselman, and Plantagenet,

The watershed is part of the St-Lawrence River drainage basin and lies in a wedge-shaped area between the St. Lawrence River and the Ottawa River, at the edge of the Canadian Shield. It was ever the seabed of the Champlain Sea. Historically, it was covered by forest and swamp but is now an agricultural-dominated watershed. Farmlands, forests, and residential areas comprise approximately 58%, 34%, and 2% of the total area, respectively. Generally, this watershed is a flat plain. The watershed soils are diverse in type, depth, and distribution and are suitable for agriculture (Eastern Ontario Warden's Caucus, 2007). Uncontrolled tile drainage exists on approximately 43% of the arable land in Ontario.

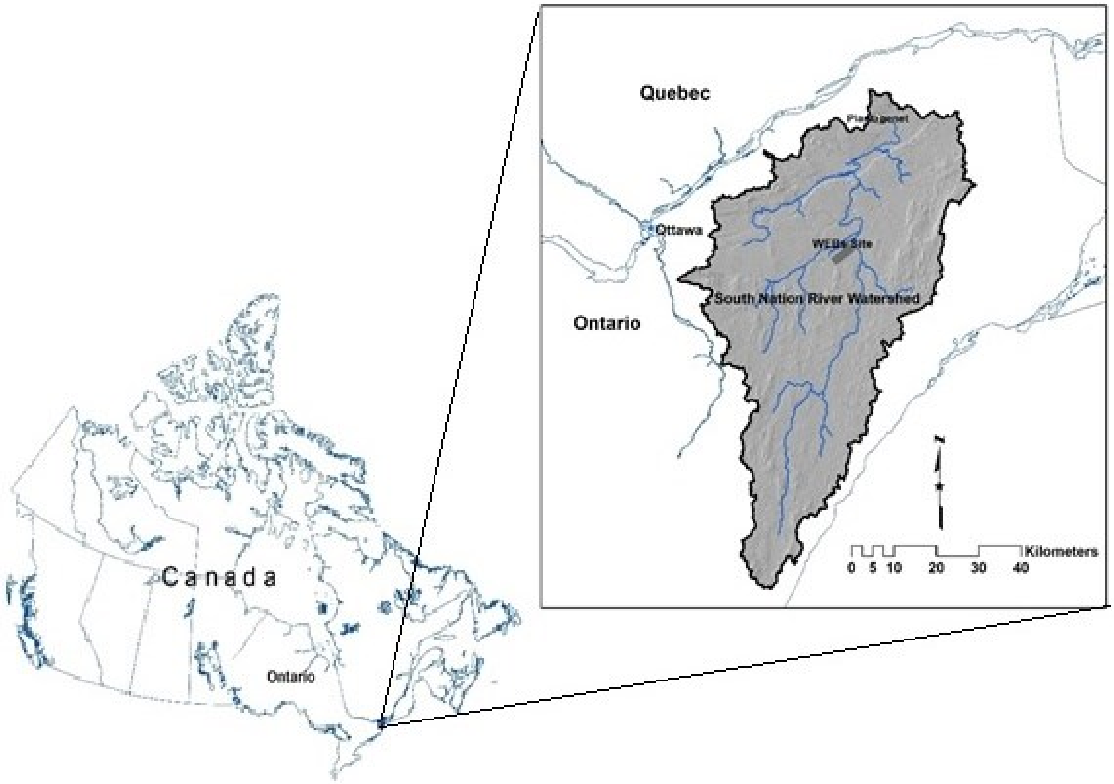

Figure 2.1 Locations of the South Nation River watershed and WEBs site

The climate of the watershed is classified as humid continental, with significant seasonal variations in precipitation and temperature (Figure 2.2). Spring and autumn are short and unpredictable, while winter is long and cloudy with land covered by snow for months. The coldest month is January at –10.3°C on average. Summer is warm and humid, and the warmest month is July at 20.7°C on average. Annual precipitation is about 962.5 mm at the Township of Russell (Environment Canada, 2012).

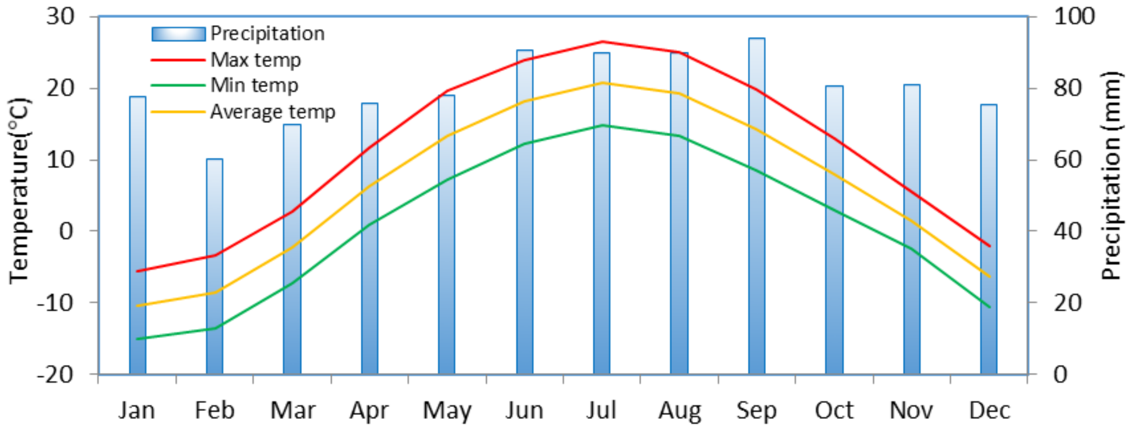

Figure 2.2 Monthly maximum, minimum, and average temperatures and precipitation

2.2 CTD and UCTD

The history of irrigation and drainage systems is as old as agriculture itself (Garrison, 1929), and archaeological evidence of ancient irrigation and drainage systems has shown that natural precipitation was often either insufficient or excessive for supporting crops, for example in Mesopotamia around 3000 BC, in Egypt in 3000 BC and, in ancient China from 2627 BC (Gulhati and Smith, 1967; Jacobsen and Adams, 1958; King, 1911). The International Commission on Irrigation and Drainage (ICID) (1979) defined drainage as the removal of excess surface and subsurface water from the land to enhance crop growth, including the removal of soluble salts from the soil. Although irrigation and drainage have the same purpose, i.e., to help create ideal conditions that are favourable for plant growth, there is a fundamental difference between the two. Irrigation involves adding water to the soil, and conversely, drainage removes excess water from the soil.

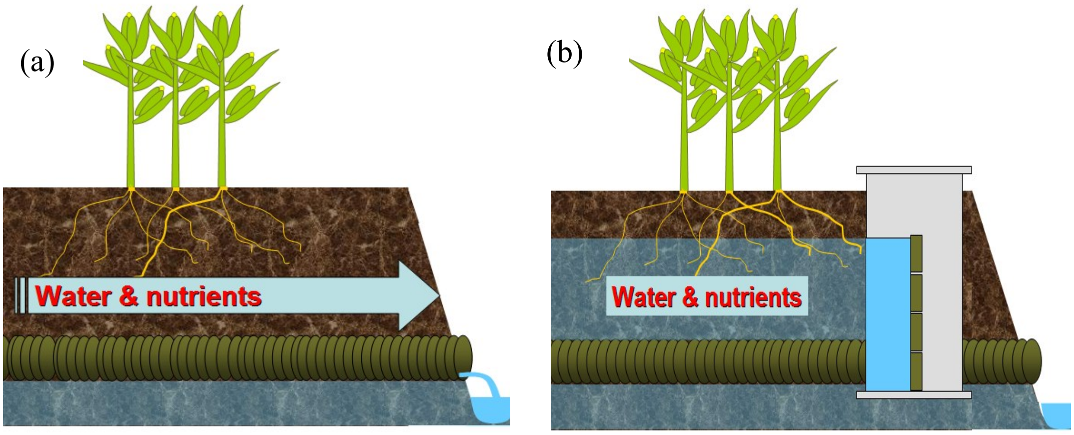

Figure 2.3 Schematic diagrams of UCTD (a) and CTD (b)

Drainage plays an essential role in maintaining water tables, soil temperatures, and oxygen supply, and in the development of crop root systems (US Bureau of Reclamation, 1993), and as a common agricultural practice, tile drainage has penitential effects on the water quality in crop fields, especially in agriculture-dominated watersheds. However, what happens naturally in landscapes with UCTD, as shown in Figure 2.3(a), is that water, sediment, and nutrients flow freely from the tiled fields into ditches or streams, and it works passively; as shown in Figure 2.3(b), CTD is a proactive and improved practice compared to UCTD, and it can manage a drainage system by using a controllable facility. Hence, it can meet various practical needs while dealing with different circumstances, such as the weather, the season, the crop, and the water table. A few field studies have examined the effects of CTD on surface water quality as shown in Table 2.1 (Skaggs and Youssef, 2008).

Table 2.1 Field studies on the effectiveness of CTD

Reference	Location	Soil	Area (ha)	Drain spacing (m)	Drain depth (m)	Control depth* (m)	Percent reduction Drainage	N Loss
Gilliam et al. (1979)	N. Carolina	Portsmouth sl	5 to 16	30 & 80	1.2	0.3–0.5	50	50
	N. Carolina	Goldsboro sl	3	30	1	0.3	85	85
Evans et al. (1989)	N. Carolina	Ballahack sl	4	18	1	0.6	56	56
	N. Carolina	Wasda muck	4	100	1.2	0.6	51	56
	N. Carolina	Wasda muck	4	18	1	0.6	17	18
Lalonde et al. (1996)	Ontario	Bainesville sil	0.63	18.3	1	0.75	49	69
						0.5	80	82
Tan et al. (1998)	Ontario	Brookston cl	2.2	9.3	0.65	0.3	20	19
Gaynor et al. (2002)	Ontario	Brookston cl	0.1	7.5	0.6	0.3	35**	***
Wesstrom et al. (2007)	Sweden	Loamy Sand	0.2	10	1	0.2–0.4	80	80
Fausey (2005)	Ohio	Hoytville sic	0.07	6	0.8	0.3	41	46

*Control typically removed during seedbed preparation, planting, and harvesting periods

**CD reduced subsurface drainage by 35%, increased surface runoff by 28% and reduced total outflow by 16%

***Nitrogen results not reported, effects on pesticide loss are reported

2.3 The WEBs project and previous CTD studies of the watershed

In cooperation with over 70 federal, provincial, municipal, academic, and non-governmental organizations in 2004, the AAFC initialed the WEBs program, which evaluated the environmental and economic performances of selected BMPs at seven watersheds from coast to coast.

Two of the BMPs, the CTD and the restricted cattle access, were examined in the South Nation River watershed in eastern Ontario shown in Figures 2.4 (Sunohara et al., 2015). A paired of drained crop fields (micro watersheds) were designed to evaluate the effects of CTD on water quality. One of them, with an area of 467 ha, was constructed with CTD control facilities, while the other, with an area of 250 ha, was equipped for UCTD.

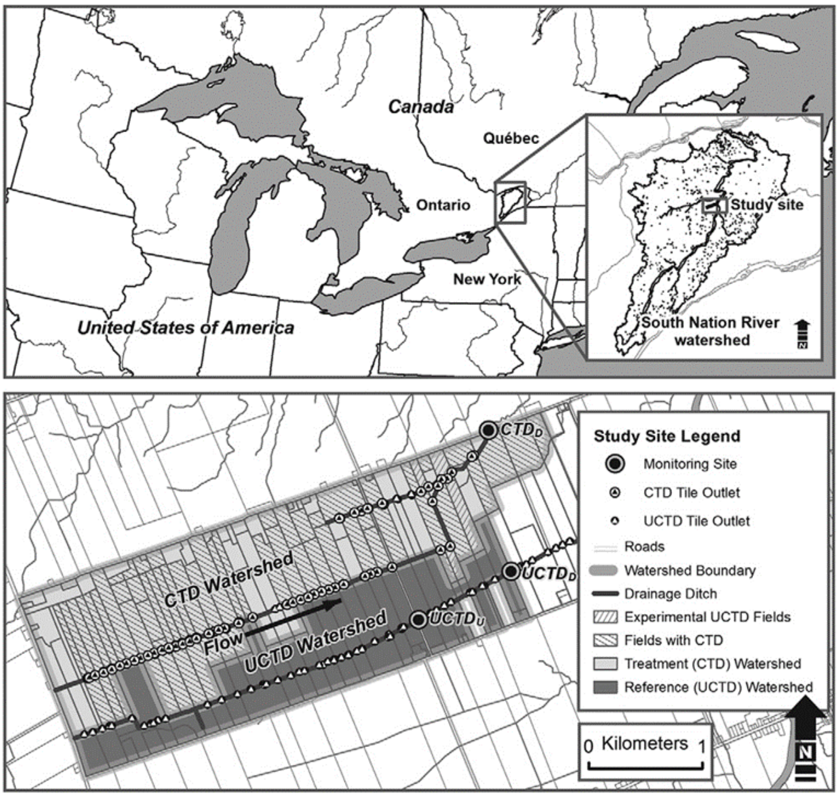

Figure 2.4 Locations of WEBs programs in Ontario, Canada

The flow was monitored and water sample were collected at each monitoring point during growing seasons from 2005 to 2014. The data for 2005 and 2014 are partial since they are the starting year and the ending year, respectively. The datasets received from WEBs are as follows in Table 2.2.

Table 2.2 Datasets from WEBs

Parameter	Starting date	Ending date	Time scale
Flow, NO3, NH4, DRP, TP	05/19/05	10/31/05	daily
	05/26/06	10/31/06	
	05/10/07	10/04/07	
	05/13/08	10/09/08	
	05/29/09	10/30/09	
	05/27/10	10/04/10	
	05/26/11	10/27/11	
	05/24/12	10/31/12	
	05/27/13	09/26/13	

Sunohara et al. (2015) noted that continuous stage and velocity measurements at a 15-min temporal resolution were collected at each monitoring site. Stage–discharge rating curves developed from the data were used to predict discharge during periods when velocity data were unavailable. Water samples were collected on a routine basis and during storm flow events from typically ice-free conditions from May to November of each year. A composite water sample (4×250-mL samples per 1-L bottle sampled every 2 h) was collected twice a week. Storm events were sampled more intensively. For water samples, the NO_2^-–N + NO_3^-–N (referred to as NO_3^-–N because NO_2^-–N levels are typically negligible) and NH_3–N + NH_4^+–N (referred to as NH_4^+–N because NH_3–N levels are also typically negligible) were analyzed calorimetrically. Dissolved reactive P was analyzed using the ascorbic acid method, and total P was analyzed using the same method preceded by a persulfate digestion. There was no data on water constituent concentrations in various soil layers.

Sunohara et al. (2015) used the collected data to show that CTD was an effective practice abating water, N, and P from crop fields in the seasons of growth during the experimental period. Based on these observations, Que et al. (2015) scaled up the watershed using the AnnAGNPS watershed water quality model. The simulation results showed that direct runoff, total N, and dissolved N were reduced by 6.6%, 3.5%, and 13.7%, respectively, during five seasons of growth (2006–2010), with the tile drainage depth set to 600 mm below the ground surface.

2.4 Water quality models

Water quality models are valuable tools for evaluating the state of aquatic environments, and a significant number of such models have been developed to cope with various situations and sites all over the world. There are many differences among these models in their theoretical origins, descriptive objectives, complexities, and sophistication. Therefore, it is crucial to select appropriate models for specific research objectives. For this purpose, the following six well-known water quality models have been reviewed, which are being applied worldwide.

2.4.1 CE-QUAL-W2

CE-QUAL-W2, a two-dimensional (longitudinal and vertical) hydrodynamic and water quality model, was initially developed by the US Army Corps of Engineers' Waterways Experiment Station (Cole and Wells, 2015). The model was an outcome of a series of developments since 1975, such as the Laterally Averaged Reservoir Model (LARM) and the Generalized Longitudinal-Vertical Hydrodynamics and Transport Model (GLVHT), version 1.0, version 2.0, and version 3.0 (Edinger and Buchak, 1975). The current formal version is 4.2.2 issued in 2020.

The model is able to simulate water surface elevation, velocity in two dimensions, temperature, a conservative tracer, water age or hydraulic residence time, coliform bacteria, contaminants, inorganic suspended solids groups, phytoplankton groups, periphyton/epiphyton groups, and carbonaceous biochemical oxygen demand (CBOD) groups, including CBOD-N and CBOD-P, as well as ammonium (NH_4^+), nitrate (NO_3^-), nitrite (NO_2^-), bioavailable phosphorus (commonly represented by orthophosphate or soluble reactive phosphorus), labile dissolved organic matter, refractory dissolved organic matter, labile particulate organic matter, refractory particulate organic matter, total inorganic carbon, alkalinity, total iron and dissolved oxygen (DO). The model can be run for long-term simulations and can cope with varying head boundary conditions such as rivers, lakes, reservoirs, and estuaries. In addition, there are other advantages such as multiple water bodies, branches and turbulence closure schemes, variable grid spacing and water quality independent of hydrodynamics. However, potential theoretical and numerical limitations exist, for example in the appropriation for large water bodies with significant lateral variations in water quality due to the assumption of lateral average hydrodynamics and transport, simplification of complex ecosystems, a shortage of sediment compartments, disadvantages of numerical transport schemes for temperature and constituents and computer limits for computation and storage.

Bowen and Hieronymus (2003) reported the application of the CE-QUAL-W2 model for the Neuse River Estuary in North Carolina, USA for a total maximum daily load (TMDL) analysis. The study simulated chlorophyll, a concentration and percentage of water quality standard exceedance for various cases of nitrogen loading reduction and found that a load reduction of approximately 5% was needed to lessen the frequency of violating the water quality standard below 10%. Debele et al. (2008) integrated CE-QUAL-W2 with the SWAT model to assess water quantity and quality, both in the upland watershed and downstream water body, and the results suggested that these two models can be used to evaluate upland watershed and downstream water bodies.

2.4.2 HSPF

The Hydrological Simulation Program–FORTRAN (HSPF) emerged in the early 1960s and was implemented with water quality processes by the USEPA in the 1970s (Johansen et al., 1984). In the 1980s, pre and post-processing software, algorithm enhancements, and the US Geological Survey (USGS) Watershed Data Management (WDM) scheme were introduced to the model by the USGS and the USEPA. An interactive version was provided in the 1990s, with version 11.0 being released in March 1997, while version 12.4 was pre-released for internal peer review in April 2014.

The model can simulate surface runoff, base flow, DO, biochemical oxygen demand (BOD), temperature, pesticides, conservatives, fecal coliforms, sediment, pH, NH_4^+, NO_2^-, NO_3^-, organic N, orthophosphate, organic P, phytoplankton, and zooplankton. The model is suitable for evaluating land use changes, reservoir operations, point or non-point source treatment alternatives and flow diversions.

Saleh and Du (2004) conducted a comparative study between the SWAT model and the HSPF in the Upper North Bosque River watershed in the USA. For monthly flow, the Nash−Sutcliffe model efficiencies for calibration and verification were 0.91 and 0.86 respectively for HSPF, while they were 0.50 and 0.78 respectively for the SWAT model. They recorded 0.72 and 0.88 for HSPF, and 0.83 and 0.59 for the SWAT model for monthly sediment. The study suggested that the SWAT model generally performed better than the HSPF for nutrient loading during the calibration and verification periods.

2.4.3 MIKE 11

MIKE 11 was initially developed by the Danish Hydraulic Institute (DHI) in 2009. The DHI is a leading software developer for water environments, and MIKE 11 is a software package for simulating flow, sediment and water quality constituents for rivers and estuaries. Alongside the nucleus module, the hydrodynamic module provides flood forecasting through simulations of flood control measures, irrigation and surface drainage system operations, channel system designs, and tidal and storm surges. The model has a range of add-on modules capable of simulating hydrology and advection-dispersion as well as models for various aspects of water quality and cohesive and non-cohesive sediment transport. MIKE 11 is a one-dimensional, fully dynamic modulated modelling tool, however, it is a distributed model, and it demands a large amount of data, high computational time, and experts. It is also a commercial software, and there was no budget to purchase this software for this study.

Doan et al. (2015) applied MIKE 11 to the Cả River in Vietnam to investigate the effect of climate change on salinity intrusion. The model fitted the observed data when the water level was calibrated and validated, and the results of the 2010 scenario revealed that the impact on salinity intrusion in the river was significant compared to the baseline scenario.

2.4.4 QUALs

Over time, a series of water quality models called QUAL2E, QUAL2E-UNCAS, QUAL2K, and QUAL2Kw were developed by the USEPA (Brown and Barnwell, 1985; Brown and Barnwell, 1987; Chapra et al., 2012; Pelletier et al., 2006). The development of the QUAL2E model can be traced back to the QUAL-II and QUAL-I models that came about in the early 1970s (Roesner et al., 1981a and b; Texas Water Development Board, 1970). As a comprehensive enhanced stream water quality model, the QUAL2E model can simulate 15 water quality indices, which are DO, BOD, temperature, algae as chlorophyll, organic nitrogen (Org-N), ammonia (NH_3-N), nitrite (NO_2^--N), nitrate (NO_3^--N), organic phosphorus (Org-P), dissolved phosphorus (Sol P) and coliform bacteria. It can also simulate one arbitrary non-conservative constituent solute and three conservative constituent solutes. The QUAL2E-UNCAS model has the capability of performing sensitivity and uncertainty analysis. Ning et al. (2001) noted that the QUAL2E model was successfully calibrated and validated using observations to predict BOD, DO, total phosphate, and NH_3-N for an entire river system in Taiwan, China. Paliwal et al. (2007) used the QUAL2E model to assess the influence of different scenarios on BOD and DO for a river near Delhi, India, and the results showed that treatment of the discharge from the drains to the river was important and the diversion of a substantial load to a canal for further treatment. Also, the uncertainty analysis performed well on simulated data. However, the QUAL2E model can only have a maximum of 25 reaches, which is less than 250 computational elements, a maximum of seven headwater elements, a maximum of six junction elements, and a maximum of 25 input and withdrawal elements. Park et al. (2003) reported that the QUAL2E model omits the role of macrophytes, whereas the HSPF model does not.

The QUAL2K model is a significant improvement over the QUAL2E model that was developed in the 2000s. The QUAL2K model inherited similar features of the QUAL2E model, such as one-dimensional, branching, steady-state hydraulic, diel heat budget, diel water quality kinetics, and heat and mass inputs. New functional elements were also incorporated into the QUAL2K model, such as a user-friendly software interface integrated with Microsoft Excel and varying model segmentation in addition to two forms of carbonaceous BOD, anoxia, sediment-water interactions, bottom algae, light extinction, pH, pathogens, reach specific kinetic parameters, and weirs and waterfalls. Zhang et al. (2012) applied the QUAL2K model to a tributary river in the Taihu Basin, a densely populated and industrialized area of China, to evaluate the impact of a range of water quality improvement scenarios, and the study found that the optimal scenario could reduce BOD, NH3-N, total N, and total P by 49.50%, 32.81%, 35.94%, and 45.27%, respectively. The QUAL2K model was considered an effective tool to assess potential water quality improvement measures. Bui et al. (2019) used the QUAL2K model to simulate T, DO, BOD, COD, and components of N and P in the downstream Cả River in Vietnam using observed water quality data and discharge simulated by the SWAT model.

The QUAL2Kw model, ver. 6 was developed with characteristics such as automatic calibration and Monte Carlo simulations in addition to addressing non-steady, non-uniform flow using kinematic wave flow routing, one-dimensional, dynamic heat budgets, dynamic water-quality kinetics, heat and mass inputs, phytoplankton and bottom algae, and variable stoichiometry (Pelletier et al., 2006). The model can simulate several constituents in a water body, including temperature, pH, CBOD, sediment oxygen demand (SOD), DO, Org-N, NH_3-N, NO_2^--N NO_3^--N, Org-P, inOrg-P, TN, total phosphorus (TP), phytoplankton, and bottom algae. Kannel et al. (2007) calibrated the QUAL2Kw model using field data from the Bagmati River in Nepal and found that the model calibration results agreed well with the observations, with the root mean square errors (RMSE) for river width, velocity, flow, temperature, pH, DO, CBOD, COD, TN and TP being 31.4%, 31.80%, 4.0%, 8.0%, 7.0%, 15.0%, 52.0%, 44.2%, 20.3% and 31%, respectively. Moreover, this model provides a genetic algorithm that assists with calibrating the selected rates automatically.

2.4.5 SWAT

The SWAT model is a physically daily based, continuous, and computationally efficient watershed water quality model developed by the USDA Agricultural Research Service (ARS) in the early 1990s. It can predict the long-term impact of management practices, such as crop rotation, drainage, fertilization, grazing, irrigation, and tillage on water, sediment, and agricultural chemical yields in large, complex watersheds under dynamic circumstances (Arnold et al., 1998). The model inherits features from several early ARS models, such as the Simulator for Water Resources in Rural Basins (SWRRB), the Chemicals, Runoff and Erosion from Agricultural Management Systems (CREAMS), the Groundwater Loading Effects on Agricultural Management Systems (GLEAMS), and the Erosion-Productivity Impact Calculator (EPIC) (Arnold et al., 1990; Knisel, 1980; Leonard et al., 1987; Williams et al., 1984; Williams et al., 1985). Over the nearly 30 years since its inception, the SWAT model has been released in a series of versions with significant improvements. These versions are SWAT94.2, SWAT96.2, SWAT98.1, SWAT99.2, SWAT2000, SWAT2005, and SWAT2009 with the current version being SWAT2012.

Since its beginning in the 1990s, the SWAT model has been broadly applied to numerous locations with different circumstances worldwide. In the first published paper related to the SWAT model, Engel et al. (1993) compared three models, i.e., the SWAT model, the Agricultural Non-Point Source Pollution Model (AGNPS), and the Areal Non-Point Source Watershed Environmental Response Simulation (ANSWERS) (Beasley et al., 1980; Young et al., 1989). They noted that the simulation results matched observed data from an 830-acre watershed in Indiana, US, which represented the Midwestern US agricultural region. On a 4,277 km^2 watershed in Texas, US, Santhi et al. (2001) calibrated and validated the SWAT model for flow, sediment, and nutrients to assess alternative management scenarios, and they achieved $R^2 \geq 0.6$ and $E \geq 0.5$ in most instances. The study documented the calibration and validation procedures for the SWAT model, and it indicated that this model could be applied to large watersheds to predict flow, sediment, and nutrients to assess the effects of alternative management scenarios. Arnold et al. (2012) described the use, calibration, and validation of the SWAT model, and they introduced an automated calibration method, SWAT-CUP, to cope with calibration, validation, sensitivity, and uncertainty analysis while accounting for the model's complicated parameterization (Abbaspour, 2014). Available optimization algorithms and calibration procedures for the SWAT model include Sequential Uncertainty Fitting Ver. 2 (SUFI2), Particle Swarm Optimization (PSO), Generalized Likelihood Uncertainty Estimation (GLUE), Parameter Solution (ParaSol), and Markov Chain Monte Carlo (MCMC) (Abbaspour et al., 1997; Abbaspour et al., 2004; Beven and Binley, 1992; Kennedy and Eberhart, 1995; Kuczera and Parent, 1998; Van Griensven and Meixner, 2006).

Golmohammadi (2014) developed the SWATDRAIN model by incorporating the DRAINMOD model into the SWAT model and proposed that CTD caused a reduction in average annual drain flow by 18%, while increasing the surface runoff by approximately 30% from June 15 to August 15 during the cropping season and from November 1 to May 1 in the non-growing season. Further, Golmohammadi et al. (2016) noted that implementing CTD resulted in a 16% reduction in the mean annual drain flow while increasing surface runoff by as much as 71% in an agricultural watershed in Ontario, Canada. Using the original SWAT model, Hanke (2018) evaluated the effects of CTD on TP losses at a site in Ontario, Canada, and the study argued that the practice of CTD would aggravate TP losses due to increasing the soil moisture and the resulting increased surface runoff. Bauwe et al. (2019) reported that a modified SWAT model on reactive P, named SWAT-P, could improve prediction accuracy for dissolved reactive phosphorus losses into streams, as well as a roughly realistic estimation of dissolved reactive phosphorus losses from tile drainage water. However, SWATDRAIN and SWAT-P were never broadly tested or applied, and the study by Hanke (2018) was limited by its small scale and by using the original model without improvement.

The SWAT model runs on a daily scale, so it is not suitable for detailed single-event flood routing. Also, as a physically distributed model, the SWAT model demands massive daily inputs and generates many files based on Hydrological Respond Units (HRUs); therefore, it is inconvenient to modify a specific parameter, especially for a large watershed. The SWAT model was designed as a watershed water quality model rather than a river (stream) water quality model, and it is limited in its ability to simulate water quality indices, such as diurnal changes in pH, bottom algae, and anoxia in water bodies, even though it is equipped with a nutrient routing adapted from the earlier version QUAL2E model. The QUAL2E model is an outdated model that emerged in the 1980s and was further developed in the 2000s, with the QUAL2Kw model being a significant improvement with many new elements compared to the QUAL2E model.

Moreover, the SWAT model was not updated with the improvements of the new QUAL2Kw model. Although the SWAT model is a watershed quality model that has some features of a river water quality model (QUAL2E), it is beyond SWAT’s capacity to simulate and evaluate river water quality. However, the SWAT model's many outputs can be used as inputs of the QUAL2Kw model, and so the simulation results from SWAT can potentially be used to drive the QUAL2Kw model and hence evaluate river water quality.

2.4.6 WASP7

The Water Quality Analysis Simulation Program (WASP7) evolved from previous versions of WASP, a model that was developed by the USEPA (Ambrose et al., 1988; Connolly and Winfield, 1984; Di Toro et al., 1983). WASP7 is a dynamic modularized water quality modelling program that includes a eutrophication module. It can simulate CBOD (1), CBOD (2), CBOD (3), ammonia, nitrate, Org-N, orthophosphate, Org-P, algae, benthic algae, detritus, sediment diagenesis, and salinity. Furthermore, it includes an organic chemical module, i.e., chemical 1, chemical 2, chemical 3, solids 1, solids 2, and solids 3 as well as a mercury module, i.e., divalent mercury, methyl mercury, sands, and fines. This model provides a pre-processor and a post-processor to assist the modeler in preparing input datasets and reviewing simulation results. Significantly, it is capable of one-, two-, or three-dimensional investigation with various pollutant types. Zou et al. (2006) linked WASP with the Environment Fluid Dynamics Code (EFDC) to predict the fate of nutrients, CBOD, algae and DO in a creek in Pennsylvania, US, with an improved periphyton dynamics module and a diurnal DO simulation module (Hamrick, 1992).

Compared to WASP, Qual2Kw is more suitable for coupling with SWAT due to its Excel interface and auto calibration procedure.

2.4.7 AnnAGNPS

AnnAGNPS, (Bingner et al., 2007) was developed by the United States Department of Agriculture Agricultural Research Service and Natural Resources Conservation Service. As a comprehensive computational model evolved from AGNPS (Young et al., 1989), it was designed to evaluate nonpoint source pollutant loads in agricultural watersheds. AnnAGNPS is a distributed simulation model that subdivides a watershed into small homogeneous sub-watersheds named cells. Cells are afterward interconnected by stream channels called reaches. Whereas, this model only simulates direct runoff.

2.4.8 DRAINMOD

Dr. Wayne Skaggs at the North Carolina State University developed the model in 1980. This model can simulate the hydrology of poorly drained, high water table soils on an hour-by-hour, day-by-day basis for long periods of climatological record. The model simulates the effects of drainage and associated water management practices on water table depths, the soil water regime and crop yields (Skaggs et al. 2012).

2.4.9 Water quality models for the study

All the three studied models in Table 2.3, SWAT, AnnAGNPS, and DRAINMOD, are capable of simulating tile flow. All three models only simulate nitrate and flow in the tiles. Given that our objective is to simulate CTD at the watershed scale, DRAINMOD was excluded. SWAT was preferred to AnnAGNPS because it can simulate baseflow and direct runoff, while AnnAGNPS can only simulate direct runoff.

Table 2.3 Summary of the reviewed models

No.	Model	Parameter simulated in tile flow	Type	Note
1	SWAT	nitrate	watershed	simulating all water with H-K tile drain functions
2	AnnAGNPS	nitrate	watershed	no groundwater simulation and H-K tile drain functions
3	DRAINMOD	nitrate	field	

The reviewed models were summarized in Table 2.4. Based on previous model reviews and an analysis of the objectives of this study, the watershed water quality model, SWAT, and the stream water quality model, QUAL2Kw, are adopted to fulfill these objectives. Specifically, the SWAT model will be applied to the watershed to evaluate the environmental effects of CTD and UCTD on the water quality of the watershed. Also, coupled with the SWAT model, the river water quality model, QUAL2Kw, will be used to assess the ecological impact of CTD and UCTD on the water quality of the river.

Table 2.4 Summary of the reviewed models

No.	Model	Type	Simulated items	Drainage module	Availability
1	CE-QUAL-W2	Stream	water surface elevation, velocity, DO, CBOD, …	No	Free
2	HSPS	Stream/watershed	surface runoff, base flow, DO, biochemical, …	No	Free
3	MIKE 11	Stream/watershed	Hydrology, advection-dispersion, water quality, and cohesive and non-cohesive sediment transport, …		Commercial
4	QUALs	Stream	Flow, DO, BOD, temperature, algae as chlorophyll, ...	No	Free
5	SWAT	Watershed	Flow, sediment, N, and P, …	Yes	Free
6	WASP7	Stream	CBOD, ammonia, nitrate, Org-N, orthophosphate, Org-P, algae, benthic algae, …	No	Free
7	AnnAGNPS	Watershed	Flow, sediment, N, and P, …	Yes	Free
8	DRAINMOD	Field	Flow, sediment, N, and P, …	Yes	Free

2.5 Theories and approaches of the QUAL2Kw model

The in-stream water quality model, QUAL2Kw, focuses on the river (stream) water quality in one dimension as described in the previous section. The model employs a segmentation scheme (Figure 2.5) to simulate a river or stream (Pelletier and Chapra, 2008). Each segment consists of a collection of reaches, while tributaries are not simulated. Tributaries can be represented as point sources.

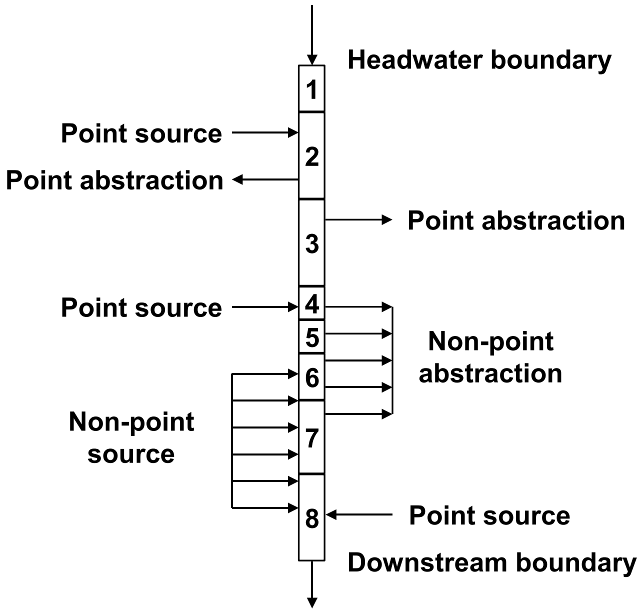

Figure 2.5 Segmentation scheme of the QUAL2Kw model

2.5.1 Flow balance

The calculation formula for a steady-state flow for each element in the model is defined in Equation 2.1, and the schematic diagram is shown in Figure 2.6 (Chapra et al., 2012).

$$Q_i = Q_{i-1} + Q_{in,i} - Q_{ab,i} - Q_{evap,i} \qquad 2.1$$

In the above equation, Q_i is the outflow from reach i into the downstream reach $i + 1$ (m^3/d), Q_{i-1} is the inflow from the upstream reach $i - 1$ (m^3/d), $Q_{in,i}$ is the total inflow into the reach from the point and non-point sources (m^3/d), $Q_{ab,i}$ is the total outflow from the reach due to point and non-point abstractions (m^3/d) and $Q_{evap,i}$ is the outflow due to evaporation (m^3/d).

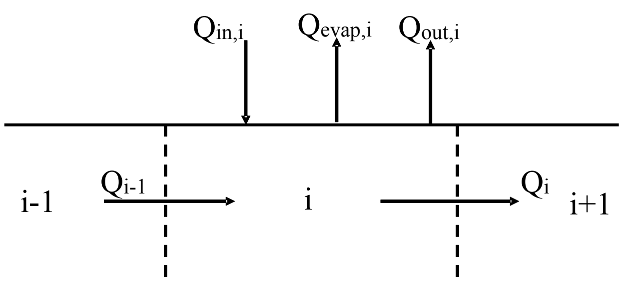

Figure 2.6 Element flow balance of the QUAL2Kw model

2.5.2 Heat balance

The heat balance considers heat transfers from adjacent reaches, loads, abstractions, the atmosphere, and sediments. The calculation formula in the model is shown in Equation 2.2:

$$\frac{dT_i}{dt} = \frac{Q_{i-1}}{V_i}T_{i-1} - \frac{Q_i}{V_i}T_i - \frac{Q_{ab,i}}{V_i}T_i + \frac{E'_{i-1}}{V_i}\left(T_{i-1} - T_i\right) + \frac{E'_i}{V_i}\left(T_{i+1} - T_i\right)$$
$$+ \frac{W_{h,i}}{\rho_w C_{pw} V_i}\left(\frac{\text{m}^3}{10^6\ \text{cm}^3}\right) + \frac{J_{h,i}}{\rho_w C_{pw} H_i}\left(\frac{\text{m}}{100\,\text{cm}}\right) + \frac{J_{s,i}}{\rho_w C_{pw} H_i}\left(\frac{\text{m}}{100\,\text{cm}}\right) \quad 2.2$$

where T_i is the temperature in reach i (°C), t is the time (d), E'_i = the bulk dispersion coefficient between reaches i and $i + 1$ (m^3/d), $W_{h,i}$ is the net heat load from point and non-point sources into reach i (cal/d), ρ_w is the density of water (g/cm^3), C_{pw} is the specific heat of the water [cal/(g °C)], $J_{h,i}$ is the air-water heat flux [cal/(cm^2 d)] and $J_{s,i}$ is the sediment-water heat flux [cal/(cm^2 d)].

2.5.3 Mass balance

For an element, the general balance of a constituent except the bottom algae variables is defined in Equation 2.3:

$$\frac{dc_i}{dt} = \frac{Q_{i-1}}{V_i}c_{i-1} - \frac{Q_i}{V_i}c_i - \frac{Q_{ab,i}}{V_i}c_i + \frac{E'_{i-1}}{V_i}\left(c_{i-1} - c_i\right) + \frac{E'_i}{V_i}\left(c_{i+1} - c_i\right) + \frac{W_i}{V_i} + S_i \quad 2.3$$

where W_i is the external loading of the constituent to reach i [g/d or mg/d] and S_i is the sources and sinks of the constituent due to reactions and mass transfer mechanisms [$g/m^3/d$ or $mg/m^3/d$]. An exchange of mass between the surface water and the hyporheic sediment zone is represented by the bulk hyporheic exchange flow in reach i.

2.6 Theories and approaches of the SWAT model

After its development in the early 1990s, as a physically based and semi-distributed watershed model, the SWAT model has been continuously improved in order to evaluate the impact of practices on water, sediment, and nutrients in complex watersheds with dynamic conditions such as soil, land use, field management and climate scenarios (Neitsch et al., 2011). The model delineates a watershed into a number of sub-watersheds representing varied spatial and temporal conditions, for example, soil, land use, climate, crop and management. Moreover, a sub-watershed in the model can be further subdivided into more HRUs, the smallest homogenous unit with respect to unique climate, crop, land use, management, soil, and topography.

2.6.1 Water

The model is driven by water balance, and it uses two major divisions, the land phase (Figure 2.7) and the routing phase (Figure 2.8) to simulate the hydrologic cycle of a watershed (Neitsch et al., 2011). The first phase covers the amount of water, sediment, nutrient, and pesticide loadings that go into the main channel in each sub-watershed, while the second phase covers the movement of water, sediment, nutrient, and pesticide loadings throughout watershed's channel network to the outlet.

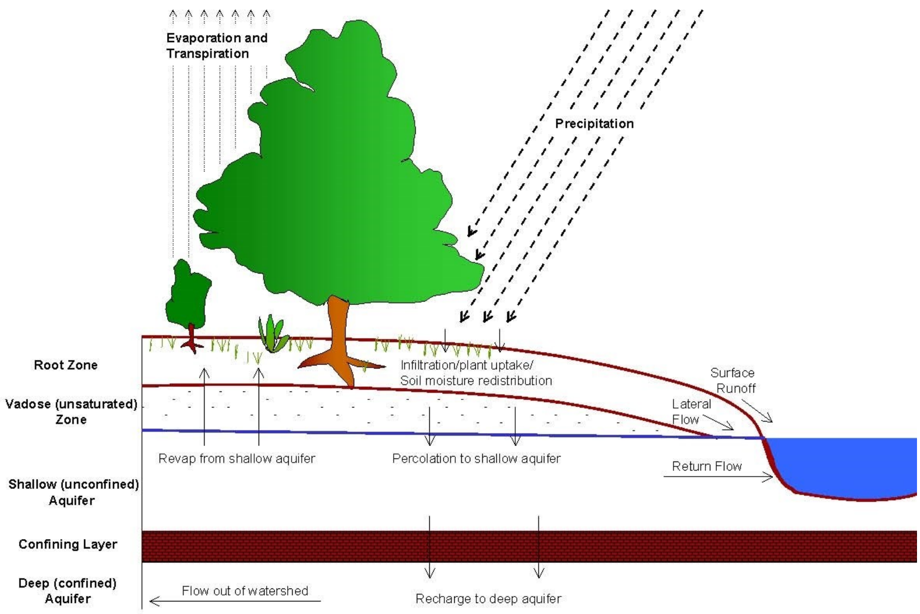

Figure 2.7 The land phase of the hydrologic cycle

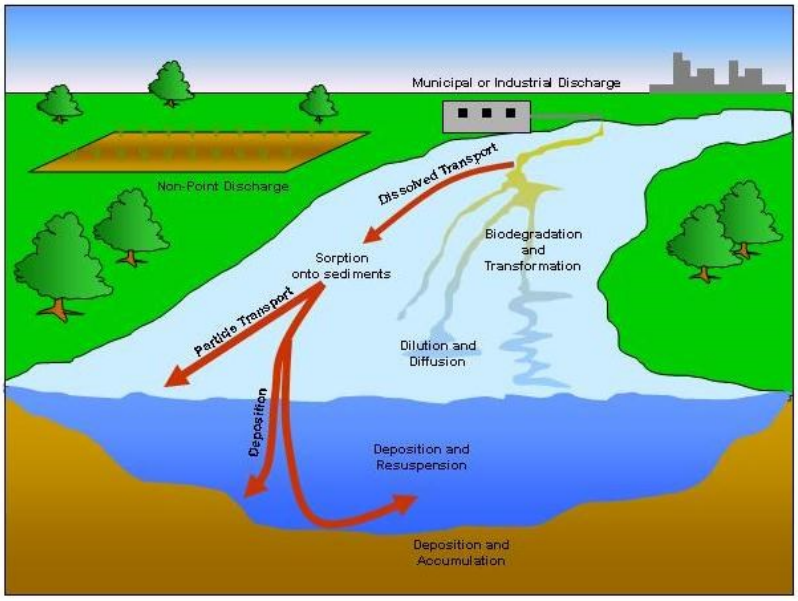

Figure 2.8 The routing phase of the hydrologic cycle

The water balance in the model can be defined in Equation 2.4

$$SW_t = SW_0 + \sum_{i=1}^{t}(R_{day} - Q_{surf} - E_a - w_{seep} - Q_{gw}) \qquad 2.4$$

where SW_t is the final soil water content (mm H_2O), SW_0 is the initial soil water content on day i (mm H_2O), t is the time (days), R_{day} is the amount of precipitation on day i (mm H_2O), Q_{surf} is the amount of surface runoff on day i (mm H_2O), E_a is the amount of evapotranspiration on day i (mm H_2O), w_{seep} is the amount of water entering the vadose zone from the soil profile on day i (mm H_2O), and Q_{gw} is the amount of return flow on day i (mm H_2O) (Neitsch et al., 2011).

The SWAT model provides two approaches to calculate surface runoff, the Soil Conservation Service (SCS) curve number (CN) method (SCS, 1972) (Equaiton. 2.5) and the Green and Ampt infiltration method (Green and Ampt, 1911).

$$Q_{surf} = \frac{(R_{day} - I_a)^2}{(R_{day} - I_a + S)} \qquad 2.5$$

In the above equation, Q_{surf} is the accumulated runoff or rainfall excess (mm H_2O). R_{day} is the rainfall depth for the day (mm H_2O). I_a is the initial abstractions, which include surface storage, interception, and infiltration prior to runoff (mm H_2O), and S is the retention parameter (mm H_2O). Runoff only occurs when $R_{day} > I_a$.

In the model, tile drainage flow is treated as lateral flow. Fields that are equipped with tile drainage generate tile drainage flow when the soil water table is higher than the tile drain depth. A detailed review and analysis of the tile drainage routines in the SWAT model are given in Sections 2.6.4 and 3.1.1.

2.6.2 Sediment

Sediment simulation in the model is based on the Modified Universal Soil Loss Equation (MUSLE) developed by Williams (1975) (Equation 2.6), which is an improved version of the Universal Soil Loss Equation (USLE) that was developed by Wischmeier and Smith (1965, 1978), as follows:

$$sed = 11.8\ (Q_{surf}\ q_{peak}\ area_{hru}\ )^{0.56}\ K_{USLE}\ C_{USLE}\ P_{USLE}\ LS_{USLE} CFRG \qquad 2.6$$

In the above equation, sed is the sediment yield on a given day (metric tons), Q_{surf} is the surface runoff volume (mm H_2O/ha), q_{peak} is the peak runoff rate (m^3/s), $area_{hru}$ is the area of the HRU (ha), K_{USLE} is the USLE soil erodibility factor (0.013 metric ton m^2 hr/(m^3-metric ton cm)), C_{USLE} is the USLE cover and management factor, P_{USLE} is the USLE support practice factor, LS_{USLE} is the USLE topographic factor and $CFRG$ is the coarse fragment factor.

2.6.3 N and P

The model simulates five different pools of N in soil generally belonging to two forms (Figure 2.9), mineral N and organic N (Neitsch et al., 2011). Mineral N includes two pools,

NH_4^+ and NO_3^-, and the other three pools, active, stable and fresh, are classified as organic N.

NITROGEN

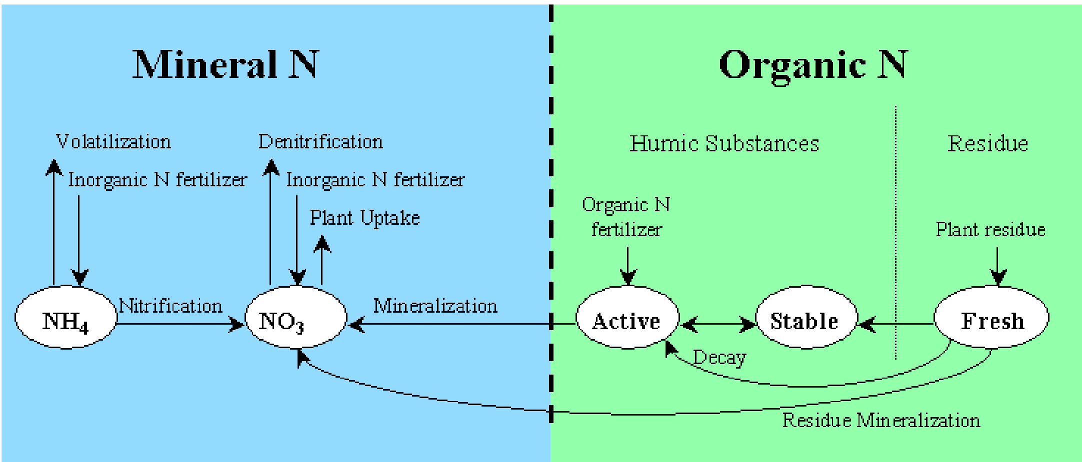

Figure 2.9 SWAT soil N pools and processes

Like N, P plays an important role in the life cycle of organisms, but there are significant differences between these two elements in reactivity, solubility, and demand. The SWAT model simulates six pools of P in the soil (Figure 2.10) (Neitsch et al., 2011). Three of these pools, stable, active and solution, are mineral P, and the other three, active, stable, and fresh, are in the organic form.

PHOSPHORUS

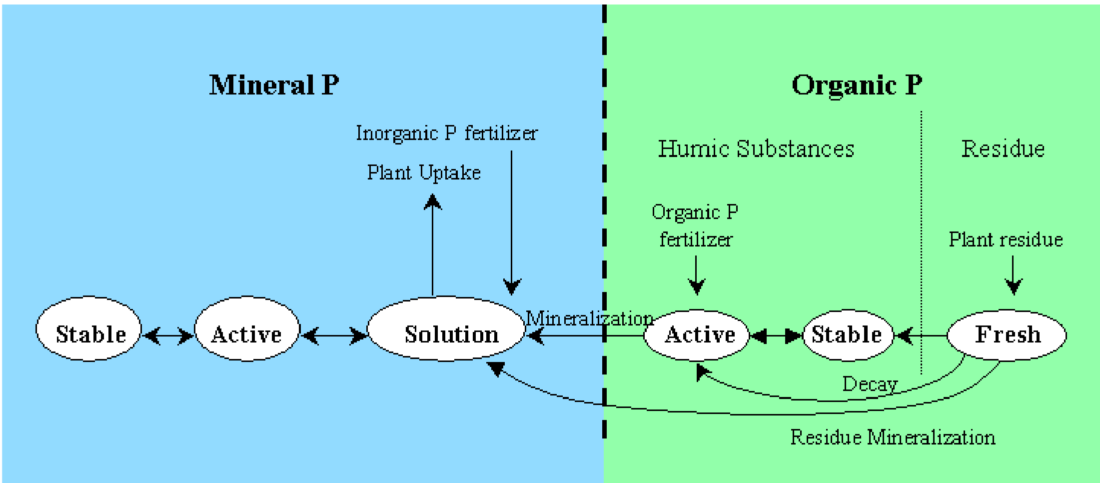

Figure 2.10 SWAT soil P pools and processes

The SWAT model assumes that due to low mobility, soluble P leaches only from the top 10 mm of soil into the first soil layer. The calculation formula is shown in Equation 2.7

$$P_{perc} = \frac{P_{solution,surf}\, w_{perc,surf}}{10\ \rho_b depth_{surf} k_{d,perc}} \qquad 2.7$$

where P_{perc} is the amount of P moving from the top 10 mm into the first soil layer (kg P/ha), $P_{solution,surf}$ is the amount of P in solution in the top 10 mm (kg P/ha), $w_{perc,surf}$ is the amount of water percolating to the first soil layer from the top 10 mm on a given day (mm H_2O), ρ_b is the bulk density of the top 10 mm (Mg/m^3) (assumed to be equivalent to the bulk density of the first soil layer), $depth_{surf}$ is the depth of the "surface" layer (10 mm), and $k_{d,perc}$ is the P percolation coefficient (m^3/Mg). The P percolation coefficient is the ratio of the concentration of P in the 10 mm of soil on the surface to the concentration of P in the percolate. Currently, the SWAT model does not simulate the soluble P pool in the shallow aquifer directly, but a concentration can be assigned, and it remains the same during the simulation period.

2.6.4 Tile drainage simulation in the SWAT model

Version 637 of the SWAT model was used in this study. It offers two methods to calculate the amount of flow from the tile drainage.

The first one is formulated as Equation 2.8 (Neitsch et al., 2011). Arnold et al. (1999) introduced two important concepts to define a restrictive soil layer at the bottom of the soil profile and allow the soil profile above the layer to fill to field capacity:

$$tile_{wtr} = \frac{(h_{wtbl} - h_{drain})}{h_{wtbl}} (SW - FC) \left(1 - \exp\left[\frac{-24}{t_{drain}}\right]\right) \quad if\ h_{wtbl} > h_{drain} \qquad 2.8$$

In the above equation, $tile_{wtr}$ is the amount of water removed from the layer on a given day by tile drainage (mm H_2O), h_{wtbl} is the height of the water table above the impervious zone (mm), h_{drain} is the height of the tile drain above the impervious zone (mm), SW is the water content of the profile on a given day (mm H_2O), *FC* is the field capacity water content of the profile (mm H_2O), and t_{drain} is the time required to drain the soil to field capacity (in hours).

To calculate the tile flow, the parameters for the height of the tile drain to the impervious layer h_{drain}, and the time required to drain the soil to field capacity t_{drain}, must be defined. Where the tile drain is applied to a saturated situation ($SW-FC>0$) and there is a tile drain underground water table (h_{wtbl} - $h_{drain} >0$), tile drain flow will occur in the model. However, this simple method has its limitations in practice. Boles et al. (2015) noted that a drawdown tile t_{drain} defined in the equation should not be the same for all storm magnitudes, and that a static time cannot capture the dynamics of tile drainage well.

The second method involves the Hooghoudt (1940) and Kirkham (1957) drainage equations implemented by Moriasi et al. (2007) (H-K equation), which are based on related tile drainage parameters such as the depth from the soil surface to the drains, the tile drain radius and the tile drain spacing (van Schilfgaarde et al., 1957).

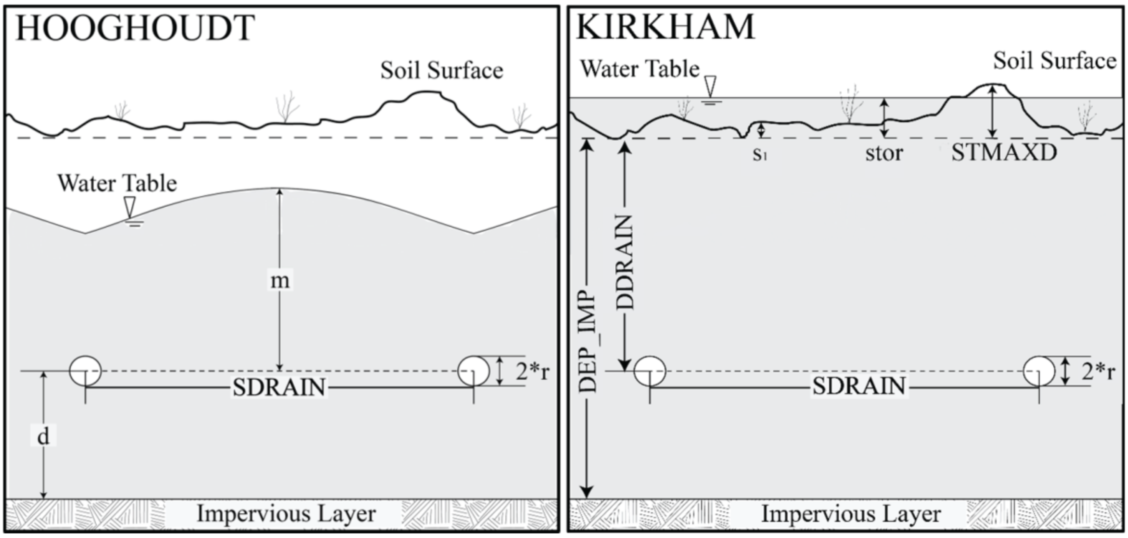

(a) (b)

Figure 2.11 Schematics of drainage for the H−K equation

The Hooghoudt equation (Equation 2.9) is used when the water table is lower than the soil surface as shown in Figure 2.11a (Boles et al., 2015).

$$q_{tile} = \frac{8K_e d_e m + 4K_e m^2}{C(SDRAIN^2)} \qquad 2.9$$

In the above equation, q_{tile} is the drainage flux (mm h^{-1}), K_e is the effective lateral saturated hydraulic conductivity (mm h^{-1}), *SDRAIN* is the distance between drains (mm), and *m* is the height of the water table above the drains measured at the midpoint (mm). d_e (mm) is the equivalent depth based on the height of the drain above the impervious layer, and *C* represents the ratio of the flow midway between the drains to the average flow between the drains. When the soil surface is submerged by the water table as illustrated in Figure 2.11b, the Kirkham equation (Equation 2.10) will be used (Boles et al., 2015).

$$q_{tile} = \frac{4\pi K_e(stor + DDRAIN - r)}{g(SDRAIN)} \qquad 2.10$$

In the above equation, *stor* is the average height of the water stored on the surface (mm), *DDRAIN* is the depth from the soil surface to the drains (mm), and *r* is the tile drain radius (mm). g is dimensionless and is calculated as a function of *d*, *SDRAIN, r,* and *DEP_IMP* mm (depth of soil profile).

The H-K method has several advantages, since it considers realistic parameters for a tile drainage system and dynamic situations, rather than a simple drawdown time, as used in the first method. Only nitrate is simulated in tile flow. Moriasi et al. (2012) evaluated the capability of the H-K method in a tile-drained watershed in Iowa, US, and found that the H-K method is a promising alternative both as a tile flow simulation method and for tile drainage design tools in the SWAT model. Furthermore, Moriasi et al. (2013) evaluated the performance of the method on NO_3^--N by using long-term monitoring data for subsurface tile drainage from an experimental field at the University of Minnesota's Agricultural Experiment Station near Waseca, southern Minnesota. This research indicated that the revised SWAT model, with the new method, simulated the water and N budgets more accurately than the first method. Boles et al. (2015) noted that the updated tile drainage equations improved the simulation of tile drainage, and Guo et al. (2017) suggested that the new method has the potential to accurately simulate hydrologic processes in mildly sloped watersheds.

2.7 Climate change

The ancient Greek philosopher Heraclitus said that "no man ever steps in the same river twice, for it's not the same river and he's not the same man." In short, this means that nothing is permanent except change, and that everything is in flux, and the climate in which we are living is not exception to this. The UN Framework Convention on Climate Change defines climate change, in Article 1 as: "a change of climate which is attributed directly or indirectly to human activity that alters the composition of the global atmosphere and which is in addition to natural climate variability observed over comparable periods" (United Nations, 1992).

As the United Nations body for assessing the science related to climate change, the Intergovernmental Panel on Climate Change (IPCC) (2014) notes that observed climate change has the strongest and most comprehensive impact on natural systems. The hydrological systems in many regions are changing due to changes in precipitation as well as melting snow and ice. As a result, this affects water resources in terms of quantity and quality. Bates et al. (2008) suggested that climate change has an effect on the function and operation of existing water infrastructure, such as structural flood defences, drainage and irrigation systems and water management practices. Therefore, it is necessary to test the performance of CTD scenarios under climate change conditions.

2.7.1 Climate models

The IPCC (2014) has defined climate models as typically numerical simulations of real-world systems calibrated and validated using observations from experiments or analogies, and then run using input data representing future climate elements. As representations of physical processes in the atmosphere, oceans, cryosphere, and land surfaces, GCMs discretize the equations for fluid motion and energy transfer and integrate them over time. These GCMs typically have a horizontal resolution of between 250 and 600 km, with 10 to 20 vertical layers for the atmosphere and sometimes as many as 30 layers for oceans. The American Meteorological Society states that a RCM is a numerical climate prediction model forced by specified lateral and ocean conditions from a GCM or observation-based dataset (re-analysis). RCMs simulates atmospheric and land surface processes, while accounting for high-resolution topographical data, land-sea contrasts, surface characteristics, and other Earth-system components.

Currently, there are numerous climate models with various spatial resolutions, both globally and regionally, that predict a variety of changes in the climate based on different assumptions and historical re-analyses.

Table 2.5 Combinations of RCM, GCM, RCP and spatial resolution

	RegCM4	WRF	CanRCM4	RCA4	HIRHAM5	RCP	ECS (°C)
HadGEM2-ES	50km	50km				8.5	4.6
CanESM3			0.44°			4.5	3.7
			0.44°			8.5	
MPI-ESM-LR	50km	50km				8.5	3.6
EC-EARTH				0.44°	0.44°	4.5	~3.3
				0.44°	0.44°	8.5	
GFDL-ESM2M	50km	50km				8.5	2.4

The climate change data used in this study were downloaded from the North American Coordinated Regional Climate Downscaling Experiment (CORDEX) Program (NA-

CORDEX), which will run from 1950 to 2100, with a spatial resolution of 0.22°/25 km or 0.44°/50 km (Mearns et al., 2017). By applying different representative concentration pathways (RCPs), the climate data for 12 climate change scenarios consists of simulation results from different RCMs driven by different GCMs as shown in Table 2.5.

With additional functionality, including well-resolved stratosphere and earth system components, the Hadley Centre Global Environment Model version 2 (HadGEM2) is the successor to HadGEM1, designed to simulate and understand the specific purpose centennial-scale evolution of climate developed by The Met Office Hadley Centre in the UK. Collins et al. (2011) note that the global climate model provided valuable results for both climate predictions and for investigating the strengths of biogeochemical feedback. The second-generation Canadian Earth System Model (CanESM2) incorporates an atmosphere-ocean general circulation model, a land-vegetation model, and a terrestrial and oceanic interactive carbon cycle model. It adequately simulates the observed twentieth-century Arctic temperature variability, including the early and late-twentieth-century warming periods and the intervening 1940–1970 period of substantial cooling (Chylek et al., 2011). The Max Planck Institute for Meteorology Earth System Model (MPI-ESM) has been applied to numerous research and practical problems worldwide. At low resolution (MPI-ESM-LR), the MPI-ESM is one of five different coupled model configurations (Mauritsen et al., 2019). As part of a Europe-wide consortium, the European community Earth-System Model (EC-Earth) is a global climate model based on the world-leading weather forecast model of the European Centre of Medium-Range Weather Forecast in its seasonal prediction configuration as the base of the climate model (Hazeleger et al., 2012). The Geophysical Fluid Dynamics Laboratory (GFDL) of the U.S. National Oceanic and Atmospheric Administration developed two new global coupled carbon–climate Earth System Models (ESMs) with different ocean dynamical/physical cores. All other components were the same, and the vertical coordinate for the ocean dynamical/physical component in the version GFDL-ESM2M is based on depth (Dunne et al., 2012; Dunne et al., 2013).

RegCM4 is the latest version derived from RegCM3. This regional climate model was developed at the National Center for Atmospheric Research and maintained in Italy's Earth System Physics of the International Center for Theoretical Physics (Giorgi et al., 2012). It was designed to be a public, open-source, user-friendly model capable of being applied to any region in the world. Designed to meet research and operational needs, the Weather Research and Forecasting (WRF) Model is used worldwide in numerical weather prediction models (Powers et al., 2017). The regional climate model was specifically developed to work with its parent global climate model, CanESM2, by the Canadian Centre for Climate Modelling and Analysis (CanRCM4), which downscales climate predictions and climate projections from CanESM2 (Scinocca et al., 2016). The latest version at the Rossby Centre of Atmospheric models is RCA4, which provides fundamental climate information via a web service. It has been used to downscale different coupled atmosphere-ocean general circulation models (Kjellström et al., 2016). The High-Resolution Limited Area Model (HIRHAM) is a numerical short-range weather forecasting system developed by the international HIRHAM Programme. It is used for routine weather forecasting at a number of meteorological institutes in Europe. Combining the most recent versions of HIRHAM and the European Centre Hamburg Model (ECHAM), HIRHAM version 5 (HIRHAM5) has become a new regional climate model (Christensen et al., 2006).

A representative concentration pathway (RCP) is a measure of greenhouse gas concentration used by the IPCC based on the assumption that cumulative emissions of CO_2 are the key driver of the future climate. RCP8.5 refers to a scenario of long-term, global emissions of greenhouse gases, with high concentrations of carbon that cause global warming at an average of 8.5 watts per square meter across the planet. Meanwhile, RCP 4.5 stands for a scenario with intermediate concentrations of carbon. The IPCC (2014) defined four pathways: a stringent mitigation scenario RCP2.6, two intermediate scenarios RCP4.5 and RCP6.0, and one scenario with very high greenhouse gas emissions RCP8.5. All scenarios were used for climate modeling and research for the IPCC's fifth Assessment Report in 2014. In this study, two pathways were explored, RCP4.5 and RCP8.5.

For a theoretical value of global warming at equilibrium for a doubling CO_2, equilibrium climate sensitivity (ECS) is vital to understanding the longer-term climate. The IPCC (2014) has stated that it has great confidence in the fact that the ECS is extremely unlikely to be less than 1°C, medium confidence that the ECS is likely to be between 1.5°C and 4.5°C, and very unlikely to be greater than 6°C.

2.7.2 Downscaling methods

GCMs or RCMs run globally or regionally, while regional analyses require information at much smaller scales, such as catchment or watershed scales. Downscaling is a process that interpolates the information from large scales generated by GCMs or RCMs to smaller scale, both spatially and temporally. Daniels et al. (2012) conceptualized the process as shown in Figure 2.12 below:

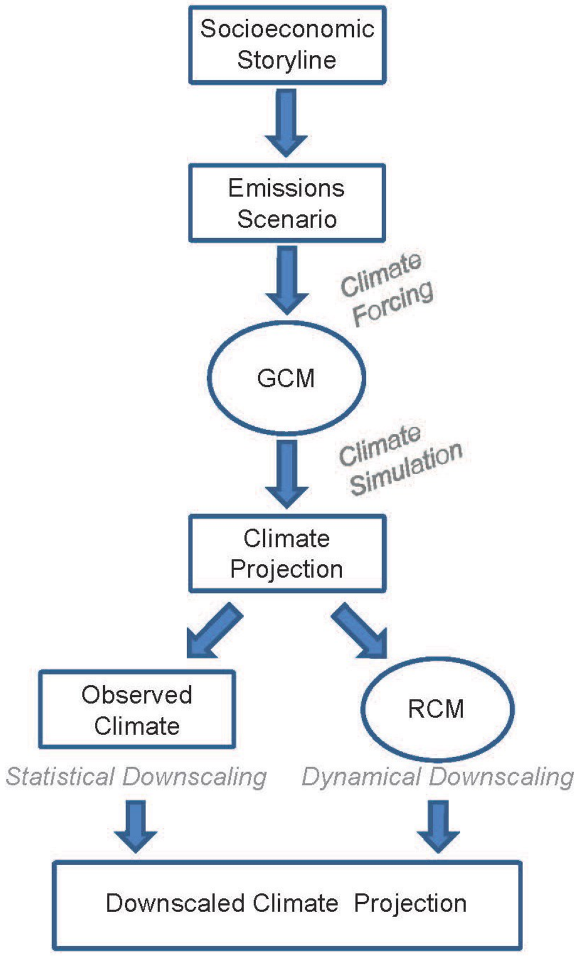

Figure 2.12 Illustration of the components and steps of downscaling

Essentially, there are two ways to apply large-scale climate predictions to local conditions, dynamical and statistical. To predict regional climate, dynamical downscaling uses higher resolution RCMs with additional regional information driven by GCMs, which is often computationally intensive.

However, statistical downscaling is based on empirical relationships from locally observed climate data. After being validated, future large-scale atmospheric conditions projected by GCMs are used to simulate local climates in the future, which is commonly done due to it's associated simplicity, flexibility, and efficiency.

Table 2.6 Statistical downscaling category, method, predictor and predictand variables, advantages, and disadvantages

Category & Method		Predictor & Predictand	Advantages	Disadvantages
Linear Methods *Spatial*	Delta method	The same type of variable (e.g., both monthly temperature, both monthly precipitation)	• Relatively straightforward to apply • Employs full range of available predictor variables	• Requires normality of data (e.g., monthly temperature, monthly precipitation, long-term average temperature) • Cannot be applied to non-normal distributions (e.g., daily rainfall) • Not suitable for extreme events
	Simple and multiple linear regression	Variables can be of the same type or different (e.g., both monthly temperature or one monthly wind and the other monthly precipitation)		
	Spatiotemporal Methods: Canonical Correlation Analysis and Singular Value Decomposition			
Weather Classification *Spatial and temporal*	Analog method	Variables can be of the same type or different (e.g., both monthly temperature, one large-scale atmospheric pressure field and the other daily rainfall)	• Yields physically interpret linkages to surface climate • Versatile, i.e., can be applied to both normally and non-normally distributed data	• Requires additional step of weather type classification • Requires a large amount of data and some computational resources • Incapable of predicting new values that are outside the range of the historical data
	Cluster analysis			
	Artificial Neural Network			
	Self-Organizing Map			
Weather Generator *Spatial and temporal*	Long Ashton Research Station Weather Generator	Same type of variable, different temporal scales (e.g., predictor is monthly precipitation and predictand is daily precipitation)	• Able to simulate the length of wet and dry spells • Produces a large number of series, which is valuable for uncertainty analysis • Production of novel scenarios	• Data-intensive • Sensitive to missing or erroneous data in the calibration set • Only some weather generators can check for the coherency between multiple variables (e.g., high insolation should not be predicted on a rainy day) • Requires generation of multiple time-series and statistical post-processing of results
	Mark Sim GCM			
	Nonhomogeneous Hidden Markov Model	Variables can be of the same type or different (e.g., both monthly temperature, one large-scale atmospheric pressure and the other daily rainfall)		

Statistical downscaling methods can be categorized into linear methods, weather classifications and weather generators. Trzaska and Schnarr (2014) summarized the advantages and disadvantages, shown in Table 2.5 as above, of some statistical downscaling methods. As one of the simplest means to statistically downscale GCM projections, the change factor (delta) method uses the ratio between future simulations of GCM and present climate observations as a multiplicative factor to obtain future local climate.

3 Development and Verification of an Improved CTD Routine for SWAT

As described in Section 2.6.4, SWAT has two tile drainage algorithms, the equation proposed by Arnold et al. (1999), and the H-K drainage equations implemented by Moriasi et al. (2007). SWAT also allows the user to dynamically change the elevations of the drains during a simulation. Despite those limitations as described in the following section, some researchers have used SWAT to simulate CTD. For instance, Hanke (2018) ran two SWAT models in parallel with tiles at two different depths and recombined the outputs of the two models to mimic the operation of a control structure. Before that, Que (2015) simulated CTD using AnnAGNPS by dynamically changing the drain depths during the simulation. He attempted to do the same with SWAT but obtained poor results. Of course, in real life, tile drain elevations cannot be changed during the growing season and comparing the outputs of two models with different configurations does not necessarily give the same results as a single model switching between configurations. It was hence decided to examine and improve the SWAT tile drainage routine so that it can better simulate CTD.

3.1 Improvements in the algorithm for calculating NO_3^--N

During initial attempts by the author to apply the SWAT's tile drainage routines to mimic CTD, it was found that the results of the CTD scenarios using the original model were not in line with the experimental observations from the paired micro watershed and previous simulation results using the AnnAGNPS model. Thus, the SWAT model must be improved in order to simulate CTD properly. After further investigation by the author, it was discovered that the algorithm used in the original SWAT for calculating NO_3^--N in tile flow does not reflect the way water leaves the field when CTD is applied. The algorithm drains water from the wrong soil layer, and possibly with the wrong nutrient concentrations. The difference between CTD and UCTD as to which soil layer water should be drawn from is illustrated in Figures 3.1, 3.2 and 3.3.

3.1.1 Algorithm for calculating NO_3^--N in the original SWAT model with CTD

The original code uses the concentration of NO_3^--N from improper soil layer when calculating NO_3^--N at certain depths when applying CTD scenarios as depicted in Figures 3.1b and 3.2b. The calculation formula for NO_3^--N in tile flow is defined as tile flow×NO_3^--N concentration of the soil layer where the tile drain is. When the tile drain depths of 200, 600, and 1,100 mm are in one layer, or the soil profile contains only one layer, the CTD scenarios are fine because they use NO_3^--N concentrations from the same soil layer. However, when there are multiple layers in the soil profile, which is in fact the general situation when modeling, the tile drain depths would possibly fall into different soil layers at 200, 600, and 1,100 mm, so the model uses NO_3^--N concentrations from different soil layer to calculate the NO_3^--N in tile flow for the CTD_{200}, CTD_{600} and UCTD scenarios (see Section 4.1.7 for CTD scenarios). The formulae for calculating NO_3^--N in tile flow in the original SWAT model for different tile drainage depths are given as below. Assuming the soil has three layers in an HRU, the method to calculate the NO_3^--N in tile flow in the original SWAT model with the CTD scenario is illustrated in Figures 3.1b, 3.2b and 3.3b.

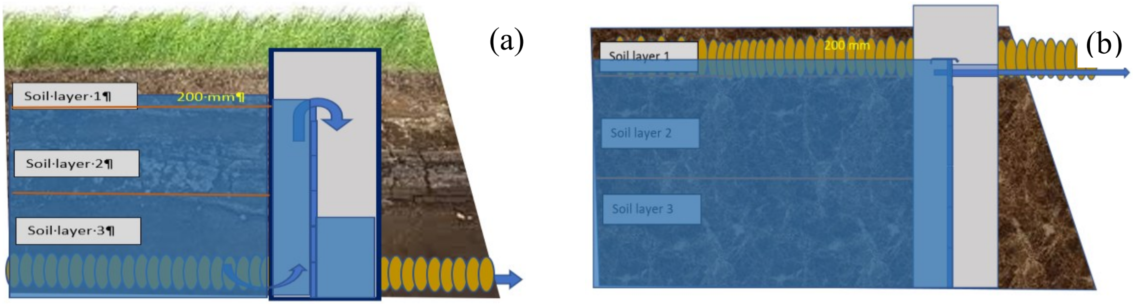

NO_3^--N_{200} = tile flow × concentration of NO_3^--N in layer 3

NO_3^--N_{200} = tile flow × concentration of NO_3^--N in layer 1

Figure 3.1 Calculating NO_3^--N for CTD_{200} in improved and original SWAT models

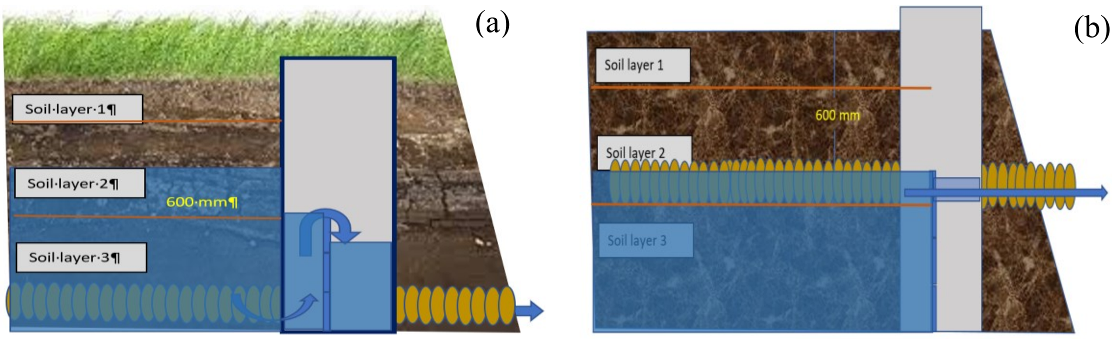

NO_3^--N_{600} = tile flow × concentration of NO_3^--N in layer 3

NO_3^--N_{600} = tile flow × concentration of NO_3^--N in layer 2

Figure 3.2 Calculating NO_3^--N for CTD_{600} in improved and original SWAT models

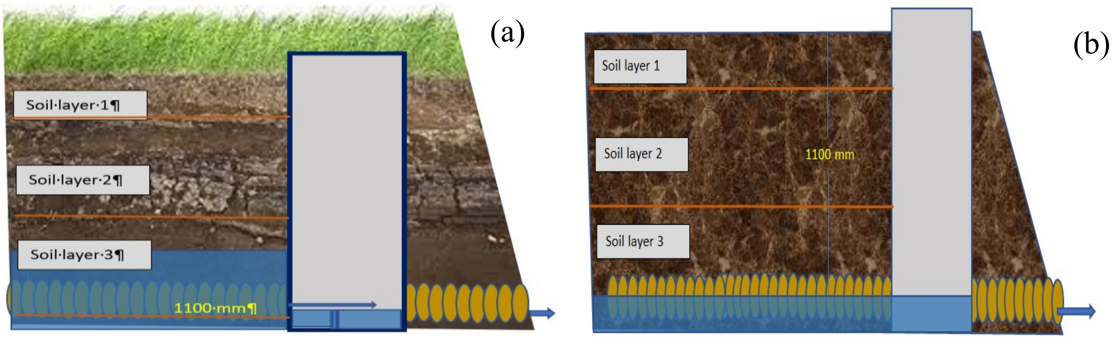

NO_3^--N_{1100} = flow × concentration of NO_3^--N in layer 3

NO_3^--N_{1100} = flow × concentration of NO_3^--N in layer 3

Figure 3.3 Calculating NO_3^--N for UCTD in improved and original SWAT models

This calculation method for NO_3^--N in the original model is not in accordance with the reality of CTD in a field, as the tile flow always comes from the tile drain instead of the soil layer. In other words, NO_3^--N in the tile flow should be calculated using the concentration of NO_3^--N in the soil layer where the tile drain is located. There does not appear to be a problem with UCTD because the tile drainage depth is normally located where the tile drain is, but it does not work in CTD scenarios because only the depth is used as the means to control the water table instead of the location of the tile drain.

3.1.2 Proposed CTD algorithm

To solve this problem, it is necessary to make the NO_3^--N concentrations in the soil layer where the default tile drain is uniform when calculating NO_3^--N in the tile flow for CTD at different tile drainage depths, as shown in Figures 3.1a, 3.2a, and 3.3a, respectively.

Thus, this way of calculating NO_3^--N in tile flow represents the reality of tile drain in field, and the CTD scenarios can be compared to the UCTD scenarios. The source codes of the model were modified accordingly.

3.2 Application of the improved SWAT model to the paired WEBs watersheds

To verify the improved algorithm for calculating NO_3^--N in the modified SWAT model, the modified SWAT model was applied to the paired micro experimental watersheds for the WEBs project, named as the CTD watershed and the UCTD watershed, respectively, implemented for CTD and UCTD scenarios in the South Nation River watershed as shown in Figure 2.1. Two SWAT models using the modified version of the SWAT model, the CTD model and UCTD model, respectively, were built for the paired experimental watersheds.

3.2.1 Materials and methods

3.2.1.1 Study areas

As noted in Section 2.3, the CTD and UCTD scenarios were experimented within two neighbouring micro watersheds (Figure 3.4), respectively. The experimental settings and results for the CTD and UCTD sites of WEBs can be found in previous publications (Sunohara et al., 2014; Sunohara et al., 2015).

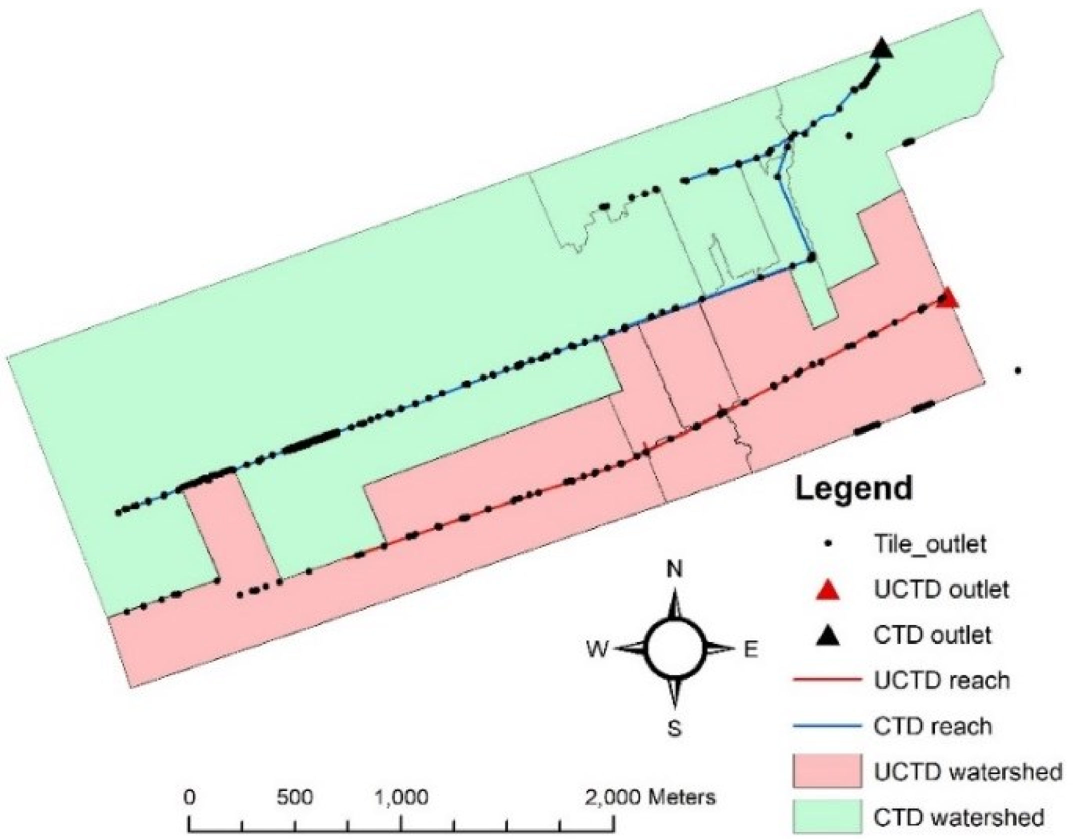

Figure 3.4 The CTD and UCTD watersheds

3.2.1.2 Topographical, hydrometeorological, field management, land use, and soil data

The digital elevation model (DEM) was obtained from AAFC with a fine resolution of 1 m × 1m, as shown in Figure 3.5.

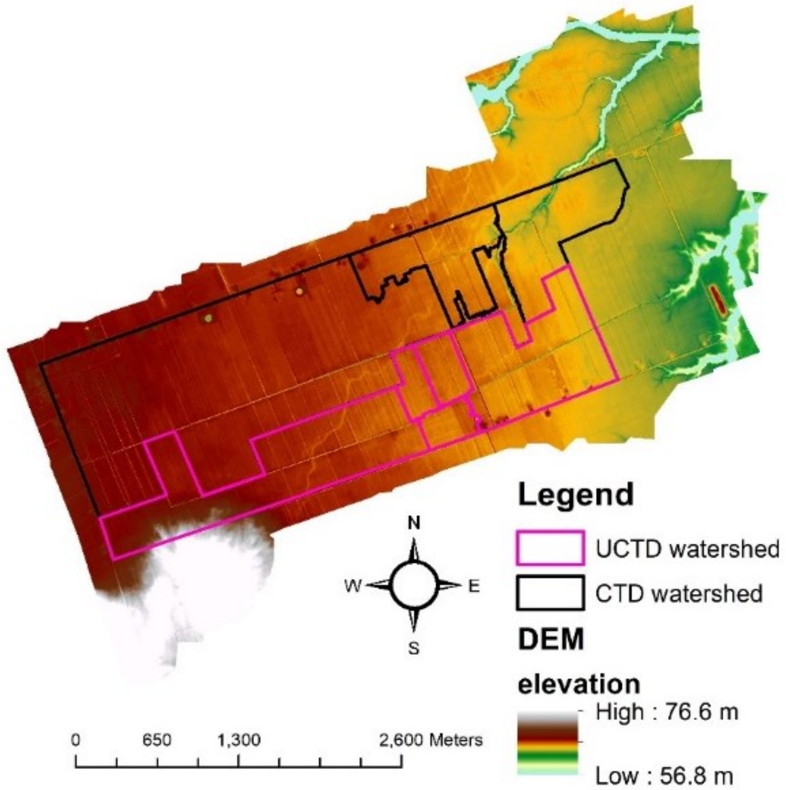

Figure 3.5 Map of the DEM with CTD and UCTD watersheds

The daily weather data required by the SWAT model, i.e., precipitation, minimum and maximum temperatures, relative humidity, solar radiation, and wind speed, were collected by a HOBO weather station within the watershed. Flow data were monitored at each outlet of the watersheds during seasons of the growth, as shown in Figure 3.6.

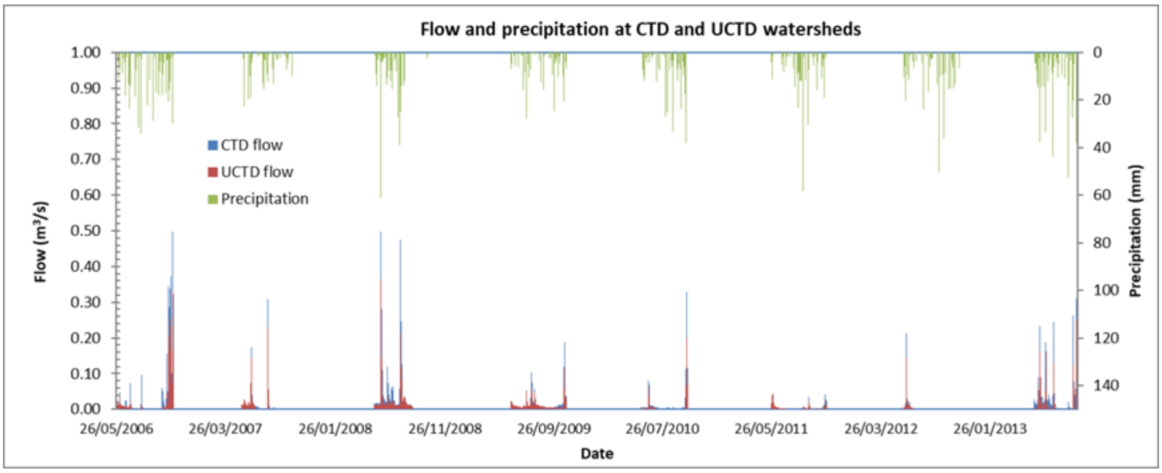

Figure 3.6 Flow and precipitation in the CTD and UCTD watersheds

Crop ration and field operations for CTD for each crop field lot were recorded by AAFC. For example, the 2006 crops in the paired watersheds were shown in Figure 3.7. Each lot has its own crop and operation schedule.

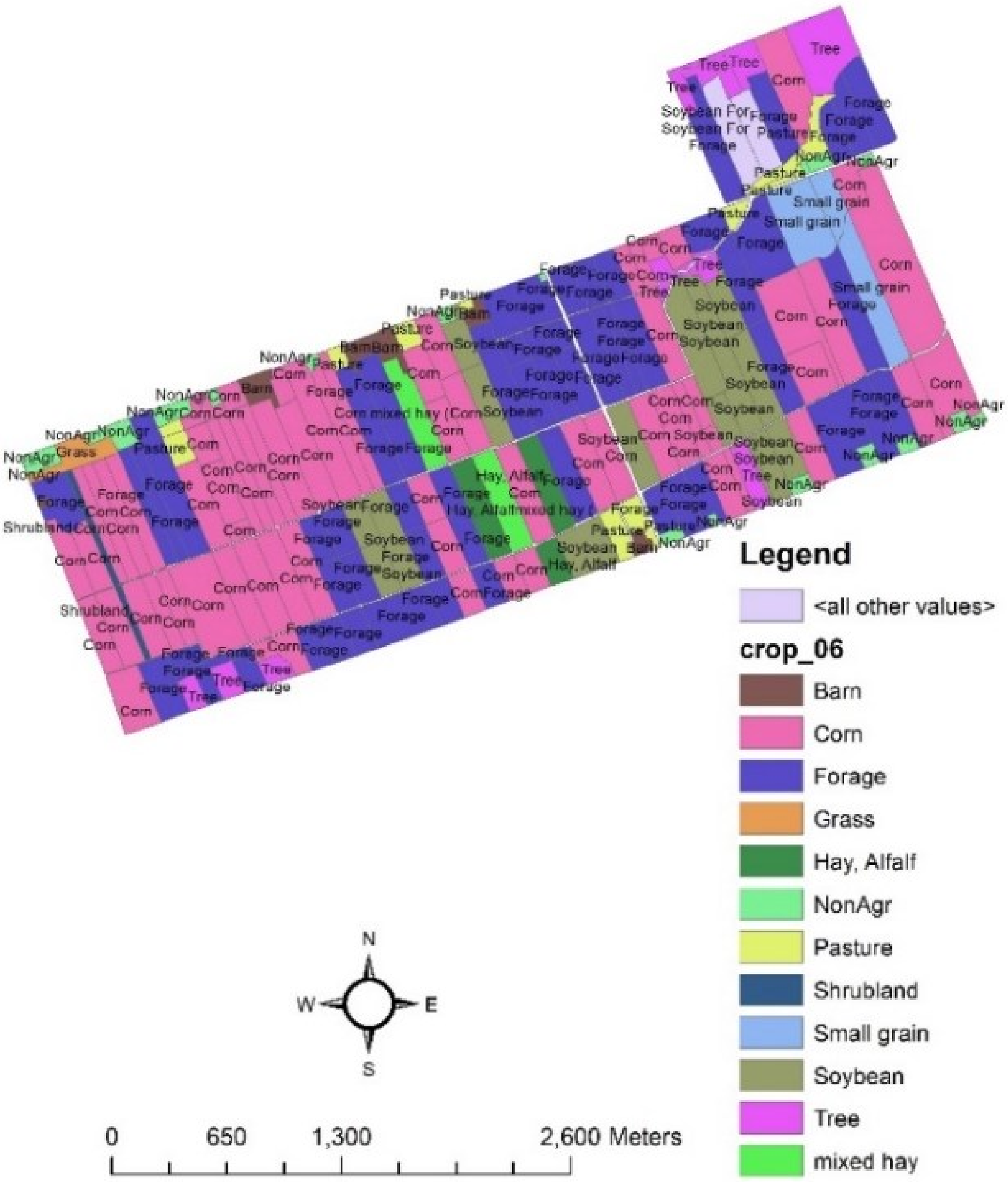

Figure 3.7 Crops in the CTD and UCTD watersheds

The soil data were obtained from AAFC (2007). The CTD and UCTD watersheds contain three and six types of soil with four layers, respectively, as shown in Figure 3.8.

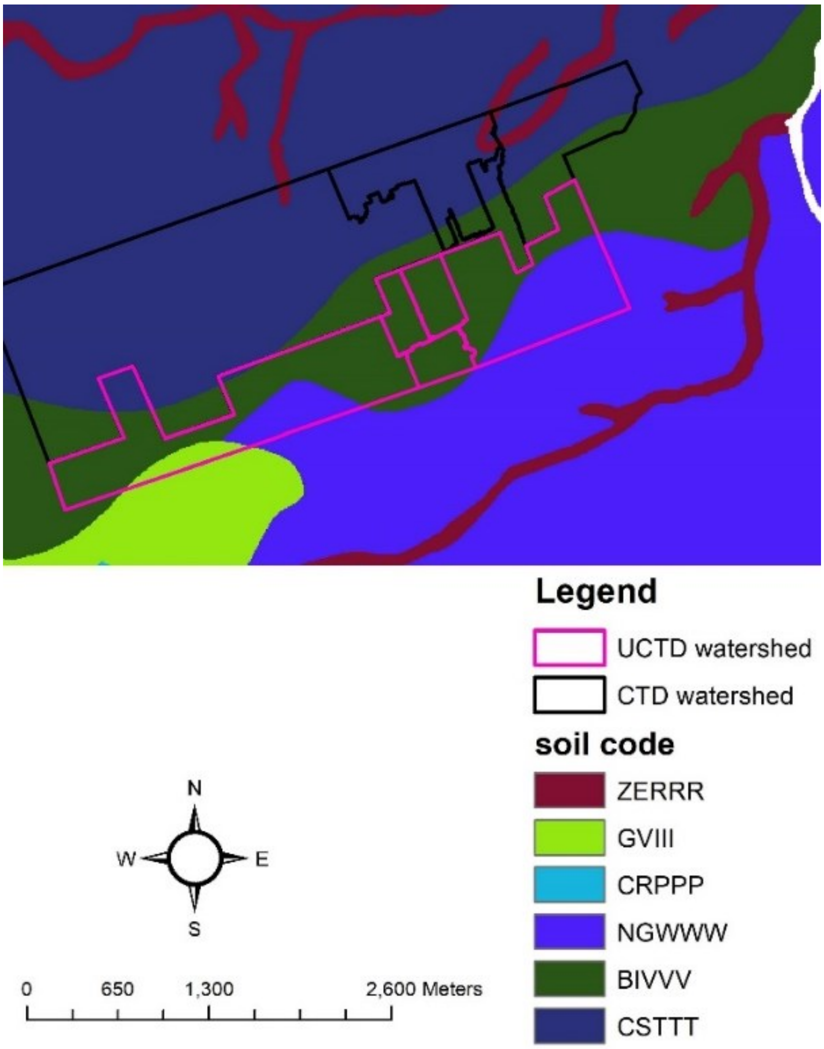

Figure 3.8 Soils within the CTD and UCTD watersheds

3.2.1.3 CTD and UCTD model setups

Given that the micro catchments were imposed, the SWAT model was developed using pre-defined watershed and stream polygons. HRUs were generated based on planting lots to precisely present each crop lot and arrange drainage operation schedules. A total of 144 and 106 HRUs were generated for the CTD and UCTD watersheds (Figure 3.9), respectively. Crop rotations and field drainage operations were scheduled for each HRU based on field records collected during the WEBs project. The field operations during crop rotation and the fertilizer application rates are summarized and shown in Table 4.1. Based on local farm field operation, at the UCTD watershed (site), the UCTD treatment (1100 mm) was applied, and the CTD treatment (600 mm) was implemented for the CTD watershed (site). So accordingly, the UCTD model tested the UCTD condition (1100 mm), and the CTD model tested the CTD treatment (600 mm).

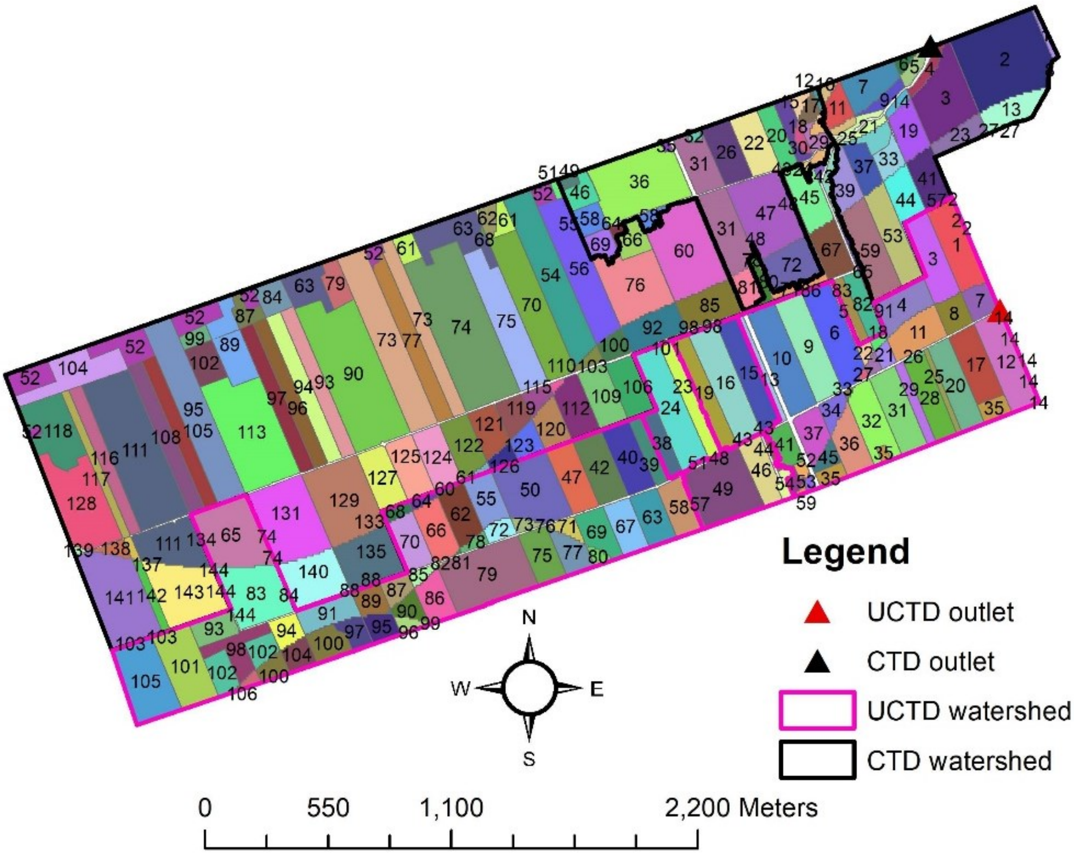

Figure 3.9 HRUs in the CTD and UCTD models

3.2.2 Verification of the benefits of CTD versus UCTD

In principle, the two models should have the same parameterizations as they are geographically close, however, there is no rule as to how to obtain common parameters. A compromise was found where each model will be calibrated independently, and then the CTD and UCTD will be compared using each of the two parameter sets.

3.2.3 Calibration and validation of the CTD and UCTD models

For calibration and validation of the model, three statistical performance measures were selected to measure the goodness of fit between the observed data and the simulated output.

These measures are the Nash–Sutcliffe efficiency (NSE) (Equation 3.1), the observations standard deviation ratio (RSR) (Equation 3.2), and the percent bias (PBIAS) (Equation 3.3) (Gupta et al., 1999; Legates and McCabe, 1999; Nash and Sutcliffe, 1970).

$$NSE = 1.0 - \frac{\sum_{i=1}^{n}(O_i - P_i)^2}{\sum_{i=1}^{n}(O_i - \bar{O})^2} \qquad 3.1$$

$$RSR = \frac{\sqrt{\frac{\sum_{i=1}^{n}(P_i - O_i)^2}{n}}}{\sqrt{\frac{\sum_{i=1}^{n}(O_i - \bar{O})^2}{n}}} \qquad 3.2$$

$$PBIAS = \frac{\sum_{i=1}^{n}(O_i - P_i)}{\sum_{i=1}^{n} O_i} \times 100 \qquad 3.3$$

In the above equations, *O* represents the observed data, *P* is the simulated data, $\overline{O}$ and $\overline{P}$ are the means of observed and simulated series, respectively, i is the sequence number of an event and *n* is the total number of events in the series.

Nash and Sutcliffe (1970) introduced NSE as a performance measure for hydrological models. Its range can be from – ∞ to 1, with 1 indicating a perfect fit between the simulated and observed data. Fundamentally, the closer to 1 the number is, the better the model can perform in its predictions. Legates and McCabe (1999) standardized the RMSE using the observation standard deviation, which ranges from zero to large positive values. The smaller the RSR, the lower the RMSE, and subsequently, the model performs better. Gupta et al. (1999) used PBIAS to measure the average tendency of the simulated data to be larger or smaller than the observations, with positive values indicating model underestimation and negative values indicating model overestimation. The best fitting number is zero, where low magnitude values indicate better simulations.

To facilitate model evaluations, Moriasi et al. (2007) studied reported ranges of values and corresponding performance ratings for statistical and graph model evaluation techniques and recommended that these three quantitative statistics be used in water quality model evaluations. The study concluded that generally, a model simulation can be judged as satisfactory if NSE > 0.50 and RSR < 0.70, and if PBIAS ±25% for stream flow, PBIAS ± 55% for sediment and PBIAS ± 70% for N and P, with performance rates being very good, good, satisfactory, or unsatisfactory.

The modification to the algorithm for calculating NO_3^-- N in tile flow in the SWAT model, then conceptually, only NO_3^-- N and accordingly TN should change (because nitrate is part of TN). N, P, and their compound are certainly affected if water and sediment loads are modified, but water and sediment are not affected by changing N and P. Also, the calculations of N and P are independent of each other. More importantly, the SWAT model only calculates nitrate in tile flow, and other parts, org N, ammonia, and nitrite, are not calculated in tile flow. Therefore, only flow and NO_3^-- N need to be calibrated for the verification of the modification to the algorithm for calculating NO_3^-- N in tile flow.

The models were calibrated in sequence. Flow was calibrated firstly, and NO_3^--N was calibrated secondly.

3.2.3.1 The CTD model

For the CTD watershed (site) of WEBs, the CTD model was calibrated and validated for monthly flow and seasonal total NO_3^--N at the tile drain depth of 600 mm. The calibration period was from 2006 to 2010, and the model was validated during 2012 and 2013.

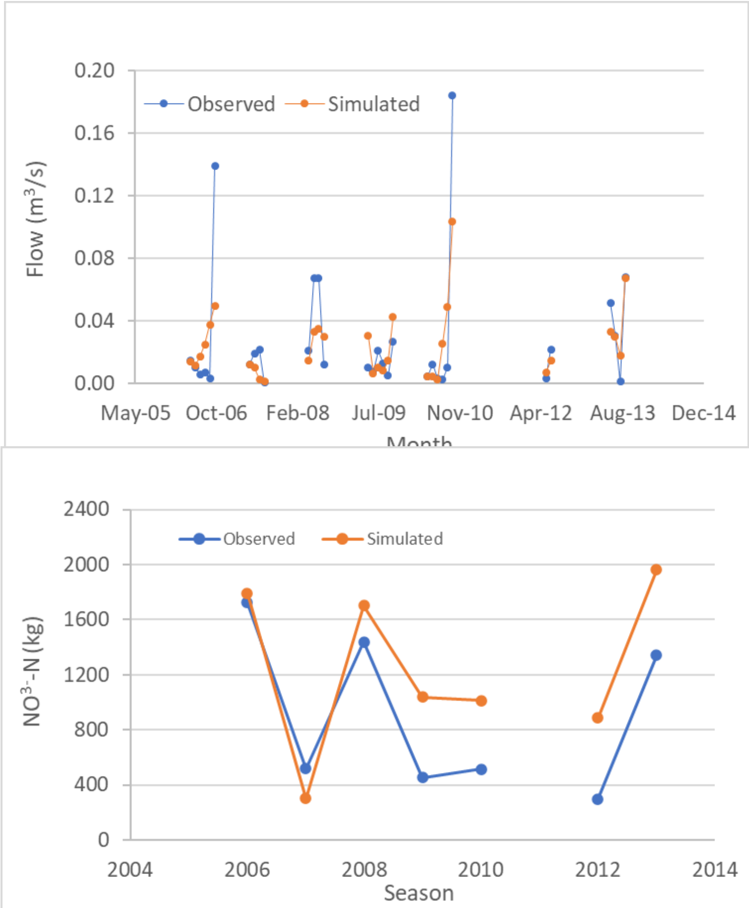

Figure 3.10 Observed and simulated flow and NO_3^--N for the CTD model

The results of the calibration and validation for flow and NO_3^-N are shown in Figure 3.10 and Table 3.1. The NSE, PBIAS, and RSR values for flow in the calibration period were 0.54, 7.32%, and 0.68, respectively, and in the validation periods they were 0.80, 4.08%, and 0.45, respectively. There seem however to be some differences in trend between the observations and simulations in some of the years, especially 2006 where the simulations are systematically increasing while the observations are decreasing, before making a large jump at the end of the season. A possible explanation for this may be erroneous measurements or wrong precipitation values.The values for NSE, PBIAS, and RSR in the calibration period for NO_3^--N were 0.51, -25.78%, and 0.70, respectively, and in the validation periods they were 0.67, -10.96%, and 0.57, respectively. Therefore, the performances of the calibration and validation for flow and NO_3^-N can be rated as very good and good, respectively (Moriasi et al., 2007).

3.2.3.2 The UCTD model

For the UCTD watershed (site) of WEBs, the UCTD model was calibrated and validated for monthly flow and seasonal total NO_3^-N at the tile depth of 1100 mm, with the calibration period being from 2006 to 2010 and the validation period being from 2012 to 2013.

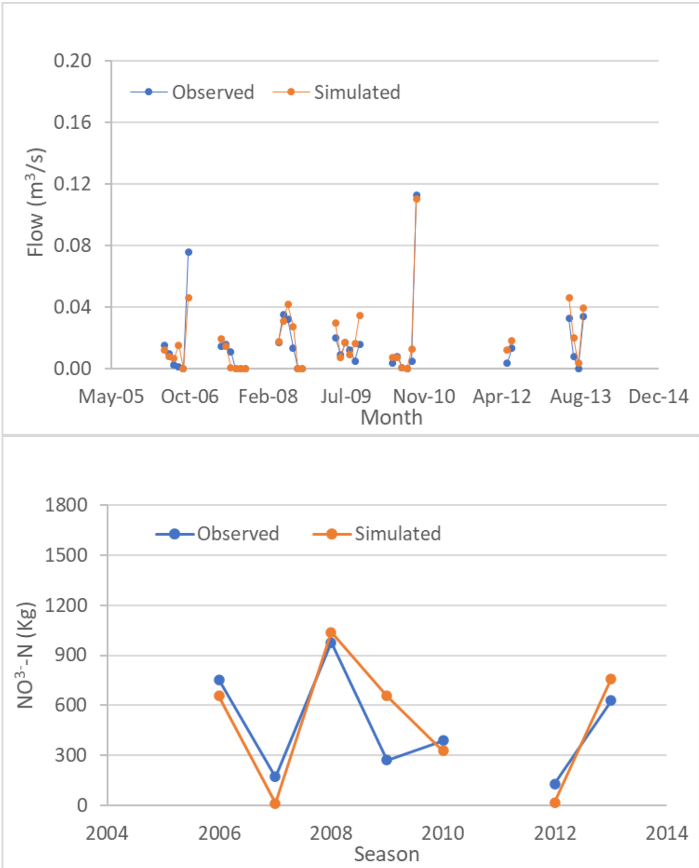

Figure 3.11 Observed and simulated flow and NO_3^--N $^-$for the UCTD model

The results of the calibration and validation for flow and NO_3^--N are shown in Figure 3.11 and Table 3.1. The values of NSE, PBIAS, and RSR in the calibration period for flow were 0.85, -9.03%, and 0.39 respectively, and in the validation periods they were 0.59, -51.25%, and 0.64, respectively. The values of NSE, PBIAS and RSR in the calibration period for NO_3^--N were 0.59, -4.97%, and 0.64, respectively, and in the validation periods they were 0.77, -0.00%, and 0.48, respectively. Therefore, the performances of both the calibration and validation for flow and NO_3^- can be rated as satisfactory and very good, respectively (Moriasi et al., 2007).

Table 3.1 Performance indices for the CTD and UCTD models

Model	Parameter	*NSE*	*PBIAS (%)*	*RSR*	Rating	Period	Scale
CTD	Flow						
	Calibration	0.54	7.32	0.68	very good	2006-2010	Monthly
	Validation	0.80	4.08	0.45	very good	2012-2013	Monthly
	NO_3^--N						
	Calibration	0.51	-25.78	0.70	good	2006-2010	Seasonal
	Validation	0.67	-10.96	0.57	very good	2012-2013	Seasonal
UCTD	Flow						
	Calibration	0.85	-9.03	0.39	very good	2006-2010	Monthly
	Validation	0.59	-51.25	0.64	satisfactory	2012-2013	Monthly
	NO_3^--N						
	Calibration	0.59	-4.97	0.64	very good	2006-2010	Seasonal
	Validation	0.77	0.00	0.48	very good	2012-2013	Seasonal

Overall, both the CTD model and the UCTD model can be considered as good, and they can be used to simulate monthly flow and seasonal total NO_3^--N for the CTD watershed and the UCTD watershed, respectively.

3.2.4 Results and discussion

3.2.4.1 Comparison between observations and simulations

The calibrated models, the CTD model and the UCTD model, were run to simulate the CTD and the UCTD sites of WEBs from 2006 to 2013, respectively. The simulation results are shown in Figure 3.12 and Table 3.2.

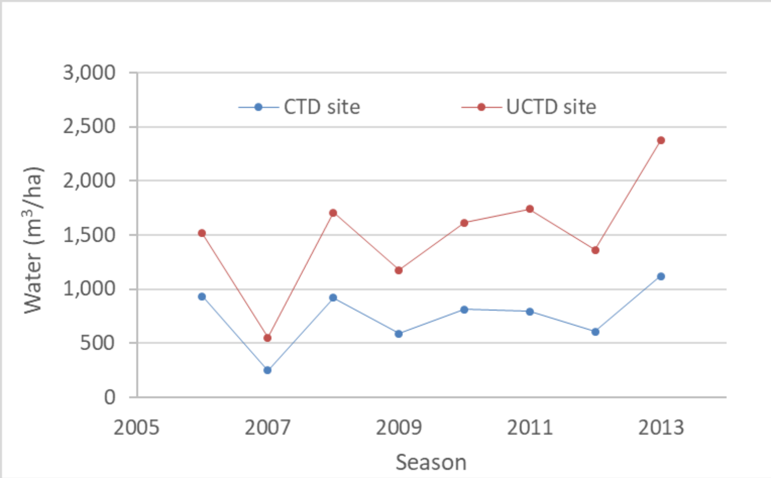

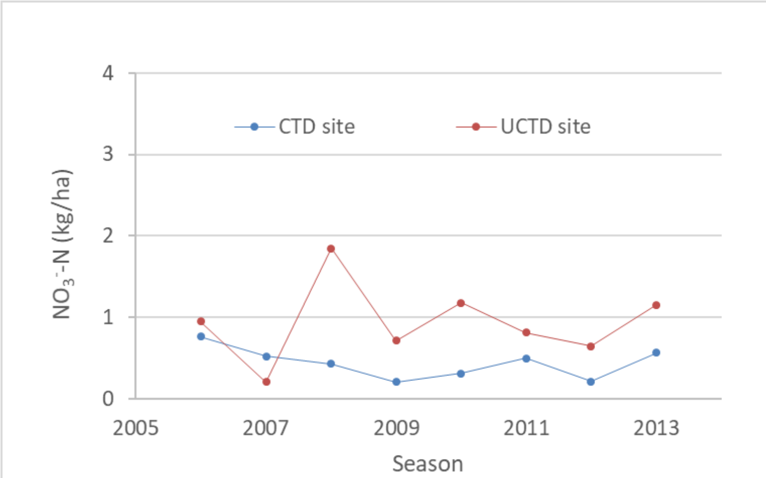

Figure 3.12 Simulated flow and NO_3^--N for the CTD and UCTD watersheds

Table 3.2 Mean seasonal mass fluxes and paired t test for the simulations

Parameter	Period	CTD (mean±SD)	UCTD (mean±SD)	CTD–UCTD (difference±SD)	n	P value	Change %
Water (m^3/ha)	2006-2013	$0.75 \pm 0.27 \times 10^3$	$1.51 \pm 0.51 \times 10^3$	$-0.76 \pm 0.24 \times 10^3$	8	0.391	-50
NO_3^--N (kg/ha)	2006-2013	0.44 ± 0.19	0.94 ± 0.48	-0.50 ± 0.29	8	0.276	-53

Sunohara et al. (2015) noted that the mean seasonal mass flux change rates for water and NO_3^--N were -20% and -25%, respectively, for the paired experimental watersheds during the treatment period (2007-2011). Generally, the change rates simulated by the CTD and UCTD models are in line with those observed change rates in Table 2.1. This indicates that the modified SWAT model was well calibrated and validated for the CTD and UCTD watersheds. Potentially, the modified SWAT model can simulate the CTD and UCTD scenarios for the watershed.

3.2.4.2 Comparisons between the CTD and UCTD scenarios by the CTD and UCTD models

To test the modified algorithm for calculating NO_3^--N in the model further, the calibrated CTD and UCTD models were run for the CTD and UCTD scenarios with the same parameter set, respectively.

3.2.4.2.1 By the CTD model at the CTD site

The simulation results of the CTD and UCTD scenarios by the calibrated CTD model are shown in Figure 3.13 and Tables 3.3 and 3.4.

Figure 3.13 Simulated flow and NO_3^--N for the CTD and UCTD scenarios using the CTD model

Table 3.3 Simulated water of the CTD and UCTD scenarios for the CTD site

May-Oct	CTD_{200} ($\times10^5$ m^3)	CTD_{600} ($\times10^5$ m^3)	UCTD ($\times10^5$ m^3)	(CTD_{200}-UCTD)/UCTD ×100	(CTD_{600}-UCTD)/UCTD ×100
2006	4.52	4.52	4.55	-0.57	-0.57
2007	1.22	1.21	1.24	-1.79	-1.85
2008	4.44	4.44	4.45	-0.18	-0.20
2009	2.86	2.86	2.86	-0.15	-0.16
2010	3.94	3.94	3.94	-0.15	-0.18
2012	2.94	2.94	2.95	-0.35	-0.40
2013	5.41	5.41	5.41	-0.06	-0.07
Total	25.32	25.32	25.40	-0.32	-0.33

Table 3.4 Simulated NO_3^--N of the CTD and UCTD scenarios for the CTD site

May-Oct	CTD_{200} (kg)	CTD_{600} (kg)	UCTD (kg)	(CTD_{200}-UCTD)/UCTD ×100	(CTD_{600}-UCTD)/UCTD ×100
2006	49.9	431.8	438.9	-88.6	-1.6
2007	247.4	259.9	289.2	-14.4	-10.1
2008	111.5	144.4	220.2	-49.4	-34.4
2009	20.5	36.7	42.9	-52.2	-14.5
2010	7.8	24.1	33.8	-77.1	-28.6
2012	10.7	63.9	72.2	-85.1	-11.6
2013	5.1	301.1	317.1	-98.4	-5.0
Total	453.0	1261.8	1414.3	-68.0	-10.8

With the same parameter set, the reduced rates of water were -0.32% and 0.33% for the CTD_{200} and CTD_{600} scenarios compared to the baseline UCTD scenario, respectively, in the simulation period for the growing seasons from 2006 to 2013. The reduced rates of NO_3^--N for the CTD_{200} and CTD_{600} scenarios were -68.0% and -10.8%, respectively.

3.2.4.2.2 By the UCTD model at UCTD site

The author compared the improved and original SWAT models under the UCTD condition at the UCTD site, and these two models gave the same results**.**

The CTD scenarios CTD_{200} and CTD_{600} were tested at the UCTD site of WEBs using the calibrated UCTD model with the same parameter set. The simulation results of , the CTD scenarios CTD_{200} and CTD_{600} at the UCTD site are shown in Figure 3.14 and Tables 3.5 and 3.6.

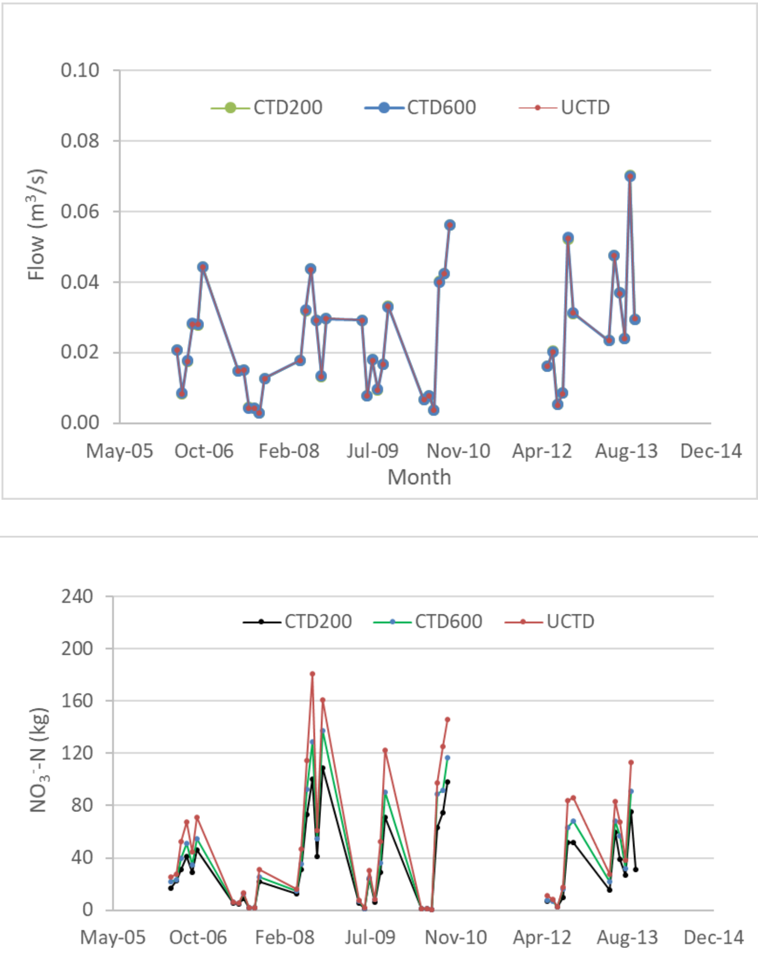

Figure 3.14 Simulated flow and NO_3^--N for the CTD and UCTD scenarios using the UCTD model

Table 3.5 Simulated water of CTD and UCTD scenarios for the UCTD site

May-Oct	CTD_{200} (×10^5 m^3)	CTD_{600} (×10^5 m^3)	UCTD (×10^5 m^3)	(CTD_{200}-UCTD)/UCTD ×100	(CTD_{600}-UCTD)/UCTD ×100
2006	3.90	3.91	3.90	-0.15	0.23
2007	1.43	1.43	1.43	0.02	-0.05
2008	4.39	4.40	4.39	-0.08	0.24
2009	3.03	3.03	3.03	-0.01	0.01
2010	4.15	4.15	4.15	0.14	-0.08
2012	3.51	3.52	3.51	-0.13	0.20
2013	6.10	6.09	6.09	0.20	0.05
Total	26.50	26.50	26.50	0.00	0.00

Table 3.6 Simulated NO_3^--N of CTD and UCTD scenarios for the UCTD site

May-Oct	CTD_{200} (kg)	CTD_{600} (kg)	UCTD (kg)	(CTD_{200}-UCTD)/UCTD ×100	(CTD_{600}-UCTD)/UCTD ×100
2006	186.0	225.0	288.8	-35.6	-22.1
2007	45.7	52.7	60.1	-24.0	-12.4
2008	366.9	463.6	580.3	-36.8	-20.1
2009	136.8	166.9	223.5	-38.8	-25.3
2010	237.5	299.0	370.5	-35.9	-19.3
2012	129.2	164.5	209.2	-38.2	-21.3
2013	215.9	306.1	374.7	-42.4	-18.3
Total	1317.9	1677.8	2107.2	-37.5	-20.4

Using the calibrated UCTD model at the UCTD site, the water for CTD_{200} and CTD_{600} scenarios were changed slightly over the simulation period, but total water remained similar. While the reductions of NO_3^--N for CTD_{200} and CTD_{600} were -37.5% and -20%, respectively.

The applications of the CTD and UCTD scenarios at the CTD and UCTD sites of WEBS demonstrate that the modification to the algorithm for calculating NO_3^--N works well for the CTD scenarios at the CTD and UCTD sites of WEBs.

3.2.4.3 Comparisons between the original and the improved SWAT models

To verify the improved algorithm for calculating NO_3^--N in tile flow, the modified SWAT model was compared to the original version using the CTD scenarios for the South Nation River watershed using the calibrated and validated model from 1981 to 2005. Ten outputs of the SWAT model, i.e., flow, sediment, Org-N, Org-P, NO_3^--N, NH_4^+-N, NO_2^--N, Min-P, TN, and TP were compared in the certification for two CTD scenario depths of 200 and 600 mm, and baseline scenario UCTD was 1100 mm. The comparisons are depicted in Table 3.7 and Figures 3.15 and 3.16 (detailed changes are given in Appendix 2).

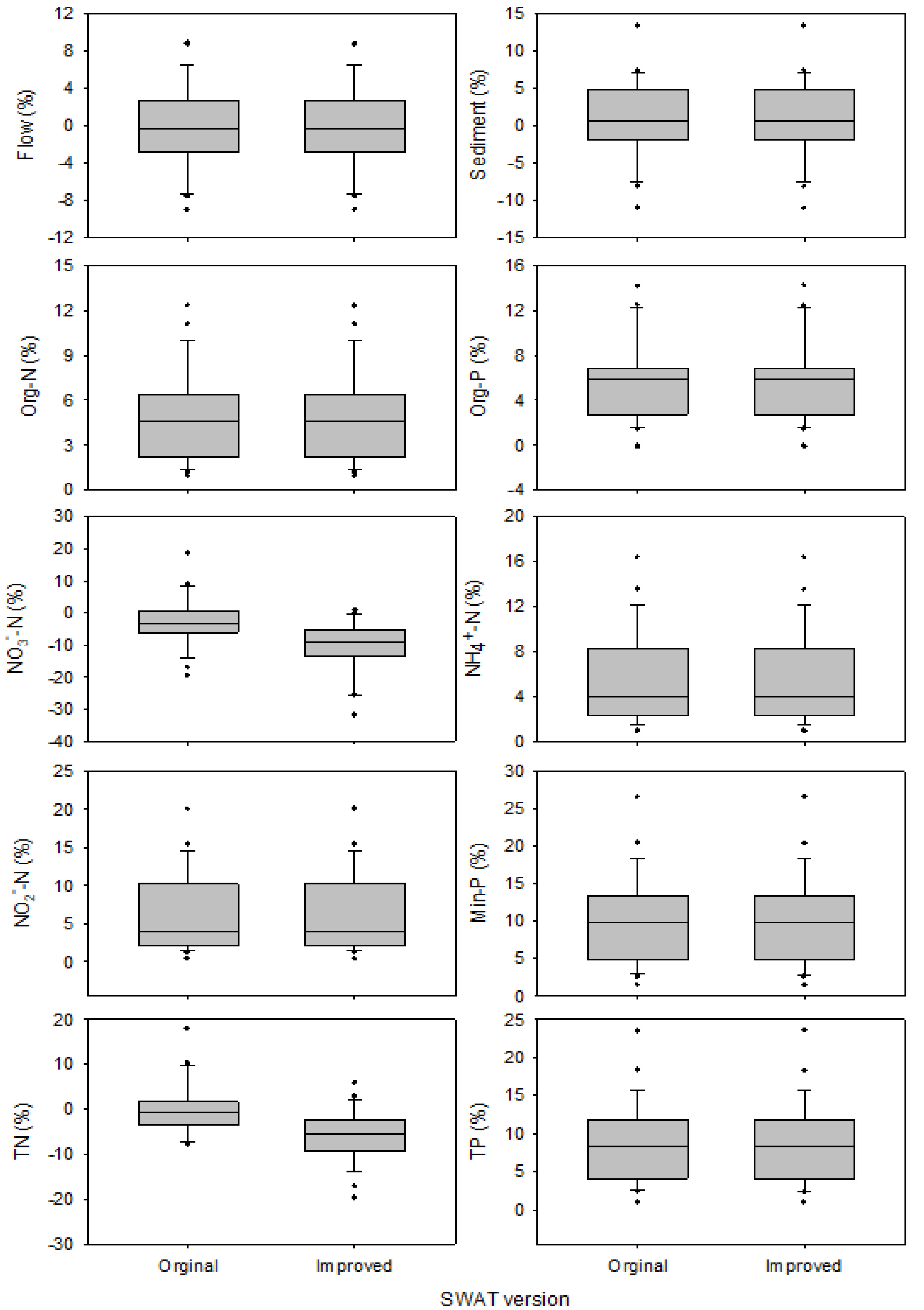

Figure 3.15 Comparisons of the original and improved SWAT model with CTD_{200}

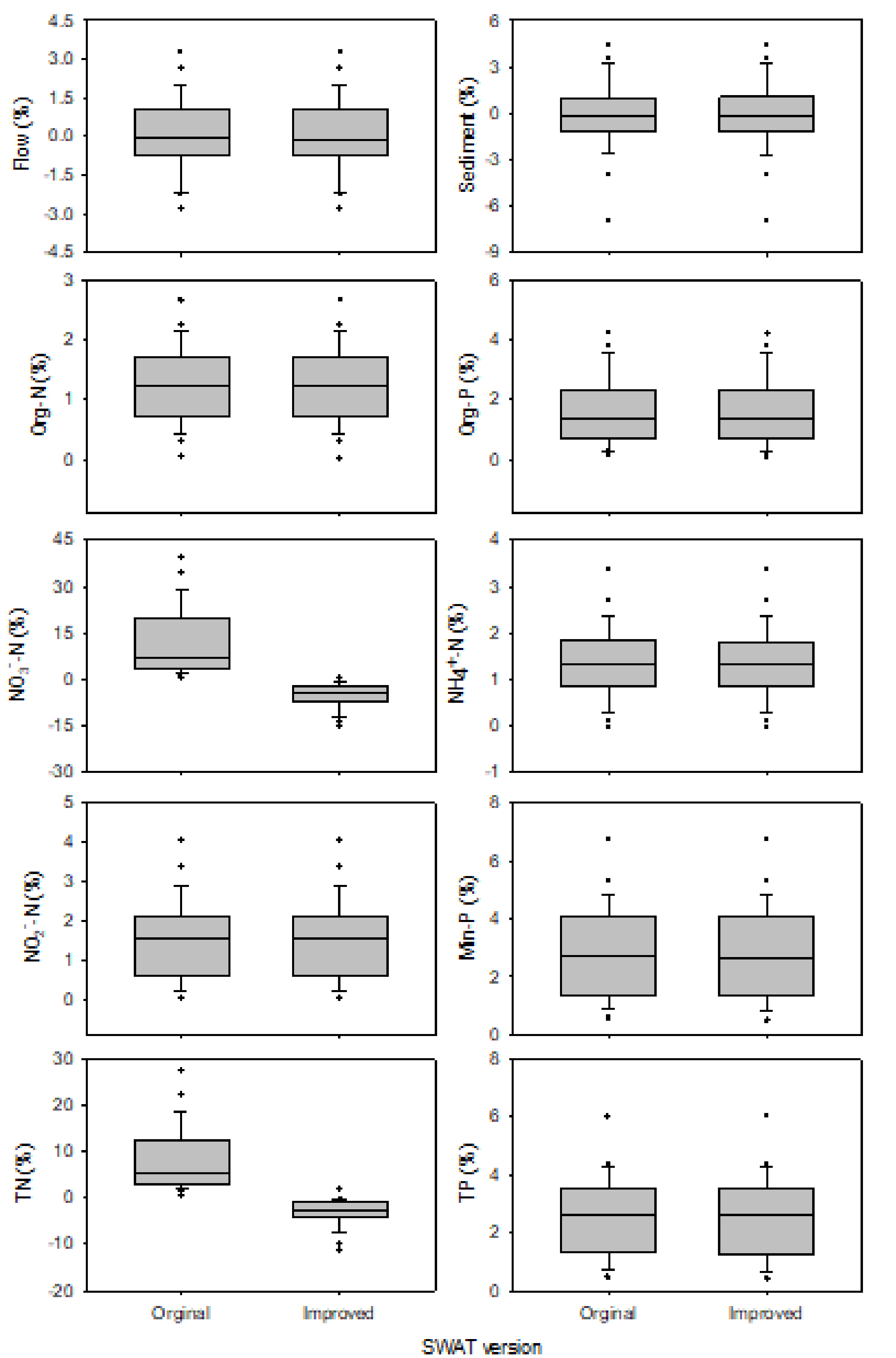

Figure 3.16 **Comparisons of the original and improved SWAT model with CTD$_{600}$**

Table 3.7 Average reductions over the comparison period from 1981 to 2005

Depth (mm)	SWAT version	Flow (%)	Sediment (%)	Org-N (%)	Org-P (%)	NO_3^--N (%)	NH_4^+-N (%)	NO_2^--N (%)	Min-P (%)	TN (%)	TP (%)
200	Original	-0.5	0.4	5.2	6.3	-1.9	6.2	7.0	11.2	0.4	9.8
	Improved	-0.5	0.4	5.2	6.3	-13.0	6.2	7.0	11.1	-7.6	9.8
600	Original	0.0	-0.1	1.3	1.8	9.7	1.4	1.6	3.1	7.4	2.7
	Improved	0.0	-0.1	1.3	1.7	-6.0	1.4	1.6	3.1	-3.9	2.7

The reductions of flow, sediment, Org-N, Org-P, NH_4^+-N, NO_2^--N, Min-P and TP at the depths of 200 and 600 mm were the same or very similar, while the reductions of NO_3^--N and TN in the two versions of the SWAT model were very different. Compared to the reductions in the original SWAT model, those in the modified SWAT model were –13.0% and –6.0% for NO_3^--N, –7.6% and –3.9% for TN at 200 and 600 mm, respectively. This indicates that the improved algorithm for calculating NO_3^--N in the modified SWAT model worked well, and the discussion in Section 4.4.2 further proves that the reductions in the modified SWAT model were in line with the previous simulation findings by Que et al. (2015) and the experimental field results (Sunohara et al., 2015).

4 MODELLING THE ENVIRONMENTAL EFFECTS OF CTD ON WATERSHED USING SWAT

4.1 Methodology and parameterization

4.1.1 Climate data

The SWAT model requires six types of climate data: precipitation, maximum temperature, minimum temperature, solar radiation, wind speed, and relative humidity. The first three types of data are available on Environment Canada's website (2014) (Figure 4.1).

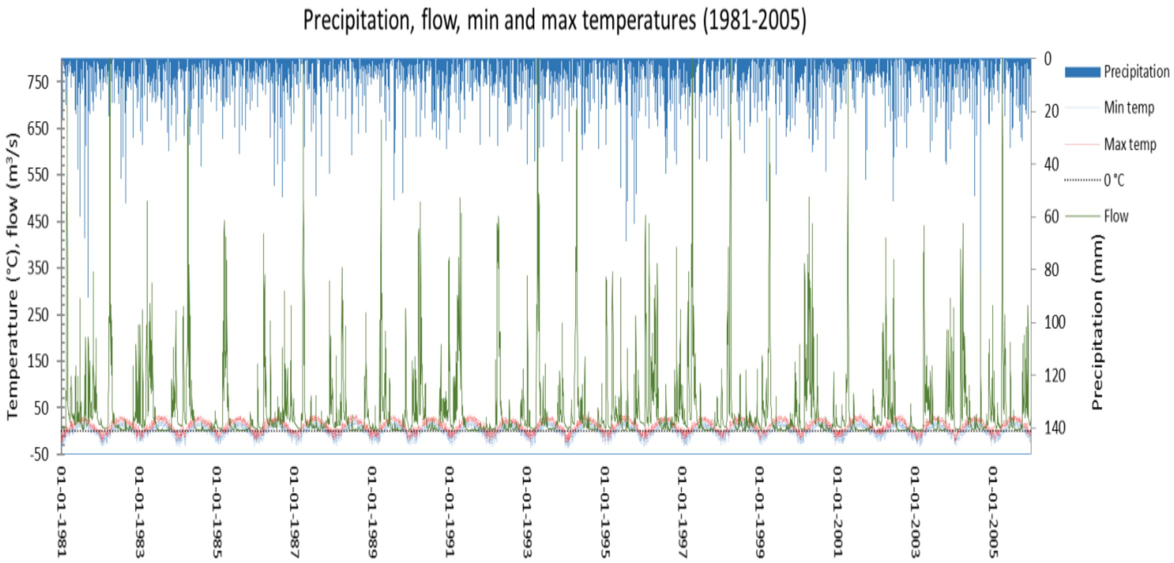

Figure 4.1 Flow, precipitation, min and max temperatures

To better present the watershed, 15 weather stations were considered initially. Finally, based on the availability of datasets and locations, eight weather stations within or near the watershed were selected for the model as shown in Figure 4.2. These stations were Angers, Brockville PCC, Montebello, Morrisburg, Ottawa Macdonald, Russell, South Mountain, and St. Albert.

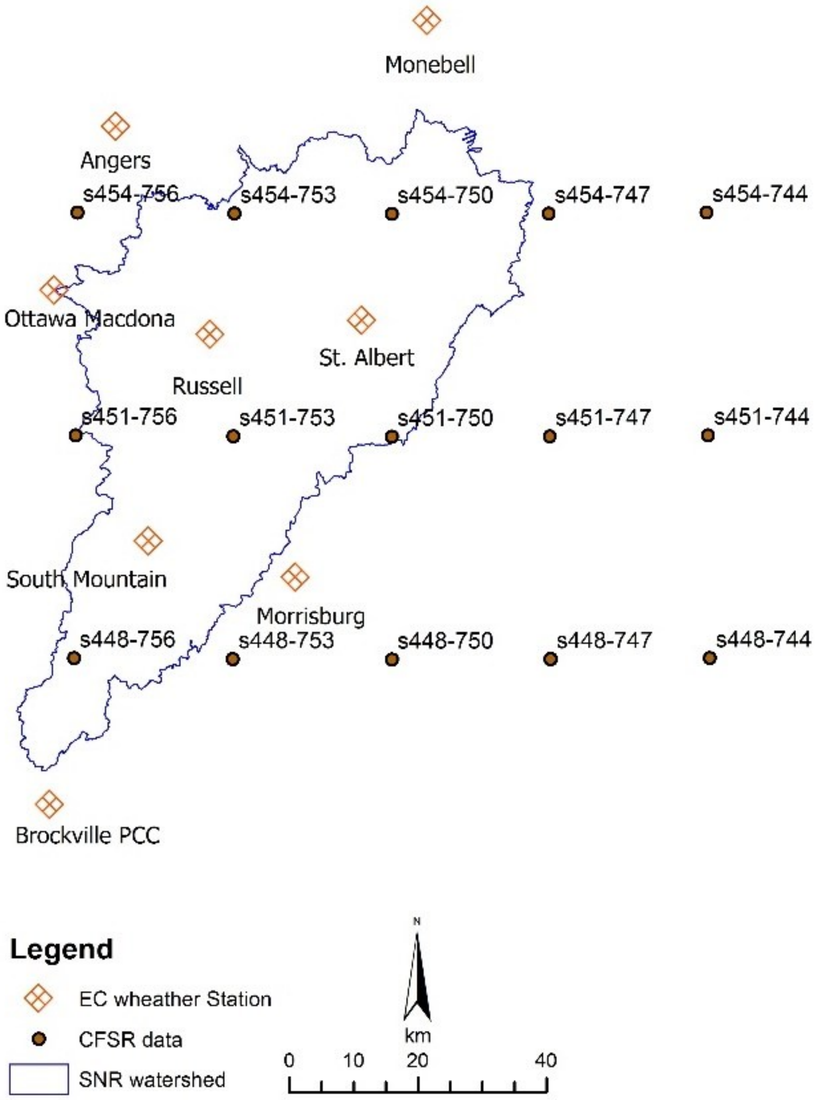

Figure 4.2 Locations of weather stations and CFSR data

Due to the scarcity of long-term continuous observations for solar radiation, wind speed and relative humidity, these three types of data came from the US National Centers for Environmental Prediction's Climate Forecast System Re-analysis (CFSR), and they were retrieved from the Spatial Sciences website of Texas A&M University (Globalweather, 2014) (Figure 4.2). The CFSR data is applicable in data-scarce areas (Dile and Srinivasan, 2014; Fuka et al., 2013). The period of the data is from 1979 to 2010.

4.1.2 Land use data

Land use data were obtained from the AAFC's Annual Crop Inventory (Agriculture and Agri-Food Canada, 2015a), and was generated from satellite imagery, using both optical and Synthetic Aperture Radar imagery (McNairn et al., 2009).

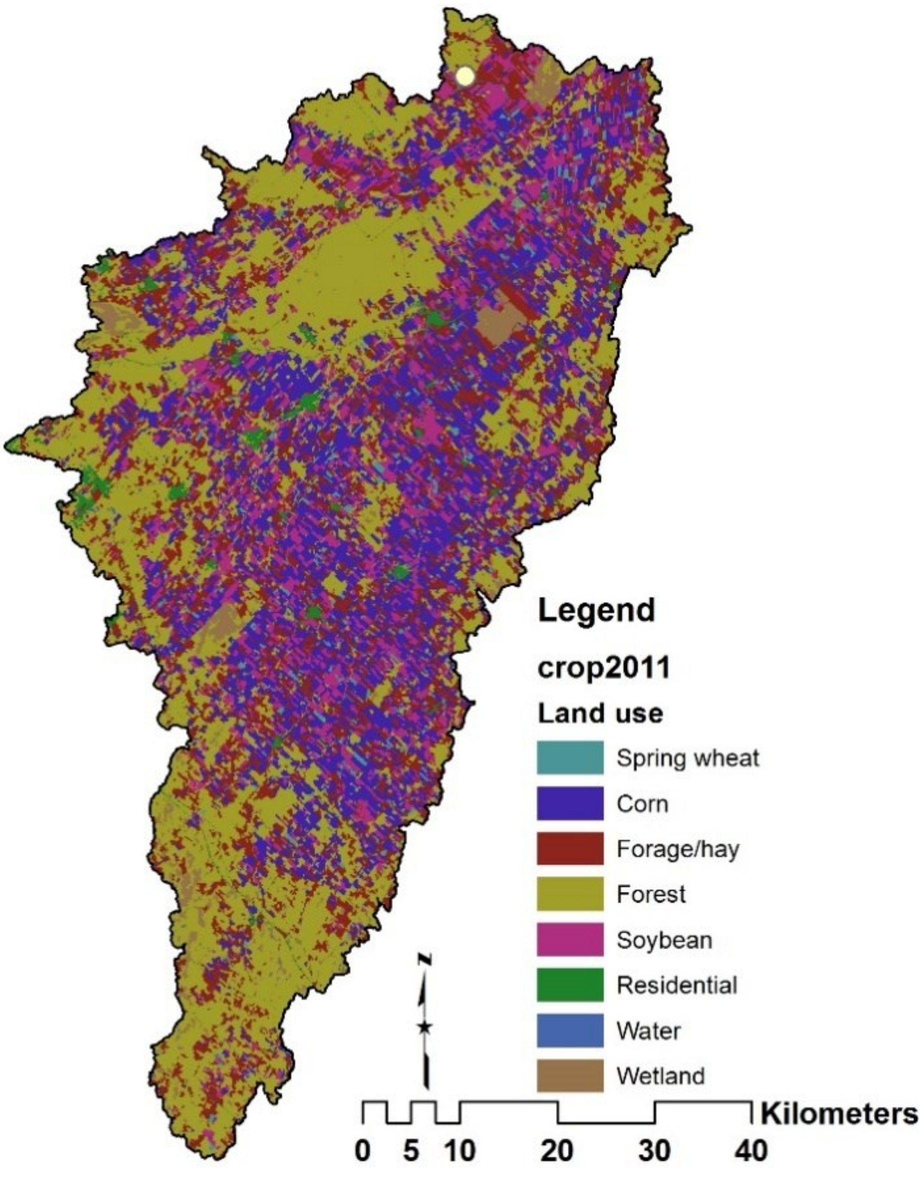

Figure 4.3 Distribution of land use over the watershed

The original data contained a variety of crop categories, and since it is unrealistic to model all of these types of crops in such a large watershed, therefore, these data were regrouped into eight land use classes: cereal (wheat), corn, forage/hay, forest, soybean, residential, water and wetland (Figure 4.3). Wheat, corn, and soybean are grown widely in this watershed. The percentages of all of these uses of the land in this watershed are presented in Figure 4.4.

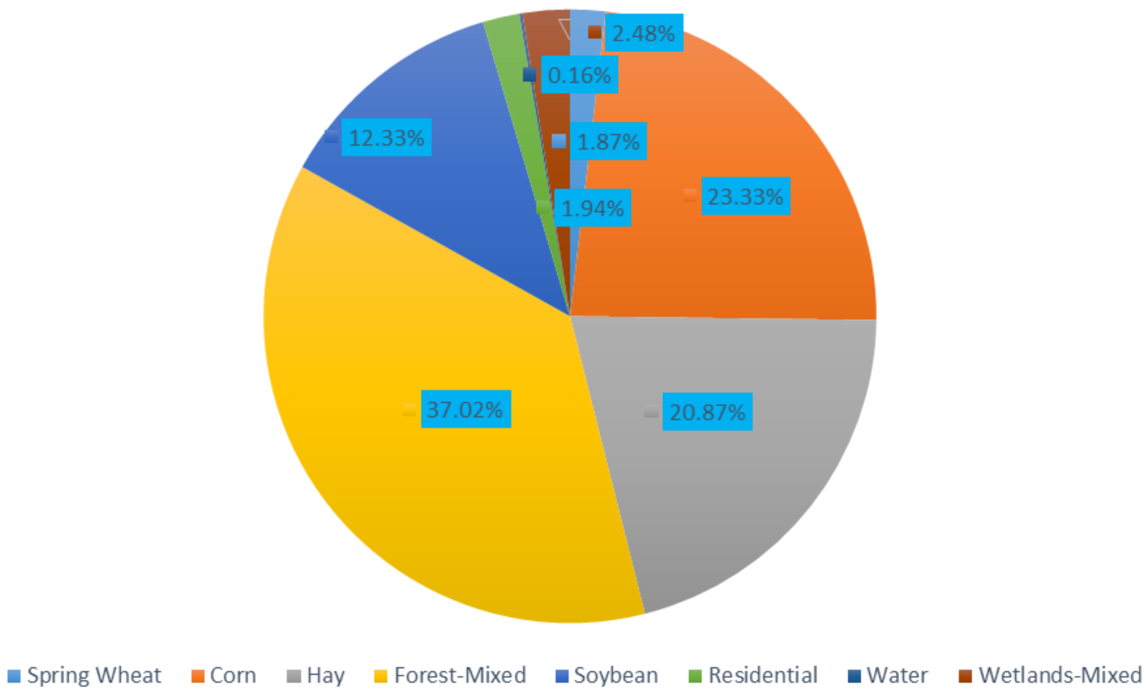

Figure 4.4 Ratios of land use in the model

4.1.3 Soil data

The soil data were extracted from Agriculture and Agri-Food Canada (2007). The watershed contains 81 types of soil with one to four layers (Wicklund and Richards, 1962).

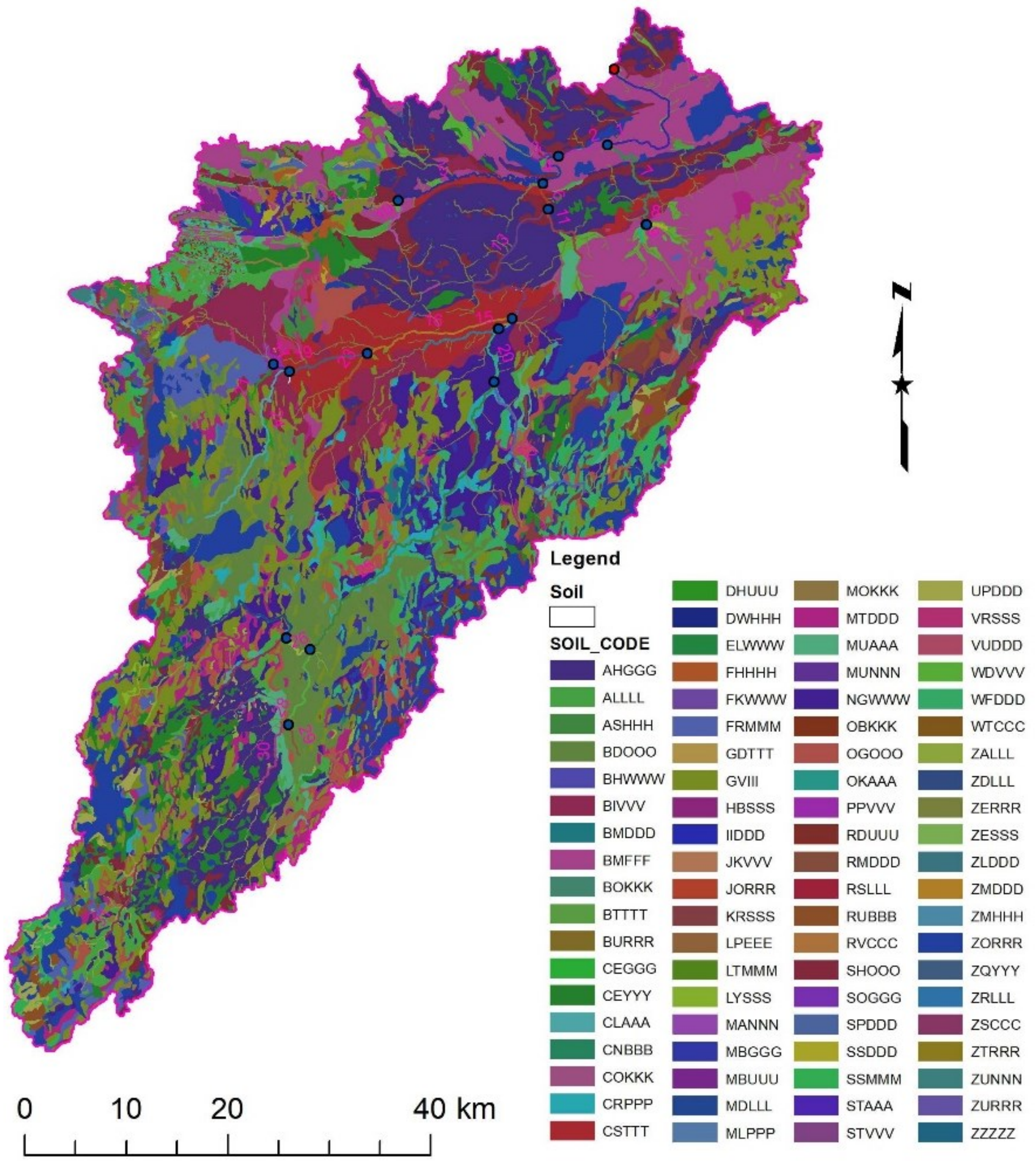

Figure 4.5 Soil distributions within the watershed

The soil definition for the model was processed in an HRU analysis. The soil distribution in the model is shown in Figure 4.5, and the area-wise percentages of soils are depicted in Figure 4.6.

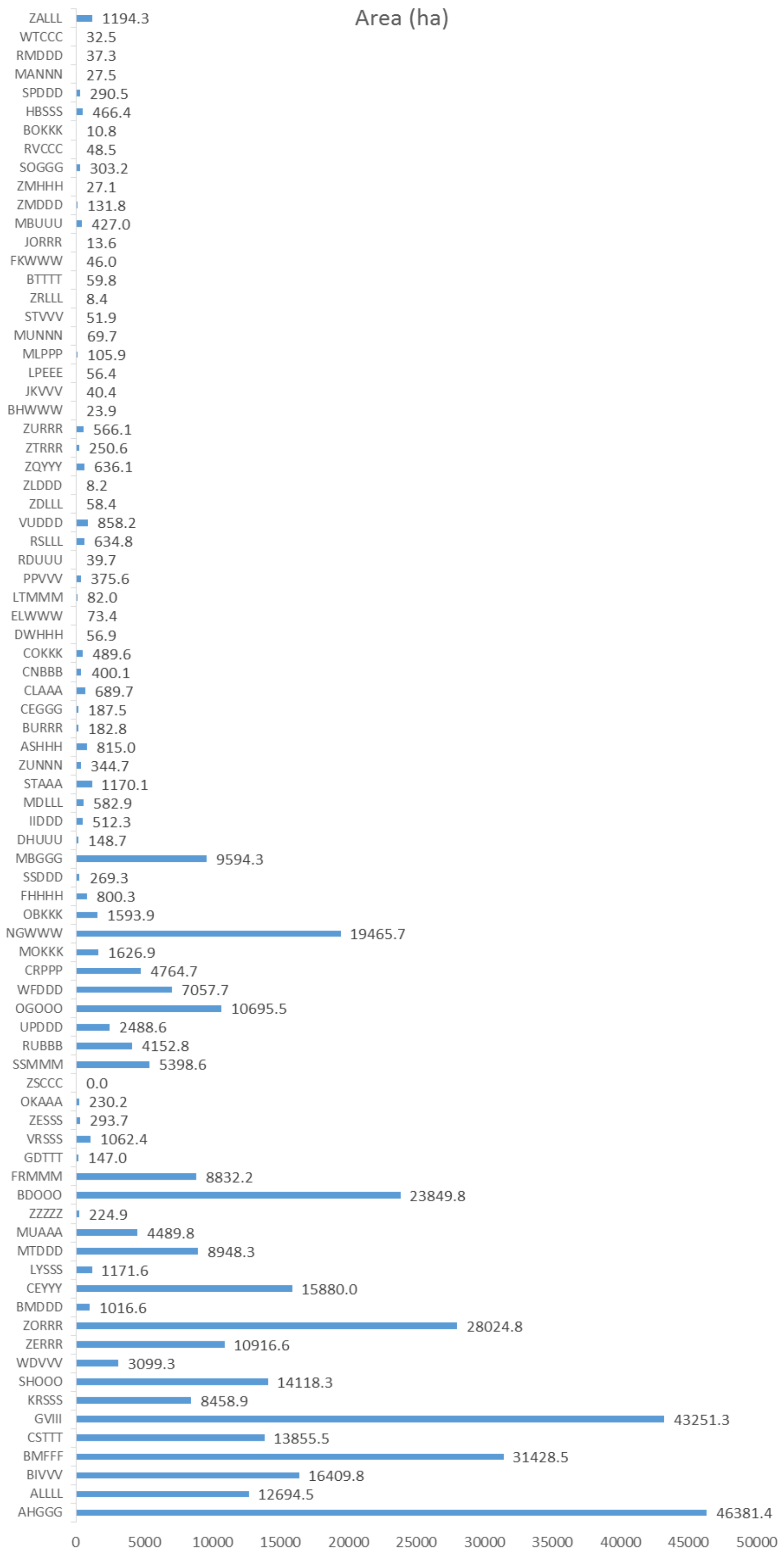

Figure 4.6 Soil ratios in the model

4.1.4 Topographical data

A 10×10 m DEM (Figure 4.7) was used to generate the spatial data, for sub-watersheds, reaches, slopes, HRUs, etc. (CH2M HILL, 2001).

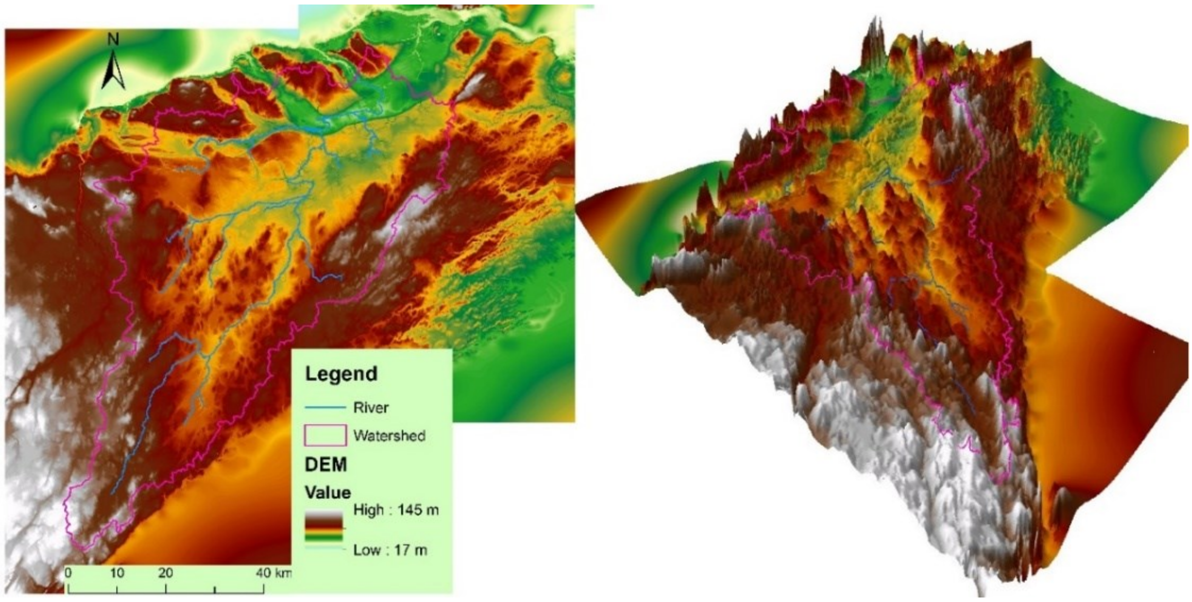

Figure 4.7 DEM map

After the delineation process, the watershed was subdivided into 31 sub-watersheds (Figure 4.8), and then these sub-watersheds were overlaid with land use and soil maps to generate HRUs for the model.

The river channel network was segmented into 31 reaches (Figure 4.8). Two slopes were classified, i.e., as less than and equal to 1% and hence suitable for CTD, and larger than 1%. In total, 6,040 HRUs for the model were obtained by overlaying the land use, soil, and slope classes.

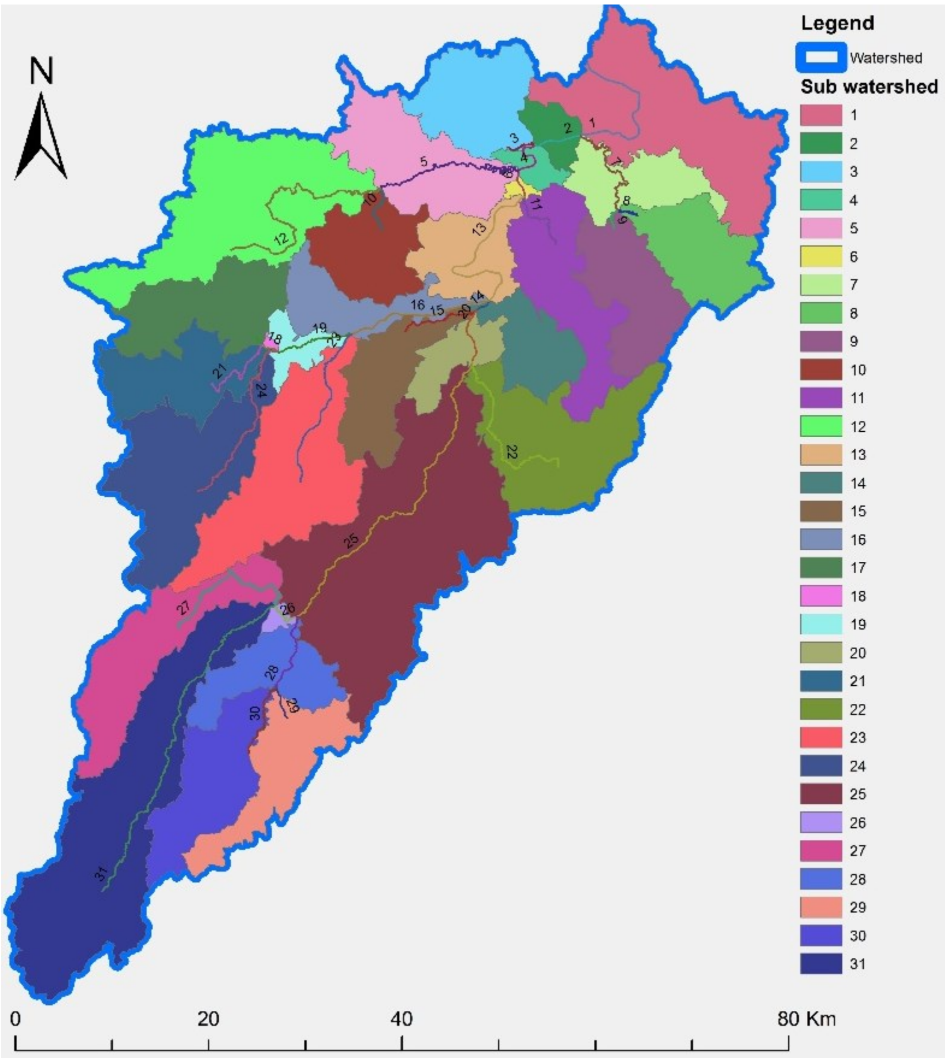

Figure 4.8 Sub watersheds in the model

4.1.5 Hydrometric and water quality data

Historical measurements of stream flow and sediment at the Plantagenet gauging station were obtained from the Water Survey Office of Environment Canada (2015), while water quality data, NO_3^--N, TN, and TP were retrieved from the Provincial Water Quality Monitoring Network (Ontario Ministry of the Environment, 2015). These data are required in order to calibrate and validate the model.

4.1.6 Crop rotation, fertilizer, and field management schedule

Based on a field survey by Pommainville (2007), there are three main crops growing in the watershed: corn, soybeans, and spring wheat.

In the model, there are two types of crop rotations, non-hay and with-hay. The rotation of the non-hay was done on a three-year cycle as corn-soybean-spring wheat, while the rotation of with-hay was set at a six-year cycle, corn-soybean-spring wheat-hay-hay-hay. The field operations during crop rotation and the fertilizer application rates are shown in Table 4.1.

Table 4.1 Crop rotations and field managements

Crop	Year	Month	Day	Operation	N (kg/ha)	P (kg/ha)
Corn	1	5	10	fertilizer application	60	40
	1	5	10	plant/began, growing season		
	1	6	20	pesticide application		
	1	6	25	fertilizer application	90	40
	1	10	15	harvest and kill operation		
	1	10	20	tillage operation		
Soybean	2	5	10	plant/began, growing season		
	2	6	10	fertilizer application		60
	2	6	25	pesticide application		
	2	9	15	harvest and kill operation		
	2	9	20	tillage operation		
Spring wheat	3	4	15	plant/began, growing season		
	3	5	20	pesticide application		
	3	6	15	fertilizer application	70	90
	3	8	25	harvest and kill operation		
	3	8	30	tillage operation		
	3	8	2	fertilizer application	500 (manure)	
Hay	4	4	25	plant/began, growing season		
	4	6	10	fertilizer application	80	70
	4	9	25	harvest and kill operation		
	4	10	5	tillage operation		
Hay	5	4	25	plant/began, growing season		
	5	6	10	fertilizer application	80	70
	5	9	25	harvest and kill operation		
	5	10	5	tillage operation		
Hay	6	4	25	plant/began, growing season		
	6	6	10	fertilizer application	80	70
	6	9	25	harvest and kill operation		
	6	10	5	tillage operation		

4.1.7 CTD and UCTD scenarios

Considering the advantages and potentialities of the H–K method, this study used this method to simulate the CTD and UCTD scenarios. Since the SWAT model was incorporated, the first simulation module for the tile drainage that occurred during the late 1990s, and the H–K method that occurred during the 2000s, have been broadly tested and reported by both the model's developer and the modeller (Arnold et al., 1999; Boles et al., 2015; Du et al., 2005; Koch et al., 2012; Moriasi et al., 2007; Moriasi et al., 2012; Rahman et al., 2011).

As shown in Figure 2.11b, DDRAIN is defined as the depth from the soil surface to the drains (mm). The effective radius of the drain and the distance between two drain tubes in the model were assigned to 40 and 15,000 mm respectively, and the default depth of tile drainage was set at a depth of 1,200 mm. To simulate CTD and UCTD, the calibrated model was run at three depths, 200 (CTD_{200}), 600 (CTD_{600}), and 1100 (UCTD) mm. Two of these depths, CTD_{200} and CTD_{600}, were taken as the CTD scenarios, and the third one, was the UCTD scenario used for the baseline scenario. A specific program running in MATLAB was developed to assist in automatic modifications of the tile drainage depth in the management files of the model (Appendix 1).

4.1.8 Potential areas of the watershed suitable for CTD

Based on the land use map, 58.4% of the watershed is cropland. The watershed is relatively flat, and tile drainage is a common practice. The Agricultural Drainage Management Systems Task Force (2012) has recommended that CTD can be applied when the slope is less than roughly 1%. In this study, all the cropland was assumed to be tile-drained, and that the practice of CTD could be employed if the slope of land surface was ≤1%.

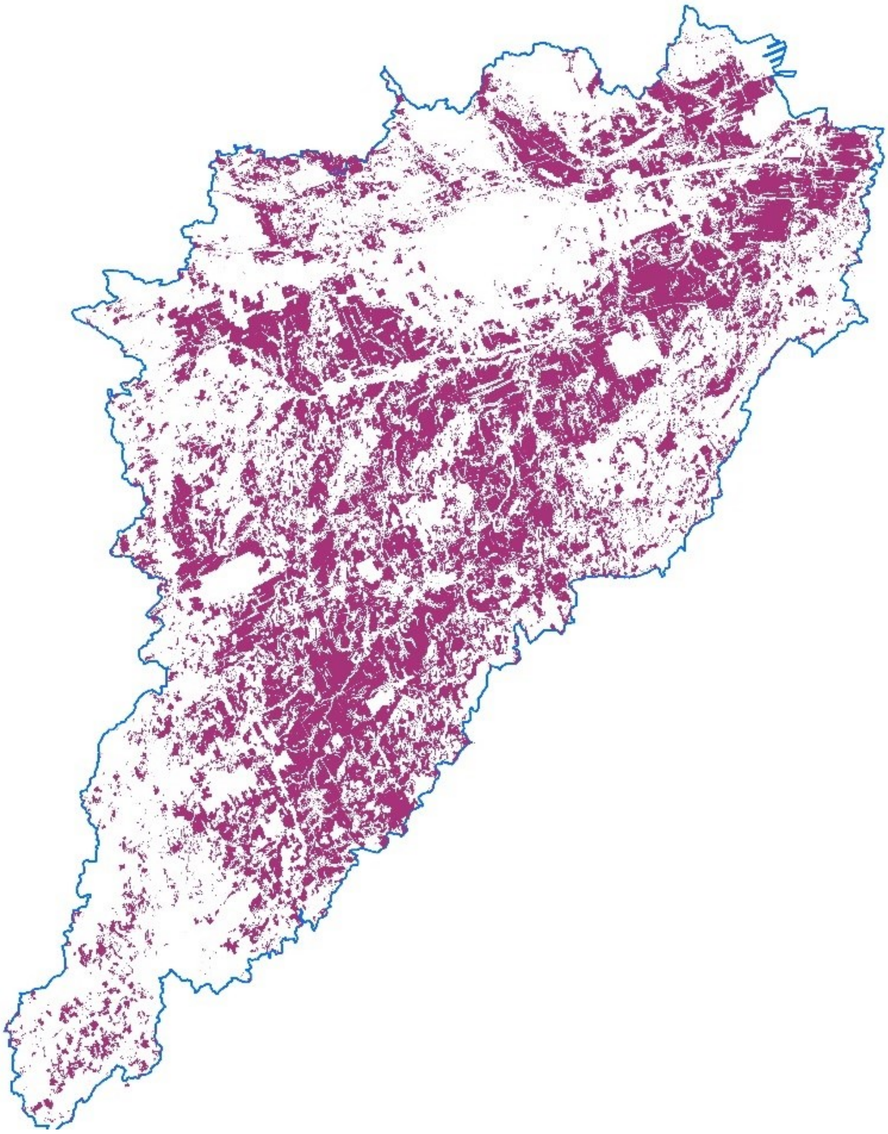

Figure 4.9 Distribution of slope less than 1% of cropland

It was found that 61% of the cropland area was suitable for CTD, as shown in Figure 4.9. Hence, 35.6% of the watershed had CTD implemented the model for the CTD scenarios.

4.2 Sensitivity analysis

The sensitivity analysis is to identify the parameters that have more influence on the model so that the model can be calibrated better. There are two indices in the SWAT-CUP model, the p-value and the t-test that are used to measure the global sensitivities of parameters (Abbaspour, 2014). These are determined by regressing the Latin Hypercube generated parameters against the objective function values (McKay et al., 1979). The smaller a p-value is, the more sensitive that parameter is. Conversely, larger t-test values in absolute values means more sensitivity for those parameters.

4.2.1 Sensitivities of parameters for flow

In 25 of the parameters involved in the flow calibration, the most sensitive parameters were CN2, followed by the snow melt base temperature (SMTMP), and the snowfall temperature (SFTMP). An overview of the results of the sensitivity analysis for these parameters is given in Figure 4.10 and Table 4.2.

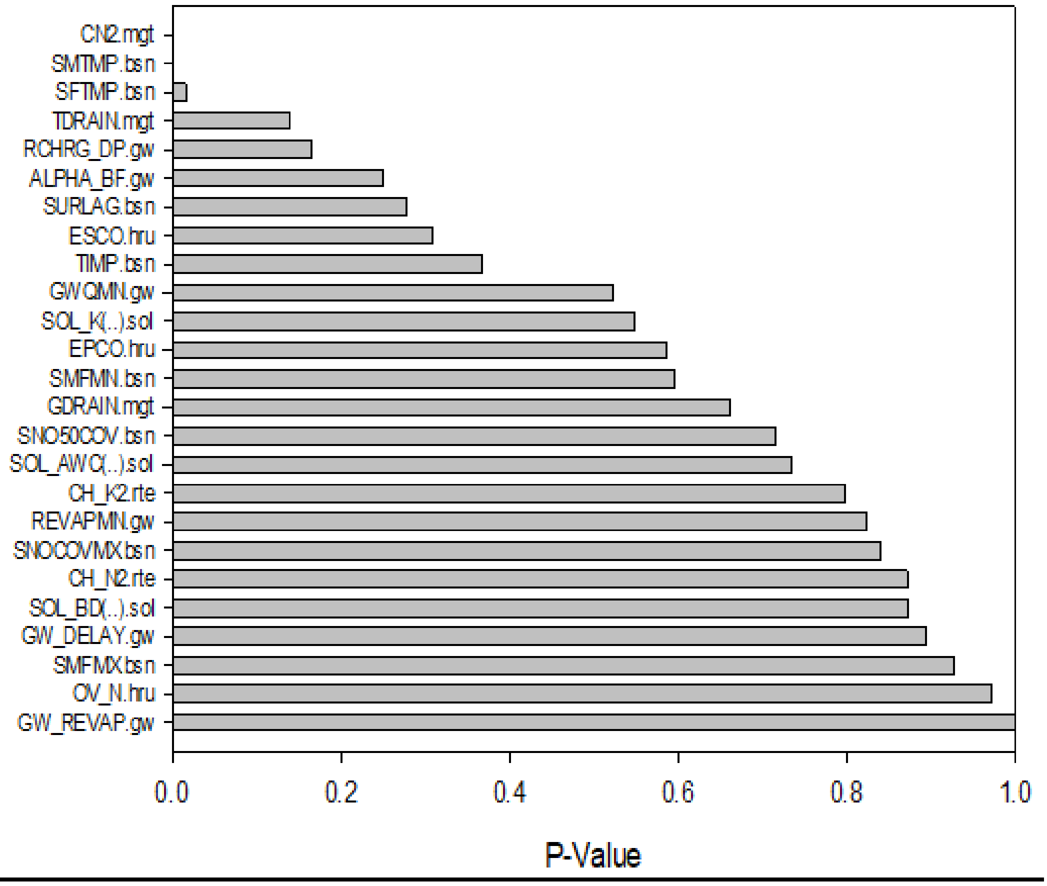

Figure 4.10 P-values of parameters for flow calibration

CN2, the SCS curve number, was found to be the most sensitive for the watershed, which represents moisture condition II, determining a large proportion of surface to subsurface flow. This result is in accordance with Que et al. (2015). As the second- and third-most sensitive parameters, SMTMP and SFTMP govern the snow melt calculation for this watershed. Specifically, this analysis shows that TDRAIN, the time to drain soil to field capacity, which influences the tile flow, is the fourth most sensitive.

Table 4.2 P-value and t-test of parameters for flow calibration

No.	Parameter	t-Stat	P-Value	No.	Parameter	t-Stat	P-Value
1	CN2.mgt	-10.968	0.000	14	GDRAIN.mgt	-0.442	0.662
2	SMTMP.bsn	-3.974	0.001	15	SNO50COV.bsn	-0.367	0.717
3	SFTMP.bsn	-2.590	0.016	16	SOL_AWC(..).sol	-0.343	0.735
4	TDRAIN.mgt	1.528	0.140	17	CH_K2.rte	-0.260	0.797
5	RCHRG_DP.gw	-1.428	0.166	18	REVAPMN.gw	0.224	0.825
6	ALPHA_BF.gw	1.177	0.251	19	SNOCOVMX.bsn	0.203	0.841
7	SURLAG.bsn	-1.109	0.278	20	CH_N2.rte	0.163	0.872
8	ESCO.hru	-1.038	0.310	21	SOL_BD(..).sol	-0.160	0.874
9	TIMP.bsn	0.918	0.368	22	GW_DELAY.gw	-0.134	0.895
10	GWQMN.gw	-0.650	0.522	23	SMFMX.bsn	-0.092	0.927
11	SOL_K(..).sol	-0.608	0.549	24	OV_N.hru	-0.035	0.972
12	EPCO.hru	0.550	0.587	25	GW_REVAP.gw	-0.001	0.999
13	SMFMN.bsn	0.536	0.597				

4.2.2 Sensitivities of parameters for sediment

Twenty-five parameters, presented in Figure 4.11, were selected for the sensitivity analysis for sediment simulation. The results of the sensitivity analysis are given in Table 4.3. Among these 25 parameters, the USLE equation for the soil erodibility K factor (USLE_K().sol), and the USLE equation for the support practice factor P (USLE_P.mgt), are the most sensitive parameters in the model for sediment. Not surprisingly, they play an important role on sediment output as the coefficients for Equation 2.6. The median particle size diameter of the channel bank sediment (CH_BNK_D50.rte), the peak rate adjustment factor for sediment routing in the main channel (PRF_BSN.bsn) and the peak rate adjustment factor for sediment routing in the sub basin (ADJ_PKR.bsn) also have a substantial influence on sediment in the model.

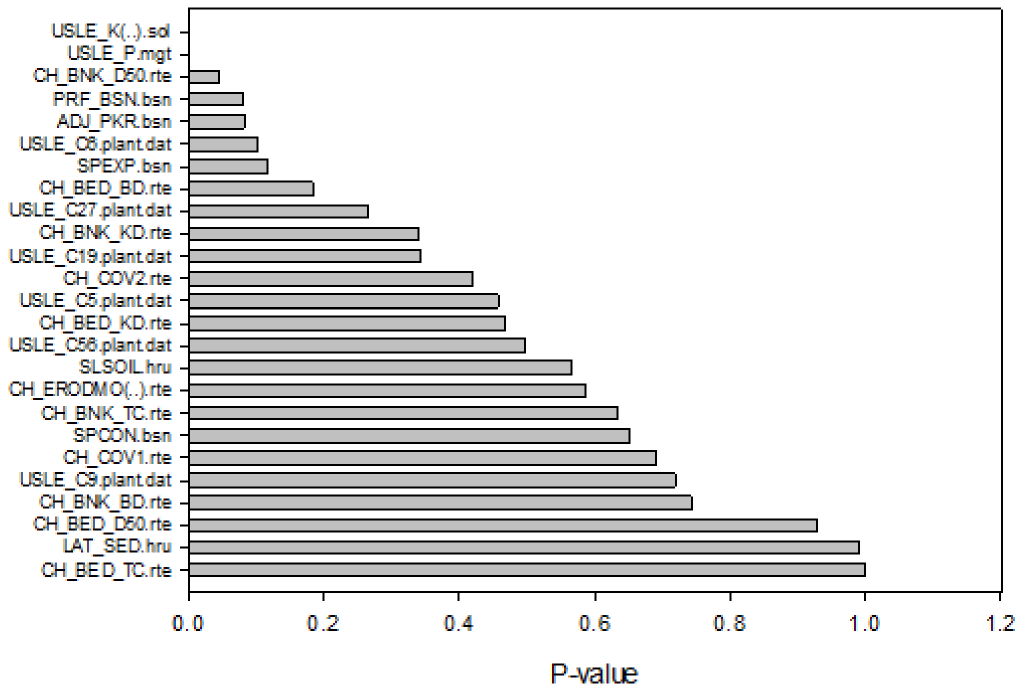

Figure 4.11 P-values of parameters for sediment calibration

Table 4.3 P-value and t-test of parameters for sediment calibration

No.	Parameter	t-Stat	P-Value	No.	Parameter	t-Stat	P-Value
1	USLE_K(..).sol	-7.844	0.000	14	CH_BED_KD.rte	0.740	0.467
2	USLE_P.mgt	-7.643	0.000	15	USLE_C{56}.plant.dat	0.689	0.498
3	CH_BNK_D50.rte	-2.106	0.046	16	SLSOIL.hru	-0.583	0.565
4	PRF_BSN.bsn	-1.829	0.080	17	CH_ERODMO(..).rte	0.553	0.585
5	ADJ_PKR.bsn	-1.814	0.082	18	CH_BNK_TC.rte	-0.482	0.634
6	USLE_C{6}.plant.dat	1.704	0.101	19	SPCON.bsn	-0.456	0.653
7	SPEXP.bsn	-1.628	0.117	20	CH_COV1.rte	0.403	0.690
8	CH_BED_BD.rte	1.371	0.183	21	USLE_C{9}.plant.dat	0.365	0.718
9	USLE_C{27}.plant.dat	1.144	0.264	22	CH_BNK_BD.rte	0.332	0.743
10	CH_BNK_KD.rte	0.976	0.339	23	CH_BED_D50.rte	0.093	0.926
11	USLE_C{19}.plant.dat	0.969	0.342	24	LAT_SED.hru	-0.011	0.992
12	CH_COV2.rte	0.821	0.420	25	CH_BED_TC.rte	0.000	1.000
13	USLE_C{5}.plant.dat	-0.756	0.457				

4.2.3 Sensitivities of parameters for N and P

For the sensitivity analysis of the parameters for N and P, 46 related parameters (presented in Figure 4.12) were analyzed, and the results of the sensitivity analysis are listed in Table 4.4.

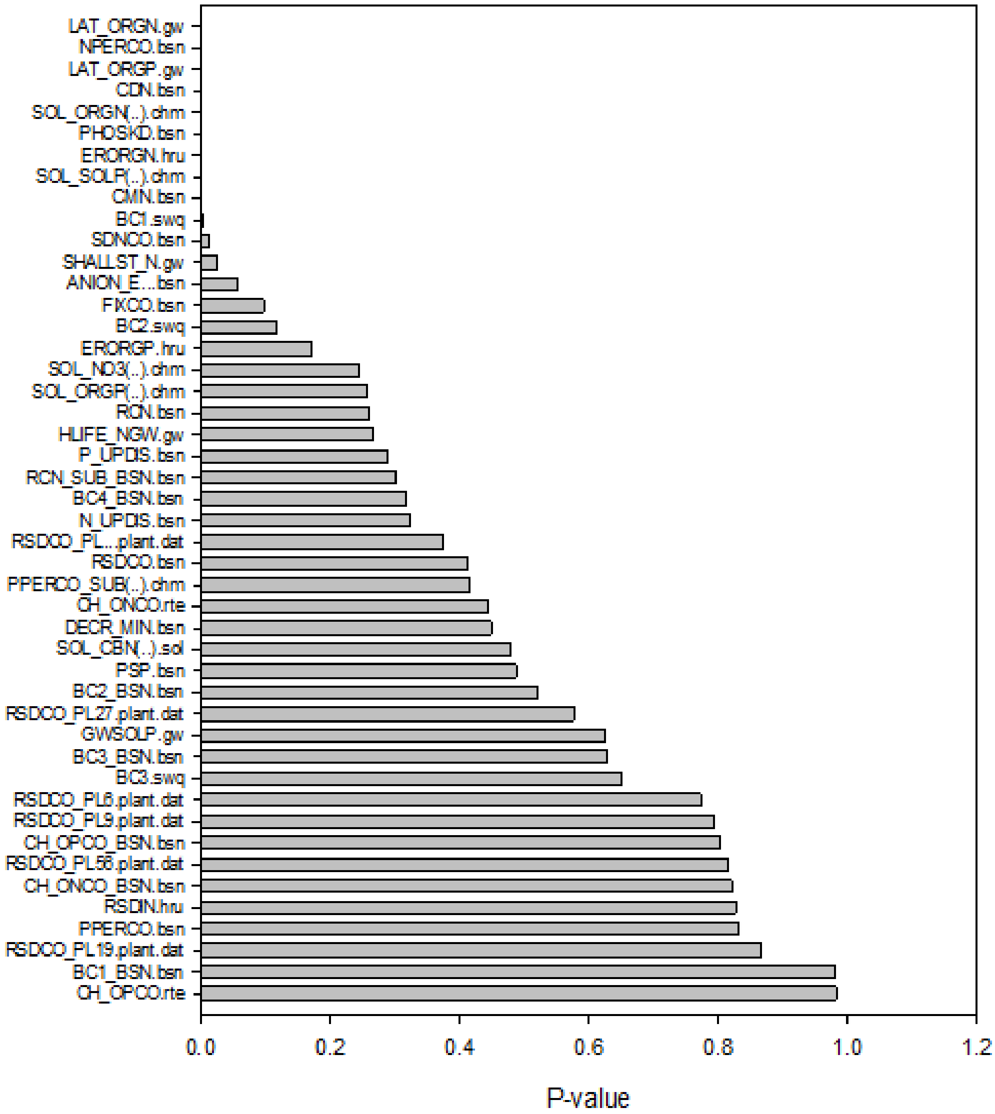

Figure 4.12 P-values of parameters for N and P calibration

Nine parameters, which are the initial organic N concentration in the soil layer (SOL_ORGN().chm), the denitrification exponential rate coefficient (CDN.bsn), the organic P in the baseflow (LAT_ORGP), the organic N in the baseflow (LAT_ORGN), the nitrogen percolation coefficient (NPERCO.bsn), the phosphorus soil partitioning coefficient (PHOSKD.bsn), the organic N enrichment ratio (ERORGN.hru), the initial P concentration in the soil layer (SOL_SOLP().chm) and the rate factor for humus mineralization of active organic nitrogen (CMN.bsn), are the most sensitive for N and P.

Table 4.4 P-value and t-test of parameters for N and P calibration

No.	Parameter	t-Stat	P-Value	No.	Parameter	t-Stat	P-Value
1	SOL_ORGN(..).chm	-13.340	0.000	24	N_UPDIS.bsn	0.995	0.324
2	CDN.bsn	24.183	0.000	25	RSDCO_PL{..}.plant.dat	0.897	0.374
3	LAT_ORGP.gw	-30.412	0.000	26	RSDCO.bsn	0.825	0.413
4	NPERCO.bsn	-38.489	0.000	27	PPERCO_SUB(..).chm	-0.821	0.416
5	LAT_ORGN.gw	-258.961	0.000	28	CH_ONCO.rte	-0.773	0.443
6	PHOSKD.bsn	6.545	0.000	29	DECR_MIN.bsn	-0.762	0.450
7	ERORGN.hru	-4.559	0.000	30	SOL_CBN(..).sol	0.712	0.480
8	SOL_SOLP(..).chm	-4.338	0.000	31	PSP.bsn	0.699	0.487
9	CMN.bsn	-4.179	0.000	32	BC2_BSN.bsn	-0.646	0.521
10	BC1.swq	3.136	0.003	33	RSDCO_PL{27}.plant.dat	-0.562	0.577
11	SDNCO.bsn	-2.583	0.013	34	GWSOLP.gw	0.494	0.623
12	SHALLST_N.gw	2.297	0.026	35	BC3_BSN.bsn	0.486	0.629
13	ANION_E...bsn	1.938	0.058	36	BC3.swq	0.458	0.649
14	FIXCO.bsn	1.686	0.098	37	RSDCO_PL{6}.plant.dat	-0.291	0.772
15	BC2.swq	1.594	0.117	38	RSDCO_PL{9}.plant.dat	-0.264	0.793
16	ERORGP.hru	-1.387	0.171	39	CH_OPCO_BSN.bsn	0.253	0.801
17	SOL_NO3(..).chm	-1.178	0.244	40	RSDCO_PL{56}.plant.dat	-0.234	0.816
18	SOL_ORGP(..).chm	1.148	0.256	41	CH_ONCO_BSN.bsn	0.229	0.820
19	RCN.bsn	-1.140	0.259	42	RSDIN.hru	0.221	0.826
20	HLIFE_NGW.gw	1.123	0.267	43	PPERCO.bsn	0.215	0.830
21	P_UPDIS.bsn	1.071	0.289	44	RSDCO_PL{19}.plant.dat	0.168	0.867
22	RCN_SUB_BSN.bsn	1.043	0.302	45	BC1_BSN.bsn	-0.024	0.981
23	BC4_BSN.bsn	1.011	0.317	46	CH_OPCO.rte	0.023	0.982

4.3 Calibration and validation of the SWAT model

4.3.1 Flow

The model was calibrated and validated for the flow on monthly scale for the periods, 1981-1995 and 1996-2005, respectively. The results of the calibration and validation for flow are depicted in Figure 4.13 and Figure 4.14, respectively.

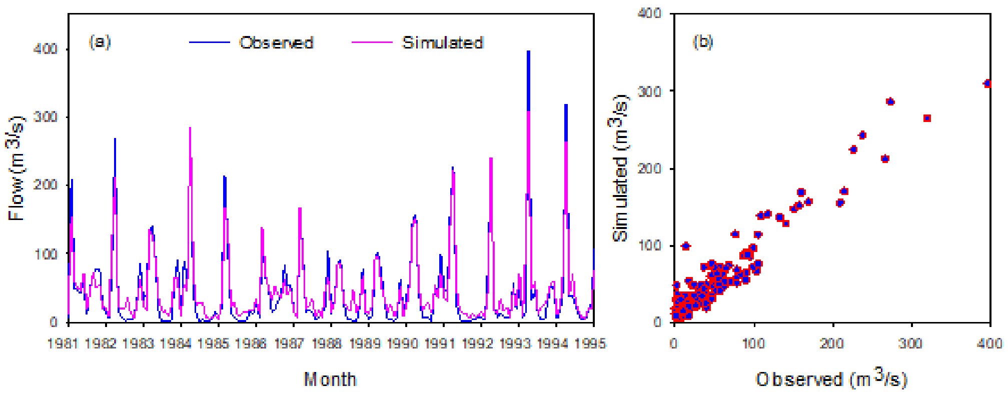

Figure 4.13 Observed and simulated monthly flow for calibration (1981–1995)

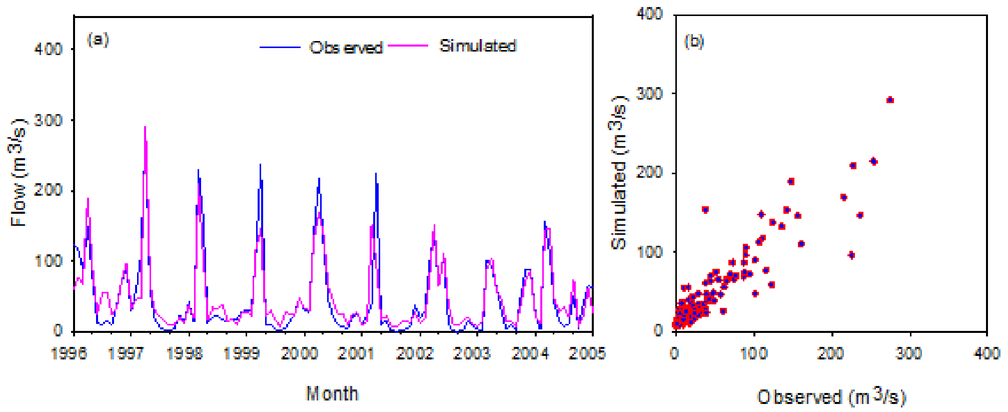

Figure 4.14 Observed and simulated monthly flow for validation (1996–2005)

Visually, these figures indicate that the simulated flow matches the observed flow very well during the calibration and validation periods. This is corroborated by the performance indices in Table 4.5. The values for NSE, PBIAS, and RSR in the calibration period for flow were 0.90%, −10.1%, and 0.31% respectively, and in the validation periods they were

0.81%, −8.3%, and 0.43%, respectively. Therefore, the performances of the calibration and validation for flow can be rated as very good (Moriasi et al., 2007).

4.3.2 Sediment

Compared to the flow data, observations for sediment are scarce and scattered. The calibration and validation periods for the sediment calibration were set to the periods, 1981-1987 and 1993-1994, respectively, and the results are shown in Figures 4.15 and 4.16.

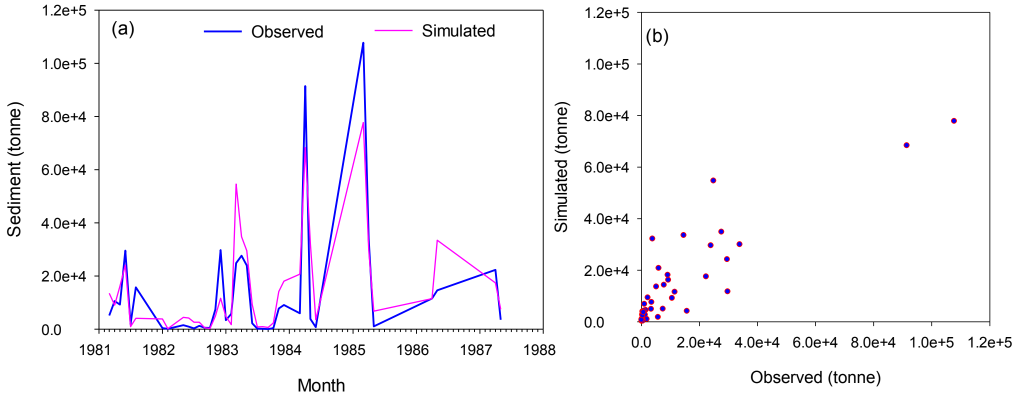

Figure 4.15 Observed and simulated monthly sediment for calibration (1981–1987)

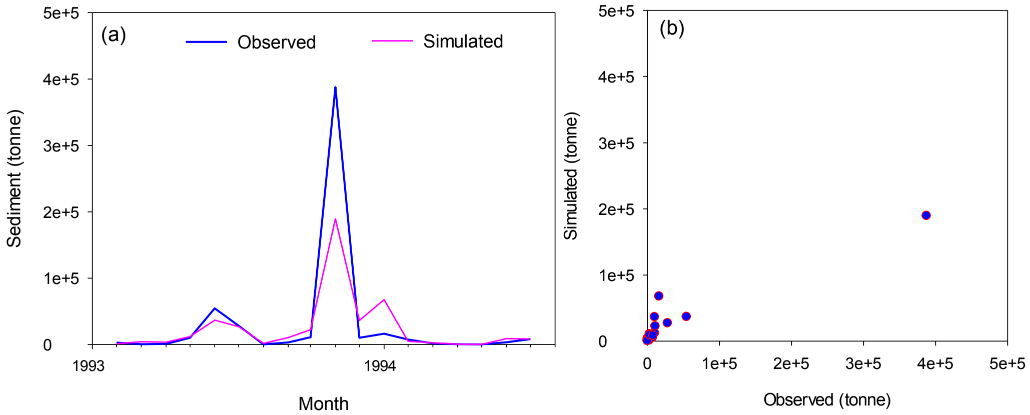

Figure 4.16 Observed and simulated monthly sediment for validation (1993–1994)

Graphically, the figures show a good fit between the simulated and observed sediment data for the calibration and validation. The values of three statistical indices, NSE, PBIAS and RSR were 0.76%, −12.8%, and 0.49% for the calibration, and 0.69%, 20%, and 0.56% for the validation, respectively, as shown in Table 4.5. The performance rating for the sediment calibration was very good, and the rating for the validation falls into the range for good (Moriasi et al., 2007).

4.3.3 Nitrogen

Like the sediment observations, the available observed nutrients, TN, NO_3^--N, and TP, were discrete and had variable lengths. All three were calibrated and validated on a monthly scale during the periods, 1996-2001 and 2002-2005, respectively.

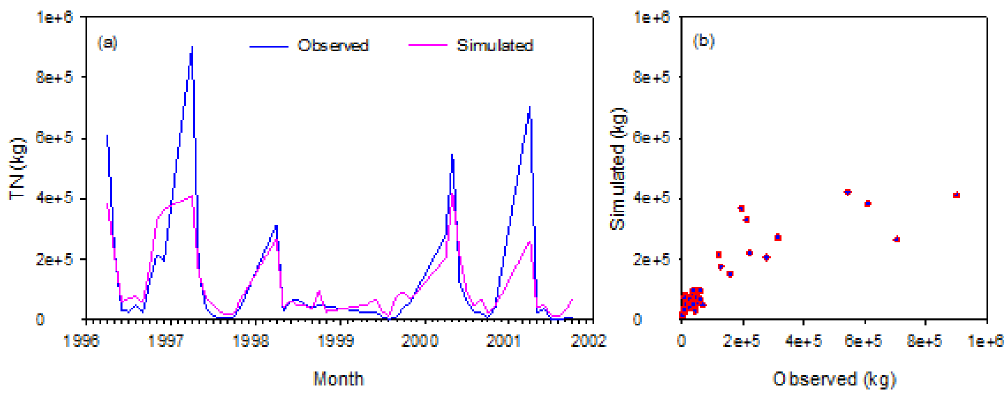

Figure 4.17 Observed and simulated monthly TN for calibration (1996–2001)

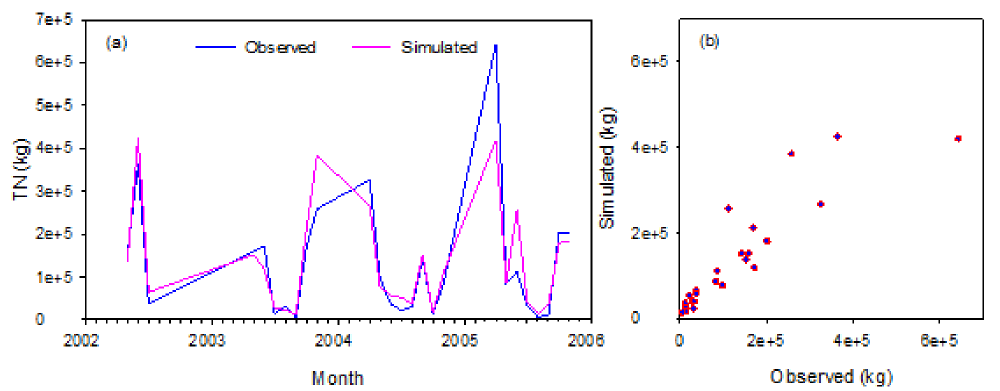

Figure 4.18 Observed and simulated monthly TN for validation (2002–2005)

Figures 4.17 and 4.18 illustrate the fitness between the simulated and observed TN during the calibration and validation periods. The NSE, PBIAS, and RSR for TN were 0.64, 2.8%, and 0.60 for the calibration and 0.80, 2.8%, and 0.44 for the validation, respectively (Table 4.5). As per Moriasi et al. (2007), the calibration was satisfactory, and the validation was very good.

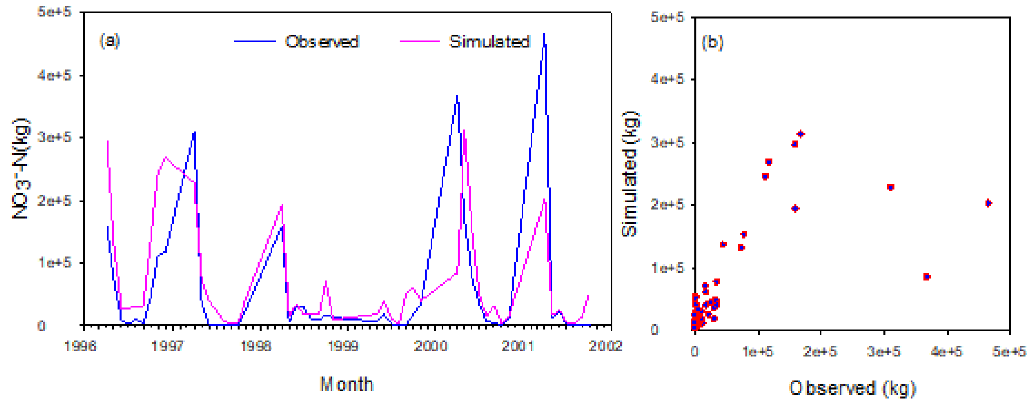

Figure 4.19 Observed and simulated monthly NO_3^--N for calibration (1996–2001)

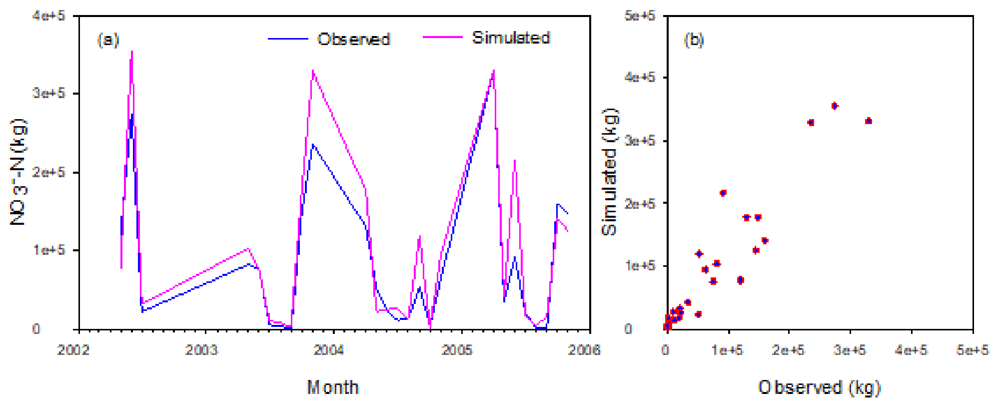

Figure 4.20 Observed and simulated monthly NO_3^--N for validation (2002–2005)

Figures 4.19 and 4.20 show the fitness between the simulated and observed values for NO_3^--N, respectively. The NSE, PBIAS, and RSR for NO_3^--N were 0.45, –18.1%, and 0.75 for the calibration and 0.79, –20.1%, and 0.46 for the validation, respectively (see Table 4.5). Here, the values of NSE and RSR for the calibration are slightly below the satisfactory performance rating, as suggested by Moriasi et al. (2007), however, given the median number of 0.26 for NSE from the literature (Moriasi et al., 2007), 0.46 for this calibration is acceptable. In contrast to the performance rating of the calibration, that for the validation is graded as very good.

4.3.4 Phosphorus

The periods of calibration and validation for TP were the same for the periods for TN and NO_3^--N. The calibration and validation were carried out on a monthly scale for the periods 1996-2001 and 2002-2005, respectively. The fitness trends are depicted in Figures 4.21 and 4.22.

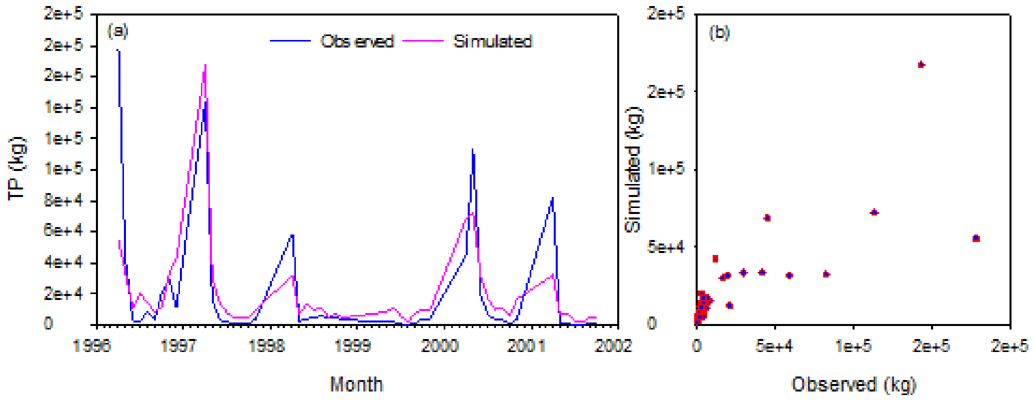

Figure 4.21 Observed and simulated monthly TP for calibration (1996–2001)

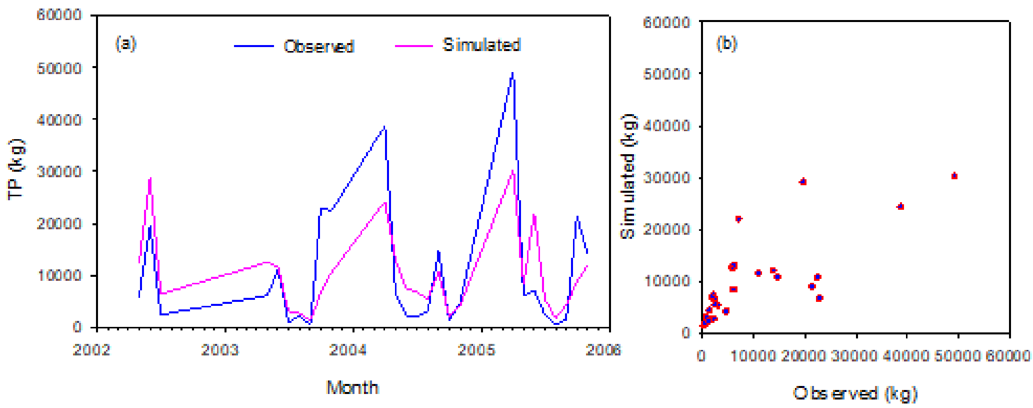

Figure 4.22 Observed and simulated monthly TP for validation (2002–2005)

The three statistical indices of NSE, PBIAS, and RSR used to evaluate the performance of the model are summarized in Table 4.5.

Table 4.5 Performance indices for calibration and validation

Parameter	*NSE*	*PBIAS (%)*	*RSR*	*Rating*
Runoff				
Calibration	0.90	–10.40	0.31	very good
Validation	0.81	–8.30	0.43	very good
Sediment				
Calibration	0.76	–12.80	0.49	very good
Validation	0.69	20.00	0.56	good
TN				
Calibration	0.64	2.80	0.60	satisfactory
Validation	0.80	–3.30	0.44	very good
NO_3^--N				
Calibration	0.45	–18.10	0.75	acceptable
Validation	0.79	–20.10	0.46	very good
TP				
Calibration	0.56	2.60	0.66	satisfactory
Validation	0.55	2.50	0.67	satisfactory

As seen in Table 4.5, NSE, PBIAS, and RSR for TP were 0.56, 2.6%, and 0.66 for the calibration and 0.55, 2.5%, and 0.67 for the validation. The performance ratings for both the calibration and the validation can be considered as satisfactory.

4.4 Simulation results and discussion for the SWAT modeling

To evaluate the environmental effects of CTD on the watershed, two CTD scenarios, CTD_{200} and CTD_{600}, were designed in Section 4.1.7. The UCTD scenario was designed as the baseline scenario for comparison with the CTD scenarios. To be in accordance with the period of observations from the paired experimental micro watersheds (Sunohara et al.,

2015) and the simulation period by Que et al. (2015), the CTD and UCTD scenarios were run for the seasons of growth (May–October) for the period 2006-2010.

4.4.1 Simulation results of CTD and UCTD scenarios

4.4.1.1 Flow

Figure 4.23 (a) and (b) illustrates the simulated flow of the CTDs compared to the UCTD scenario for the season of growth for each year from 2006 to 2010. The results show that the flow decreased with the height of the crest of the CTD structure.

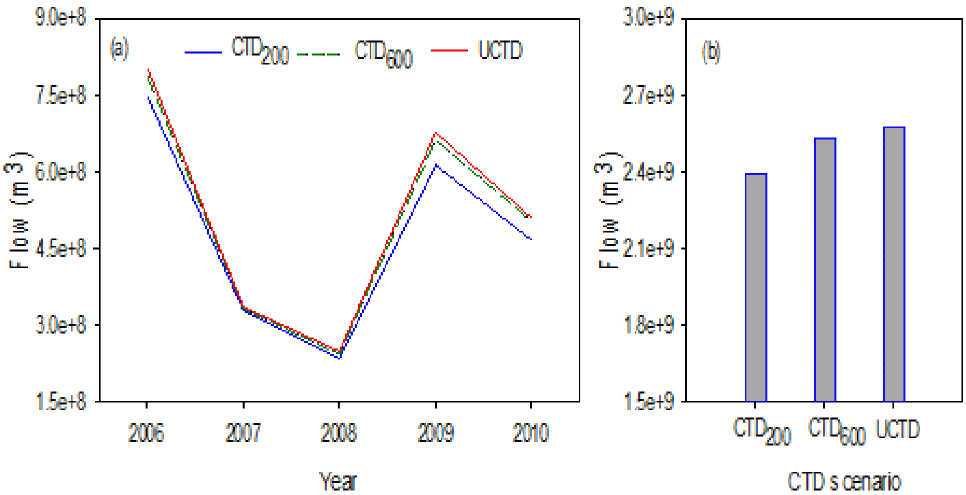

Figure 4.23 Growing seasonal (a) and total (b) simulated flow

However, due to climate variability, the reduction ratios for these two CTD scenarios performed differently in each season of growth. For CTD_{200}, they varied from –1.95% (2007) to –9.42% (2009), while for CTD_{600}, they varied from –0.96% (2007) to –2.13% (2008), a narrower range.

Table 4.6 Simulated flow of CTD and UCTD scenarios in five seasons of growth

Year	CTD_{200} $\times10^8$ m^3	CTD_{600} $\times10^8$ m^3	UCTD $\times10^8$ m^3	$(CTD_{200}$ - UCTD)/UCTD × 100 %	$(CTD_{600}$ - UCTD)/UCTD × 100 %
2006	7.48	7.87	8.03	-6.88	-2.01
2007	3.29	3.33	3.36	-1.95	-0.96
2008	2.35	2.44	2.49	-5.48	-2.13
2009	6.13	6.63	6.77	-9.42	-2.12
2010	4.67	5.03	5.10	-8.47	-1.28
Total	23.93	25.30	25.75	-7.09	-1.77

For the watershed, the simulated flow of the CTD scenarios at depths of 200 and 600 mm for the five seasons of growth during the simulation period were 23.93×10^8 m^3 and 25.30×10^8 m^3, respectively, and that of the UCTD scenario increased to 25.75×10^8 m^3.

Therefore, compared to the baseline UCTD scenario, the reduction ratios of the CTD_{200} and CTD_{600} scenarios were –7.09 and –1.77%, respectively, as shown in Table 4.6.

4.4.1.2 Sediment

Sediment loads were found to decrease when the depth of the crest of the CTD structure was lowered, as shown in Figure 4.24 (a) and (b). The percent increase in the sediment load when CTD was used instead of UCTD ranged from 2.99% (2007) to 7.97% (2009) for CTD_{200} and 0.33% (2008) to 3.02% (2009) for CTD_{600}, respectively.

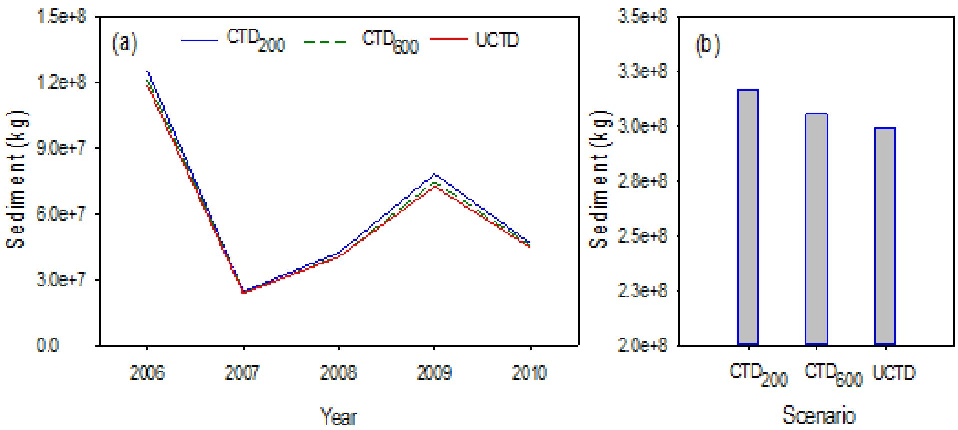

Figure 4.24 Growing seasonal (a) and total (b) simulated sediment

For the five periods of growth, the sediment loads for CTD_{200} and CTD_{600} increased by 5.67% and 2.21%, respectively, compared to that of UCTD, as tabulated in Table 4.7. The simulation results from the SWAT model for the sediment from the CTD and UCTD scenarios generally agree with the increases of 2.56% for CTD_{200} and 0.23% for CTD_{600} as simulated by the AnnAGNPS model (Que et al., 2015).

Table 4.7 Simulated sediment of CTD and UCTD scenarios in five seasons of growth

Year	CTD_{200} $\times10^8$ kg	CTD_{600} $\times10^8$kg	UCTD $\times10^8$ kg	$(CTD_{200}$ - UCTD)/UCTD × 100 %	$(CTD_{600}$ - UCTD)/UCTD × 100 %
2006	1.25	1.21	1.18	5.63	2.34
2007	0.24	0.24	0.24	2.99	1.27
2008	0.42	0.41	0.40	4.73	0.33
2009	0.78	0.74	0.72	7.97	3.02
2010	0.47	0.46	0.45	4.35	2.15
Total	3.16	3.05	2.99	5.67	2.12

4.4.1.3 Nitrogen

The SWAT model categorizes N into two main forms, mineral N and organic N. Furthermore, mineral N is subdivided into NH_4^+-N, NO_2^--N, and NO_3^--N. The SWAT model then simulates four forms of N, Org-N, NH_4^+-N, NO_2^--N, and NO_3^--N. Each of them performs under the CTD and UCTD scenarios, as discussed below

4.4.1.3.1 Org-N

Of the five different pools of nitrogen in the soil simulated by the SWAT model, three pools are organic forms of nitrogen: fresh Org-N associated with crop residue and microbial biomass, and active and stable Org-Ns associated with the soil humus (Figure 2.9). The simulated loads of Org-N in the seasons of growth are shown in Figure 4.25 (a) and (b). Both decrease with the height of the weir of the CTD control structure.

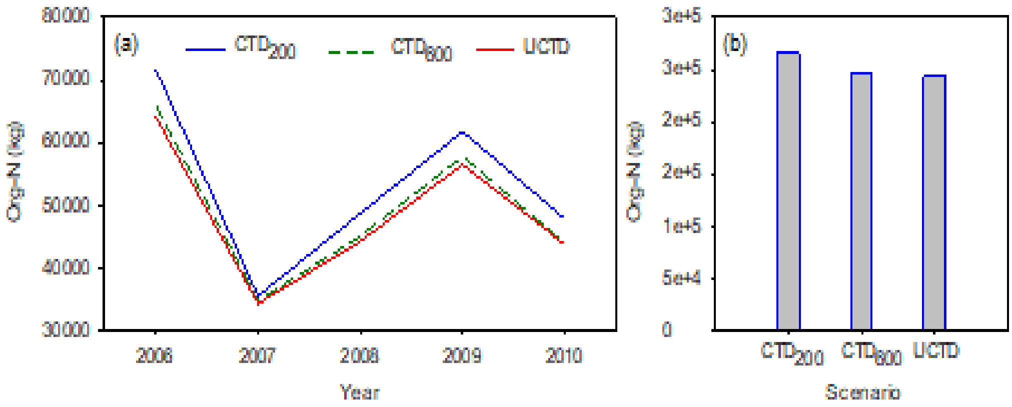

Figure 4.25 Growing seasonal (a) and total (b) simulated Org-N

During the simulation period 2006-2010, Org-N increased the most in 2006 and the least in 2007, whereas it reached 11.88% and 3.50% for CTD_{200}. Compared to the large variation in CTD_{200}, the increase of Org-N for CTD_{600} varied in a relatively limited range from 0.44% in 2010 to 2.86% in 2006. Over the five connected seasons of growth, incremental Org-Ns were 9.34% for CTD_{200} and 1.90% for CTD_{600}, respectively, as listed in Table 4.8.

Table 4.8 Simulated Org-N of CTD and UCTD scenarios in five seasons of growth

Year	CTD_{200} $\times 10^5$ kg	CTD_{600} $\times 10^5$ kg	UCTD $\times 10^5$ kg	$(CTD_{200} - UCTD)/UCTD \times 100$ %	$(CTD_{600} - UCTD)/UCTD \times 100$ %
2006	0.72	0.66	0.64	11.88	2.86
2007	0.35	0.35	0.34	3.50	1.38
2008	0.49	0.45	0.44	10.10	1.82
2009	0.62	0.58	0.56	9.33	2.32
2010	0.48	0.44	0.44	9.44	0.44
Total	2.65	2.47	2.43	9.34	1.90

4.4.1.3.2 NH_4^+-N

NH_4^+-N is only a small fraction of TN, and Figure 4.26 (a) and (b) shows that it decreases along with the height of the weir of the CTD control structure.

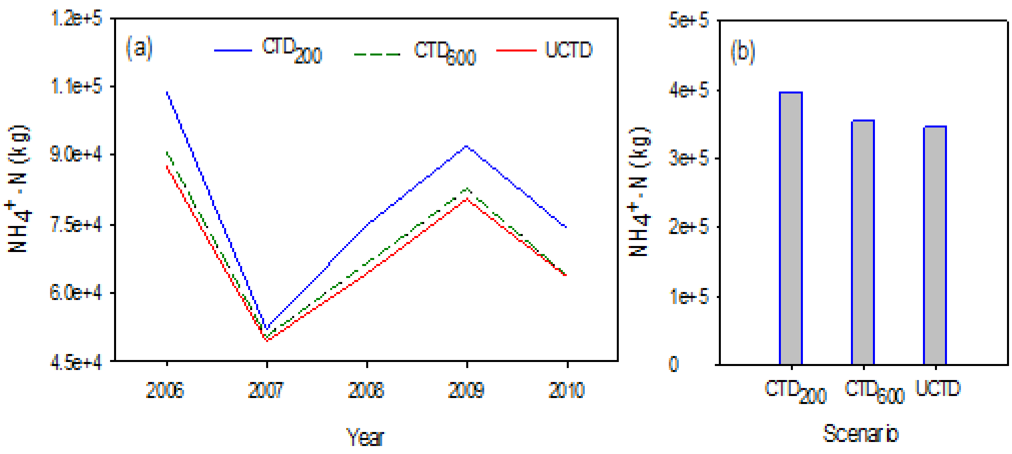

Figure 4.26 Growing seasonal (a) and total (b) simulated NH_4^+-N

The changes in NH_4^+-N when CTD is used instead of UCTD ranged from 5.52% (2007) to 18.6% (2006) for CTD_{200} and 0.31% (2010) to 3.66% (2008) for CTD_{600}, as detailed in Table 4.9. The increases in NH_4^+-N over the five growing seasons were 14.95% and 2.58% for CTD_{200} and CTD_{600}, respectively.

Table 4.9 Simulated NH_4^+-N of CTD and UCTD scenarios in five seasons of growth

Year	CTD_{200} $\times 10^5$ kg	CTD_{600} $\times 10^5$ kg	UCTD $\times 10^5$ kg	(CTD_{200} - UCTD)/UCTD × 100 %	(CTD_{600} - UCTD)/UCTD × 100 %
2006	1.04	0.90866	0.88	18.61	3.60
2007	0.52	0.5053	0.50	5.52	2.03
2008	0.75	0.66578	0.64	16.46	3.66
2009	0.92	0.82727	0.81	14.29	2.74
2010	0.74	0.63714	0.64	16.57	0.31
Total	3.97	3.54415	3.45	14.95	2.58

4.4.1.3.3 NO_2^--N

Like NH_4^+-N, NO_2^--N is a small fraction of TN compared to NO_3^--N. The simulated NO_2^--N loads under CTD_{200}, CTD_{600}, and UCTD are shown in Figure 4.27 (a) and (b) and Table 4.10. The two CTD scenarios, NO_2^--N decreased along with the increasing height of the tile drainage.

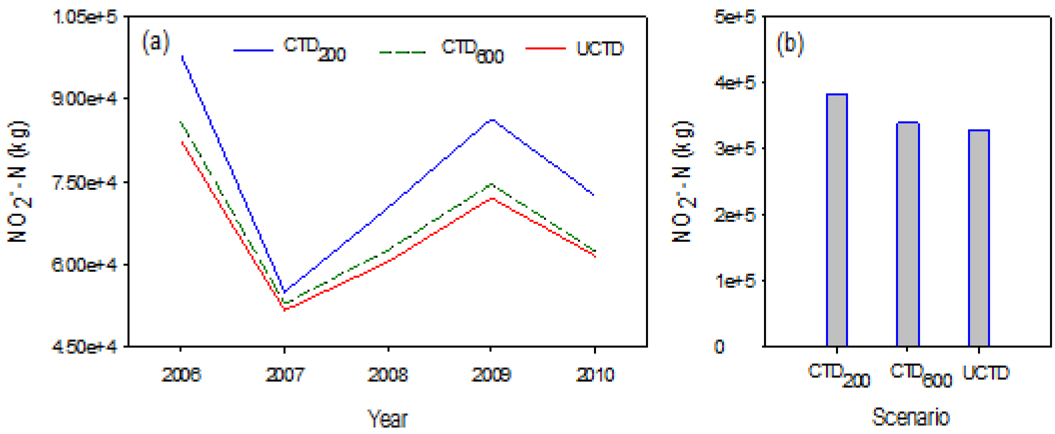

Figure 4.27 Growing seasonal (a) and total (b) simulated NO_2^--N

For the season of growth each year, NO_2^--Ns varied from 6.35% (2007) to 19.78% (2009) and from 1.30% (2010) to 4.12% (2006) for CTD_{200} and CTD_{600}, respectively. During the five seasons of growth, the total increments of CTD_{200} and CTD_{600} were 16.35% and 3.06%, respectively.

Table 4.10 Simulated NO_2^--N of CTD and UCTD scenarios in five seasons of growth

Year	CTD_{200} $\times 10^5$ kg	CTD_{600} $\times 10^5$ kg	UCTD $\times 10^5$ kg	$(CTD_{200} - UCTD)/UCTD \times 100$ %	$(CTD_{600} - UCTD)/UCTD \times 100$ %
2006	0.98	0.85788	0.82	18.87	4.12
2007	0.55	0.52971	0.52	6.35	2.31
2008	0.70	0.62753	0.61	16.19	3.60
2009	0.86	0.74646	0.72	19.78	3.45
2010	0.72	0.62459	0.62	17.50	1.30
Total	3.82	3.38617	3.29	16.35	3.06

4.4.1.3.4 NO_3^--N

NO_3^--N is the main constituent of TN, and therefore, the trends for NO_3^--N in the simulation results correspond to the trends for TN. Figure 4.28 shows the NO_3^--N decreases with the increasing tile drainage depths.

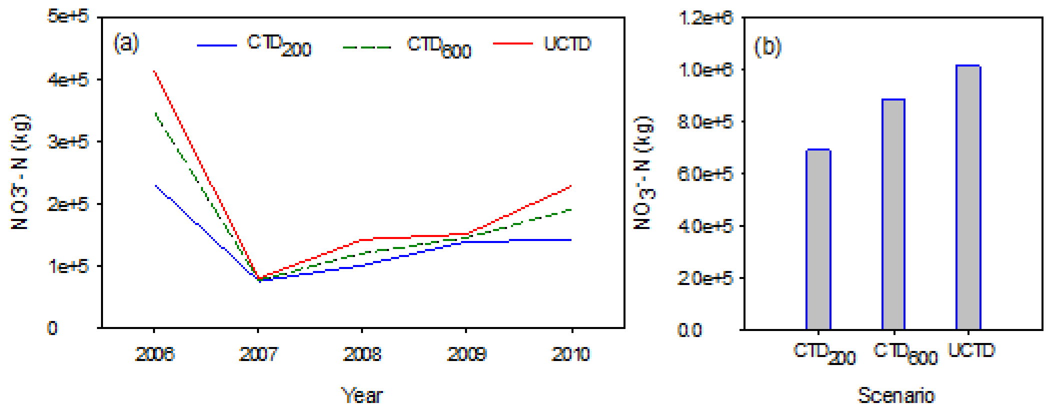

Figure 4.28 Growing seasonal (a) and total (b) simulated NO_3^--N

The reduction ratios for NO_3^--N for CTD_{200} and CTD_{600} varied in a larger range, from –5.63% (2007) to –43.74% (2006) and –3.30% (2007) to –16.31% (2010), respectively, and for the total, the reduction ratios under CTD_{200} and CTD_{600} were –31% and –13.04%, respectively, as shown in Table 4.11.

Table 4.11 Simulated NO_3^--N of CTD and UCTD scenarios in five seasons of growth

Year	CTD_{200} $\times 10^5$ kg	CTD_{600} $\times 10^5$ kg	UCTD $\times 10^5$ kg	(CTD_{200} - UCTD)/UCTD × 100 %	(CTD_{600} - UCTD)/UCTD × 100 %
2006	2.32	3.47	4.12	-43.74	-15.87
2007	0.76	0.78	0.81	-5.63	-3.30
2008	1.02	1.22	1.44	-28.96	-15.15
2009	1.40	1.47	1.52	-7.95	-3.66
2010	1.42	1.92	2.29	-37.93	-16.31
Total	6.93	8.86	10.18	-31.97	-13.04

4.4.1.3.5 TN

As noted previously, TN consists of five forms of N, Org-N, NH_4^+-N, NO_2^--N, and NO_3^--N. Of all the forms of N, NO_3^--N is the only one simulated directly in the tile-flow module in the model, and the other four forms of N, Org-N, NH_4^+-N, and NO_2^--N react indirectly to the changes in depth for CTD_{200} and CTD_{600} through the flow and sediment.

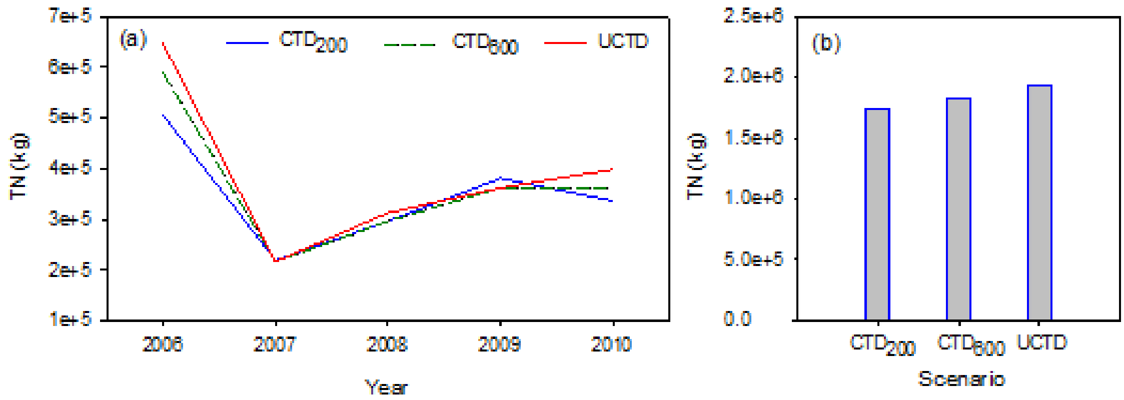

Figure 4.29 Growing seasonal (a) and total (b) simulated TN

Figure 4.29 (a) illustrates the variations in the growth seasons' TN from 2006 to 2010 under CTD_{200} and CTD_{600}. Depending on the year, CTD can lead to an increase or a decrease in TN (Table 4.12). Overall, the TN is reduced by 5.56% at the outlet of the watershed.

Table 4.12 Simulated TN of CTD and UCTD scenarios in five seasons of growth

Year	CTD_{200} $\times 10^5$ kg	CTD_{600} $\times 10^5$ kg	UCTD $\times 10^5$ kg	$(CTD_{200}$ - UCTD)/UCTD × 100 %	$(CTD_{600}$ - UCTD)/UCTD × 100 %
2006	5.05	5.89	6.46	-21.80	-8.84
2007	2.19	2.17	2.16	1.24	0.00
2008	2.96	2.96	3.13	-5.35	-5.25
2009	3.80	3.62	3.62	5.23	0.13
2010	3.37	3.62	3.98	-15.47	-9.10
Total	17.38	18.26	19.35	-10.21	-5.65

Figure 4.29 (b) shows the trends of the growth seasons' TN under CTD_{200} and CTD_{600} for the simulation period. TN is reduced by –10.21% and –5.56% for CTD_{200} and CTD_{600}, respectively (Table 4.12). These results are consistent with the findings by Que et al. (2015) using AnnAGNPS.

4.4.1.4 Phosphorus

The SWAT model differentiates P into two forms: Org-P and Min-P, while the model does not partition Org-P and Min-P into smaller items as it does for N (Figure 2.10).

4.4.1.4.1 Org-P

The Org-P simulation results for CTD_{200} and CTD_{600} are shown in Figure 4.30 (a) and (b). Org-P increased for both CTD scenarios over each season of growth, and the total amounts for the five simulated seasons rose with increases in the depth of tile drainage.

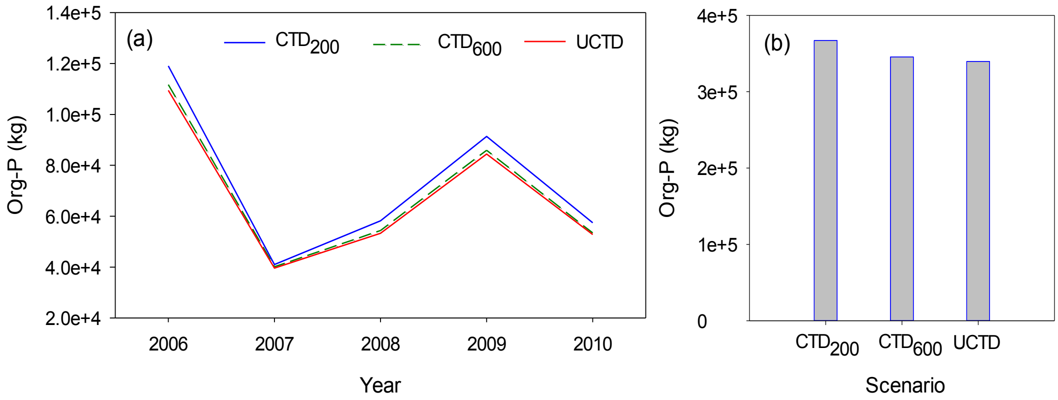

Figure 4.30 Growing seasonal (a) and total (b) simulated Org-P

In Table 4.13, it can be seen that Org-P increased from 3.58% (2007) to 9.27% (2008) and from 1.30% (2007) to 2.15% (2008) for CTD_{200} and CTD_{600}, respectively. The total increments for the five years for Org-P were 8.09% and 1.77% for CTD_{200} and CTD_{600}, respectively.

Table 4.13 Simulated Org-P of CTD and UCTD scenarios in five seasons of growth

Year	CTD_{200} $\times 10^4$ kg	CTD_{600} $\times 10^4$ kg	UCTD $\times 10^4$ kg	$(CTD_{200}$ - UCTD)/UCTD × 100 %	$(CTD_{600}$ - UCTD)/UCTD × 100 %
2006	1.19	1.12	1.09	8.76	2.04
2007	0.41	0.40	0.40	3.58	1.30
2008	0.58	0.54	0.53	9.27	2.15
2009	0.91	0.86	0.84	8.16	1.76
2010	0.57	0.53	0.53	8.76	1.22
Total	3.67	3.46	3.40	8.09	1.77

4.4.1.4.2 Min-P

Min-P increases alone with increases in tile drainage depth in the CTD scenarios, as depicted in Figure 4.31 (a) and (b). Independent of the tile depth, Min-P increases when UCTD is replaced by CTD.

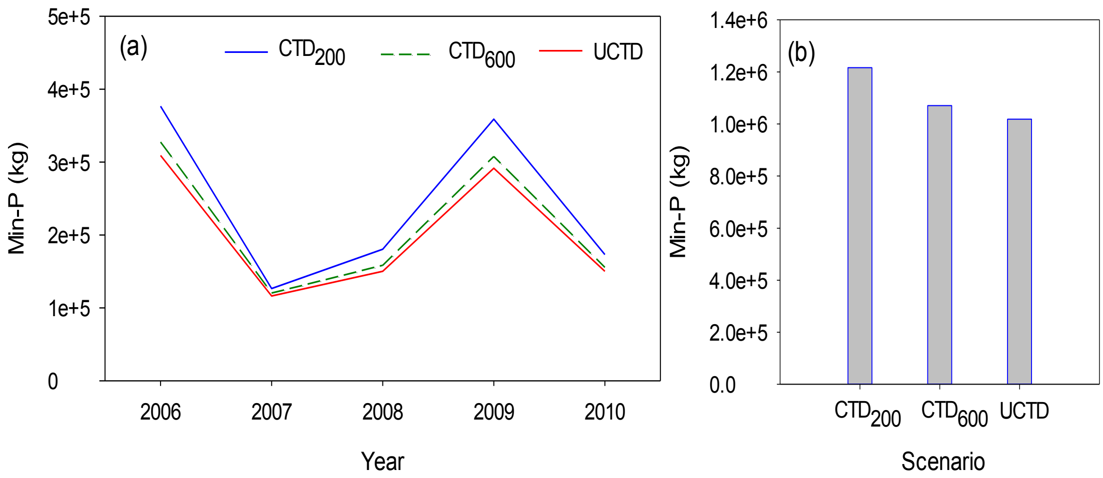

Figure 4.31 Growing seasonal (a) and total (b) simulated Min-P

The ratios of Min-P increased from 8.90% (2007) to 23.07% (2009) and 3.50% (2007) to 5.88% (2006) for CTD_{200} and CTD_{600}, respectively. The total Min-P for the five years of the simulation period was 19.48% and 5.15% for CTD_{200} and CTD_{600}, respectively (Table 4.14).

Table 4.14 Simulated Min-P of CTD and UCTD scenarios in five seasons of growth

Year	CTD_{200} ×10^4 kg	CTD_{600} ×10^4 kg	UCTD ×10^4 kg	(CTD_{200} - UCTD)/UCTD × 100 %	(CTD_{600} - UCTD)/UCTD × 100 %
2006	3.77	3.28	3.09	21.81	5.88
2007	1.27	1.21	1.16	8.90	3.58
2008	1.81	1.59	1.50	20.15	5.65
2009	3.59	3.08	2.92	23.07	5.58
2010	1.73	1.56	1.50	15.25	3.50
Total	12.17	10.71	10.18	19.48	5.15

4.4.1.4.3 TP

As addressed in Section 2.6.3, six different pools of P were simulated by the model: three Min-P pools and three Org-P pools. The three Min-P pools are solution, active, and stable, with the fresh Org-P being associated with crop residue and microbial biomass, and the active and stable Org-P are associated with the soil humus, and constitute the three Org-P pools (Neitsch et al., 2011). Given that both Org-P and Min-P increased along with increased tile drainage depth, TP reacts positively to the increasing depth, as shown in Figure 4.32 (a) and (b).

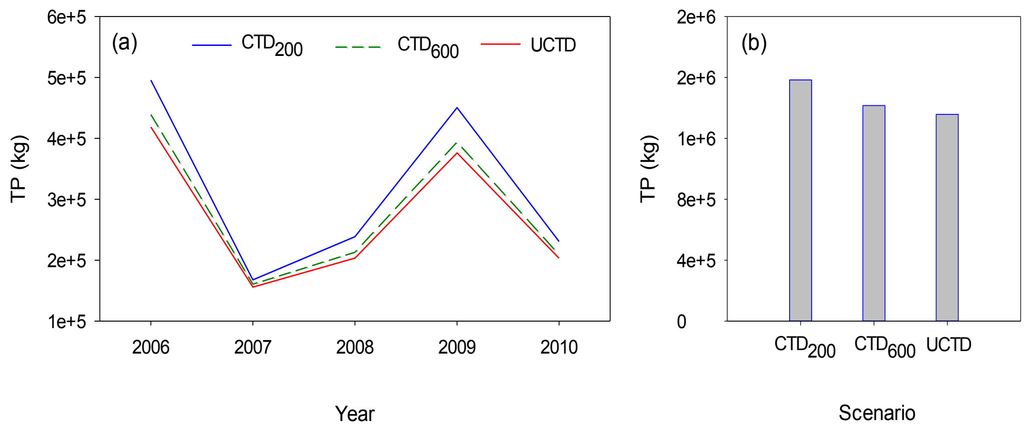

Figure 4.32 Growing seasonal (a) and total (b) simulated TP

Although the TP varied from 7.54% (2007) to 19.72% (2009) and 2.90% (2010) to 4.86% (2006) for CTD_{200} and CTD_{600}, respectively, it increased throughout the simulation period of five years. For the five seasons of growth during the simulation period, the increments of TP were 16.62% and 4.29% for CTD_{200} and CTD_{600}, respectively (Table 4.15).

Table 4.15 Simulated TP of CTD and UCTD scenarios in five seasons of growth

Year	CTD_{200} $\times10^4$ kg	CTD_{600} $\times10^4$ kg	UCTD $\times10^4$ kg	$(CTD_{200}$ - UCTD)/UCTD × 100 %	$(CTD_{600}$ - UCTD)/UCTD × 100 %
2006	4.96	4.39	4.19	18.36	4.86
2007	1.68	1.61	1.56	7.54	3.01
2008	2.39	2.13	2.04	17.32	4.74
2009	4.50	3.94	3.76	19.72	4.71
2010	2.31	2.09	2.03	13.56	2.90
Total	15.84	14.16	13.58	16.62	4.29

4.4.2 Discussion

Starting with SWAT2000, a tile flow calculation component was added to the model (Arnold et al., 1999). Moriasi et al. (2007) added another option for tile drainage that uses the H-K drainage equations. After the model incorporated the first tile-drain simulation module during the late 1990s and then the H-K method during the 2000s, it matured gradually into simulating traditional tile drainage after it was broadly tested and reported by both the model developer and the modeller (Arnold et al., 1999; Du et al., 2005; Moriasi et al., 2007; Rahman et al., 2011; Koch et al., 2012; Moriasi et al., 2012; Boles et al., 2015).

The original model was unable to simulate CTD properly due to the model's method for calculating NO_3^--N in the tile flow. However, as has been discussed, after improvements in the calculation procedure for NO_3^--N in the tile flow, the model was capable of simulating CTD.

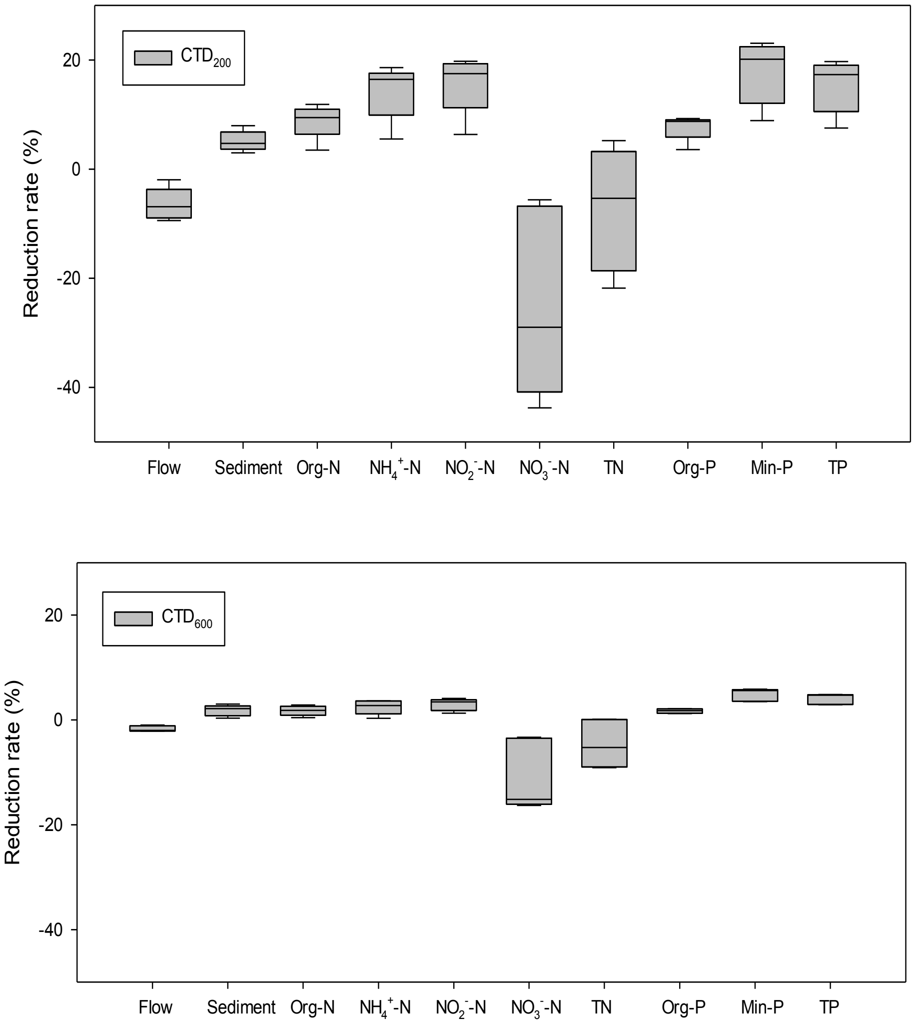

Figure 4.33 Changes in water quantity and quality by CTD_{200} and CTD_{600}

Under the current climate and land use managements during the period 2006-2010, replacing UCTD with CTD leads to changes of –7.09, 5.67, 9.34, 14.95, 16.35, –31.97, –10.21, 8.09, 19.48, and 16.62% under CTD_{200}, and –1.77, 2.12, 1.90, 2.58, 3.06, –13.04, –5.56, 1.77, 5.15, and 4.29% under CTD_{600} for water, sediment, Org-N, NH_4^+-N, NO_2^--N, NO_3^--N, TN, Org-P, Min-P, and TP, respectively, as shown in Figure 4.33. Obviously, the CTD_{200} scenario leads greater changes in output in either a positive or negative way. The -7.09% reduction in flow under TD_{200} is in line with the previous finding of –7.28% (Que et al., 2015), whereas the reduction of -1.77% under CTD_{600} is less than the previous finding of –6.62% by Que et al. (2015). The difference under the CTD_{600} scenario is likely caused by the fact that the SWAT model and AnnAGNPS simulate flow (discharge) and runoff differently. AnnAGNPS only simulates direct flow, while the SWAT model simulates all parts, including the ground water. Hence, these simulation results for CTD_{200} and CTD_{600} by the improved SWAT model are generally in agreement with the previous simulation findings by Que et al. (2015).

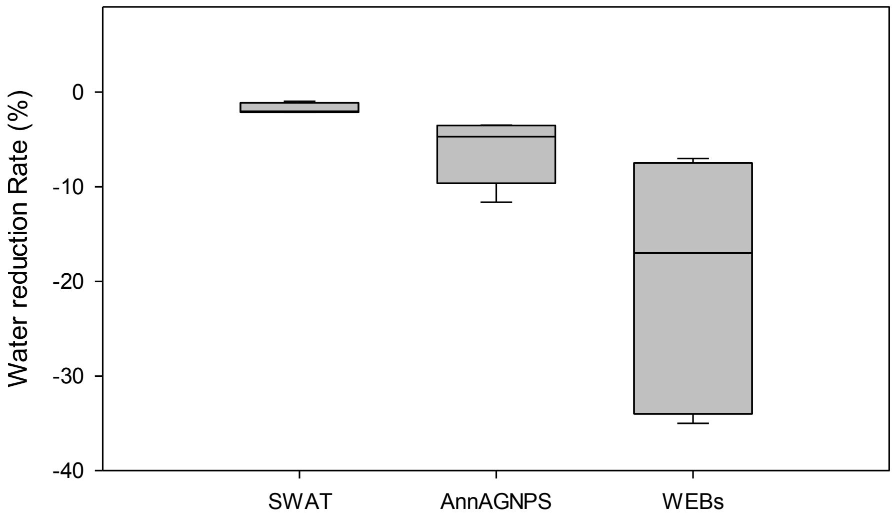

Figure 4.34 CTD_{600} water reductions of SWAT, AnnAGNPS, and WEBs

The water reduction rates from WEBs, AnnAGNPS, and the improved SWAT model decrease gradually, as depicted in Figure 4.34. The one-way ANOVA reflects that the differences in the median values among the three treatment groups are greater than what would be expected by chance; thus, there is a statistically significant difference. It can be reasonably explained that these reduction rates arise from different situations, i.e., WEBs is based on a mere comparison of CTD and UCTD; AnnAGNPS only simulates direct runoff; and the improved SWAT model covers all types of water, including groundwater. Tile drained areas in the watershed model and WEBs were different. The CTD experiment of WEBs had high tile drained filed, and the tile drained area is about 36% of the watershed, so more water reduction for WEBs is reasonable.

The SWAT model uses the MUSLE approach to simulate sediment (Williams, 1975), which is the same approach adopted by the AnnAGNPS model. The t-test shows that the difference in the median values between the two groups is not great enough to exclude the possibility that the difference is due to random sampling variability; there is no statistically significant difference, as shown in Figure 4.35.

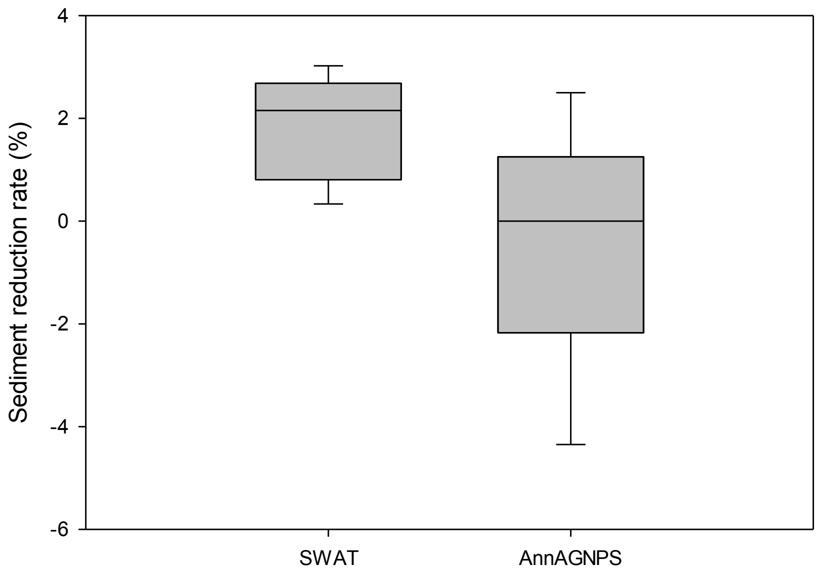

Figure 4.35 CTD_{600} Sediment reduction rates of the SWAT model and AnnAGNPS

As noted previously, in the SWAT and AnnAGNPS models, TN consists of four forms of N, Org-N, NH_4^+-N, NO_2^--N, and NO_3^--N. Of all the forms of N, NO_3^--N is the only one simulated directly in the tile-flow module in the model, and the other three forms of N, Org-N, NH_4^+-N, and NO_2^--N, react indirectly to the changes in depth for CTD_{200} and CTD_{600} through the flow and sediment.

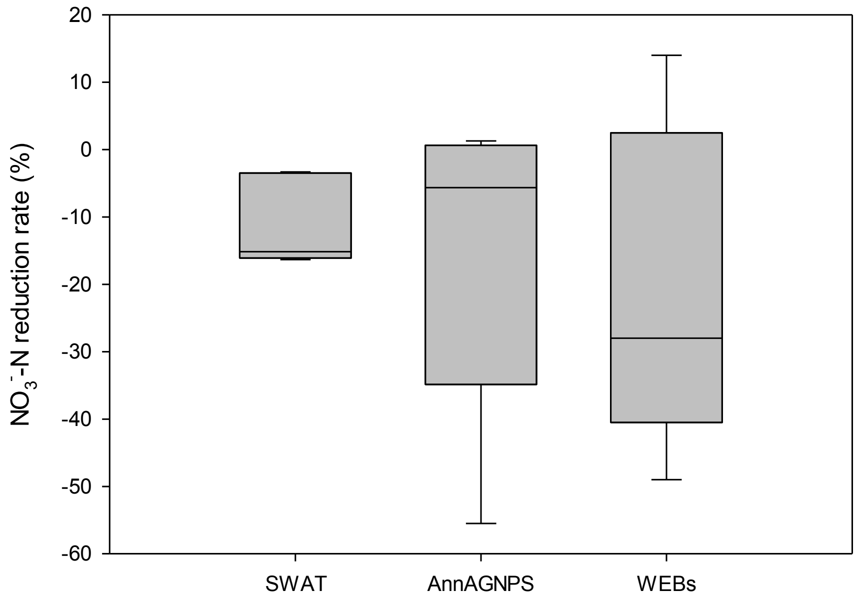

Figure 4.36 CTD_{600} NO_3^--N reductions of SWAT, AnnAGNPS (dissolved N), and mass fluxes of WEBs

The one-way ANOVA reflects that the differences in the mean values for NO_3^--N among the three treatment groups are not great enough to exclude the possibility that the difference is due to random sampling variability; there is no statistically significant difference (Figure 4.36). Therefore, the simulation results for NO_3^--N by the SWAT and AnnAGNPS models are consistent with the observations from the two experimental micro-watersheds.

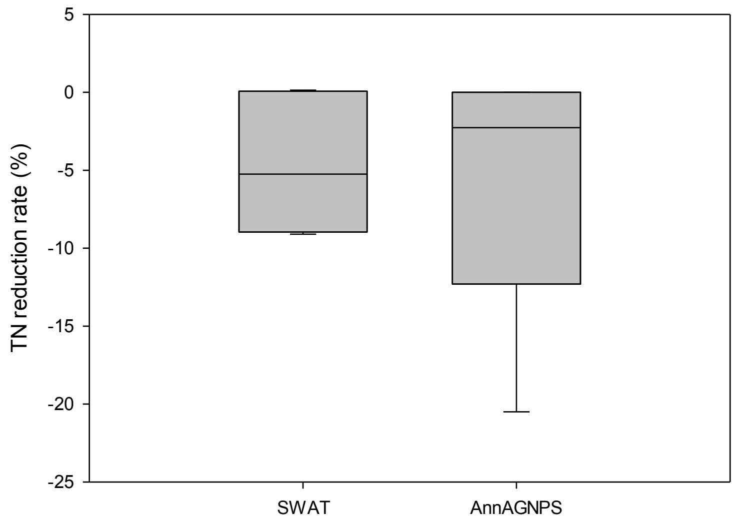

Figure 4.37 CTD$_{600}$ TN reduction rates of the SWAT model and AnnAGNPS

Similarly, the t-test of the results shows that there is no statistically significant difference between the TN results of the SWAT and AnnAGNPS models (Figure 4.37).

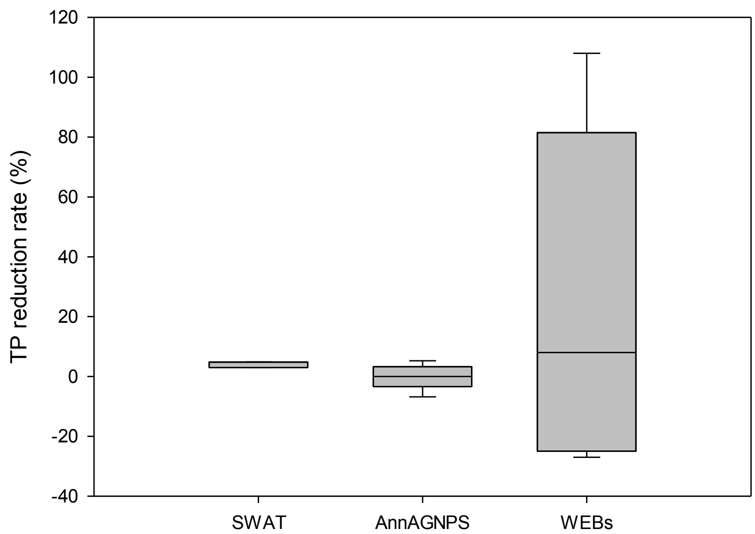

Figure 4.38 CTD$_{600}$ TP reduction rates of the SWAT model, AnnAGNPS, and WEBs

For the TP, the one-way ANOVA also shows that there is no statistically significant difference between the TP results of the SWAT and AnnAGNPS models and WEBs (Figure 4.38).

4.5 Performances of the CTD scenarios under climate changes

4.5.1 Climate change scenarios

As discussed in Section 2.7, numerous climate models are applied worldwide. This study uses the statistical downscaling results from coupling GCMs and RCMs with different configurations, as listed in Table 2.5.

In order to test the performances of the CTD scenarios under dynamic climate circumstances and a long period of climate change, using the improved SWAT model, 12 climate change datasets were prepared for the model based on a combination of GCM and RCM configurations, which are: CanESM3+ CanRCM4+4.5 (CAN45), CanESM3+ CanRCM4+8.5 (CAN85), EC-EARTH+RCA4+4.5 (ECER45), EC-EARTH+RCA4+8.5 (ECER85), EC-EARTH+ HIRHAM5+4.5 (ECEH45), EC-EARTH+ HIRHAM5+8.5 (ECEH85), GFDL-ESM2M+RegCM4+8.5 (GFDLR85), GFDL-ESM2M+WRF+8.5 (GFDLW85), HadGEM2-ES+RegCM4+8.5 (HADR85), HadGEM2-ES+WRF+8.5 (HADW85), MPI-ESM-LR+ RegCM4+8.5 (MPIR85), and MPI-ESM-LR+WRF+8.5 (MPIW85).

4.5.2 Simulations and discussion of climate change scenarios

The CTD scenarios were examined for two equal simulation periods, the reference period (1981–2010) as a baseline and one future period (2021–2050), in order to represent a change in climate. In the baseline period from 1981 to 2010, the modified SWAT model was run with historical climate data (BASE), while for the climate change period from 2021 to 2050, 12 climate datasets were applied to the improved SWAT model. The crop distribution, fertilizer application rate and physical features of the watershed were unchanged.

4.5.2.1 Output variations of climate change scenarios over 30 years

For the current tile drainage condition (UCTD) using the modified SWAT model, the outputs of each climate change and baseline scenario are shown in Figures 4.39–4.48.

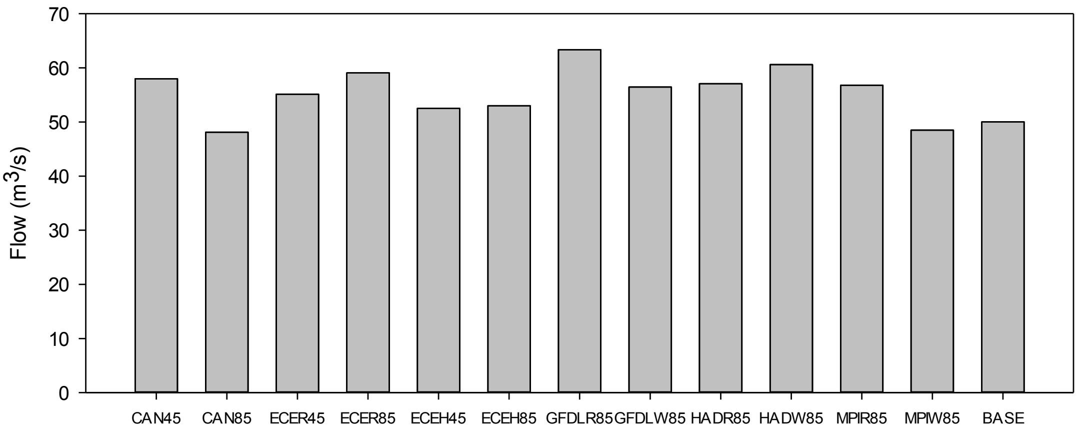

Figure 4.39 Average flow under the baseline and future climate

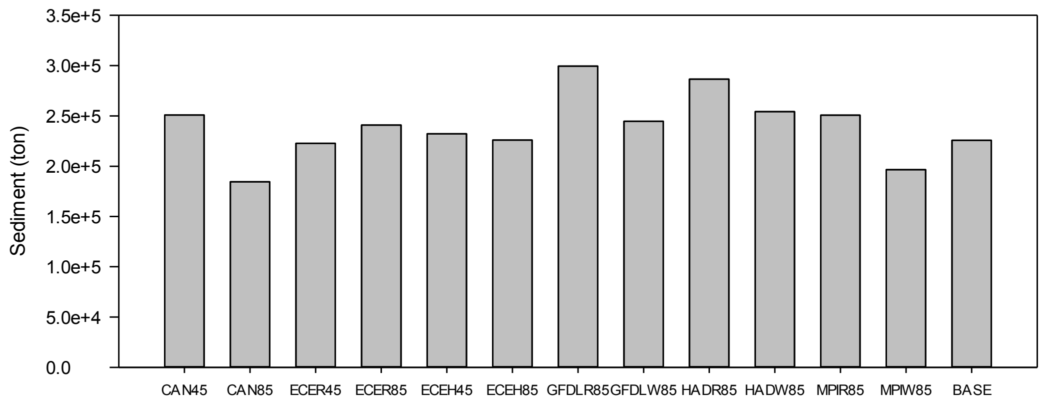

Figure 4.40 Average sediment under the baseline and future climate

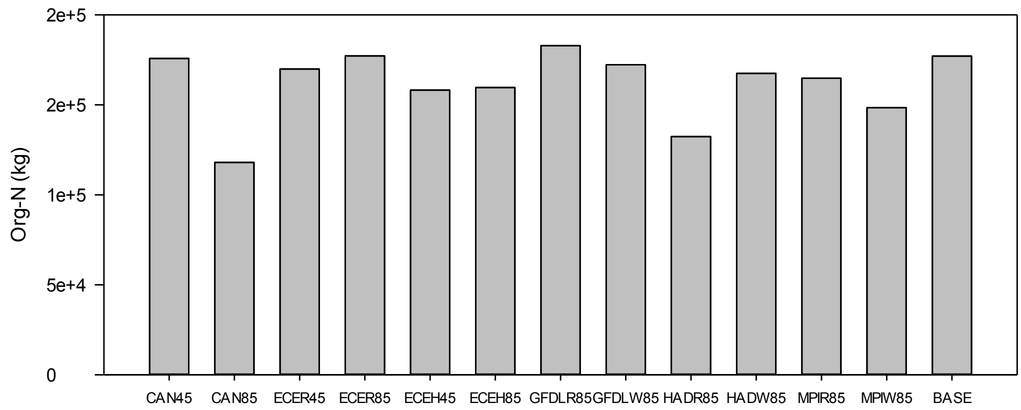

Figure 4.41 Average Org-N under the baseline and future climate

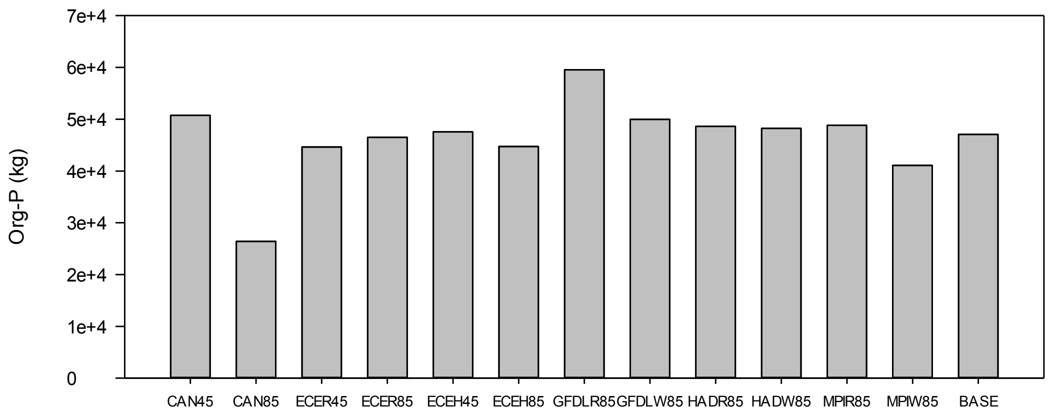

Figure 4.42 Average Org-P under the baseline and future climate

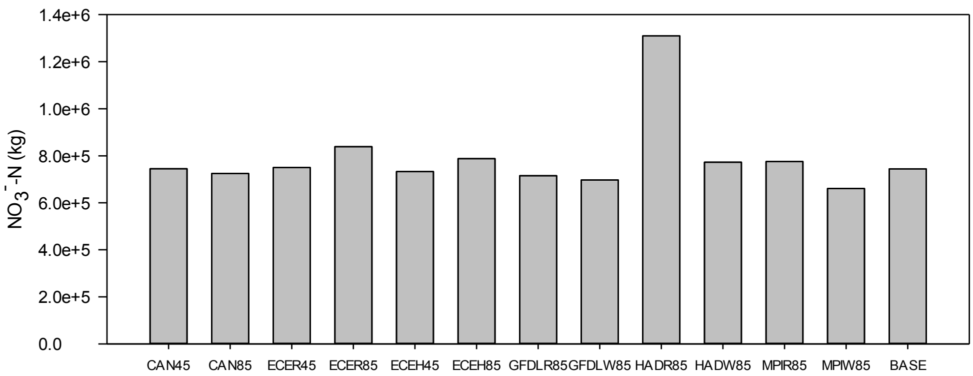

Figure 4.43 Average NO_3^--N Under the baseline and future climate

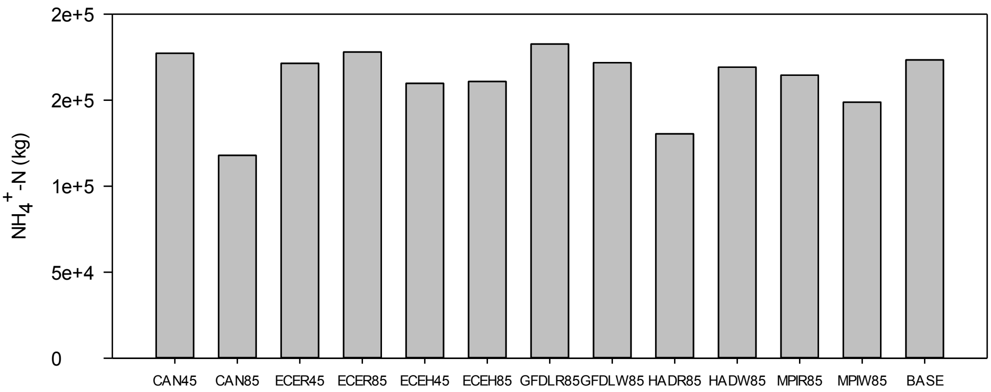

Figure 4.44 Average NH_4^+-N under the baseline and future climate

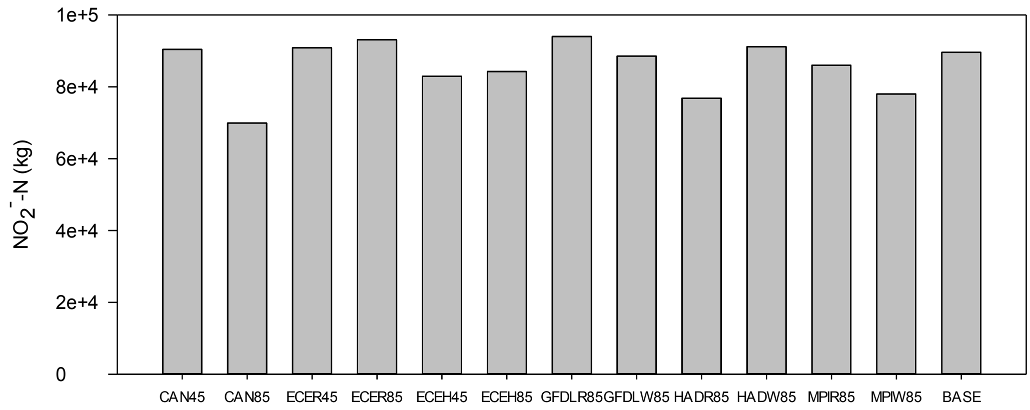

Figure 4.45 Average NO_2^--N under the baseline and future climate

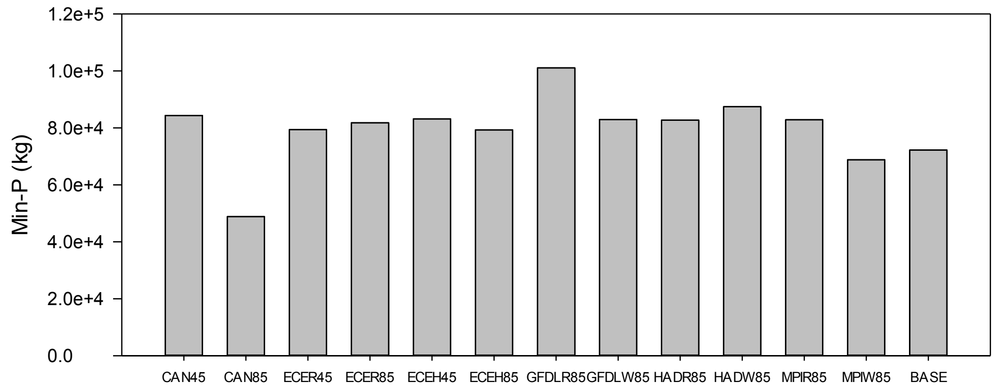

Figure 4.46 Average Min-P under the baseline and future climate

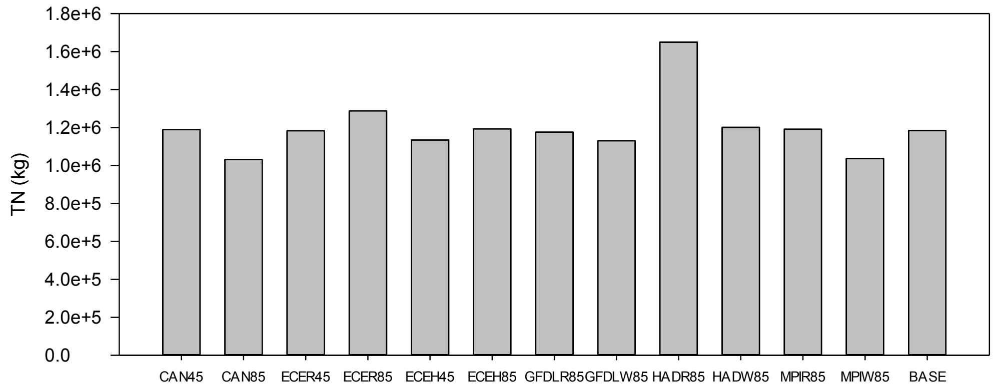

Figure 4.47 Average TN under the baseline and future climate

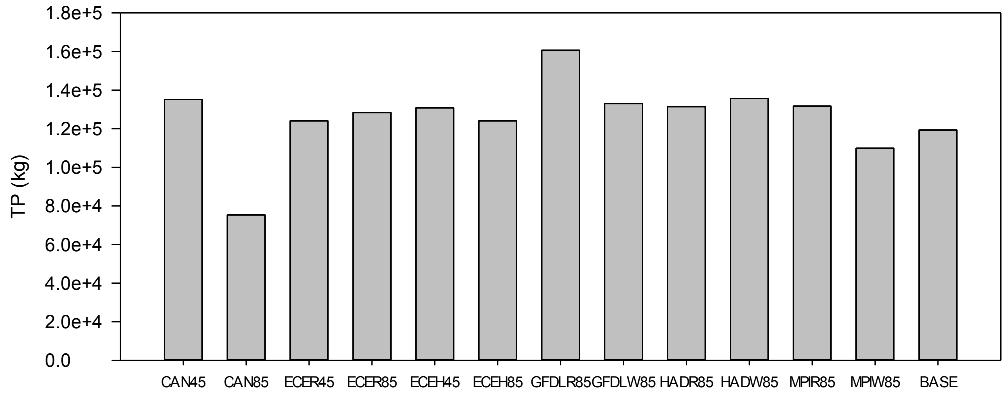

Figure 4.48 Average TP under the baseline and future climate

The simulation results suggest that flow, sediment, NO_3^--N, TN, and TP will increase in the future period compared to the baseline (Table 4.16), which means that the nutrient loadings from the watershed will be more likely to increase with climate changes. Flow, sediment, NO_3^--N, TN, and TP are expected to increase by 13.2, 7.57, 0.44, 0.10, and 9.85%, respectively. Consequently, the pollution caused by agricultural activities will likely worsen in the future.

Table 4.16 Annual water quantity and quality parameters in baseline and future periods

Climate scenario	Flow (m^3/s)	Sediment (ton)	Org-N (kg)	Org-P (kg)	NO_3^--N (kg)	NH_4^+-N (kg)	NO_2^--N (kg)	Min-P (kg)	TN (kg)	TP (kg)
CAN45	5.8E+01	2.5E+05	1.8E+05	5.1E+04	7.4E+05	1.8E+05	9.0E+04	8.4E+04	1.2E+06	1.4E+05
CAN85	4.8E+01	1.8E+05	1.2E+05	2.6E+04	7.2E+05	1.2E+05	7.0E+04	4.9E+04	1.0E+06	7.5E+04
ECER45	5.5E+01	2.2E+05	1.7E+05	4.5E+04	7.5E+05	1.7E+05	9.1E+04	7.9E+04	1.2E+06	1.2E+05
ECER85	5.9E+01	2.4E+05	1.8E+05	4.6E+04	8.4E+05	1.8E+05	9.3E+04	8.2E+04	1.3E+06	1.3E+05
ECEH45	5.3E+01	2.3E+05	1.6E+05	4.8E+04	7.3E+05	1.6E+05	8.3E+04	8.3E+04	1.1E+06	1.3E+05
ECEH85	5.3E+01	2.3E+05	1.6E+05	4.5E+04	7.9E+05	1.6E+05	8.4E+04	7.9E+04	1.2E+06	1.2E+05
GFDLR85	6.3E+01	3.0E+05	1.8E+05	6.0E+04	7.2E+05	1.8E+05	9.4E+04	1.0E+05	1.2E+06	1.6E+05
GFDLW85	5.6E+01	2.4E+05	1.7E+05	5.0E+04	7.0E+05	1.7E+05	8.9E+04	8.3E+04	1.1E+06	1.3E+05
HADR85	5.7E+01	2.9E+05	1.3E+05	4.9E+04	1.3E+06	1.3E+05	7.7E+04	8.3E+04	1.6E+06	1.3E+05
HADW85	6.1E+01	2.5E+05	1.7E+05	4.8E+04	7.7E+05	1.7E+05	9.1E+04	8.7E+04	1.2E+06	1.4E+05
MPIR85	5.7E+01	2.5E+05	1.6E+05	4.9E+04	7.8E+05	1.6E+05	8.6E+04	8.3E+04	1.2E+06	1.3E+05
MPIW85	4.8E+01	2.0E+05	1.5E+05	4.1E+04	6.6E+05	1.5E+05	7.8E+04	6.9E+04	1.0E+06	1.1E+05
Mean	5.7E+01	2.4E+05	1.7E+05	4.8E+04	7.5E+05	1.7E+05	8.7E+04	8.3E+04	1.2E+06	1.3E+05
BASE	5.0E+01	2.3E+05	1.8E+05	4.7E+04	7.4E+05	1.7E+05	9.0E+04	7.2E+04	1.2E+06	1.2E+05

4.5.2.2 Annual reductions of climate change and baseline scenarios over 30 years

The ensemble of climate change experiments covered a broad range of plausible future climate regimes. The modified SWAT model was used to simulate CTD_{200} and CTD_{600} under the baseline and future climate regimes, and the results are shown in Table 4.17 and Figure 4.49. In the future period, the average change when the CTD_{200} is employed instead of the UCTD range from –0.45 to –0.18, –0.30 to 1.30, 6.00 to 9.84, 8.58 to 14.81, –11.62 to –9.19, 5.45 to 10.03, 5.34 to 10.43, 11.55 to 16.24, –6.21 to –2.71, and 10.47 to 15.74% for flow, sediment, Org-N, Org-P, NO_3^--N, NH_4^+-N, NO_2^--N, Min-P, TN, and TP, respectively. In the baseline period from 1981 to 2010, the average reductions by the CTD_{200} scenario were –0.3, 0.1, 4.6, 4.8, –11.7, 5.0, 6.0, 7.1, –5.4, and 6.2 for flow, sediment, Org-N, Org-P, NO_3^--N, NH_4^+-N, NO_2^--N, Min-P, TN, and TP, respectively. The reductions in the baseline period were not significantly different from those in the future, which means that the CTD_{200} scenario under the various climate scenarios works well in the future.

Table 4.17 Annual reductions of CTDs under baseline and climate change scenarios

CTD_{200}	Flow (%)	Sediment (%)	Org-N (%)	Org-P (%)	NO_3^--N (%)	NH_4^+-N (%)	NO_2^--N (%)	Min-P (%)	TN (%)	TP (%)
BASE	-0.30	0.13	4.63	4.84	-11.65	5.02	5.96	7.14	-5.41	6.20
CAN45	-0.31	0.97	8.34	10.01	-9.58	8.30	8.89	12.87	-2.87	11.79
CAN85	-0.45	0.50	6.00	14.81	-9.47	5.45	5.34	16.24	-4.99	15.74
ECER45	-0.26	-0.30	7.57	9.11	-9.22	7.59	8.44	11.77	-3.01	10.84
ECER85	-0.26	0.58	8.35	10.68	-9.31	8.25	9.15	13.55	-3.12	12.51
ECEH45	-0.19	0.57	8.16	8.58	-9.58	8.08	8.75	11.55	-3.27	10.47
ECEH85	-0.29	0.74	7.89	9.34	-11.62	7.88	8.73	12.54	-4.94	11.38
GFDLR85	-0.28	1.09	8.28	8.87	-9.84	8.01	8.63	11.63	-2.76	10.62
GFDLW85	-0.26	0.16	7.90	8.75	-10.38	7.83	8.76	11.74	-3.33	10.62
HADR85	-0.24	1.30	9.84	12.03	-10.43	10.03	10.43	15.13	-6.21	13.99
HADW85	-0.18	0.81	8.78	11.26	-9.19	8.87	9.67	14.12	-2.71	13.11
MPIR85	-0.34	0.75	8.82	9.68	-10.32	8.83	9.54	12.81	-3.58	11.65
MPIW85	-0.29	0.13	8.57	9.76	-10.77	8.38	9.18	12.80	-3.75	11.66
CTD_{600}										
BASE	-0.06	0.00	1.36	1.64	-5.97	1.38	1.50	2.13	-3.21	1.93
CAN45	-0.08	0.31	2.08	2.84	-5.13	2.03	2.05	3.31	-2.45	3.13
CAN85	-0.01	-0.15	0.54	3.19	-2.89	0.31	0.30	3.14	-1.92	3.16
ECER45	-0.07	-0.08	2.28	2.89	-4.00	2.24	2.35	3.35	-1.70	3.21
ECER85	-0.06	0.37	2.31	3.18	-4.19	2.24	2.33	3.69	-1.94	3.50
ECEH45	-0.05	0.06	2.24	2.52	-4.90	2.21	2.38	3.11	-2.37	2.90
ECEH85	-0.06	0.05	2.08	2.67	-5.67	2.01	2.07	3.38	-3.06	3.11
GFDLR85	-0.09	0.34	2.19	2.65	-5.24	2.13	2.28	3.24	-2.34	3.02
GFDLW85	-0.06	0.07	2.13	2.56	-5.97	2.00	2.11	3.15	-2.89	2.93
HADR85	-0.05	0.20	1.84	2.84	-4.30	1.82	1.89	3.10	-3.03	3.01
HADW85	-0.03	0.18	2.52	3.50	-4.43	2.55	2.63	4.05	-1.94	3.87
MPIR85	-0.07	0.35	2.35	2.85	-5.04	2.34	2.45	3.58	-2.45	3.31
MPIW85	-0.06	-0.04	2.14	2.71	-4.89	2.00	2.10	3.13	-2.37	2.97

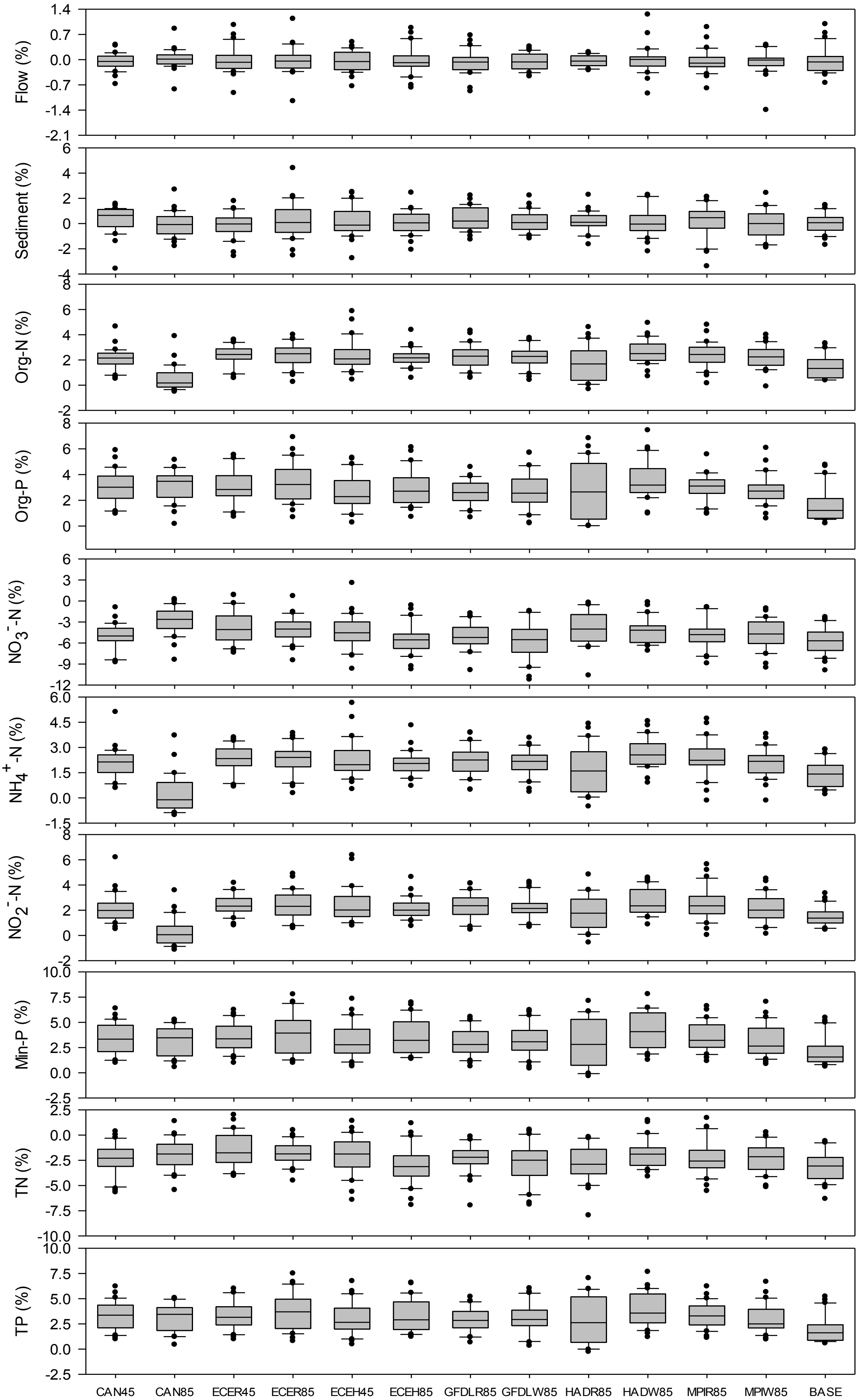

Figure 4.49 Annual reductions of CTD_{600} under baseline and climate change scenarios

The changes when UCTD is replaced by CTD_{600} in the 12 climate experiments ranged from –0.09 to –0.18, –0.15 to 0.37, 6.00 to 9.84, 8.58 to 14.81, –11.62 to –9.19, 5.45 to 10.03, 11.55 to 16.24, –6.21 to –2.71, and 10.47 to 15.74% for flow, sediment, Org-N, Org-P, NO_3^--N, NH_4^+-N, NO_2^--N, Min-P, TN, and TP, respectively. In the baseline period from 1981 to 2010, the average changes by the CTD_{600} scenario were –0.1, 0.0, 1.4, 1.6, –6.0, 1.4, 1.5, 2.1, –3.2, and 1.9 for flow, sediment, Org-N, Org-P, NO_3^--N, NH_4^+-N, NO_2^--N, Min-P, TN, and TP, respectively. The CTD_{600} behaved the same as the CTD_{200} scenario under the 12 climate scenarios, and it functioned well under the future dynamic climates.

Thus, compared to the baseline, the outputs, flow, sediment, NO_3^--N, TN, and TP of the climate change scenarios increase in the watershed, and subsequently the pollution from the agricultural field will deteriorate under the current uncontrolled tile drainage. Comparisons between the simulations for the baseline period and the predicted period of the CTD scenarios indicate that the CTD scenarios performed effectively and stably with the current modeling settings using the improved SWAT model.

5 Modeling the Ecological Impacts of CTD on River Using QUAL2Kw

5.1 Rationale

As described in Section 1.2.1, although many studies have examined CTD for fields or watersheds, there has been no assessment of the environmental effects of CTD on combined watershed and river system. Most CTD studies have focused on how much pollutants can migrate from either a field or watershed, but did not further assess the ecological impacts of CTD on a river system. Therefore, this chapter intends to further investigate the ecological effects of CTD on a river system by coupling the watershed water quality model SWAT and the river water quality model QUAL2Kw.

5.2 Methodology and parameterization

5.2.1 Study river

The South Nation River runs for about 175 km and has several major branches, i.e., the North Branch South Nation River, Sandy Creek, Payne River, Castor River, Moose Creek, Bear Brook, Scotch River, and Caledonia Creek. In this study, the main channel of the river from the source to Plantagenet in Ontario was modeled. The total length of the river in the model is 152 km.

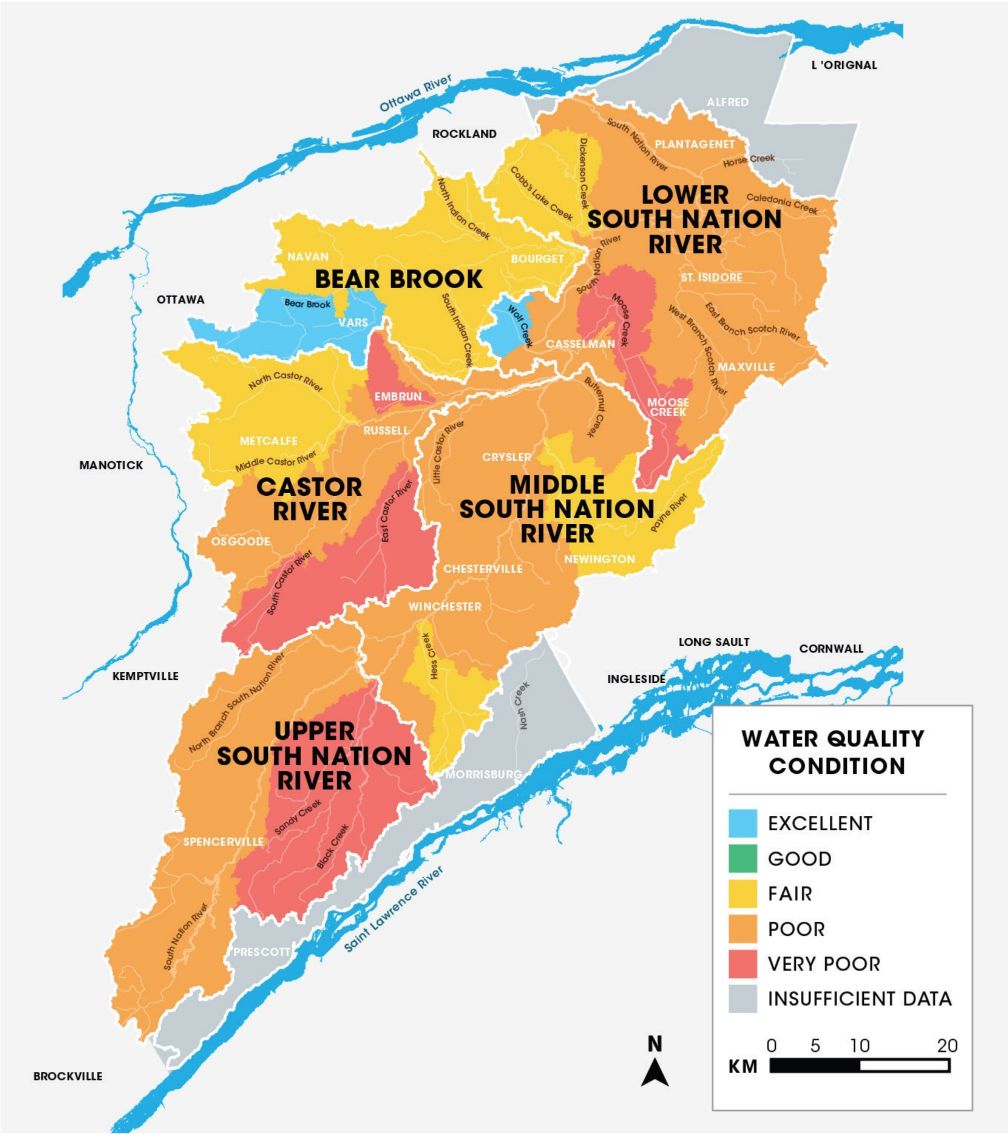

Figure 5.1 State of the surface water quality of South Nation River

The surface water quality of the South Nation River and its branches varies from excellent to very poor, as shown in Figure 5.1 (South Nation Conservation, 2018).

5.2.2 Segmentation of the river for the QUAL2Kw model

As descripted in Section 2.5, the model simulates the main channel of a river through smaller segments, which are obtained by subdividing the channel into smaller units. Based on the watershed delineation by the SWAT model (Figure 5.2), the main channel of the river was segmented into 10 smaller units with nine branches, as shown in Figure 5.3.

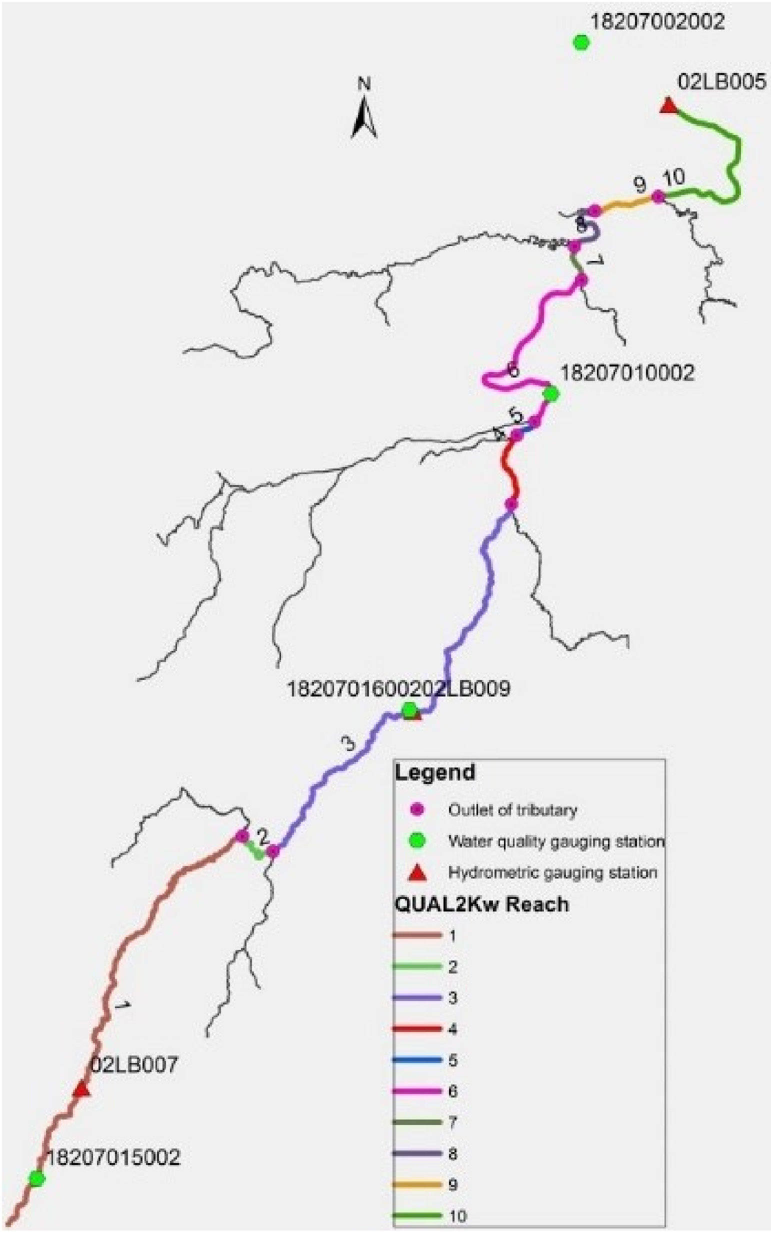

Figure 5.2 Reaches of the QUAL2Kw model

The flow, sediment, and N and P compounds from the SWAT model for the nine branches of the river are presented as point sources flowing into the main channel at corresponding positions (outlets of tributaries). Meanwhile, the output of the main channel (reaches) from the SWAT model contributes directly to the reaches in the QUAL2Kw model.

Figure 5.3 Segmentation of river and locations of pollution sources

5.2.3 Preparation of the inputs for the QUAL2Kw model

The model is integrated in Microsoft Excel and programmed in the Visual Basic for Applications (VBA) language, and a set of predesigned worksheets in Excel are used as the graphical user interface to prepare inputs for the model.

As a complex model aimed at simulating the water quality of a river or stream, running QUAL2Kw requires numerous types of parameters (Chapra, 2012). These parameters can be grouped into several categories: river geometric parameters, such as stream length and reach segment; meteorological parameter, such as air temperature, dew point, wind speed, solar radiation, cloud cover, and shade; hydrologic parameters, such as headwater, tributary inflow, and diversions; hydraulic parameters, such as slope and bottom roughness; water quality parameters, such as inflow and upstream boundary conditions; effluent parameters, such as flow rates and concentrations; and reaction rate parameters, such as oxidation, reaction, and settling rate coefficients (US EPA, 1997). Some of these can be obtained from observations and the outputs of the SWAT model, and the others have to be based on empirical estimations (model default).

5.2.3.1 Inputs from the observations

The water quality parameters, such as alkalinity, conductivity, dissolved oxygen, and pH, were retrieved from the database of the Provincial (Stream) Water Quality Monitoring Network (PWQMN) (Ontario Ministry of the Environment, 2015). This network only works on a seasonal basis, typically from May to November, and the sampling frequency is once monthly at gauging stations. In this study, the water quality and effluent data came from four water quality gauging stations, 18207015002, 18207016002, 18207010002, and 18207002002, which are located on reaches one, three, six, and 10, respectively, as shown in Figure 5.2.

Diel meteorological parameters, air temperature, dew point, wind speed, solar radiation, and cloud cover data were obtained from the Canadian Weather Energy and Engineering Datasets (CWEEDS) (Environment Canada, 2017).

5.2.3.2 Inputs from the SWAT model

5.2.3.2.1 Inputs of the QUAL2Kw model and outputs of the SWAT model

All the river's geometric parameters, e.g., the length and elevation of each reach, latitude, and longitude, were generated by the SWAT model, and were derived from the DEM. Also, the flow, sediment, and water quality parameters for the main channel and branches of the river, i.e., NH_4^+-N, NO_2^--N, NO_3^--N, Org-N, Min-P, and Org-P, were calculated based on the outputs of the SWAT model.

The time scale for the outputs of the SWAT model is daily, while the QUAL2Kw model requires hourly inputs, so the outputs of the SWAT model must be interpolated into a diel time scale. Moreover, the outputs of the SWAT model are mostly in weight form, e.g., kg and tonnes, however, the QUAL2Kw model uses concentration for its input and output, and therefore the units of weight must be converted into concentration, e.g., mg/l and ug/l.

5.2.3.2.2 Conversion of the SWAT model outputs into the inputs of the QUAL2Kw model

Unlike the SWAT model, which runs on a daily basis and is capable of long-term simulations, the QUAL2Kw model runs on a diel heat budget and on diel water quality kinetics; hence, it is essentially a diel model demanding hourly inputs. The required inputs for the QUAL2Kw model – flow, sediment, NH_4^+-N, NO_2^--N, NO_3^--N, Org-N, Min-P, and Org-P – were retrieved by output.rch, the main channel output file of the SWAT model, which contains summary information for each routing reach in the watershed.

5.2.3.2.2.1 Headwater

A worksheet (Figure 5.4) is used to enter the flow and concentration for the system's boundaries. The headwater came from the inflow of sub-watershed 31 in the SWAT model (reach 31), and the nutrient concentrations can be calculated by using the inflow and nutrient mass. For instance, the calculation formula of the concentration of NO_3^--N is defined, as in Equation 5.1.

$$Concentration_{NO_3^- - N} = \frac{Mass_{NO_3^- - N}(kg) \times 100000000(\frac{\mu g}{kg})}{Inflow(\frac{m^3}{s}) \times 24 \times 60 \times 60(s) \times 1000(\frac{L}{m^3})} \qquad \text{Equation 5.1}$$

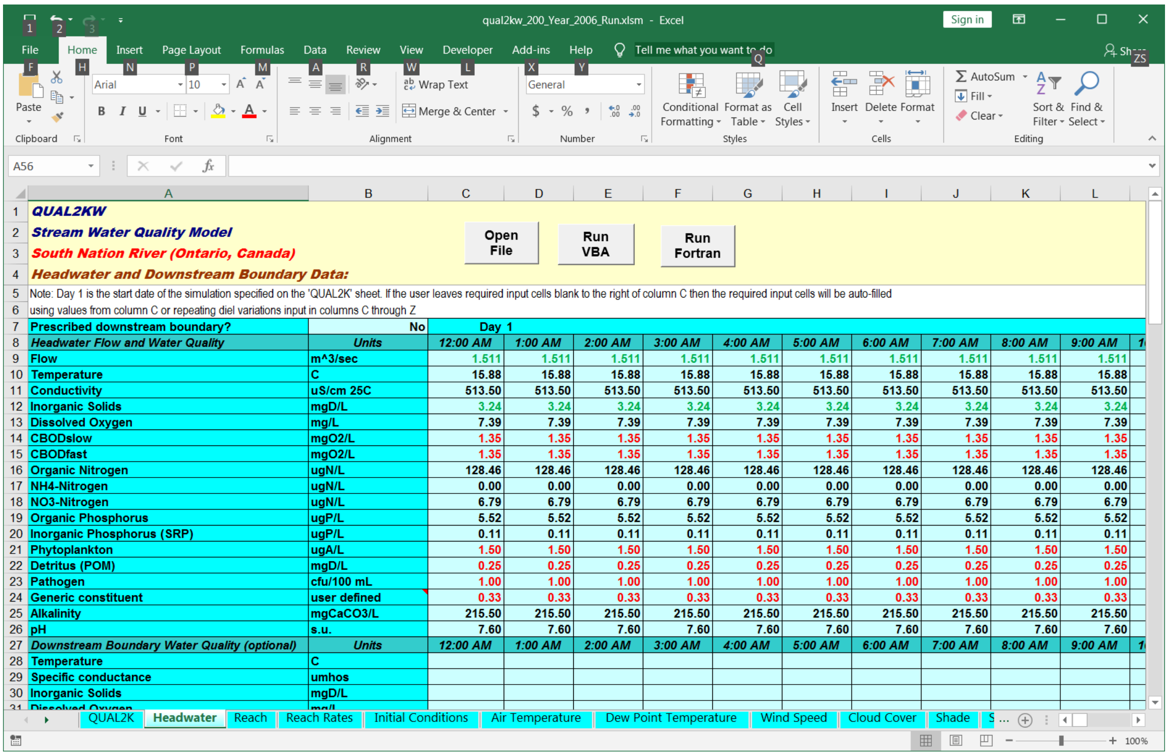

Prescribed downstream boundary?	No	Day 1									
Headwater Flow and Water Quality	**Units**	12:00 AM	1:00 AM	2:00 AM	3:00 AM	4:00 AM	5:00 AM	6:00 AM	7:00 AM	8:00 AM	9:00 AM
Flow	m^3/sec	1.511	1.511	1.511	1.511	1.511	1.511	1.511	1.511	1.511	1.511
Temperature	C	15.88	15.88	15.88	15.88	15.88	15.88	15.88	15.88	15.88	15.88
Conductivity	uS/cm 25C	513.50	513.50	513.50	513.50	513.50	513.50	513.50	513.50	513.50	513.50
Inorganic Solids	mgD/L	3.24	3.24	3.24	3.24	3.24	3.24	3.24	3.24	3.24	3.24
Dissolved Oxygen	mg/L	7.39	7.39	7.39	7.39	7.39	7.39	7.39	7.39	7.39	7.39
CBODslow	mgO2/L	1.35	1.35	1.35	1.35	1.35	1.35	1.35	1.35	1.35	1.35
CBODfast	mgO2/L	1.35	1.35	1.35	1.35	1.35	1.35	1.35	1.35	1.35	1.35
Organic Nitrogen	ugN/L	128.46	128.46	128.46	128.46	128.46	128.46	128.46	128.46	128.46	128.46
NH4-Nitrogen	ugN/L	0.00	0.00	0.00	0.00	0.00	0.00	0.00	0.00	0.00	0.00
NO3-Nitrogen	ugN/L	6.79	6.79	6.79	6.79	6.79	6.79	6.79	6.79	6.79	6.79
Organic Phosphorus	ugP/L	5.52	5.52	5.52	5.52	5.52	5.52	5.52	5.52	5.52	5.52
Inorganic Phosphorus (SRP)	ugP/L	0.11	0.11	0.11	0.11	0.11	0.11	0.11	0.11	0.11	0.11
Phytoplankton	ugA/L	1.50	1.50	1.50	1.50	1.50	1.50	1.50	1.50	1.50	1.50
Detritus (POM)	mgD/L	0.25	0.25	0.25	0.25	0.25	0.25	0.25	0.25	0.25	0.25
Pathogen	cfu/100 mL	1.00	1.00	1.00	1.00	1.00	1.00	1.00	1.00	1.00	1.00
Generic constituent	user defined	0.33	0.33	0.33	0.33	0.33	0.33	0.33	0.33	0.33	0.33
Alkalinity	mgCaCO3/L	215.50	215.50	215.50	215.50	215.50	215.50	215.50	215.50	215.50	215.50
pH	s.u.	7.60	7.60	7.60	7.60	7.60	7.60	7.60	7.60	7.60	7.60
Downstream Boundary Water Quality (optional)	**Units**	12:00 AM	1:00 AM	2:00 AM	3:00 AM	4:00 AM	5:00 AM	6:00 AM	7:00 AM	8:00 AM	9:00 AM
Temperature	C										
Specific conductance	umhos										
Inorganic Solids	mgD/L										

Figure 5.4 Headwater inputs of the QUAL2Kw model

Similarly, the other parameters, i.e., the inorganic suspended solid (sediment), NH_4^+-N, NO_3^--N, Org-N, Min-P, and Org-P, can be calculated from the output.rch file. The columns for these parameters in the output.rch file are listed in Table 5.1.

Table 5.1 Column of headwater parameter in output.rch

No.	Parameter	Column
1	Flow	6
2	Sediment	10
3	Org-N	13
4	Org-P	15
5	NO_3^--N	17
6	NH_4^+-N	19
7	Min-P	23

5.2.3.2.2.2 Continuous sources

Continuous simulations need continuous source inputs. Continuous sources include two parts, main channel reaches (Figure 5.5) and branches (inflows from tributaries) (Figure 5.6).

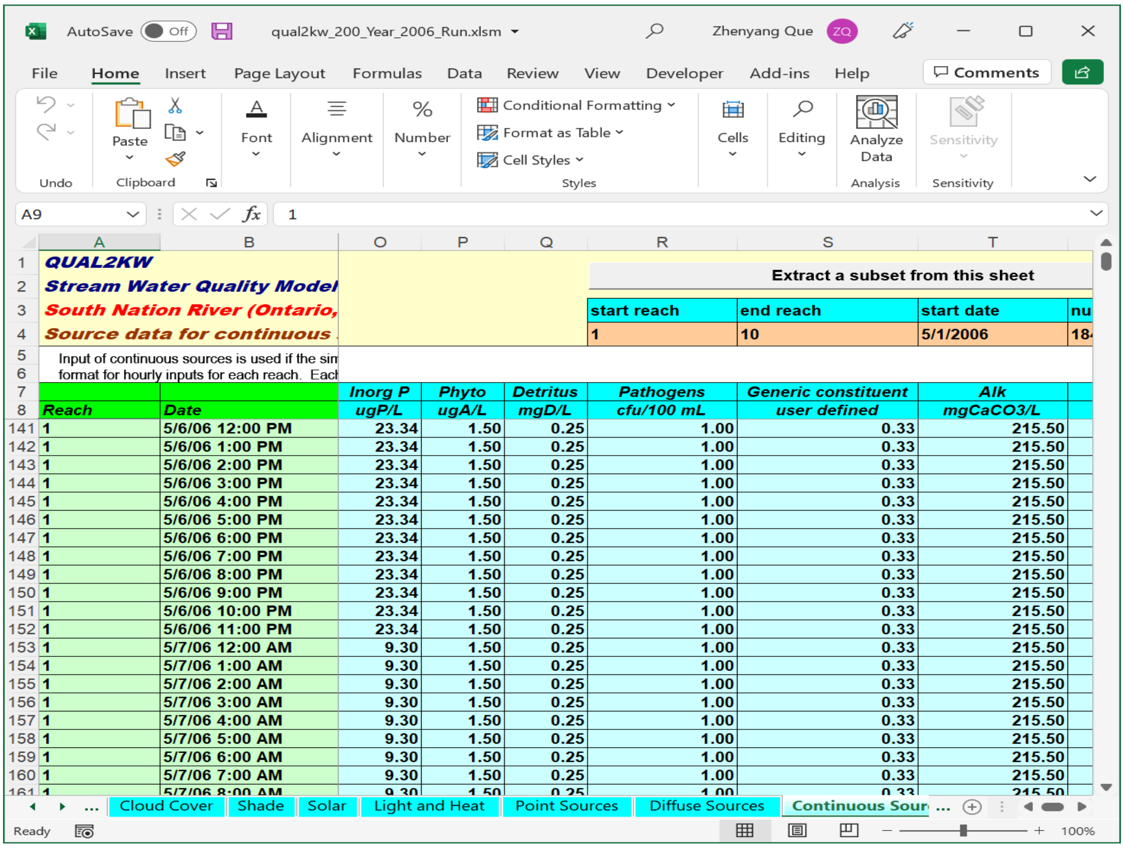

Figure 5.5 Reach inputs of the QUAL2Kw model

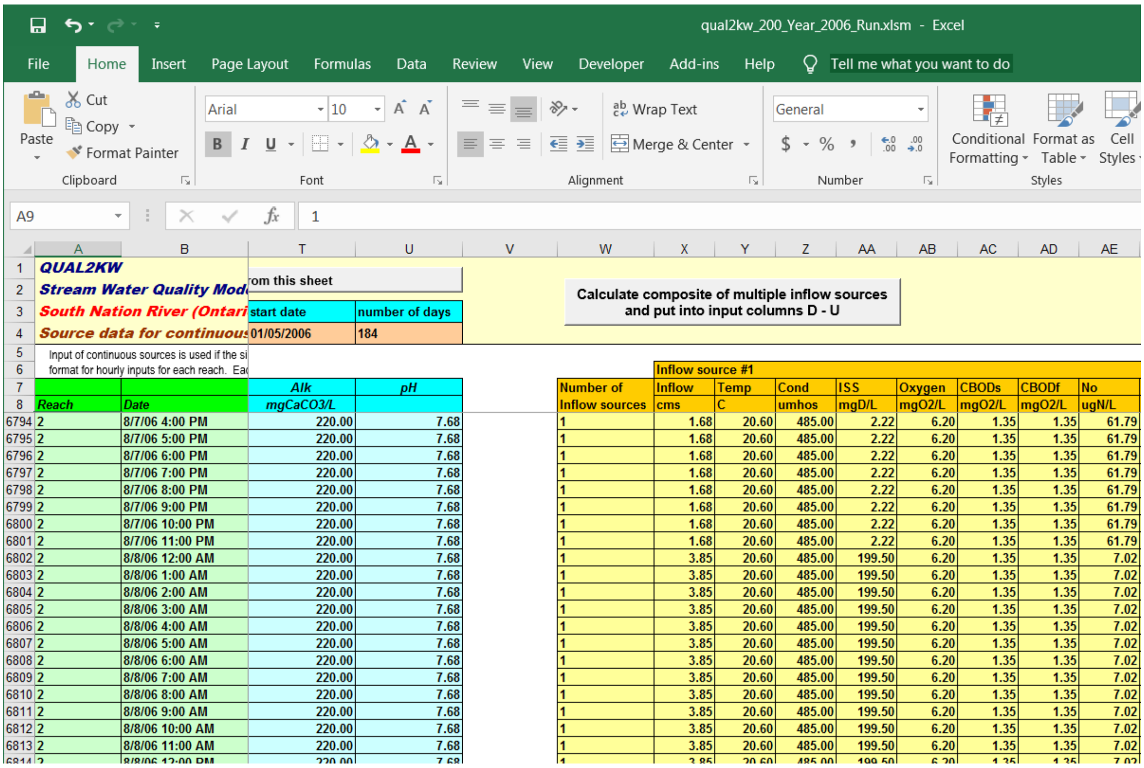

Figure 5.6 Inflow source inputs of the QUAL2Kw model

Based on Figures 4.8, 5.2, and 5.3, the corresponding reaches of the output.rch file for the main channel and branches of the QUAL2Kw model and the SWAT model are shown in Tables 5.2 and 5.3.

Table 5.2 Corresponding reaches for reach inputs

Reach in QUAL2Kw	Reach in SWAT
1	31
2	26
3	25
4	20
5	14
6	13
7	6
8	4
9	2
10	1

Table 5.3 Corresponding reaches for inflow source inputs

Reach in QUAL2Kw	Reach in SWAT
1	
2	27
3	28
4	22
5	15
6	16
7	11
8	5
9	3
10	7

The columns for these parameters in the output.rch file are listed in Table 5.4.

Table 5.4 Column of reach and inflow source parameter in output.rch

No.	Parameter	Column
1	Flow	7
2	Sediment	11
3	Org-N	14
4	Org-P	16
5	NO_3^--N	18
6	NH_4^+-N	20
7	NO_2^--N	22
8	Min-P	24

After all the daily input parameters are retrieved and calculated from the output.rch file, they have to be converted into a diel format (24 hours). Diel data equal to daily data. There are 184 days in one growing season from May 1st to October 31st, so there will be 184 × 24 = 4416 records for each parameter each year. The five years of the simulations for the three scenarios demand 4416 × 5 × 3 × 19 (reach) = 1,258,560 records for each parameter.

5.2.4 CTD and UCTD scenarios for the QUAL2Kw model

In order to evaluate the effects of CTD on the water quality of the river, the CTD and UCTD scenarios for the QUAL2Kw model were developed based on the outputs of the CTD and UCTD scenarios of the SWAT model. To be more precise, the scenario at 200 mm of the tile drainage depth for the model, CTD200, employed outputs from the CTD_{200} scenario simulated by the improved SWAT model. Similarly, the scenario at 600 mm (CTD600) and the UCTD scenario (UCTD) were designed based on the outputs of the CTD_{600} and UCTD scenarios of the improved SWAT model, respectively. The outputs from the CTD and UCTD scenarios simulated by the improved SWAT model for the branches of the river, sediment, NH_4^+-N, NO_2^--N, NO_3^--N, Org-N, TN, Min-P, Org-P, and TP, were transformed into form of concentration as the input parameters for the QUAL2K model, and the other parameters required by the QUAL2Kw model remained the same. As a result, the effects of CTD on the water quality of the river can be evaluated by the CTD scenarios.

Although the model is capable of continuous simulation, it has a limit of 365 days, as mentioned previously. Continuous simulation requires a vast number of hourly inputs. In this study, the model simulated five seasons of growth from 2006 to 2010. With the simulation time limit, this study had to set up a yearly model, and thus 15 models were built for the three scenarios and the five years.

5.2.5 Calibration and verification of the QUAL2Kw model

5.2.5.1 Limitation of the automatic calibration procedure and manual extension

QUAL2Kw uses a genetic algorithm that modifies the kinetic rate parameters and constants to find a best fit for a model application compared to observations (Pelletier et al., 2006). The automatic calibration approach adopts a subroutine developed by Charbonneau and Knapp (1995). This approach calculates the RMSE between the simulated and the observed data, and the inverse of the RMSE for all the parameters in the calibration are defined as the "goodness of fit", which indicates the performance of the model. Therefore, the model performs better when the RMSE decreases and the fitness increases.

However, the QUAL2Kw model can only be calibrated and verified automatically on one specific day, so in order to calibrate and verify the model for a longer period, this study calibrated and verified the model manually to extend it to three seasons of growth from 2006 to 2008, and two seasons of growth from 2009 to 2010 respectively. By doing so, the model was calibrated and verified for five consecutive growing seasons from 2006 to 2010, and it improved and secured the performance of the model.

5.2.5.2 The observed data and the periods of the calibration and verification

As a one-dimensional diel kinetics river water-quality model, QUAL2Kw is capable of continuous simulation with a limitation of 365 days. The calibration and verification days were chosen based on the availability of the observed water quality and quantity data from the PWQMN and the Canadian hydrometric data, which is operated by Ontario Ministry of the Environment and Environment and Climate Change Canada, respectively.

The PWQMN in the watershed was operated monthly, so the observations of the water quality for the river were only available on specific day in a month during the seasons of growth. Similarly, the hydrometric data and flow were discrete and only available on some days at certain hydrometric gauging stations.

To calibrate and verify the QUAL2Kw model, eight types of data, i.e., alkalinity, DO, electrical conductivity (EC), flow, pH, temperature (T), TN, and TP, were obtained from four water quality gauging stations, coded as 18207015002, 18207016002, 18207010002, and 18207002002, and two hydrometric gauging stations, 02LB007 and 02LB005, along the river (Figure 5.2). To be in accordance with the periods of the calibration and validation of the SWAT model, the calibration period was set as the three seasons of growth from 2006 to 2008, and the validation period was the two seasons of growth from 2009 to 2010.

5.2.5.3 Measurements of the performance of the calibration and verification

In this study, the subtlety of the QUAL2Kw model's calibration and verification was demonstrated both graphically and statistically. Graphs provided a visual method to examine the agreement between the simulated and observed data, and statistical indices gave a numerical way to evaluate the performance of the model for the simulation. The adopted statistical index was calculated as relative RMSE (RRMSE), as shown below.

$$RRMSE = \frac{RMSE}{\bar{O}} \qquad 5.2$$

where $\bar{O}$ is the mean of the observed data. The value of 0 for RRMSE is for an ideal situation, while a value between 0.0 and 1.0 is acceptable for the performance of the model to simulate a river (Gikas, 2014).

5.2.5.4 Calibration of the QUAL2Kw model

Using the observed water quality and hydrometric data from the four water quality gauging stations and two hydrometric gauging stations along the river, the model was calibrated and verified using eight parameters, that affected the water quality of the river the most. Figure 5.7 and Table 5.5 present the calibration results of the QUAL2Kw model.

- ❖ Alkalinity

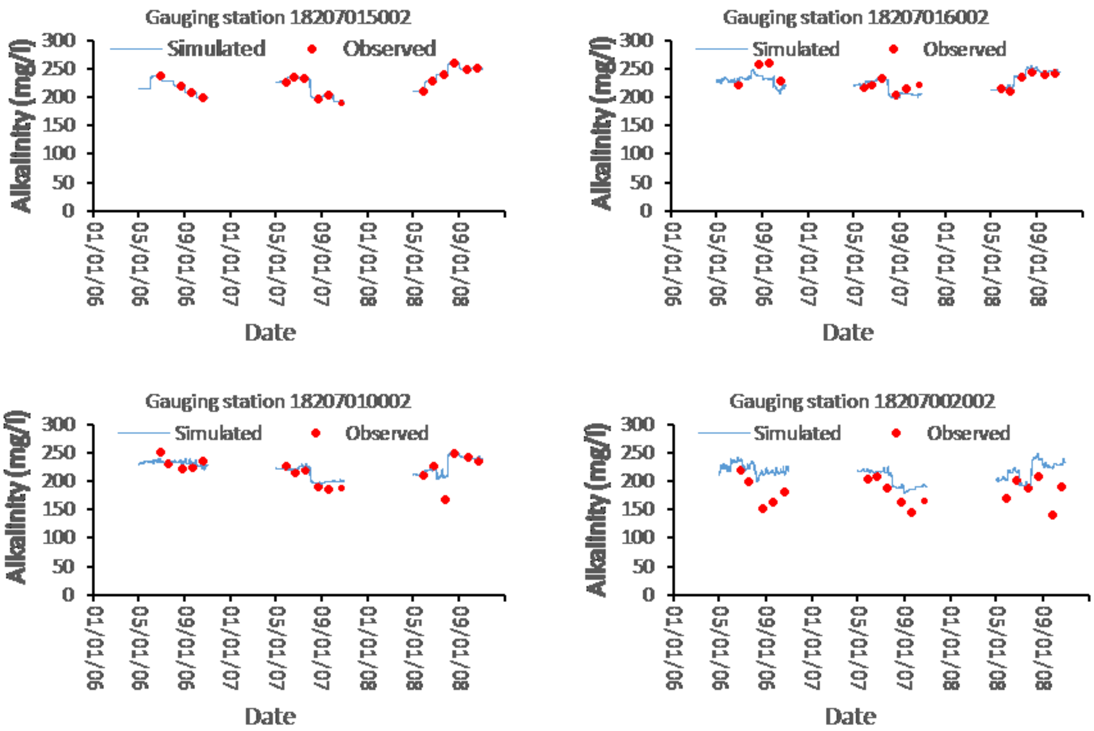

❖ DO

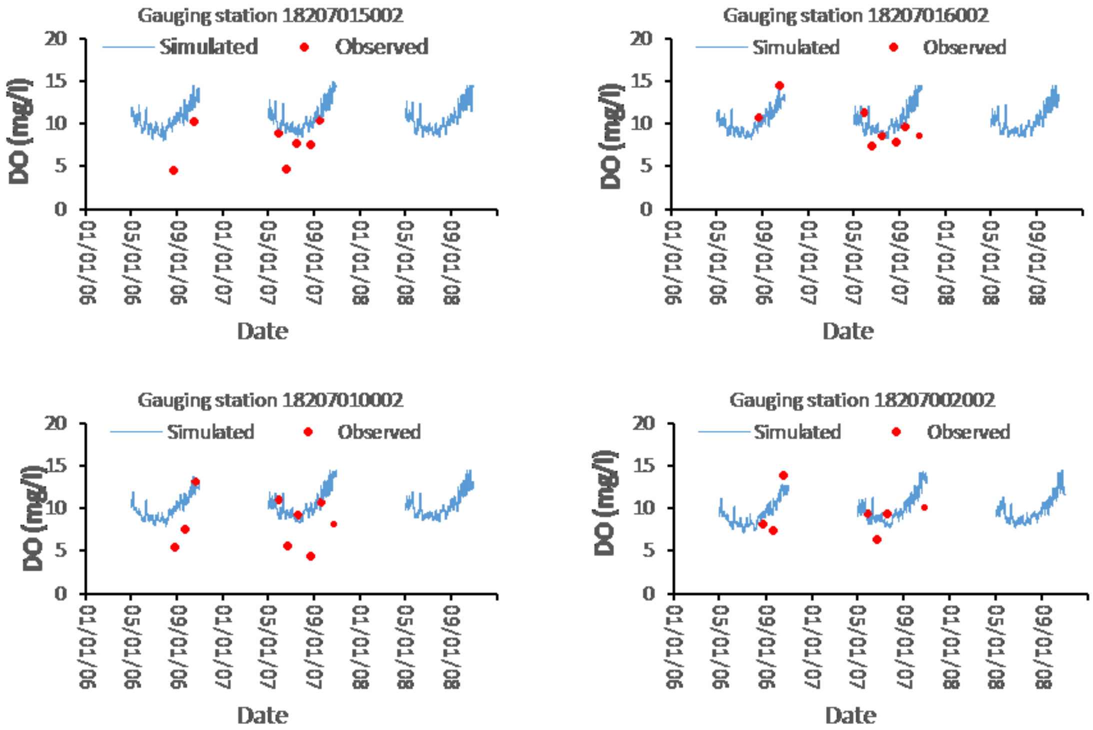
Gauging station 18207015002
Gauging station 18207016002
Gauging station 18207010002
Gauging station 18207002002
Simulated
Observed
DO (mg/l)
0
5
10
15
20
01/01/06
05/01/06
09/01/06
01/01/07
05/01/07
09/01/07
01/01/08
05/01/08
09/01/08
Date

❖ EC

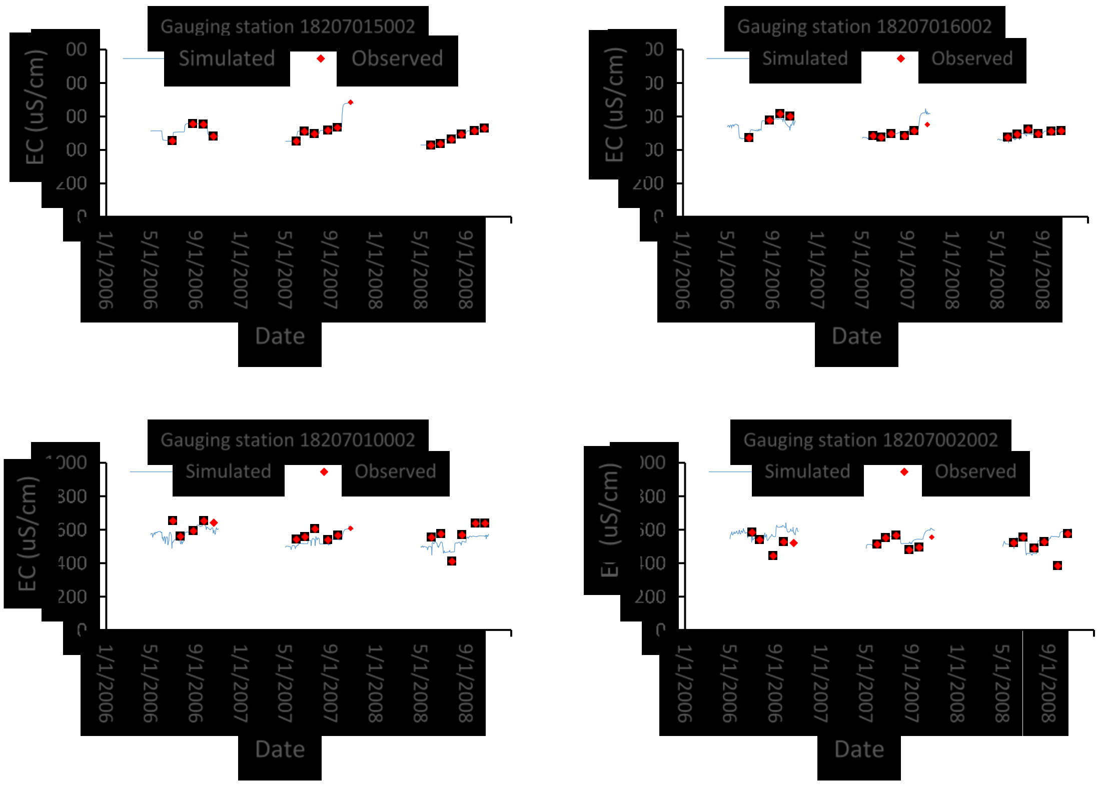
Gauging station 18207015002
Gauging station 18207016002
Gauging station 18207010002
Gauging station 18207002002
Simulated
Observed
EC (uS/cm)
1/1/2006
5/1/2006
9/1/2006
1/1/2007
5/1/2007
9/1/2007
1/1/2008
5/1/2008
9/1/2008
Date

❖ Flow

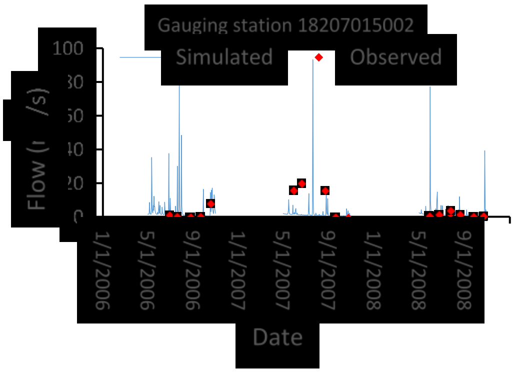
Gauging station 18207015002
Simulated
Observed
100
Date
1/1/2006
5/1/2006
9/1/2006
1/1/2007
5/1/2007
9/1/2007
1/1/2008
5/1/2008
9/1/2008

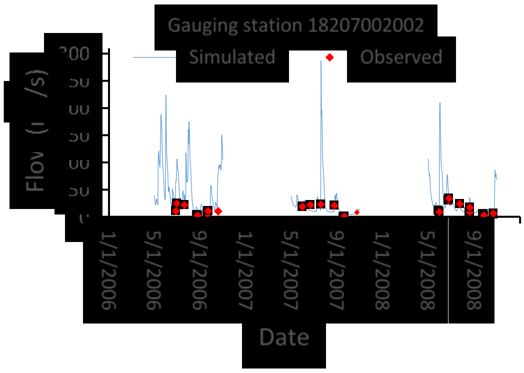
Gauging station 18207002002
Simulated
Observed
Date
1/1/2006
5/1/2006
9/1/2006
1/1/2007
5/1/2007
9/1/2007
1/1/2008
5/1/2008
9/1/2008

❖ pH

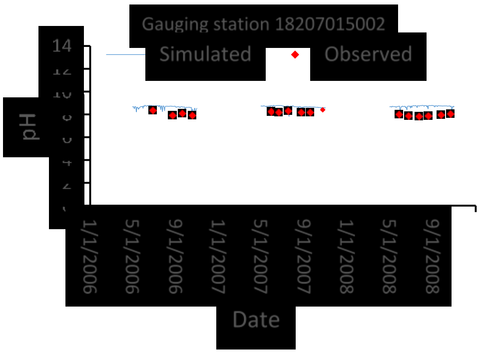
Gauging station 18207015002
Simulated
Observed
14
pH
Date
1/1/2006
5/1/2006
9/1/2006
1/1/2007
5/1/2007
9/1/2007
1/1/2008
5/1/2008
9/1/2008

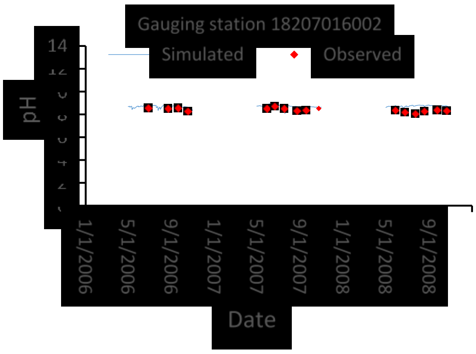
Gauging station 18207016002
Simulated
Observed
14
pH
Date
1/1/2006
5/1/2006
9/1/2006
1/1/2007
5/1/2007
9/1/2007
1/1/2008
5/1/2008
9/1/2008

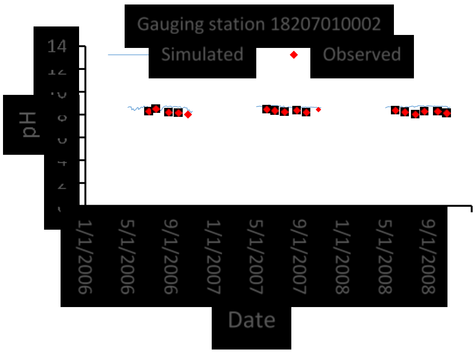
Gauging station 18207010002
Simulated
Observed
14
pH
Date
1/1/2006
5/1/2006
9/1/2006
1/1/2007
5/1/2007
9/1/2007
1/1/2008
5/1/2008
9/1/2008

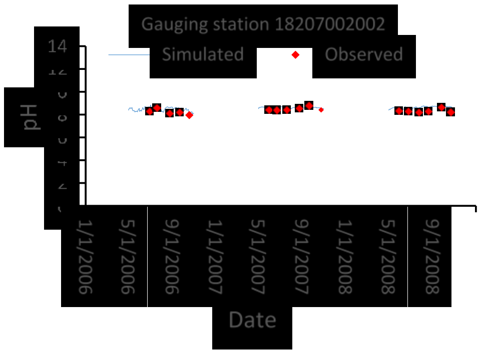
Gauging station 18207002002
Simulated
Observed
14
pH
Date
1/1/2006
5/1/2006
9/1/2006
1/1/2007
5/1/2007
9/1/2007
1/1/2008
5/1/2008
9/1/2008

❖ T

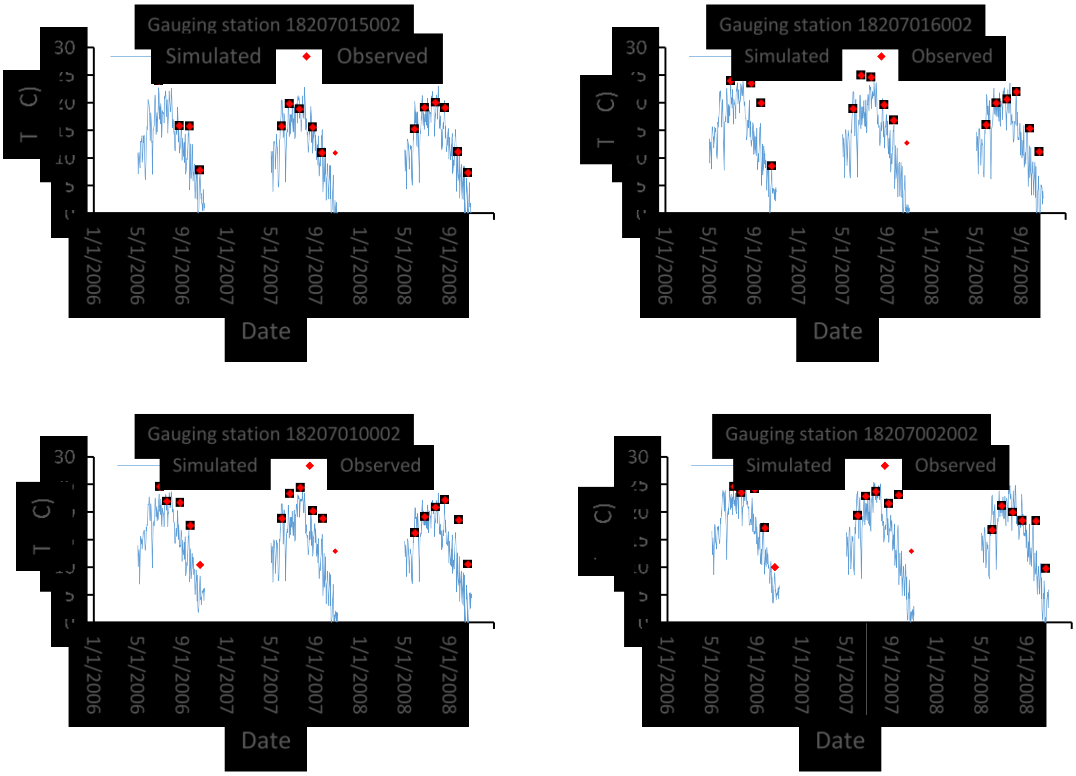
Gauging station 18207015002
Simulated
Observed
Gauging station 18207016002
Gauging station 18207010002
Gauging station 18207002002
30
1/1/2006
5/1/2006
9/1/2006
1/1/2007
5/1/2007
9/1/2007
1/1/2008
5/1/2008
9/1/2008
Date

❖ TN

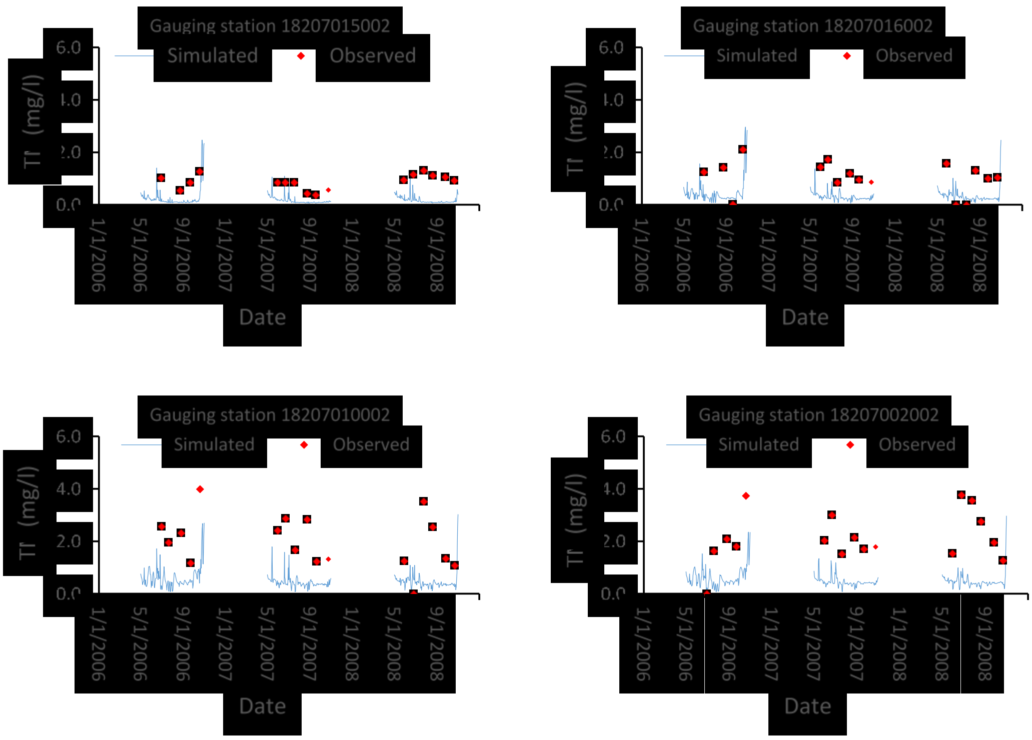
Gauging station 18207015002
Simulated
Observed
Gauging station 18207016002
Gauging station 18207010002
Gauging station 18207002002
(mg/l)
6.0
4.0
2.0
0.0
1/1/2006
5/1/2006
9/1/2006
1/1/2007
5/1/2007
9/1/2007
1/1/2008
5/1/2008
9/1/2008
Date

❖ TP

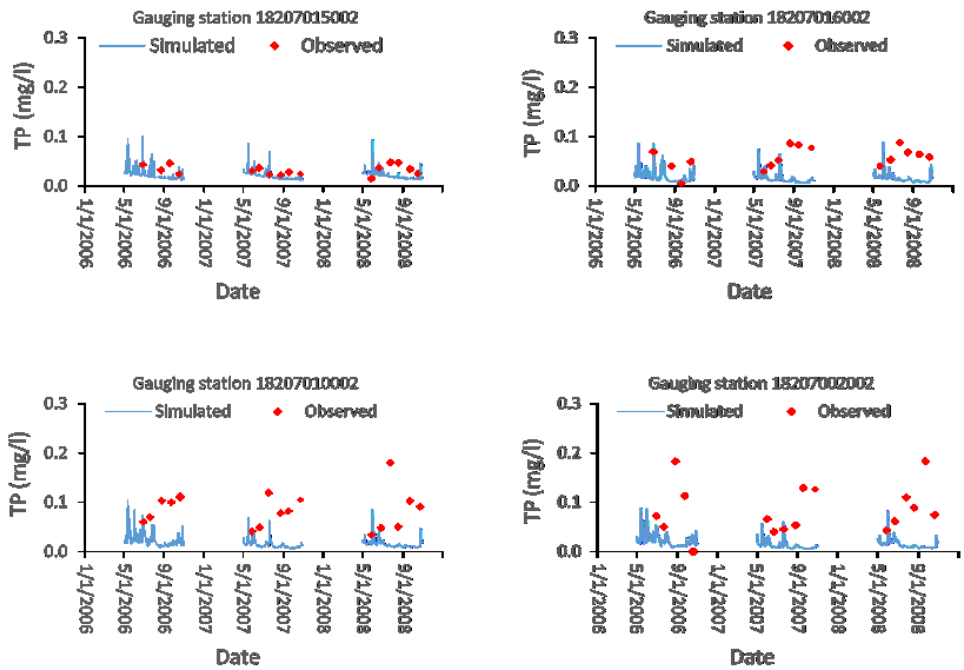

Figure 5.7 Calibration of QUAL2Kw in three growing seasons from 2006 to 2008

5.2.5.5 Verification of the QUAL2Kw model

Based on the availability of the observed water quality data from the four water quality gauging stations and the flow data from the two hydrometric gauging stations along the river, the calibrated model was verified using the observed data for the two seasons of growth from 2009 to 2010.

❖ Alkalinity

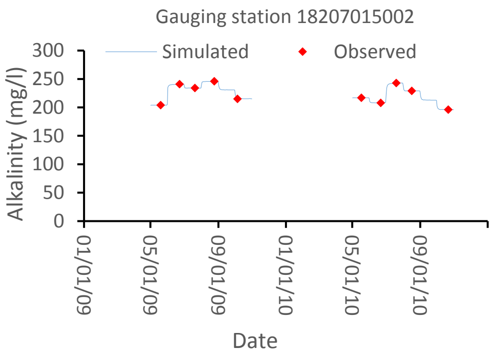

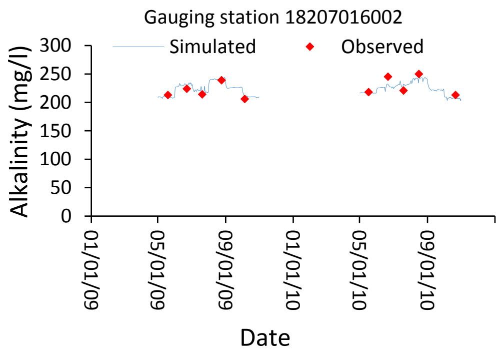

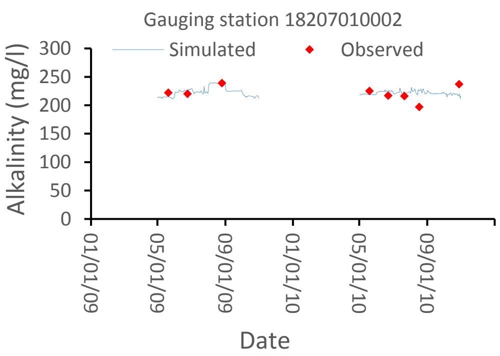

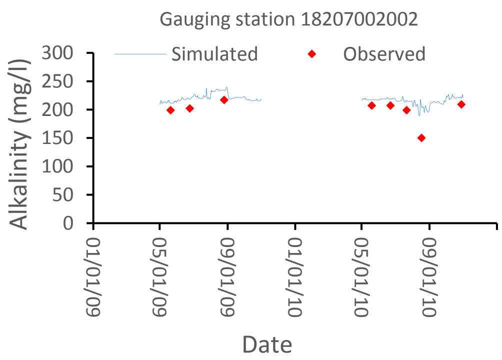

❖ DO

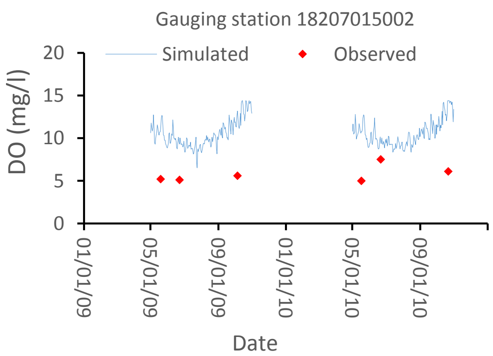

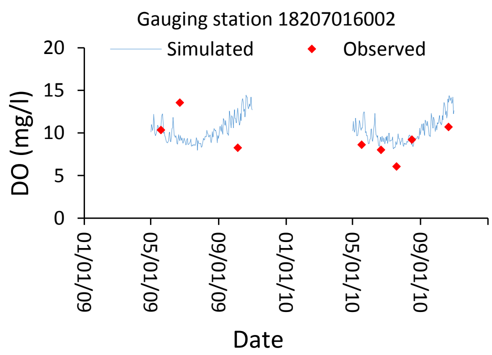

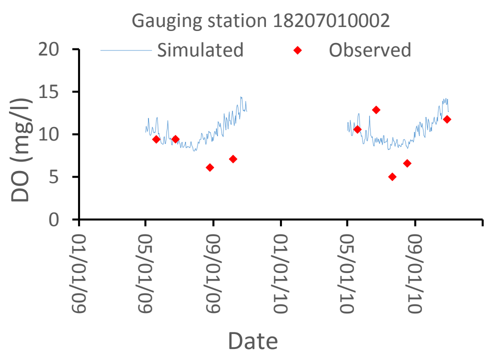

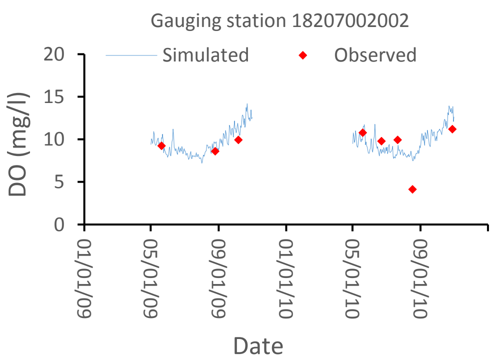

- EC

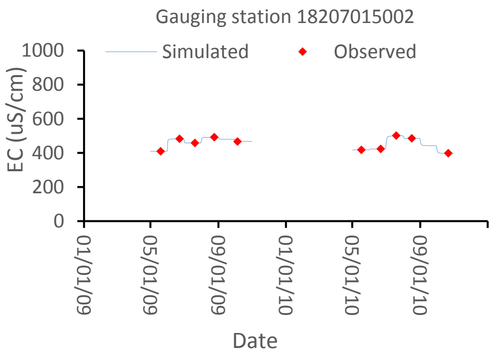
Gauging station 18207015002
Simulated
Observed
EC (uS/cm)
1000
800
600
400
200
0
01/01/09
05/01/09
09/01/09
01/01/10
05/01/10
09/01/10
Date

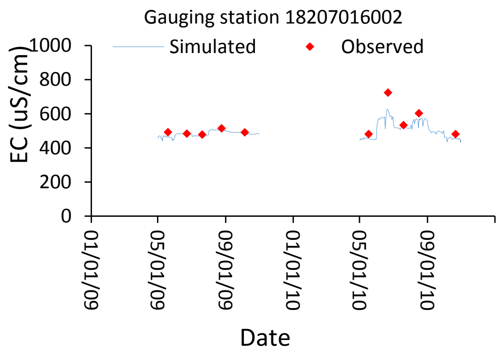
Gauging station 18207016002
Simulated
Observed
EC (uS/cm)
1000
800
600
400
200
0
01/01/09
05/01/09
09/01/09
01/01/10
05/01/10
09/01/10
Date

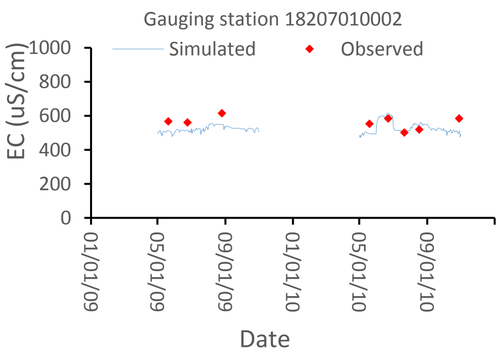
Gauging station 18207010002
Simulated
Observed
EC (uS/cm)
1000
800
600
400
200
0
01/01/09
05/01/09
09/01/09
01/01/10
05/01/10
09/01/10
Date

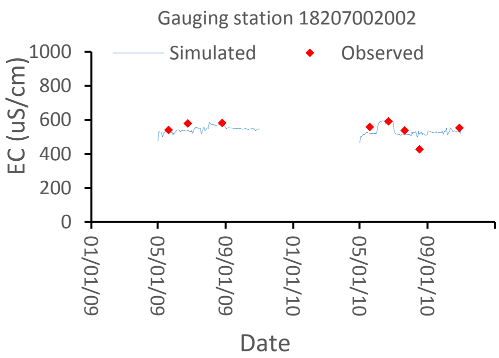
Gauging station 18207002002
Simulated
Observed
EC (uS/cm)
1000
800
600
400
200
0
01/01/09
05/01/09
09/01/09
01/01/10
05/01/10
09/01/10
Date

- Flow

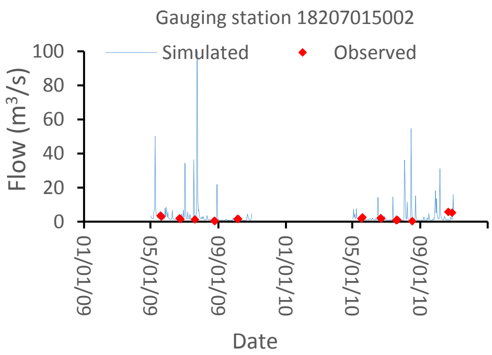
Gauging station 18207015002
Simulated
Observed
Flow (m3/s)
100
80
60
40
20
0
01/01/09
05/01/09
09/01/09
01/01/10
05/01/10
09/01/10
Date

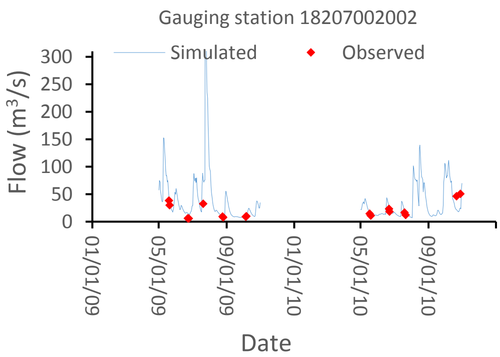
Gauging station 18207002002
Simulated
Observed
Flow (m3/s)
300
250
200
150
100
50
0
01/01/09
05/01/09
09/01/09
01/01/10
05/01/10
09/01/10
Date

❖ pH

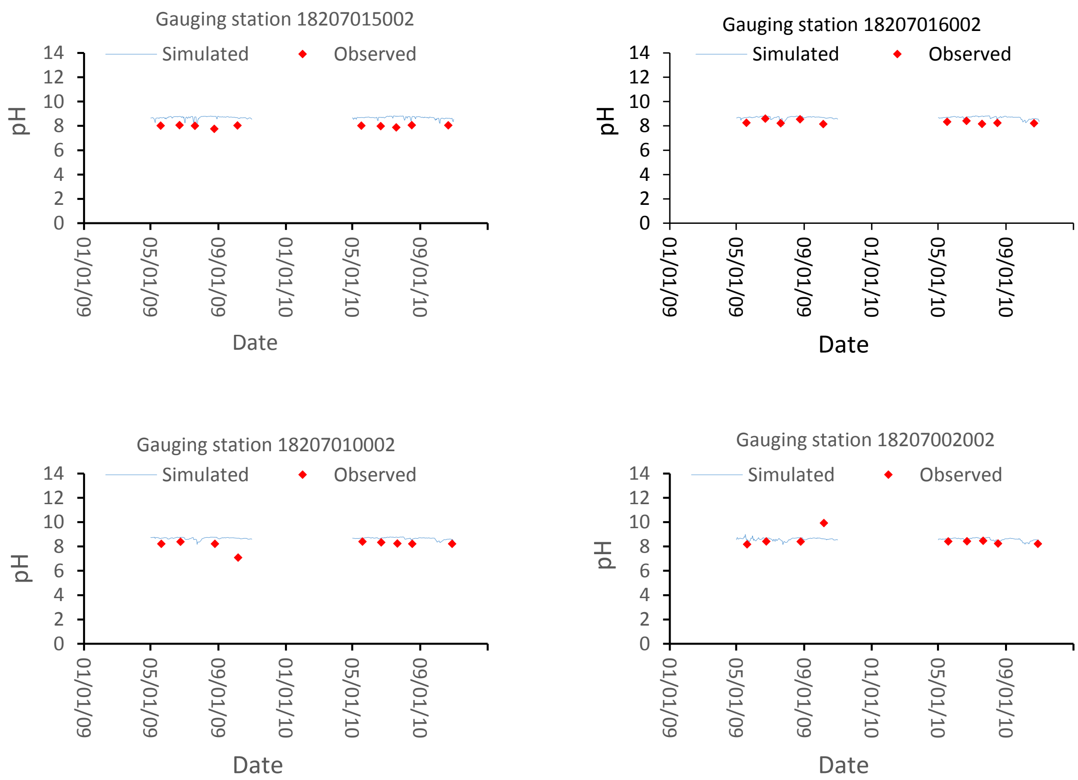
Gauging station 18207015002
Gauging station 18207016002
Gauging station 18207010002
Gauging station 18207002002
Simulated
Observed
pH
14
12
10
8
6
4
2
0
01/01/09
05/01/09
09/01/09
01/01/10
05/01/10
09/01/10
Date

❖ T

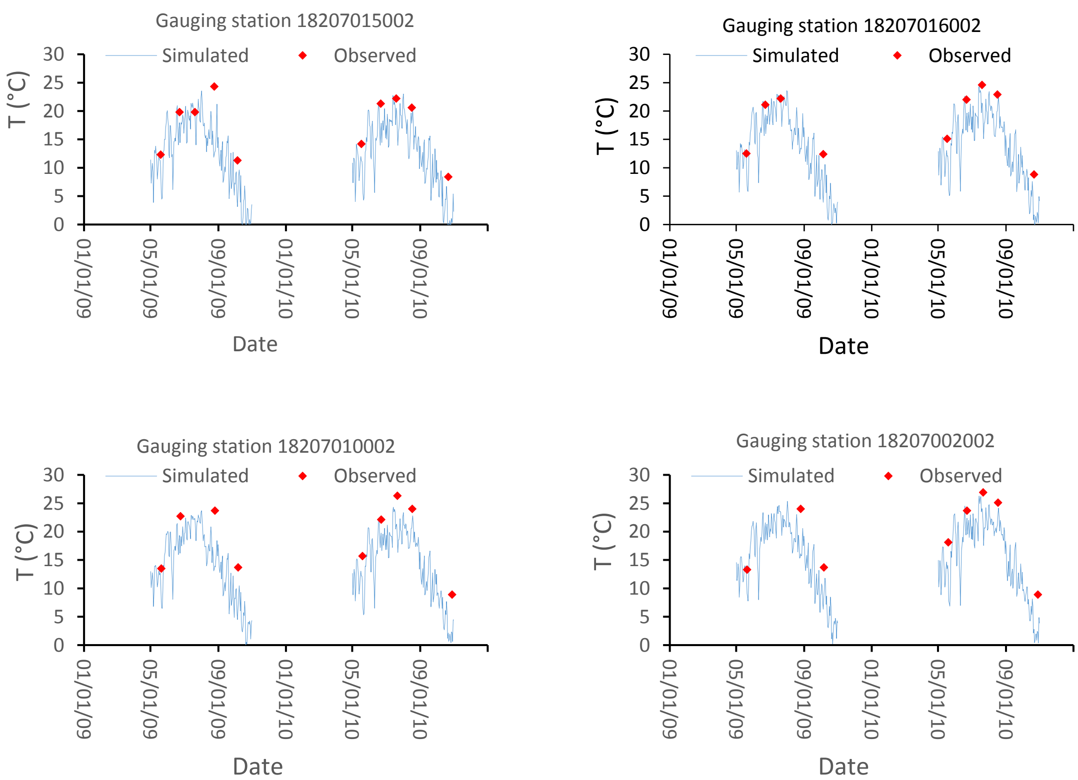
Gauging station 18207015002
Gauging station 18207016002
Gauging station 18207010002
Gauging station 18207002002
Simulated
Observed
T (°C)
30
25
20
15
10
5
0
01/01/09
05/01/09
09/01/09
01/01/10
05/01/10
09/01/10
Date

❖ TN

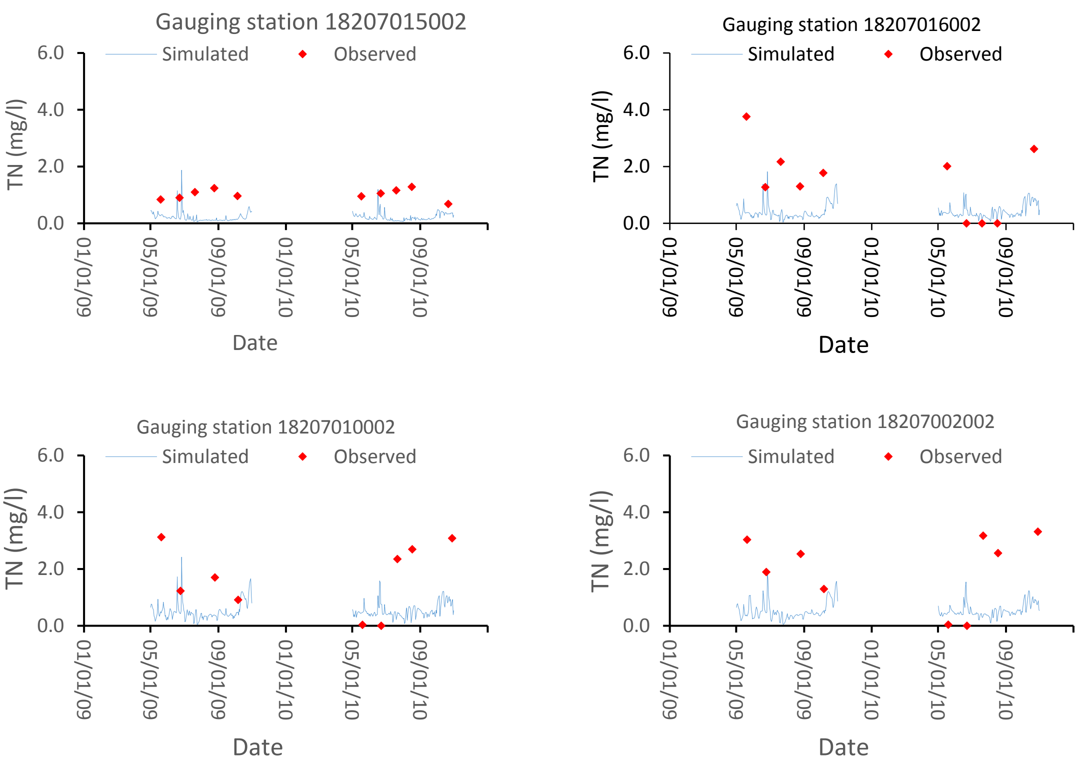

❖ TP

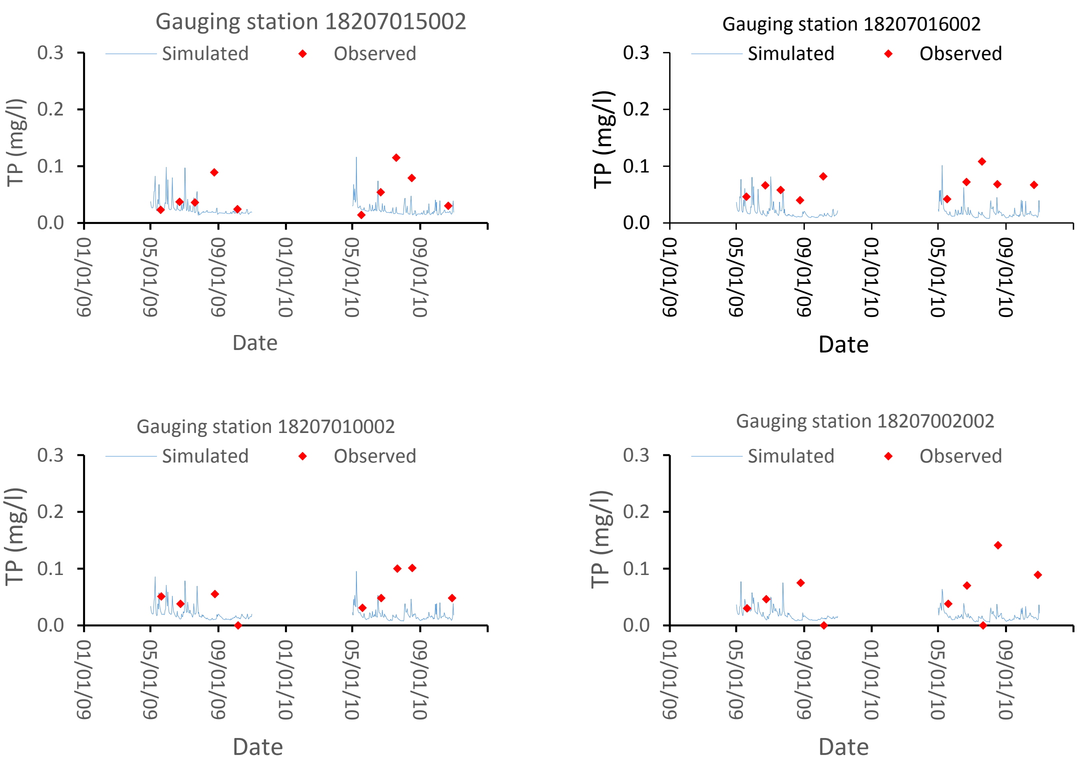

Figure 5.8 Verification of QUAL2Kw in two seasons of growth from 2009 to 2010

As seen in Figures 5.7 and 5.8, generally, the simulated followed the trends of the observed for all eight aimed parameters of the model. More importantly, for the alkalinity, DO, EC, pH, and T, the model performed quite well, and the RRMSE values of these parameters ranged from 0.07 to 0.47 for the calibration and verification, which reflected the excellent agreement between the simulated and the observed during the five seasons of growth from 2006 to 2010. For the nutrient parameters, TN and TP, the RRMSE values were slightly higher at 0.87 and 0.94, which are still under the acceptable criteria of one. Only one index of the flow calibration, 1.74, exceeded the criteria, while the verification index was within the acceptable range.

The statistical indices for the calibration and verification of the model are listed in Table 5.5 below.

Table 5.5 Statistical indices for the calibration and validation of the model

No.	Parameter	RRMSE								Ave.	
		18207015002		18207016002		18207010002		18207002002			
		Cal	Val	Cal	Val	Cal	Val	Cal	Val	Cal	Val
1	Alkalinity	0.00	0.00	0.05	0.03	0.06	0.06	0.21	0.12	**0.08**	**0.05**
2	DO	0.77	1.05	0.25	0.30	0.45	0.35	0.26	0.19	**0.43**	**0.47**
3	EC	0.00	0.00	0.06	0.07	0.10	0.09	0.12	0.07	**0.07**	**0.06**
4	Flow	1.98	0.94					1.50	0.73	**1.74**	**0.83**
5	pH	0.07	0.09	0.04	0.05	0.05	0.08	0.03	0.06	**0.05**	**0.07**
6	T	0.28	0.33	0.00	0.00	0.00	0.00	0.00	0.00	**0.07**	**0.08**
7	TN	0.86	0.85	0.97	1.07	0.92	0.98	0.84	0.84	**0.90**	**0.94**
8	TP	0.67	0.84	0.83	0.80	0.93	0.92	1.03	1.08	**0.87**	**0.91**

Considering the long periods of the calibration and verification covering five seasons of growth from 2006 to 2010 and the observed data from the four water quality gauging stations and two hydrometric gauging stations covering the entire river, the calibration and verification of the model are considered as satisfactory, and it is suitable for the assessment of the ecological effects of CTD on the water quality of the river system.

The following Table 5.6 lists the calibrated parameters for the QUAL2Kw model.

Table 5.6 Calibrated parameters for the QUAL2Kw model

Parameter	Value	Units	Auto-cal	Min value	Max value
Stoichiometry:					
Carbon	37.41	gC	Yes	30.00	60.00
Nitrogen	6.06	gN	Yes	5.00	9.00
Phosphorus	1.49	gP	Yes	0.50	2.00
Dry weight	100.00	gD	Yes	100.00	100.00
Chlorophyll	0.93	gA	Yes	0.50	2.00
Inorganic suspended solids:					
Settling velocity	1.37	m/d	Yes	0.00	2.00
Oxygen:					
Reaeration model	User model		f(u h)		
User reaeration model parameter A	3.73			3.00	6.00
User reaeration model parameter B	0.81			0.50	1.00
User reaeration model parameter C	-1.67			-1.85	-1.50
Temp correction for reaeration	1.02				
Reaeration wind effect	None				
O2 for carbon oxidation	2.67	gO2/gC			
O2 for NH4 nitrification	4.57	gO2/gN			
Oxygen inhib model CBOD oxidation	Exponential				
Oxygen inhib parameter CBOD oxidation	0.60	L/mgO2	No	0.60	0.60

Oxygen inhib model nitrification	Exponential				
Oxygen inhib parameter nitrification	0.60	L/mgO2	No	0.60	0.60
Oxygen enhance model denitrification	Exponential				
Oxygen enhance parameter denitrification	0.60	L/mgO2	No	0.60	0.60
Oxygen inhib model phyto resp	Exponential				
Oxygen inhib parameter phyto resp	0.60	L/mgO2	No	0.60	0.60
Oxygen enhance model bot alg resp	Exponential				
Oxygen enhance parameter bot alg resp	0.60	L/mgO2	No	0.60	0.60
Slow CBOD:					
Hydrolysis rate	0.13	/d	Yes	0.05	0.25
Temp correction	1.05		No	1.00	1.07
Oxidation rate	2.78	/d	Yes	0.00	5.00
Temp correction	1.05		No	1.00	1.07
Fast CBOD:					
Oxidation rate	1.06	/d	Yes	0.00	5.00
Temp correction	1.05		No	1.00	1.07
Organic N:					
Hydrolysis	0.08	/d	Yes	0.05	0.30
Temp correction	1.07		No	1.00	1.07
Settling velocity	0.05	m/d	Yes	0.05	2.00
Ammonium:					
Nitrification	1.56	/d	Yes	0.05	3.00
Temp correction	1.07		No	1.00	1.07
Nitrate:					

Denitrification	0.32	/d	Yes	0.00	2.00
Temp correction	1.07		No	1.00	1.07
Sed denitrification transfer coeff	0.46	m/d	Yes	0.00	1.00
Temp correction	1.07		No	1.00	1.07
Organic P:					
Hydrolysis	0.23	/d	Yes	0.05	0.30
Temp correction	1.07		No	1.00	1.07
Settling velocity	0.06	m/d	Yes	0.05	2.00
Inorganic P:					
Settling velocity	0.44	m/d	Yes	0.00	2.00
Sed P oxygen attenuation half sat constant	1.98	mgO2/L	Yes	0.00	2.00
Phytoplankton:					
Max Growth rate	2.50	/d	No	1.50	3.00
Temp correction	1.07		No	1.00	1.07
Respiration rate	0.10	/d	No	0.05	0.50
Temp correction	1.07		No	1.00	1.07
Death rate	0.00	/d	No	0.00	1.00
Temp correction	1.00		No	1.00	1.07
Nutrient limitation model for N and P	Minimum				
Nitrogen half sat constant	15.00	ugN/L	No	10.00	25.00
Phosphorus half sat constant	2.00	ugP/L	No	1.00	5.00
Inorganic carbon half sat constant	0.00	moles/L	No	0.00	0.00
Phytoplankton use HCO3- as substrate	Yes				
Light model	Half saturation				

Light constant	57.60	langleys/d	No	40.00	110.00
Ammonia preference	25.00	ugN/L	No	15.00	30.00
Settling velocity	0.15	m/d	No	0.05	2.00
Include transport of phytoplankton	Yes				
Nitrogen uptake water column fraction	1.00		No	0.00	1.00
Phosphorus uptake water column fraction	1.00		No	0.00	1.00
Bottom plants:					
Growth model	Zero-order				
Max growth rate	51.02	gD/m2/d or /d	Yes	50.00	200.00
Temp correction	1.07		No	1.00	1.07
First-order model carrying capacity	100.00	gD/m2	No	50.00	200.00
Basal respiration rate	0.48	/d	No	0.02	0.20
Photo-respiration rate parameter	0.00	unitless	No	0.00	0.60
Temp correction	1.07		No	1.00	1.07
Excretion rate	0.28	/d	Yes	0.00	0.50
Temp correction	1.07		No	1.00	1.07
Death rate	0.49	/d	Yes	0.00	0.50
Temp correction	1.07		No	1.00	1.07
Scour function	Flow				
Coefficient of scour function	0.00	/d/cms or /d/mps	No	0.00	0.10
Exponent of scour function	0.00		No	0.00	2.00
Minimal biomass after scour event	0.00	gD/m^2	No	0.00	10.00
Catastrophic scour rate during flood event	0.00	/d	No	0.00	100.00
Critical flow or vel for catastrophic scour	0.00	cms or m/s	No	0.00	50.00

External nitrogen half sat constant	215.56	ugN/L	Yes	100.00	500.00
External phosphorus half sat constant	78.74	ugP/L	Yes	25.00	100.00
Inorganic carbon half sat constant	0.00	moles/L	Yes	0.00	0.00
Bottom algae use HCO3- as substrate	Yes				
Light model	Half saturation				
Light constant	109.72	langleys/d	Yes	40.00	110.00
Ammonia preference	26.33	ugN/L	Yes	15.00	30.00
Nutrient limitation model for N and P	Minimum				
Subsistence quota for nitrogen	23.50	mgN/gD	Yes	7.20	36.00
Subsistence quota for phosphorus	2.55	mgP/gD	Yes	1.00	5.00
Maximum uptake rate for nitrogen	1147.43	mgN/gD/d	Yes	350.00	1500.00
Maximum uptake rate for phosphorus	175.50	mgP/gD/d	Yes	50.00	200.00
Internal nitrogen half sat ratio	4.61		Yes	1.05	5.00
Internal phosphorus half sat ratio	1.35		Yes	1.05	5.00
Nitrogen uptake water column fraction	1.00		No	0.00	1.00
Phosphorus uptake water column fraction	1.00		No	0.00	1.00
Detritus (POM):					
Dissolution rate	0.18	/d	Yes	0.05	0.50
Temp correction	1.07		No	1.07	1.07
Settling velocity	0.05	m/d	Yes	0.05	2.00
Pathogens:					
Decay rate	0.80	/d	No	0.00	20.00
Temp correction	1.07		No	1.00	1.07
Settling velocity	1.00	m/d	No	0.00	2.00
Alpha constant for light mortality	1.00	/d per ly/hr	No	0.00	1.00

pH:					
Partial pressure of carbon dioxide	347.00	ppm			
Hyporheic metabolism					
Model for biofilm oxidation of fast CBOD	Zero-order				
Max biofilm growth rate	5.00	gO2/m^2/ d or /d	No	0.00	20.00
Temp correction	1.05		No	1.05	1.05
Fast CBOD half-saturation	0.50	mgO2/L	No	0.00	2.00
Oxygen inhib model	Exponential				
Oxygen inhib parameter	0.60	L/mgO2	No	0.60	0.60
Respiration rate	0.20	/d	No	0.20	0.20
Temp correction	1.07		No	1.07	1.07
Death rate	0.05	/d	No	0.05	0.05
Temp correction	1.07		No	1.07	1.07
External nitrogen half sat constant	15.00	ugN/L	No	15.00	15.00
External phosphorus half sat constant	2.00	ugP/L	No	2.00	2.00
Ammonia preference	25.00	ugN/L	No	25.00	25.00
First-order model carrying capacity	100.00	gD/m2	No	100.00	100.00
Generic constituent					
Decay rate	0.00	/d	No	0.00	20.00
Temp correction	1.07		No	1.00	1.07
Settling velocity	0.00	m/d	No	0.00	2.00
Use generic constituent as COD?	No				
Photosynthetic quotient and respiratory quotient for phytoplankton and bottom algae					

Photosynthetic quotient for NO_3 vs NH_4 use	1.29	No	1.20	1.80
Respiratory quotient	1.00	No	0.85	1.00

5.3 Simulation results and discussions for the QUAL2Kw modeling

5.3.1 Simulation results of the CTD and UCTD scenarios

The CTD and UCTD scenarios were simulated for two time scales, diel (24 hours) and growing season (May–Oct.). The simulation of the diel scale demonstrated how the CTD and UCTD scenarios performed during a diel cycle, and the simulation of the seasonal scale showed the general trends of the effects of the CTD and UCTD scenarios on the water quality of the river over five consecutive seasons of growth from 2006 to 2010.

5.3.1.1 Diel simulation results of the CTD and UCTD scenarios

The simulation of the diel cycle was set for June 23, 2008, and to assess the impacts of the CTD and UCTD scenarios on the river, nine parameters were evaluated: flow, DO, pH, EC, phytoplankton, Org-N, dissolved inorganic-N (NH_4^+-N, NO_2^--N, NO_3^--N), TN, and TP. The model's simulation results for the CTD and UCTD scenarios are presented in Figure 5.9, and Tables 5.7 and 5.8 show the reductions by the CTD scenarios. The ratio calculation formula is (CTD concentration -UCTD concentration)/ concentration × 100.

As Figure 4.9 shows, the simulated flows of the CTD200, CTD600, and UCTD scenarios became successively greater, which corresponds to the flow simulation results of the CTD and UCTD scenarios from the SWAT model.

Table 5.7 Reduced ratios by the CTD200 for the diel simulation

Distance km	Flow %	DO %	pH %	EC %	Phytoplankton %	DissInor-N %	Org-N %	TN %	TP %
152.6	0.6	0.0	0.0	0.0	0.0	0.0	0.8	0.8	0.5
108.1	0.5	0.0	0.0	0.0	0.5	0.3	1.1	1.0	1.0
103.7	-1.2	0.0	0.0	0.0	-1.8	-0.4	1.5	0.9	0.3
63.2	-12.7	0.1	0.1	-0.1	-13.7	1.4	6.6	3.9	-1.3
56.9	-10.3	0.0	0.0	0.0	-3.3	16.7	42.4	28.5	14.8
55.0	-10.9	0.0	0.0	0.2	-1.7	-3.4	81.1	40.1	27.0
33.3	-1.1	0.0	0.0	0.5	2.5	-12.8	96.3	42.3	35.5
30.3	-1.2	0.0	0.0	0.4	2.4	-19.8	99.7	42.2	37.3
24.2	-0.6	0.0	0.0	0.3	2.4	-20.0	86.7	37.2	34.8
18.8	-0.5	0.0	0.0	0.3	2.8	-25.1	79.0	36.1	36.3
0.0	1.0	0.0	0.0	0.2	4.4	-26.8	67.5	32.0	34.4

Table 5.8 Reduced ratios by the CTD600 for the diel simulation

Distance km	Flow %	DO %	pH %	EC %	Phytoplankton %	DissInor-N %	Org-N %	TN %	TP %
152.6	0.7	0.0	0.0	0.0	0.0	-0.4	0.1	0.1	0.0
108.1	0.7	0.0	0.0	0.0	0.5	0.0	0.4	0.4	0.4
103.7	0.4	0.0	0.0	0.0	-0.1	0.1	0.5	0.4	0.3
63.2	-6.3	0.1	0.1	-0.1	-7.0	0.7	3.3	2.0	-0.6
56.9	-4.4	0.0	0.0	0.0	-1.0	8.9	8.1	7.8	4.6
55.0	-4.4	0.0	0.0	0.2	-0.2	4.1	21.0	12.5	7.9
33.3	-0.3	0.0	0.0	0.5	1.2	0.7	26.5	13.5	9.8
30.3	-0.4	0.0	0.0	0.4	1.2	-1.4	27.8	13.5	10.1
24.2	-0.2	0.0	0.0	0.3	1.1	-2.9	25.1	12.0	9.5
18.8	-0.1	0.0	0.0	0.3	1.3	-4.8	23.3	11.6	9.8
0.0	0.6	0.0	0.0	0.2	1.8	-6.0	20.0	10.2	9.3

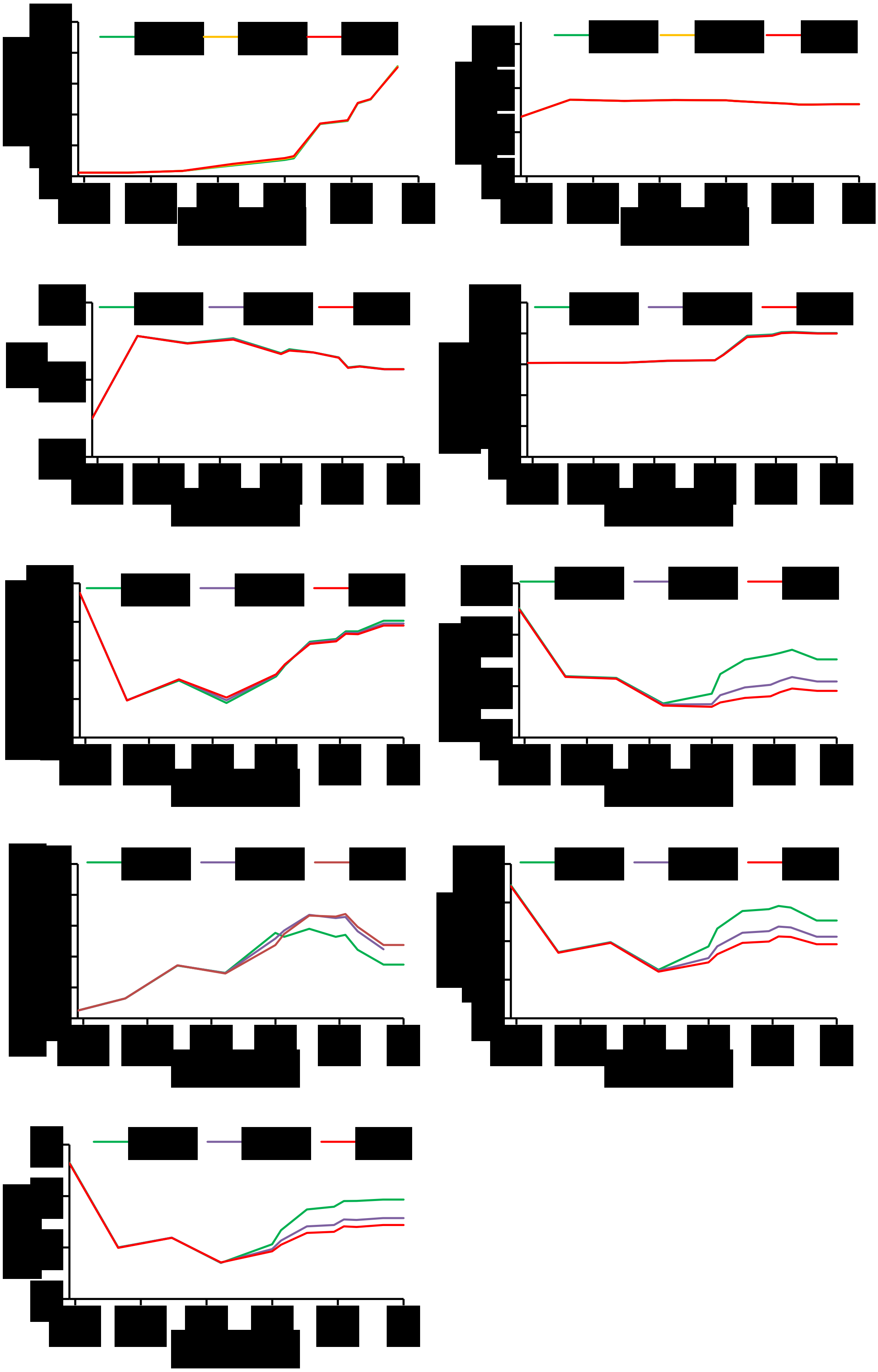

Figure 5.9 Diel simulations of CTD and UCTD scenarios

The indices of the water quality, DO, pH, and EC, changed over the distance to the outlet of the river. The EC for CTD_{200} was slightly higher than that of the other two scenarios CTD_{600} and UCTD, while the differences between the three scenarios for DO and pH were negligible. Therefore, the CTD scenarios had no significant impact on these three indices of water quality in the river. The ecological indices, the phytoplankton, behaved differently over the length of the river. The CTDs reduced the phytoplankton midstream, whereas the CTD scenarios encouraged phytoplankton growth downstream.

In the model, TN consists of inorganic-N, and Org-N, which increased over the river. For the dissolved inorganic-N compounds, NH_4^+-N and NO_2^--N+NO_3^--N, there was a significant reduction between the CTDs and the UCTD scenarios at the end of the river. As a major part of TN, the Org-N of the two CTD scenarios was clearly greater than that in the UCTD scenario, and this resulted in the TN of the two CTD scenarios increasing compared to the UCTD scenario. Likewise, the TP from the CTD scenarios increased when the tile drainage depth was decreased.

5.3.1.2 Continuous simulations of the CTD scenarios over five seasons of growth

To continuously assess the effects of the CTD scenarios on the water quality of the river, the calibrated model simulated the river for five consecutive seasons of growth between 2006 and 2010. Since the model is only capable of simulating 365 days, there must be one model for a certain year and a certain CTD scenario. Therefore, there were 5 (year) × 3 (CTD200, CTD600, and UCTD) models, with 15 models in total, and each model covered 184 days from May 1st to October 31st.

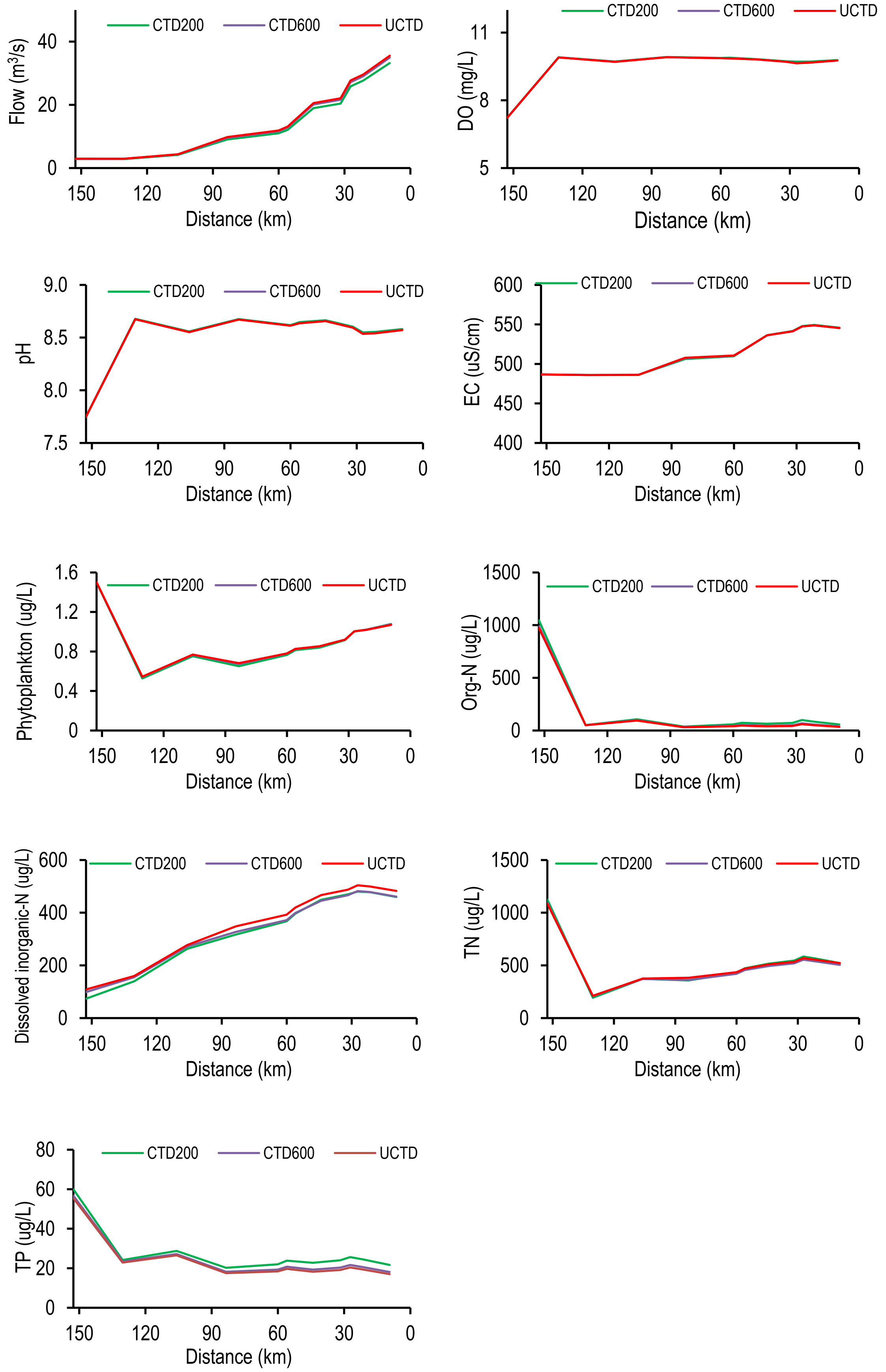

Figure 5.10 Continuous simulations of CTD and UCTD scenarios

The simulation results were represented as the daily averages of the five seasons (daily sum/5/184 days). Like the diel simulation, nine parameters were simulated, which were flow, DO, pH, EC, phytoplankton, Org-N, dissolved inorganic-N, TN, and TP. The simulation results are shown in Figure 5.10, and the reduced ratios for CTD_{200} and CTD_{600} are listed in Tables 5.9 and 5.10.

Table 5.9 Reduced ratios by CTD200 for the continuous simulation

Distance	Flow	DO	pH	EC	Phytoplankton	DissInor-N	Org-N	TN	TP
km	%	%	%	%	%	%	%	%	%
152.6	-4.6	0.0	0.0	0.0	0.0	-32.3	7.7	3.6	8.3
108.1	-4.7	0.1	0.0	0.0	-3.2	-12.5	3.4	-8.7	5.7
103.7	-4.9	0.2	0.1	0.0	-2.1	-5.2	12.0	-0.8	8.3
63.2	-7.6	0.1	0.1	-0.3	-4.5	-8.9	19.7	-6.6	15.7
56.9	-7.5	0.1	0.1	-0.2	-2.0	-6.3	45.9	-1.4	19.5
55.0	-8.1	0.3	0.1	-0.1	-1.6	-5.5	55.2	0.6	21.3
33.3	-7.7	0.1	0.1	0.0	-1.6	-3.9	62.4	1.4	25.0
30.3	-7.6	0.2	0.1	0.1	-0.6	-3.7	67.4	2.1	25.5
24.2	-6.8	0.8	0.2	0.1	-0.1	-4.7	64.8	2.7	26.0
18.8	-6.5	0.5	0.2	0.1	0.2	-4.3	66.2	2.1	26.5
0.0	-6.5	0.1	0.1	0.1	0.9	-4.8	65.9	0.0	27.2

Table 5.10 Reduced ratios by the CTD600 for the continuous simulation

Distance	Flow	DO	pH	EC	Phytoplankton	DissInor-N	Org-N	TN	TP
km	%	%	%	%	%	%	%	%	%
152.6	-1.3	0.0	0.0	0.0	0.0	-9.3	1.9	0.8	2.4
108.1	-1.3	0.0	0.0	0.0	-0.6	-2.9	1.6	-1.8	2.2
103.7	-1.3	0.0	0.0	0.0	-0.5	-2.0	2.8	-0.8	2.4
63.2	-2.2	0.0	0.0	-0.1	-1.4	-6.1	4.1	-5.2	4.2
56.9	-2.2	0.0	0.0	-0.1	-0.4	-5.2	9.7	-3.8	5.0
55.0	-2.3	0.0	0.0	0.0	-0.2	-4.8	13.1	-3.0	5.5
33.3	-2.2	0.0	0.0	0.0	-0.3	-4.6	13.3	-3.2	6.0
30.3	-2.2	0.0	0.0	0.0	0.0	-4.3	13.7	-2.8	6.1
24.2	-2.0	0.1	0.0	0.0	0.1	-4.3	13.2	-2.4	6.2
18.8	-1.9	0.0	0.0	0.0	0.2	-4.3	12.8	-2.7	6.3
0.0	-1.7	0.0	0.0	0.0	0.5	-4.5	13.4	-3.2	6.4

Some patterns of the water quality parameters for the continuous simulation results of the CTD and UCTD scenarios resembled those in the diel simulation, while others performed differently. The flows for CTD200, CTD600, and UCTD differentiated themselves from the midstream. Compared to the UCTD, the CTD600 and the CTD200, all of them lowered the flow in each scenario as simulated by the SWAT model. For DO, pH, and EC, the simulation results for the CTD200 and CTD200 scenarios were almost the same.

CTD200 reduced phytoplankton along all the reaches, except for reaches 9 and 10, and CTD600 reduced phytoplankton along reaches 1 to 6 and increased slightly along reaches 8 to 10.

For the dissolved inorganic N, both CTD scenarios yielded less than the UCTD scenario, and the CTD200 outputted the least. CTD600 decreased TN along the river, while CTD200 reduced TN upstream and increased it slightly downstream. All the CTDs showed that the TP concentrations increased along the river channel.

5.3.2 Discussion

To assess the ecological impact of CTD on the river, two CTD scenarios, CTD200 and CTD600, were developed and evaluated using the calibrated QUAL2Kw model at two different time scales, diel and seasonal. The diel simulation only represented the changes in river water quality over the distance on a specific day, and the general trend of the changes in river water quality required long-term continuous simulation. However, most recent QUAL2K models were the diel scale, and continuous simulation over a long period was rare.

In this study, for the five seasons of growth from May to October between 2006 and 2010, the continuous simulation of the CTD scenarios revealed different trends concerning how the water quality evolved over time. Compared to the baseline UCTD, the CTD scenarios reduced the biologically available dissolved inorganic-N levels in the river. McIsaac et al. (2001) documented that NO_3^--N was the major contributor to eutrophication, and from this point of view, the simulation results of the CTD scenarios indicated that CTD is beneficial to the water quality of the river. Moreover, the general trends shown by the continuous simulation suggested that the CTD scenarios could improve the water quality of the river by reducing the dissolved inorganic-N and TN levels. Less dissolved inorganic-N would discourage the growth of phytoplankton in the water body, and the concentrations of phytoplankton in both the CTD200 and CTD600 scenarios were decreased along most river sections.

The QUAL2Kw model requires varieties of water quality and biological inputs to simulate a river. However, collecting these field data is a costly and time-consuming task, especially for a river running along 175 km. This study did not have the budget to collect the required field water quality and climate data required by the QUAL2Kw model, and therefore it relied on data from public sources, e.g., PWQMN, CWEEDS, and the National Hydrometric Program operated by the Water Survey of Canada. This model simulates a diel heat budget and water-quality kinetics, and consequently it demands diel input to simulate diel water quality dynamics in a river given certain initial conditions. This resulted in preparing large amounts of input data for the model. Moreover, the river was segmented into reaches and tributaries, all required related inputs.

5.4 Climate changes on river water quality with CTD scenarios

As modeled in Section 5.3, the practice of CTD had ecological effects on the river water quality. Also, climate change plays a big role in the future of river water quality (Rehana and Mujumdar, 2011; Whitehead et al., 2009), and so it is necessary to further investigate the combined effects of CTD and climate change on river water quality under dynamic climate change scenarios.

Two climate change scenarios, CAN45 and CAN85, were used to predict the combined effects of CTD and climate change on the river. As described in Section 5.2.3.2, the QUAL2Kw model was fed with the outputs of the climate change scenarios and simulated by the SWAT model. The simulation period was the five connective seasons of growth from 2056 to 2060 in order to compare it to the baseline period from 2006 to 2010.

5.4.1 Simulations of CTDs under climate changes

Like the previous simulation for the observed period 2006–2010, the climate change scenarios were examined with two CTD scenarios, CTD200 and CTD600. The reductions predicted by the two CTD scenarios under the climate change scenarios are shown in Figures 5.11 and 5.12 and Tables 5.11 and 5.12.

The impacts of the two CTDs on water quality under the two climate change scenarios were highly similar. For CTD200, flow reductions varied from –5.5% to –3.5% and –4.3% to –2.1% along the river under CAN45 and CAN85, respectively, while for CTD600, they ranged from –1.5% to –0.9% and –0.9% to 0.2% under CAN45 and CAN85, respectively. Although the combined CTD and climate changes increase DO and decrease EC, the effects are negligible, and the changes of the pH are invisible during the simulation period. For phytoplankton, the reductions along the river ranged from –3.5% to 1.1% and –2.9% to 0.4% by CTD200, –1.6% to 0.0%, and –1.2% to 0.4% by CTD600 under CAN45 and CAN85, respectively.

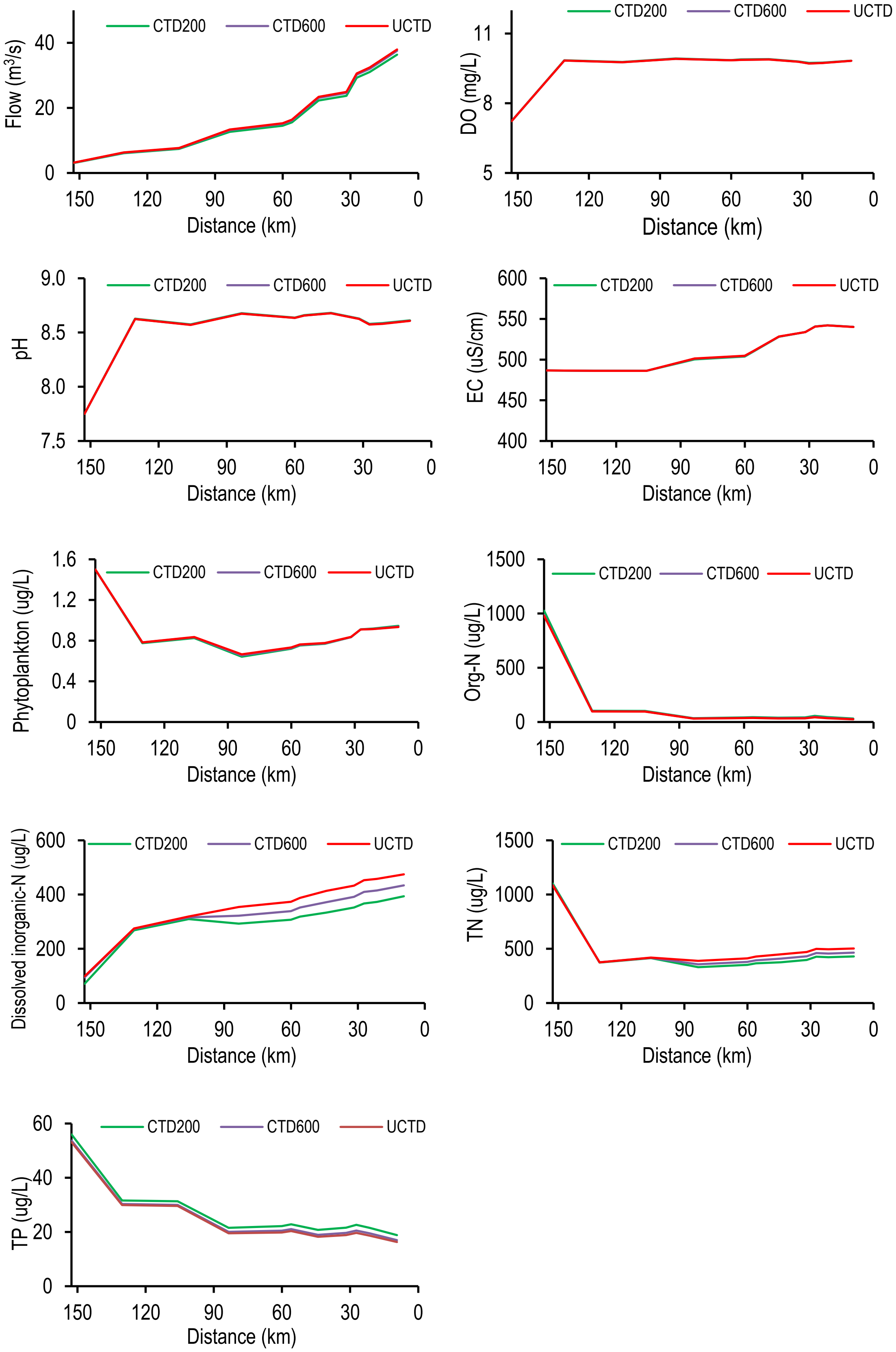

Figure 5.11 Continuous simulations of CTD and UCTD under CAN45

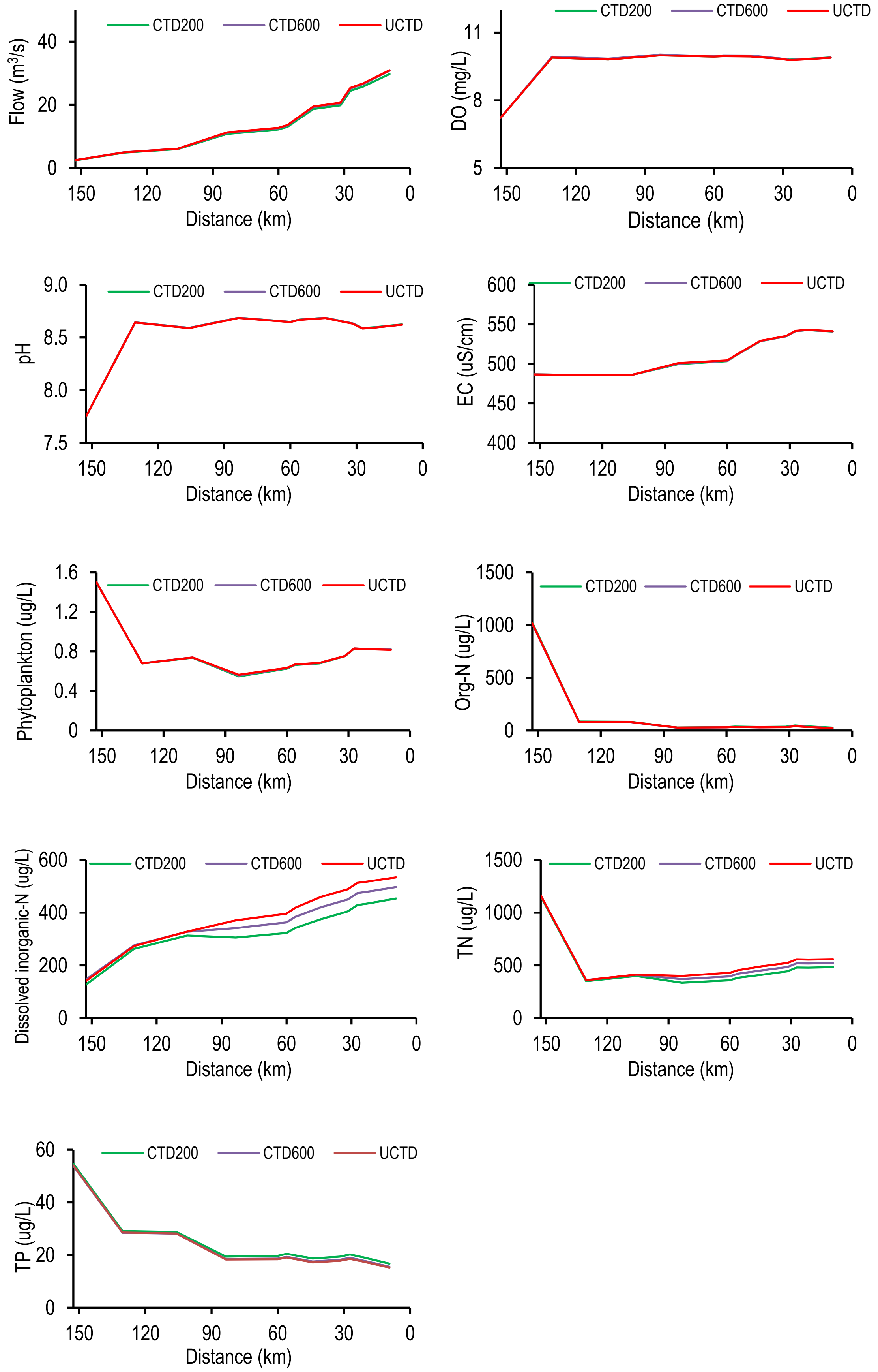

Figure 5.12 Continuous simulations of CTD and UCTD under CAN85

Table 5.11 Reductions by CTD scenarios under CAN45 for the QUAL2Kw model

Distance km	Flow %	DO %	pH %	EC %	Phytoplankton %	DissInor-N %	Org-N %	TN %	TP %
CTD200									
152.6	-3.5	0.0	0.0	0.0	0.0	-28.2	4.7	1.7	5.4
108.1	-3.5	0.1	0.0	0.0	-0.9	-2.5	5.7	-0.4	5.6
103.7	-3.6	0.1	0.1	0.0	-1.1	-3.1	6.2	-1.0	5.8
63.2	-5.3	0.2	0.0	-0.2	-3.5	-17.4	11.5	-15.0	10.3
56.9	-5.1	0.1	0.0	-0.2	-1.8	-17.7	17.9	-14.5	11.7
55.0	-5.3	0.2	0.0	-0.1	-1.3	-17.8	20.3	-14.4	12.3
33.3	-4.9	0.1	0.0	-0.1	-1.0	-19.4	22.0	-16.3	14.1
30.3	-4.8	0.1	0.0	0.0	-0.2	-18.6	24.6	-15.4	14.6
24.2	-4.3	0.3	0.1	0.0	0.2	-19.0	31.2	-14.6	15.2
18.8	-4.2	0.2	0.1	0.0	0.4	-18.6	33.1	-14.8	15.5
0.0	-4.2	0.1	0.1	0.0	1.1	-17.0	27.7	-14.7	15.6
CTD600									
152.6	-0.9	0.0	0.0	0.0	0.0	-4.0	0.8	0.4	1.1
108.1	-0.9	0.0	0.0	0.0	-0.2	-0.4	1.3	0.0	1.3
103.7	-0.9	0.0	0.0	0.0	-0.3	-1.1	1.0	-0.6	1.3
63.2	-1.5	0.0	0.0	-0.1	-1.6	-9.1	2.0	-8.2	2.8
56.9	-1.4	0.0	0.0	-0.1	-0.8	-9.3	4.5	-8.0	3.3
55.0	-1.5	0.0	0.0	0.0	-0.6	-9.2	5.0	-7.9	3.5
33.3	-1.4	0.0	0.0	0.0	-0.5	-10.0	5.3	-8.8	4.0
30.3	-1.4	0.0	0.0	0.0	-0.2	-9.5	6.3	-8.3	4.3
24.2	-1.2	0.1	0.0	0.0	0.0	-9.5	9.1	-7.9	4.5
18.8	-1.3	0.1	0.0	0.0	0.1	-9.3	9.2	-7.9	4.5
0.0	-1.1	0.0	0.0	0.0	0.3	-8.6	6.7	-7.8	4.2

Both CTD scenarios significantly reduced dissolved inorganic-N and TN under two climate change scenarios. The reduction of dissolved inorganic-N by CTD200 ranged from –28% to –2.5% and –18.5% to –4.0% and –10.0% to –0.4% and –8.5% to 4.1% by CTD600 under CAN45 and CAN85, respectively. Although the CTD scenarios increased Org-N, the levels of TN were decreased moderately because the reductions of dissolved inorganic-N were highly significant. The CTD scenarios raised the level of TP under two climate changes.

Table 5.12 Reductions by CTD scenarios under CAN85 for the QUAL2Kw model

Distance	Flow	DO	pH	EC	Phytoplankton	DissInor-N	Org-N	TN	TP
km	%	%	%	%	%	%	%	%	%
CTD200									
152.6	-2.1	0.0	0.0	0.0	0.0	-9.9	0.7	-0.6	1.2
108.1	-2.1	0.0	0.0	0.0	-0.1	-4.0	1.8	-2.6	1.9
103.7	-2.2	0.0	0.0	0.0	-0.4	-4.4	1.4	-3.3	2.0
63.2	-4.3	0.1	0.0	-0.3	-2.9	-17.6	2.3	-16.2	6.0
56.9	-4.0	0.0	0.0	-0.2	-1.3	-18.5	8.3	-16.5	6.9
55.0	-4.1	0.1	0.0	-0.1	-0.8	-18.3	13.3	-15.9	7.4
33.3	-4.1	0.0	0.0	-0.1	-0.8	-18.4	14.2	-16.3	8.6
30.3	-4.1	0.1	0.0	-0.1	-0.3	-17.1	15.3	-15.1	8.7
24.2	-3.7	0.2	0.0	0.0	0.0	-16.5	17.3	-13.9	9.0
18.8	-3.7	0.2	0.0	0.0	0.1	-16.1	19.3	-13.8	9.2
0.0	-3.9	0.1	0.0	0.0	0.4	-15.0	19.4	-13.5	9.5
CTD600									
152.6	-0.1	0.0	0.0	0.0	0.0	4.1	-0.5	0.1	-0.3
108.1	0.2	0.4	0.0	0.0	0.2	0.8	-1.0	0.4	-0.2
103.7	0.1	0.4	0.0	0.0	0.0	-0.2	-1.3	-0.4	-0.2
63.2	-0.9	0.3	0.0	-0.2	-1.2	-7.8	-3.8	-7.5	0.9
56.9	-0.9	0.1	0.0	-0.1	-0.5	-8.3	0.4	-7.6	1.3
55.0	-0.9	0.3	0.0	-0.1	-0.3	-8.2	1.4	-7.5	1.4
33.3	-0.9	0.4	0.0	-0.1	-0.3	-8.5	1.0	-7.9	2.0
30.3	-0.9	0.2	0.0	-0.1	0.0	-8.0	2.2	-7.3	2.1
24.2	-0.9	0.1	0.0	0.0	0.1	-7.6	2.7	-6.8	2.2
18.8	-0.8	0.1	0.0	0.0	0.2	-7.4	2.9	-6.7	2.2
0.0	-0.5	0.0	0.0	0.0	0.3	-6.9	1.1	-6.5	1.9

5.4.2 Comparisons of climate change scenarios to the baseline

During the simulation period 2056 - 2060, the predicted reductions in the two CTD scenarios under CAN45 and CAN85 are compared to the baseline simulation of the observed period 2006 - 2010 (OBS), as shown in Figures 5.13 and 5.14.

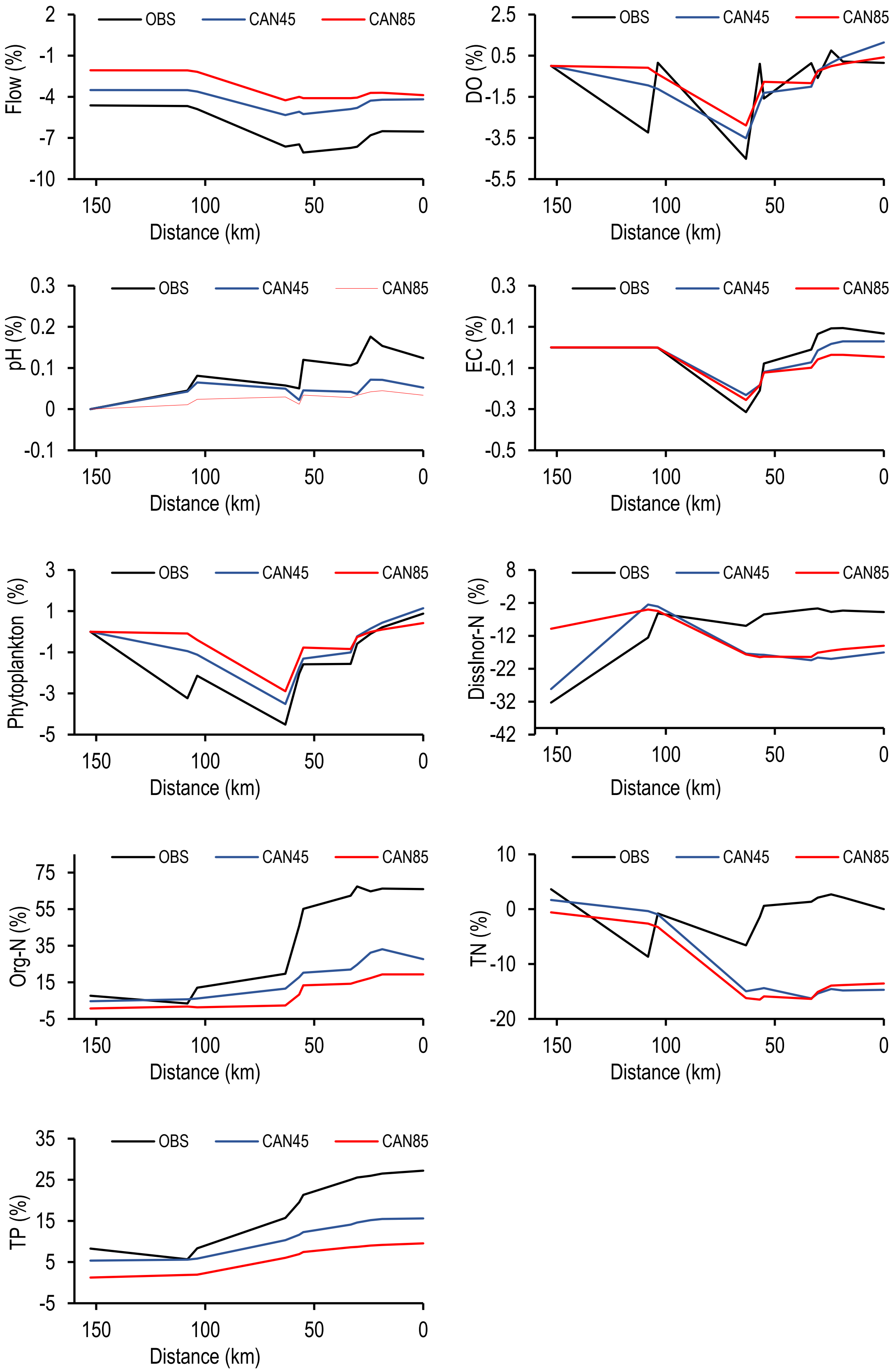

Figure 5.13 Reductions of CTD200 under OBS, CAN45, and CAN85

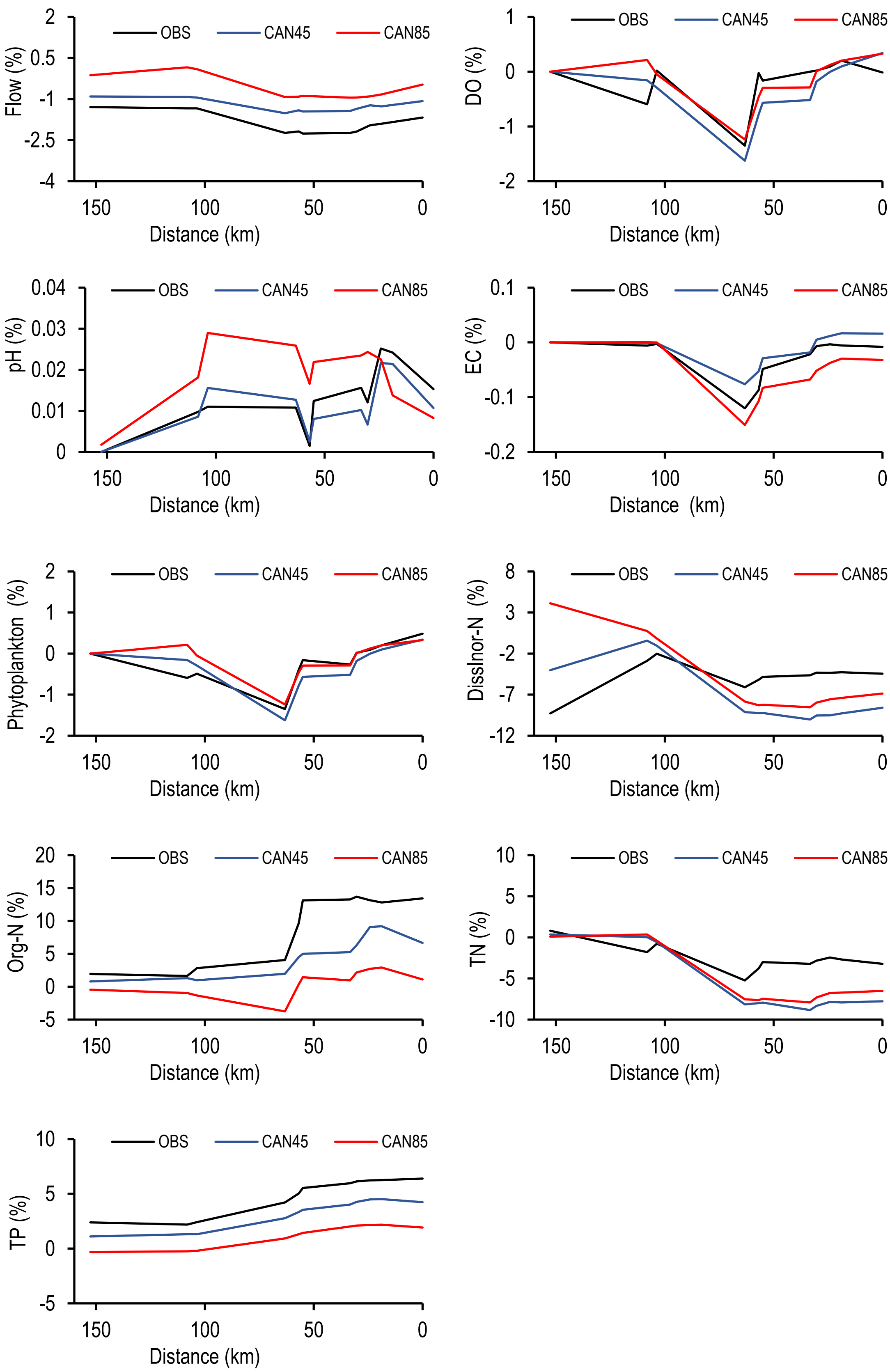

Figure 5.14 Reductions of CTD600 under OBS, CAN45, and CAN85

Generally, the predicted reductions of CTD200 and CTD600 under CAN45 and CAN85 are in line with the findings under OBS, and they had similar trends along the river. The simulations of both CTD scenarios under the observed period 2006 to 2010 and the two future climate change scenarios during the period 2056 to 2060 suggest that CTD can reduce biologically available dissolved inorganic-N and TN and discourage phytoplankton growth in the river.

This study evaluated the biological effects of two CTD scenarios on river water quality at two different time scales, diel and seasonal, and it developed innovative approaches and programs to retrieve and prepare necessary inputs required by the QUAL2Kw model from the outputs of the SWAT model, which distinguishes this study from other QUALs models. Furthermore, this study applies climate changes to the modeling and investigates the behaviour of CTD under dynamic climate changes in the future. Long periods of continuous simulation and climate change scenarios also make this study stand out from other QUALs modeling.

6 CONCLUSIONS AND RECOMMENDATIONS

In this study, the algorithm for calculating NO_3^--N in tile flow was improved in order to simulate CTD properly. The improvement in the algorithm was verified with the paired experimental micro watersheds. The improvement enhanced the SWAT model and expanded the scope of its application to CTD. According to the author's knowledge, this is the first successful attempt to assess the environmental effects of CTD on watershed using the SWAT model.

The modified model was calibrated and validated by comparing the model results with field observations at the outlet of the watershed near Plantagenet, an agriculture-dominated sub watershed of the Ottawa River basin, in eastern Ontario, Canada. The statistical performance indices for flow, sediment, NO_3^--N, TN, and TP were 0.90, 0.76, 0.45, 0.64, and 0.56 for NSE, –10.40, –12.80, –18.10, 2.80, and 2.60 for PBIAS, and 0.31, 0.49, 0.75, 0.60, and 0.66 for RSR respectively, for the calibration, 0.81, 0.69, 0.79, 0.64, and 0.55 for NES, –8.30, –20.00, –20.10, –3.30, and 2.50 for PBIAS, and 0.43, 0.56, 0.46, 0.44, and 0.67 for RSR, respectively, for the validation. The calibration and validation of the model are satisfactory, and the model can represent the watershed and be used to evaluate the CTD and UCTD scenarios.

These results are in line with those of Que (2015), who performed a similar simulation using AnnAGNPS. Despite SWAT and AnnAGNPS having very different flow simulation algorithms, the results of this study are consistent with those of the AnnAGNPS model and field project WEBs. This finding further verifies those of previous studies in this watershed and helps with understanding the environmental effects and operating mechanism of CTD on flow, sediment, and nutrient loadings at a watershed scale, which aids in better drainage management practices in an effort to reduce nutrient loadings in agricultural runoff, specifically in agricultural-dominated watersheds. Moreover, the performances of the CTD scenarios were examined under a matrix of climate change scenarios, and the results indicated that the CTD scenarios would perform effectively and stably under broad climate change scenarios based on varieties of GCMs and RCMs with different configurations. Also, the climate change scenarios predicted that the nutrient loadings from the watershed will increase during the simulation period 2021 to 2050. Thus, the pollution from the agricultural field will deteriorate with the current uncontrolled tile drainage.

To assess the ecological impacts of CTD on a river, this study applied the river water quality model, QUAL2Kw, to the South Nation River in eastern Ontario, Canada by addressing the preparation of input data, model setup, calibration and verification, and evaluation under CTD and UCTD scenarios evolving from the outputs of the SWAT model. The model was calibrated and verified at observed locations along the river during the five seasons of growth from 2006 to 2010. The calibration and verification of the model are satisfactory, and thus the model is capable of assessing the ecological effects of CTD on the water quality of the river.

This study evaluated the biological effects of two CTD scenarios on river water quality at two different time scales, diel and seasonal. The diel simulation results indicated that the CTD could lower the flow rate, NH_4^+-N, NO_2^--N, NO_3^--N, and phytoplankton levels, increase the TN and TP levels, and have marginal effects on DO, EC, and Min-P. Considering that the CTD scenarios could reduce the dissolved N levels in the river, NH_4^+-N, NO_2^--N and NO_3^--N, the study suggests that CTD was beneficial to the water quality of the river since biologically available dissolved N is the major contributor to eutrophication and seasonal hypoxia. However, the diel simulation only represented the changes in river water quality over the distance on a specific day, and the general trend of the changes of river water quality required long-term continuous simulation. So, in this study, CTD was continuously simulated for the five seasons of growth from May to October during the period 2006 to 2010. The continuous simulation suggested that the practice of CTD could significantly improve the water quality of the river by reducing dissolved inorganic-N levels and thereby impeding phytoplankton growth in the river. Most previous QUAL2Ks modeling has been conducted at a diel scale, and continuous simulation over a long period such as in this study is rare. Also, the evaluations were scrutinized under climate change scenarios. Long periods of continuous simulation and climate change scenarios also make this study stand out from other QUALs modeling studies.

To the author's knowledge, this study is the first attempt to date to assess the environmental effects of CTD on a watershed and river by coupling the modified SWAT model and the QUAL2Kw model. The findings in the place indicated that CTD implementation in a watershed can benefit not only the watershed by barring N from leaving fields, but also the river by reducing biologically available dissolved N and thereby impeding phytoplankton growth in the river. The findings have expanded the current scope of knowledge in the area of the environmental effects of CTD on watersheds and rivers under current and future climate regimes.

This study successfully achieved its objectives and creatively extended the capabilities of the SWAT model and the QUAL2Kw model to simulate CTD bridging the SWAT model and the QUAL2Kw model and laying a foundation for other research. However, there are some limitations. The SWAT model does not have a function for calculating P in tile flow, and so the model cannot directly assess the effects of CTD on the P cycle in tile flow. This might result in underestimating P outputs in the CTD and UCTD scenarios and therefore compromise the performance of CTD. The QUAL2Kw model has a running limit of 365 days, which restricts the application of the model for longer periods. This study managed to simulate consecutive seasons of growth for the period 2006-2010 through building one model for one season.

This study suggests that the P cycle in tile flow should be further investigated for the SWAT model. The function for calculating P in tile flow may be irrelevant for watersheds without tile drainage, but it is indispensable for watersheds with tile drainage. It will compromise the performance of the SWAT model, particularly for heavily tile-drained watersheds.

REFERENCES

Abbaspour K. C. 2014. SWAT-CUP 2012: SWAT Calibration and Uncertainty Programs – A User Manual. Swiss Federal Institute of Aquatic Science and Technology, Eawag. Retrieved from http://swat.tamu.edu/media/114860/usermanual_swatcup.pdf. (Accessed August 2015)

Abbaspour, K. C., A. Johnson, M. Th. van Genuchten. 2004. Estimating uncertain flow and transport parameters using a sequential uncertainty fitting procedure. Vadose Zone Journal 3:1340-1352.

Abbaspour, K. C., M. Th. van Genuchten, R. Schulin, and E. Schläppi. 1997. A sequential uncertainty domain inverse procedure for estimating subsurface flow and transport parameters. Water Resour. Res. 33:1879-1892.

Agricultural Drainage Management Systems Task Force (ADMSTF). 2012. http://hostedweb.cfaes.ohio-state.edu/usdasdru/ADMS/ADMSindex. htm (accessed 21 Aug. 2013).

Agriculture and Agri-Food Canada. 2007. Soil landscapes of Canada Version 3.1.1. Retrieved from http://sis.agr.gc.ca/cansis/nsdb/slc/index.html (accessed 16 Feb.2015).

Agriculture and Agri-Food Canada. 2015a. Annual Crop Inventory. Retrieved from http://open.canada.ca/en/apps/aafc-crop-inventory (accessed on July 15, 2015)

Agriculture and Agri-Food Canada. 2015b. Watershed Evaluation of Beneficial Management Practices. Retrieved from http://www.agr.gc.ca/eng/?id=1285354752471. (Accessed on July 10, 2015)

Ale, S., L.C. Bowling, P.R. Owens, S.M. Brouder, and J.R. Frankenberger. 2012. Development and application of a distributed modeling approach to assess the watershed-scale impact of drainage water management. Agric. Water Manage. 107:23–33.

Ambrose, R.B. et al. 1988. WASP4, A Hydrodynamic and Water Quality Model—Model Theory, User's Manual, and Programmer's Guide. U.S. Environmental Protection Agency, Athens, GA. EPA/600/3-87-039.

Anderson, D. M., P. M. Glibert, and J. M. Burkholder. 2002. Harmful algal blooms and eutrophication: Nutrient sources, composition, and consequences. Estuaries 25(4B):704-726.

Arnold, J.G., D. N. Moriasi, P. W. Gassman, K. C. Abbaspour, M. J. White,R. Srinivasan, C. Santhi, R. D. Harmel, A. van Griensven, M. W. Van Liew, N. Kannan, M. K. Jha. 2012. SWAT: Model Use, Calibration, and Validation. Transactions of the ASABE. Vol. 55(4): 1491-1508.

Arnold, J.G., J.R. Williams, A.D. Nicks, and N.B. Sammons. 1990. SWRRB: A basin scale simulation model for soil and water resources management. Texas A&M Univ. Press, College Station, TX.

Arnold, J.G., P.W. Gassman, K.W. King, A. Saleh, and U. Sunday. 1999. Validation of the Subsurface Tile Flow Component in the SWAT Model. Presented at the ASAE/CSAESCGR Annual International Meeting. American Society of Agricultural Engineers Paper No. 992138. St. Joseph, MI: American Society of Agricultural Engineers.

Arnold, J. G., R. Srinivasin, R. S. Muttiah, and J. R. Williams. 1998. Large area hydrologic modeling and assessment part I: Model development. Journal of the American Water Resources Association, 34(1): 73–89.

Bates, B.C., Z.W. Kundzewicz, S. Wu and J.P. Palutikof, Eds., 2008: Climate Change and Water. Technical Paper of the Intergovernmental Panel on Climate Change, IPCC Secretariat, Geneva, 210 pp.

Bauwe, A., Eckhardt, K. U., and Lennartz, B. 2019. Predicting dissolved reactive phosphorus in tile-drained catchments using a modified SWAT model. Ecohy-drology and Hydrobiology, 19(2), 198-209. https://doi.org/10.1016/j.ecohyd.2019.03.003

Beven, K. and Binley, A., 1992. The Future of Distributed Models - Model Calibration and Uncertainty Prediction. Hydrological Processes, 6(3): 279-298.

Beasley, D. B., L. F. Huggins, and E. J. Monke. 1980. ANSERS: A model for watershed planning. Trans. ASAE. 23(4):938-944.

Beman, J. M., K. R. Arrigo, and P. A. Matson. 2005. Agricultural runoff fuels large phytoplankton blooms in vulnerable areas of the ocean. Nature 434(7030):211-214.

Boles, C. M., J. R. Frankenberger, and D. N. Moriasi, D. N: 2015. Tile Drainage Simulation in SWAT2012: Parameterization and Evaluation in an Indiana Watershed, Trans. ASABE, 58, 1201-1213, doi: 10.13031/trans.58.10589.

Bingner, R.L., F.D. Theurer and Y. Yuan 2007. AnnAGNPS Technical Processes. Available at:ftp://199.133.90.201/pub/outgoing/AGNPS/AGNPS_Web_Files/pdf_files/AnnAGNPS_Technical_Documentation.pdf.

Borah, D.K., G. Yagow, A. Saleh, P.L. Barnes, W. Rosenthal, E.C. Krug, and L.M. Hauck. 2006. Sediment and nutrient modeling for TMDL development and implementation. Trans. ASABE 49(4):967–986.

Bowen, J. D. and J. W. Hieronymus. 2003. A CE-QUAL-W2 Model of Neuse Estuary for Total Maximum Daily Load Development. J. Water Resour. Plann. Manage., 129(4), 283–294.

Brown, L. C., and T. O. Barnwell. 1985. Computer program documentation for the enhanced stream water quality model QUAL2E. Environmental Research Laboratory, Office of Research and Development, US Environmental Protection Agency.

Brown, L.C. and T.O. Barnwell, Jr. 1987. The enhanced water quality models QUAL2E and QUAL2E-UNCAS documentation and user manual. EPA document EPA/600/3-87/007. USEPA, Athens, GA.

Bui, H.H., Ha, N.H., Nguyen, T.N.D., Nguyen, A.T., Pham, T.T.H., Kandasamy, J., Nguyen, T.V., 2019. Integration of swat and qual2k for water quality modeling in a data scarce basin of cau river basin in vietnam. Ecohydrol. Hydrobiol. 19, 210–223.

Bunting, L., P. R. Leavitt, B. Wissel, K. R. Laird, B. F. Cumming, A. St. Amand, and D. R. Engstrom. 2011. Sudden ecosystem state change in Lake Winnipeg, Canada, caused by eutrophication arising from crop and livestock production during the 20th century. Manitoba Water Stewardship, Winnipeg, MB. 72pp.

Chambers P.A., M. Guy, E.S. Roberts, M.N. Charlton, R. Kent, C. Gagnon, G. Grove, and N. Foster. 2001. Nutrients and their impact on the Canadian environment. Agriculture and Agri-Food Canada, Environment Canada, Fisheries and Oceans Canada, Health Canada and Natural Resources Canada. 241 p.

CH2M HILL. 2001. Eastern Ontario Water Resources Management Study final report. CH2M HILL, Ottawa, ON.

Clearwater, R. L., T. Martin and T. Hoppe (eds.). 2016. Environmental sustainability of Canadian agriculture: Agri-environmental indicator report series – Report #4. Ottawa, ON: Agriculture and Agri-Food Canada.

Chapra, S.C., Pelletier, G.J. and Tao, H. 2012. QUAL2K: A Modeling Framework for Simulating River and Stream Water Quality, Version 2.12: Documentation and User's Manual. Civil and Environmental Engineering Dept., Tufts University, Medford, MA,

Charbonneau, P. and B. Knapp. 1995. *A user's guide to PIKAIA 1.0,* NCAR Tech. Note 418+IA, National Center for Atmospheric Research, Boulder, Colorado.

Christensen, O. B., Drews, M., Christensen, J. H., Dethloff, K., Ketelsen, K., Hebestadt, I. and Rinke, A.: The HIRHAM regional climate model version 5., DMI Technical Report, DMI, Copenhagen, Denmark. [online] Available from: https://www.dmi.dk/fileadmin/Rapporter/TR/tr06-17.pdf, 2006.

Chylek, P., Li, J., Dubey, M. K., Wang, M., and Lesins, G.: Observed and model simulated 20th century Arctic temperature variability: Canadian Earth System Model CanESM2, Atmos. Chem. Phys. Discuss., 11, 22893–22907, https://doi.org/10.5194/acpd-11-22893-2011, 2011.

Cole, T. M., and S. A. Wells. 2015. "CE-QUAL-W2: A two-dimensional, laterally averaged, hydrodynamic and water quality model, version 3.72," Department of Civil and Environmental Engineering, Portland State University, Portland, OR.

Collins, W. J., Bellouin, N., Doutriaux-Boucher, M., Gedney, N., Halloran, P., Hinton, T., Hughes, J., Jones, C. D., Joshi, M., Liddicoat, S., Martin, G., O'Connor, F., Rae, J., Senior, C., Sitch, S., Totterdell, I., Wiltshire, A., and Woodward, S.: Development and evaluation of an Earth-System model – HadGEM2, Geosci. Model Dev., 4, 1051–1075, https://doi.org/10.5194/gmd-4-1051-2011, 2011.

Connolly, J.P. and R. Winfield. 1984. A User's Guide for WASTOX, a Framework for Modeling the Fate of Toxic Chemicals in Aquatic Environments. Part 1: Exposure Concentration. U.S. Environmental Protection Agency, Gulf Breeze,FL. EPA-600/3-84-077.

Daniels, A.E.; Morrison, J.F.; Joyce, L.A.; Crookston, N.L.; Chen, S.C.; McNulty, S.G. 2012. Climate projections FAQ. Gen. Tech. Rep. RMRS-GTR-277WWW. Fort Collins, CO: U.S. Department of Agriculture, Forest Service, Rocky Mountain Research Station. 32 p.

Debele B., R. Srinivasan, J. Y. Parlange. 2008. Coupling upland watershed and downstream waterbody hydrodynamic and water quality models (SWAT and CE-QUAL-W2) for better water resources management in complex river basins. Environ. Model Asses. 13(1):135–153.

DHI. 2009. MIKE 11 – a modeling system for rivers and channels. Danish Hydraulic Institute.

Di Toro, D. M., J. J. Fitzpatrick, and R. V. Thomann. 1981, rev. 1983. Water Quality Analysis Simulation Program (WASP) and Model Verification Program (MVP)-Documentation. Hydroscience, Inc., Westwood, NY, for US EPA, Duluth, MN. Contract, (68-01), 3872.

Dile, Y. T. and R. Srinivasan, 2014. Evaluation of CFSR climate data for hydrologic prediction in data-scarce watersheds: an application in the Blue Nile River Basin. Journal of the American Water Resources Association (JAWRA) 1-16.

Doan, Q. T., N. C. Don, Y. C. Chen, and P. K. Mishra. 2015. Applying numerical method to understand the effect of climate change on the salinity intrusion in Ca River basin, Vietnam. Lowland Technology International 17 (2): 93-104.

Du, B., J. G. Arnold, A. Saleh, and D. B. Jaynes. 2005. Development and application of SWAT to landscapes with tiles and potholes. Trans. ASAE 48(3): 1121-1133.

Dunne, J. P., John, J. G., Adcroft, A. J., Griffies, S. M., Hallberg, R. W., Shevliakova, E., Stouffer, R. J., Cooke, W., Dunne, K. A., Harrison, M. J., Krasting, J. P., Malyshev, S. L., Milly, P. C. D., Phillipps, P. J., Sentman, L. T., Samuels, B. L., Spelman, M. J., Winton, M., Wittenberg, A. T., and Zadeh, N.: GFDL's ESM2 Global Coupled Climate–Carbon Earth System Models. Part I: Physical Formulation and Baseline Simulation Characteristics, J. Climate, 25, 6646–6665, 2012.

Dunne, J. P., John, J. G., Shevliakova, E., Stouffer, R. J., Krast-ing, J. P., Malyshev, S. L., Milly, P. C. D., Sentman, L. T., Ad-croft, A. J., Cooke, W., Dunne, K. A., Griffies, S. M., Hallberg,R. W., Harrison, M. J., Levy, H., Wittenberg, A. T., Phillips, P. J.,and Zadeh, N. 2013. GFDL's ESM2 Global Coupled Climate-CarbonEarth System Models. Part II: Carbon

System Formulation and Baseline Simulation Characteristics, J. Climate, 26, 2247–2267. https://doi.org/10.1175/JCLI-D-12-00150.1.

Eastern Ontario Warden's Caucus. 2007. A Profile of Eastern Ontario (Regional Data Set). The Eastern Ontario Rural Policy Project, ON, Canada. Retrieved from http://www.eowc.org/en/futuredirections/resources/Profile_Eastern_Ont-Regional_Data-Mar3107.pdf. (Accessed on May 20, 2015)

Edinger, J. E. and E. M. Buchak. 1975. "A Hydrodynamic, Two-Dimensional Reservoir Model: The Computational Basis", prepared for US Army Engineer Division, Ohio River, Cincinnati, Ohio.

Eman Mostafa Foda, Mohamed Mohamed Foad Sobeih, Gehan Abd El - Hakeem Salam, Ashraf Fathy Saber Ellayn, and Yasser Mohamed Atta. 2020. Long-term effects of using controlled drainage on: Crop yields and soil salinity in Egypt, Water Science, 34:1, 143-154, DOI: 10.1080/11104929.2020.1807169.

Engel, B. A., R. Srinivasan, J. Arnold, C. Rewerts, S. J. Brown, 1993. Nonpoint source (NPS) pollution modeling using models integrated with geographic information systems (GIS). Water Science & Technology, 28(3-5), 685-690.

Environment Canada. 2001. Threads to Source of Drinking Water and Aquatic Ecosystem Health in Canada. National Water Research Institute, Burlington, Ontario. NWRI Scientific Assessment Report Series No.1. 72p.

Environment Canada. 2012. National climate data and information archive: Climate normals from 1971-2000. Environment Canada, Ottawa, Ontario.

Environment Canada. 2014. Climate data online. Retrieved from http://climate.weather.gc.ca/index_e.html (accessed on Feburary 15, 2014).

Environment Canada. 2015. Historical hydrometric data. Retrieved from https://wateroffice.ec.gc.ca/mainmenu/historical_data_index_e.html (accessed April 18, 2015).

Environment Canada. 2017. Engineering Climate Datasets. http://climate.weather.gc.ca/prods_servs/engineering_e.html (accessed 16 Sept. 2017).

Environment Canada and Manitoba Water Stewardship. 2011. State of Lake Winnipeg. Ottawa and Winnipeg: Government of Canada and the Government of Manitoba. Retrieved from http://www.gov.mb.ca/waterstewardship/water_quality/state_lk_winnipeg_report/pdf/state_of_lake_winnipeg_rpt_technical_low_resolution.pdf. (Accessed on March 25, 2015)

Environment Canada and the U.S. Environmental Protection Agency. 2014. State of the Great Lakes 2011. Cat No. En161-3/1-2011E-PDF. EPA 950-R-13-002. Retrieved from http://binational.net. (Accessed on April 25, 2015)

European Environment Agency. 2005. Source apportionment of nitrogen and phosphorus inputs into the aquatic environment. EEA Report No. 7 / 2005. European Environment Agency, Copenhagen, Denmark.

Evans, R.O., J.E. Parsons, K. Stone, and B. Wells. 1992. Water table management on a watershed scale. J. Soil Water Conserv. 47:58–64.

Fuka, D.R., C.A. MacAllister, A.T. Degaetano, and Z.M. Easton. 2013. Using the Climate Forecast System Reanalysis dataset to improve weather input data for watershed models. Hydrol. Proc. 28(22):5613–5623.

Garrison, F. H. 1929. The history of drainage, irrigation, sewage-disposal and water-supply. Bulletin of the New York Academy of Medicine, 5(10), 887–938.

Gikas G. D. 2014. Water quality of drainage canals and assessment of nutrient loads using QUAL2Kw. Environ Process 1(4):369–385.

Giorgi F, Coppola E, Solmon F, Mariotti L, Sylla MB, Bi X et al (2012) RegCM4: model description and preliminary tests over multiple CORDEX domains. Clim Res 52:7–29. https ://doi.org/10.3354/cr01018

Globalweather, 2014. NCEP Climate Forecast System Reanalysis (CFRS). Retrieved from http://globalweather.tamu.edu/. (Accessed on December 22, 2014)

Golmohammadi, G. 2014. Development and evaluation of SWATDRAIN, a new model to simulate the hydrology of agricultural tile-drained watersheds. [Doctoral dissertation, McGill University]. https://escholarship.mcgill.ca/concern/theses/kk91fq062

Golmohammadi, G., Rudra, R., Prasher, S. et al. Modeling the effects of controlled drainage at a watershed scale using SWATDRAIN. Arab J Geosci 9, 582 (2016). https://doi.org/10.1007/s12517-016-2608-2

Green, W.H. and G.A. Ampt. 1911. Studies on soil physics, 1. The flow of air and water through soils. Journal of Agricultural Sciences 4:11-24.

Gulhati, N.D. and W.Ch. Smith 1967. Irrigated agriculture: a historical review. In: R.M. Hagan, H.R. Haise and T.W. Edminster (eds.), Irrigation of agricultural lands. Agronomy 11, American Society of Agronomy, Madison. pp. 3-11.

Guo, T., Gitau, M., Merwade, V., Arnold, J., Srinivasan, R., Hirschi, M., and Engel, B.: Comparison of performance of tile drainage routines in SWAT 2009 and 2012 in an extensively tile-drained watershed in the Midwest, Hydrol. Earth Syst. Sci., 22, 89–110, https://doi.org/10.5194/hess-22-89-2018, 2018.

Gupta, H.V., S. Sorooshian, and P.O. Yapo. 1999. Status of automatic calibration for hydrologic models: Comparison with multilevel expert calibration. J. Hydrol. Eng. 4(2):135–143. doi:10.1061/(ASCE)1084-0699(1999)4:2(135)

Hamilton, P. A. and T. L. Miller. 2002. Lessons from the national water-quality assessment. Journal of Soil and Water Conservation 57(1):16A- 21A.

Hamrick, J. M. 1992. "A three-dimensional environmental fluid dynamics computer code: Theoretical and computational aspects." Special Rep. No. 317, the College of William and Mary, Virginia Institute of Marine Science, VA.

Hanke K. 2018. Impacts of Climate Change and Controlled Tile Drainage on Water Quality and Quantity in Southern Ontario, Canada. UWSpace. http://hdl.handle.net/10012/13757

Hazeleger W, Wang X, Severijns C, Ştefãnescu S, Bintanja R, Sterl A, Wyser K, Semmler T, Yang S, Van den Hurk B, Van Noije T (2012) EC-Earth V2. 2: description and validation of a new seamless earth system prediction model. Clim Dyn 39(11):2611–2629

Hooghoudt, S. B. 1940. General consideration of the problem of field drainage by parallel drains, ditches, water courses, and channels. Contribution to the Knowledge of Some Physical Parameters of the Soil, Publication No. 7. Groningen. The Netherlands: Bodemkundig Instituut.

ICID. 1979. Amendments to the constitution, Agenda of the International Council Meeting at Rabat. International Commission on Irrigation and Drainage, Morocco. ICID, New Delhi, pp. A-156-163.

IPCC, 2014: Climate Change 2014: Synthesis Report. Contribution of Working Groups I, II and III to the Fifth Assessment Report of the Intergovernmental Panel on Climate Change [Core Writing Team, R.K. Pachauri and L.A. Meyer (eds.)]. IPCC, Geneva, Switzerland, 151 pp.

Jacobsen, T. and R.M. Adams. 1958. Salt and silt in ancient Mesopotamian agriculture. Science 128(3334):1251-1258.

James, E., P. Kleinman, T. Veith, R. Stedman, and A. Sharpley. 2007. Phosphorus contributions from pastured dairy cattle to streams of the Cannonsville Watershed, New York. Journal of Soil and Water Conservation 62(1):40-47.

Johansen, N. B., J. C. Imhoff, J. L. Kittle, and A. S. Donigian. 1984. Hydrological Simulation Program − Fortran (HSPF): User's Manual. EPA−600/3−84−066. Athens, GA, USEPA.

Kennedy, J.; R. Eberhart. 1995. Particle Swarm Optimization. Proceedings of IEEE International Conference on Neural Networks IV. pp. 1942–1948.

King, F.H. 191 I. Farmers of forty centuries, or permanent agriculture in China, Korea and Japan. Rodale, 441 p.

Knisel, W.G. 1980. CREAMS, a field scale model for chemicals, runoff and erosion from agricultural management systems. USDA Conservation Research Rept. No. 26.

Kannel, P. R., S. Lee, Y. S. Lee, S. R. Kanel, and G. J Pelletier. 2007. Application of automated QUAL2Kw for water quality modeling and management in the Bagmati River, Nepal. Ecological Modelling, 202(3), 503-517.

Kjellström E, Bärring L, Nikulin G, Nilsson C, Persson G and Strandberg G 2016 Production and use of regional climate model projections—A Swedish perspective on building climate services Clim. Serv. 2 15–29.

Koch, S., A. Bauwe, and B. Lennartz. 2012. Application of the SWAT model for a tile-drained lowland catchment in North-Eastern Germany on subbasin scale, Water Resour. Manage., 27, 791-805, doi:10.1007/s11269-012-0215-x.

Kuczera, G., Parent, E., 1998. Monte Carlo assessment of parameter uncertainty in conceptual catchment models: the Metropolis algorithm. Journal of Hydrology, 211(1-4):69-85.

Leonard, R.A., W.G. Knisel, and D.A. Still. 1987. GLEAMS: Groundwater loading effects on agricultural management systems. Trans. ASAE 30(5):1403-1428.

Lalonde, V., C. A. Madramootoo, L. Trenholm, and R. S. Broughton. 1996. Effects of controlled drainage on nitrate concentrations in subsurface drain discharge. Agric. Water Manage. 29:187–199.

Legates, D.R. and G.J. McCabe. 1999. Evaluating the use of "goodness-of-fit" measures in hydrologic and hydroclimatic model validation. Water Resources Res. 35(1): 233-241.

Luo, W., G.R. Sands, M. Youssef, J.S. Strock, I. Song, and D. Canelon. 2010. Modeling the impact of alternative drainage practices in the northern Corn-belt with DRAINMOD-NII. Agric. Water Manage. 97:389–398.

Mauritsen, T., Bader, J., Becker, T., Behrens, J., Bittner, M., Brokopf, R., et al. (2019). Developments in the MPI-M Earth System Model version 1.2 (MPI-ESM1.2) and its response to increasing CO2. Journal of Advances in Modeling Earth Systems, 11, 998–1038. https://doi.org/10.1029/2018MS001400.

McKay, M.D., R. J. Beckman, W. J. Conover. 1979. A comparison of three methods for selecting values of input variables in the analysis of output from a computer code. Technometrics. 21, 239-245.

McIsaac, G. F., M. B. David, G. Z. Gertner, and D. A. Goolsby. 2001. Eutrophication: Nitrate flux in the Mississippi River. Nature, 414(6860), 166-167.

McNairn, H., C. Champagne, J. Shang, D. Holmstrom, G. Reichert. 2009. Integration of optical and Synthetic Aperture Radar (SAR) imagery for delivering operational annual crop inventories, ISPRS Journal of Photogrammetry and Remote Sensing, Vol. 64(5), p. 434-449.

Mearns, L.O., et al., 2017: The NA-CORDEX dataset, version 1.0. NCAR Climate Data Gateway, Boulder CO, accessed [date], https://doi.org/10.5065/D6SJ1JCH.

Michalak, A.M., E.J. Anderson, D. Beletsky, S. Boland, N.S. Bosch, T.B. Bridgeman, J.D. Chaffin, K. Cho, R. Confesor, I. Daloğlu, J.V. DePinto, M.A. Evans, G.L. Fahnenstiel, L. He, J.C. Ho, L. Jenkins, T.H. Johengen, K.C. Kuo, E. LaPorte, X. Liu, M.R. McWilliams, M.R. Moore, D.J. Posselt, R.P. Richards, D. Scavia, A.L. Steiner, E. Verhamme, D.M. Wright, and M.A. Zagorski. 2013. Record-setting algal bloom in Lake Erie caused by agricultural and meteorological trends consistent with expected future conditions. Proc. Natl. Acad. Sci. USA 110(16):6448–6452.

Moriasi, D. N., C. Rossi, J. G. Arnold, and M. Tomer. 2012. Evaluating hydrology of the Soil and Water Assessment Tool (SWAT) with new tile drain equations. J. Soil Water Cons., 67(6), 513-524.

Moriasi, D. N., J. G. Arnold, and C. H. Green. 2007. Incorporation of Hooghoudt and Kirkham tile drain equations into SWAT2005. Proc. 4th Intl. SWAT Conf. Delft, The Netherlands: UNESCO-IHE. pp. 139-147.

Moriasi, D.N., J.G. Arnold, M.W. Van Liew, R.L. Bingner, R.D. Harmel, and T.L. Veith. 2007. Model evaluation guidelines for systematic quantification of accuracy in watershed simulations. Trans. ASABE 50(3):885–900. doi:10.13031/2013.23153.

Moriasi, D. N., P. H. Gowda, J. G. Arnold, D. J. Mulla, S. Ale, J. L. Steiner, and M. D. Tomer. 2013. Evaluation of the Hooghoudt and Kirkham tile drain equations in the Soil and Water Assessment Tool to simulate tile flow and nitrate-nitrogen.J. Environ. Qual., 42(6), 1699-1710. http://dx.doi.org/10.2134/jeq2013.01.0018.

Neitsch, S. L., J. G. Arnold, J. R. Kiniry, J. R. and Williams. 2011. Soil and Water Assessment Tool Theoretical Documentation Version 2009, Texas Water Resources Institute Technical Report 406, Texas A&M University System, College Station (Texas).

Ng, H.Y.F., C.S. Tan, C.F. Drury, and J.D. Gaynor. 2002. Controlled drainage and subirrigation influences tile nitrate loss and corn yields in a sandy loam soil in southwestern Ontario. Agric. Ecosyst. Environ. 90:81–88.

Ning, S.K., Ni-Bin Chang, L. Yang, H.W. Chen and H.Y. Hsu. 2001. Assessing pollution prevention program by QUAL2E simulation analysis for the Kao-Ping River Basin-Taiwan. Journal of Environmental Management 61 (1): 61–76.

Nash, J.E., and J.V. Sutcliffe. 1970. River flow forecasting through conceptual models: Part I. A discussion of principles. J. Hydrol. 10(3):282–290. doi:10.1016/0022-1694(70)90255-6.

Ontario Ministry of the Environment. 2015. The Provincial (Stream) Water Quality Monitoring Network (PWQMN). Retrieved from http://www.ontario.ca/data/provincial-stream-water-quality-monitoring-network (accessed April 19, 2015).

Paliwal, R., P. Sharma, and A. Kansal. 2007. Water quality modelling of the river Yamuna (India) using QUAL2E-UNCAS. Journal of Environmental Management, 83(2):131–144.

Park, S. S., Y. Na, C. G. Uchrin. 2003. An oxygen equivalent model for water quality dynamics in a macrophyte dominated river. Ecological modelling, 168(1), 1-12.

Parris K. 2011. Impact of Agriculture on Water Pollution in OECD Countries: Recent Trends and Future Prospects, International Journal of Water Resources Development, 27:1, 33-52, DOI: 10.1080/07900627.2010.531898.

Pelletier, G. J. and S. C. Chapra. 2008. "QUAL2Kw theory and documentation (version 5.1)." Environmental Assessment Program, Olympia, Washington.

Pelletier, G. J., S. C. Chapra, and H. Tao. 2006. QUAL2Kw, A framework for modeling water quality in streams and rivers using a genetic algorithm for calibration. Environmental Modelling and Software, vol. 21, p. 419-425.

Pommainville A. 2007 Survey on Agricultural Management Practices. Alfred, ON, Canada.

Powers, J. G., and Coauthors, 2017: The Weather Research and Forecasting Model. Overview, system efforts, and future direction. Bull. Amer. Meteor. Soc., 98, 1717–1737, https://doi.org/10.1175/BAMS-D-15-00308.1.

Que, Z., O. Seidou, R.L. Droste, G.A. Wilkes, M. Sunohara, E. Topp, and D. R. Lapen. 2015. Using AnnAGNPS to predict the effects of tile drainage control on nutrient and sediment loads for a river basin. Journal of Environmental Quality, 44, pp. 1-13.

Rabalais, N.N., R.E. Turner, and W.J. Wiseman, Jr. 2002. Gulf of Mexico hypoxia, a.k.a. “The Dead Zone”. Annu. Rev. Ecol. Syst. 33:235–263.

Rahman, M. M., Z. Lin, and D.N. Moriasi. 2011. Applying SWAT for impact analysis of tile drainage on streamflow in a snow dominated watershed. ASABE Paper No. 1110866. St. Joseph, Mich.: ASABE.

Rehana S, and P.P. Mujumdar. 2011. River water quality response under hypothetical climate change scenarios in Tunga–Bhadra river, India. Hydrological Processes. DOI: 10.1002/hyp.8057

Roesner, L.A., P.R. Giguere, and D.E. Evenson. 1981a. User’s Manual for Stream Quality Model (QUAL – II). USEPA, Athens, GA, EPA-600/9-81-014.

Roesner, L.A., P.R. Giguere, and D.E. Evenson. 1981b. User’s Manual for Stream Quality Model (QUAL – II). USEPA, Athens, GA, EPA-600/9-81-015.

Saleh, A. and B. Du. 2004. Evaluation of SWAT and HSPF within BASINS program for the Upper North Bosque River watershed in Central Texas. In Trans. ASAE.

Soil Conservation Service (SCS). 1972. Section 4: Hydrology in National Engineering Handbook. SCS.

Santhi, C., R. Srinivasan, J.G. Arnold, and J.R. Williams. 2006. A modeling approach to evaluate the impacts of water quality management plans implemented in a watershed in Texas. Environ. Model. Softw. 21:1141– 1157.

Santhi, C., J. G. Arnold, J. R. W illiams, W. A. Dugas, R. Srinivasan, and L. M. Hauck. 2001. Validation of the SWAT model on large river basin with point and nonpoint sources. J. Am. Water Resources Assoc. 37(5):1169–1188.

Scinocca, J., and Coauthors, 2016: Coordinated global and regional climate modeling. J. Climate, 29, 17–35, https://doi.org/10.1175/JCLI-D-15-0161.1.

Skaggs, R.W. and M.A. Youssef. 2008. Effect of Drainage Water Management on Water Conservation and Nitrogen Losses to Surface Waters. Presented at the 16th National Nonpoint source monitoring Workshop, Columbus, OH. Sept. 14-18, 2008.

Skaggs, R.W., Youssef, M.A. and Chescheir, G.M., 2012. 'DRAINMOD: model use, calibration and validation'. American Society of Agricultural and Biological Engineers, vol. 55 (4), pp. 1509 -1522

Smith, V. H., S. B. Joye, and R. W Howarth. 2006. Eutrophication of freshwater and marine ecosystems. Limnol. Oceanogr. 51:351–355.

South Nation Conservation. 2018. State of the nation - Watershed Report Card. http://www.nation.on.ca/water/reports/watershed-report-cards (March 25, 2018)

Sunohara, M.D., E. Craiovan, E. Topp, N. Gottschall, C.F. Drury, and D.R. Lapen. 2014. Comprehensive nitrogen budgets for controlled tile drainage fields in eastern Ontario, Canada. J. Environ. Qual. 43:617–630.

Sunohara, M.D., N. Gottschall, G. Wilkes, E. Craiovan, E. Topp, Z. Que, O. Seidou, S. Frey, and D. R. Lapen. 2015. Long term observations of nitrogen and phosphorus export in paired-agricultural watersheds under controlled and conventional tile drainage management. Journal of Environmental Quality, 44(5):1589-604.

Tan, C. S., C. F. Drury, H. Y. F. Ng, and J. D. Gaynor. 1999. Effect of controlled drainage and subirrigation on subsurface tile drainage nitrate loss and crop yield at the farm scale. Can. Water Resour. J. 24(3):177–186.

Texas Water Development Board. 1970. QUAL-I — Simulation of Water Quality in Stream and Canals: Program Documentation and User's Manual. Austin, TX, US.

Thorp, K.R., D.B. Jaynes, and R.W. Malone. 2008. Simulating the long-term performance of drainage water management across the midwestern United States. Trans. ASABE 51:961–976.

Trzaska, S. and Schnarr, E. 2014. A Review of Downscaling Methods for Climate Change Projections: African and Latin American Resilience to Climate Change (ARCC).

http://www.ciesin.org/documents/Downscaling_CLEARED_000.pdf

United Nations. 1992. United Nations Framework Convention on Climate Change. [New York]: United Nations, General Assembly.

US EPA. (1997). "Streams and rivers." Technical guidance manual for performing waste load allocations, Streams and Rivers, United States Environmental Protection Agency, Washington, DC.

US Bureau of Reclamation. 1993. Drainage Manual (Revised Reprint). United States Department of the Interior, Bureau of Reclamation, Denver, Colorado, USA, 212-218, 321 pp.

USEPA (US Environment Protection Agency). 1984. Report to Congress: Nonpoint Source Pollution in the U.S.; U.S. Environmental Protection Agency, Office of Water: Washington, DC.

USGAO (US General Accounting Office). 1990. Water pollution: Greater EPA leadership needed to reduce nonpoint source pollution. RCED-91.10. Gaithersburg, MD: US Government Accounting Office. http://www.gao.gov/assets/150/149860.pdf. (Accessed on January 25, 2015)

Van Griensven, A. and T. Meixner. 2006. Methods to quantify and identify the sources of uncertainty for river basin water quality models. Water Science and Technology, 53(1):51-59.

van Schilfgaarde, J., F. Engelund, D. Kirkham, D. F. Peterson, and M. Maasland. 1957. Theory of land drainage. In Drainage of Agricultural Lands. Agronomy Monograph No. 7. Madison,Wisc.: ASA.

Vörösmarty, C. J., P. B. McIntyre, M. O. Gessner, D. Dudgeon, A. Prusevich, P. Green, S. Glidden, S. E. Bunn, C. A. Sullivan, C. Reidy Liermann, and P. M. Davies. 2010. Global threats to human water security and river biodiversity. Nature 467, 555–561

Wesström, I., and I. Messing. 2007. Effects of controlled drainage on N and P losses and n dynamics in a loamy sand with spring crops. Agric. Water Manage. 87:229–240.

Whitehead P. G., R. L. Wilby, R. W. Battarbee, M. Kernan and A. J. Wade. 2009. A review of the potential impacts of climate change on surface water quality, Hydrological Sciences Journal, 54:1, 101-123, DOI: 10.1623/hysj.54.1.101

WHO and UNICEF (World Health Organization/United Nations Children's Fund). 2015. Progress on sanitation and drinking water: 2015 Update and MDG assessment. New York, WHO/UNICEF Joint Monitoring Programme for Water Supply and Sanitation.

Wicklund, R.E., and N.R. Richards. 1962. Soil survey of Russell and Prescott Counties. Rep No. 33 of the Ontario Soil Survey, Research Branch. Canada Department of Agriculture, Ottawa, ON, Canada.

Williams, J. R. 1975. Sediment routing for agricultural watersheds. Water Resour. Bull. 11(5):965-974.

Williams, J.R., A.D. Nicks, and J.G. Arnold. 1985. Simulator for water resources in rural basins. Journal of Hydraulic Engineering 111(6): 970-986.

Williams, J.R., C.A. Jones and P.T. Dyke. 1984. A modeling approach to determining the relationship between erosion and soil productivity. Trans. ASAE 27(1):129-144.

Wischmeier, W.H. and D.D. Smith. 1965. Predicting rainfall-erosion losses from cropland east of the Rocky Mountains. Agriculture Handbook 282. USDA-ARS.

Wischmeier, W.H., and D.D. Smith. 1978. Predicting rainfall losses: A guide to conservation planning. USDA Agricultural Handbook No. 537. U.S. Gov. Print. Office, Washington, D. C.

Withers, P. J. A.; C. Neal, H. P. Jarvie, D. G Doody. 2014. Agriculture and eutrophication: where do we go from here? Sustainability, 6, 5853-5875.

Working Group on the State of the St. Lawrence Monitoring. 2014. Overview of the State of the St. Lawrence 2014. St. Lawrence Action Plan. Environment Canada, Québec's ministère du Développement durable, de l'Environnement et de la Lutte contre les changements climatiques), Québec's ministère des Forêts, de la Faune et des Parcs, Parks Canada, Fisheries and Oceans Canada, and Stratégies Saint‑Laurent. 52 p.

World Bank. 2013. Retrieved from http://data.worldbank.org/indicator/ER.H2O.INTR.K3. (Accessed on July 20, 2015).

WWAP (World Water Assessment Programme). 2012. The United Nations World Water Development Report 4: Managing Water under Uncertainty and Risk. Paris, UNESCO.

WWAP (United Nations World Water Assessment Programme). 2015. The United Nations World Water Development Report 2015: Water for a Sustainable World. Paris, UNESCO.

WWAP (United Nations World Water Assessment Programme). 2016. The United Nations World Water Development Report 2016: Water and Jobs. Paris, UNESCO.

Young, R.A., C.A. Onstad, D.D. Bosch, and W.P. Anderson. 1989. AGNPS: A nonpoint-source pollution model for evaluating agricultural watersheds. J. Soil Water Conserv. 44(2):168–173.

Youssef, M.A.; Abdelbaki, A.M.; Negm, L.M.; Skaggs, R.W.; Thorp, K.R.; Jaynes, D.B. 2018. DRAINMOD-simulated performance of controlled drainage across the U.S. Midwest. Agric. Water Manag., 197, 54–66.

Yuan, Y., R.L. Bingner, and J. Boydstun. 2006. Development of TMDL watershed implementation plan using annualized ANGPS. Land Use Water Resour. Res. 6:2.1–2.8.

Yuan, Y., R.L. Bingner, M.A. Locke, F.D. Theurer, and J. Stafford. 2011. Assessment of subsurface drainage management practices to reduce nitrogen loadings using AnnAGNPS. Appl. Eng. Agric. 27(3):335–344.

Zhang, R., X. Qian, H. Li, X. Yuan, R. Ye. 2012. Selection of optimal river water quality improvement programs using QUAL2K: A case study of Taihu Lake Basin, China. Sci. Total Environ. 431: 278–285.

Zhang, W. L., S. X. Wu, H. J. Ji, and H. Kolbe. 2004. Estimation of agricultural non-point source pollution in China and the alleviating strategies: I. Estimation of agricultural non-point source pollution in China in early 21 century. Sci. Agric. Sin. 37(7):1008–1017. (In Chinese)

Zou, R., S. Carter, L. Shoemaker, A. Parker, and T. Henry, T. 2006. Integrated hydrodynamic and water quality modeling system to support nutrient total maximum daily load development for Wissahickon Creek, Pennsylvania. Journal of Environmental Engineering, 132(4), 555-566.

APPENDICES

i. Appendix 1 Tile drainage depth program

```
% Read SWAT model mgt files that contain tile drain depth and replace with desired tile
% drain depth 600 mm.
% By Que, zhenyang. Septemper, 2015 in Morden, MB

for k = 1:31
   % Create a text file name, and read the file.
   if k <=9
      for j = 1:600
         if j<=9
            textFileName = ['0000' num2str(k) '000' num2str(j) '.hru'];
            if exist(textFileName, 'file')
               fid = fopen(textFileName,'r');

               depth_to_change = '          6000    ';
               new_depth = '          3000    ';
               % Find the tile depth to change
               while ~feof(fid)
                  tline = fgetl(fid);
                  temp = strsplit(tline,'|'); % Split the tile drain line into 2 cells
                  if strcmp(temp{1},depth_to_change)
                     newline = strrep(tline,temp{1},new_depth);
                     frewind(fid); % Go back to start of the file
                     fulltext = fread(fid,'*char')'; % Reserve entire file prior to discarding
                     fclose(fid);
                     fid = fopen(textFileName,'w'); % Loading with write flag discards the file
contents
                     fulltext = strrep(fulltext,tline,newline); % Replace tile depth
                     fprintf(fid,'%s',fulltext); % Write modified text back to file
                     fclose(fid);
                     fprintf('Tile depth in file %s has been changed successfully!\n',
textFileName);
                    break
                  end
```

```
            end
            fclose('all');
        else
            fprintf('File %s does not exist.\n', textFileName);
        end
    elseif (10<= j)&&(j <= 99)
        textFileName = ['0000' num2str(k) '00' num2str(j) '.hru'];
        if exist(textFileName, 'file')
           fid = fopen(textFileName,'r');
            depth_to_change = '           6000     ';
            new_depth = '            3000     ';
            % Find the tile depth to change
            while ~feof(fid)
                tline = fgetl(fid);
                temp = strsplit(tline,'|'); % Split the tile drain line into 2 cells
                if strcmp(temp{1},depth_to_change)
                    newline = strrep(tline,temp{1},new_depth);
                    frewind(fid); % Go back to start of the file
                    fulltext = fread(fid,'*char')'; % Reserve entire file prior to discarding
                    fclose(fid);
                    fid = fopen(textFileName,'w'); % Loading with write flag discards the file
contents
                    fulltext = strrep(fulltext,tline,newline); % Replace tile depth
                    fprintf(fid,'%s',fulltext); % Write modified text back to file
                    fclose(fid);
                    fprintf('Tile depth in file %s has been changed successfully!\n',
textFileName);
                    break
                end
            end
            fclose('all');
        else
            fprintf('File %s does not exist.\n', textFileName);
        end
    elseif (100 <= j)&&(j <=600)
        textFileName = ['0000' num2str(k) '0' num2str(j) '.hru'];
        if exist(textFileName, 'file')
```

```
                fid = fopen(textFileName,'r');
                depth_to_change = '            6000    ';
                new_depth = '            3000    ';
                % Find the tile depth to change
                while ~feof(fid)
                    tline = fgetl(fid);
                    temp = strsplit(tline,'|'); % Split the tile drain line into 2 cells
                    if strcmp(temp{1},depth_to_change)
                        newline = strrep(tline,temp{1},new_depth);
                        frewind(fid); % Go back to start of the file
                        fulltext = fread(fid,'*char')'; % Reserve entire file prior to discarding
                        fclose(fid);
                        fid = fopen(textFileName,'w'); % Loading with write flag discards the file
contents
                        fulltext = strrep(fulltext,tline,newline); % Replace tile depth
                        fprintf(fid,'%s',fulltext); % Write modified text back to file
                        fclose(fid);
                        fprintf('Tile depth in file %s has been changed successfully!\n',
textFileName);
                        break
                    end
                end
                fclose('all');
            else
                fprintf('File %s does not exist.\n', textFileName);
            end
        end
    end
else
    for j = 1:600
        if j<=9
            textFileName = ['000' num2str(k) '000' num2str(j) '.hru'];
            if exist(textFileName, 'file')
               fid = fopen(textFileName,'r');
                depth_to_change = '            6000    ';
                new_depth = '            3000    ';
                % Find the tile depth to change
```

```
        while ~feof(fid)
          tline = fgetl(fid);
          temp = strsplit(tline,'|'); % Split the tile drain line into 2 cells
          if strcmp(temp{1},depth_to_change)
            newline = strrep(tline,temp{1},new_depth);
            frewind(fid); % Go back to start of the file
            fulltext = fread(fid,'*char')'; % Reserve entire file prior to discarding
            fclose(fid);
            fid = fopen(textFileName,'w'); % Loading with write flag discards the file
contents
            fulltext = strrep(fulltext,tline,newline); % Replace tile depth
            fprintf(fid,'%s',fulltext); % Write modified text back to file
            fclose(fid);
            fprintf('Tile depth in file %s has been changed successfully!\n',
textFileName);
            break
          end
        end
        fclose('all');
      else
        fprintf('File %s does not exist.\n', textFileName);
      end
    elseif (10<= j)&&(j <= 99)
      textFileName = ['000' num2str(k) '00' num2str(j) '.hru'];
      if exist(textFileName, 'file')
       fid = fopen(textFileName,'r');
        depth_to_change = '           6000    ';
        new_depth = '           3000    ';

        % Find the tile depth to change
        while ~feof(fid)
          tline = fgetl(fid);
          temp = strsplit(tline,'|'); % Split the tile drain line into 2 cells
          if strcmp(temp{1},depth_to_change)
            newline = strrep(tline,temp{1},new_depth);
            frewind(fid); % Go back to start of the file
            fulltext = fread(fid,'*char')'; % Reserve entire file prior to discarding
```

```
                fclose(fid);
                fid = fopen(textFileName,'w'); % Loading with write flag discards the file
contents
                fulltext = strrep(fulltext,tline,newline); % Replace tile depth
                fprintf(fid,'%s',fulltext); % Write modified text back to file
                fclose(fid);
                fprintf('Tile depth in file %s has been changed successfully!\n',
textFileName);
                break
            end
        end
        fclose('all');
    else
        fprintf('File %s does not exist.\n', textFileName);
    end
elseif (100 <= j)&&(j <=600)
    textFileName = ['000' num2str(k) '0' num2str(j) '.hru'];
    if exist(textFileName, 'file')
        fid = fopen(textFileName,'r');
        depth_to_change = '          6000    ';
        new_depth = '          3000    ';
        % Find the tile depth to change
        while ~feof(fid)
            tline = fgetl(fid);
            temp = strsplit(tline,'|'); % Split the tile drain line into 2 cells
            if strcmp(temp{1},depth_to_change)
                newline = strrep(tline,temp{1},new_depth);
                frewind(fid); % Go back to start of the file
                fulltext = fread(fid,'*char')'; % Reserve entire file prior to discarding
                fclose(fid);
                fid = fopen(textFileName,'w'); % Loading with write flag discards the file
contents
                fulltext = strrep(fulltext,tline,newline); % Replace tile depth
                fprintf(fid,'%s',fulltext); % Write modified text back to file
                fclose(fid);
                fprintf('Tile depth in file %s has been changed successfully!\n',
textFileName);
```

```
                break
            end
        end

        fclose('all');
    else
        fprintf('File %s does not exist.\n', textFileName);
    end
  end
 end
end
end
```

Appendix 2 Comparison the original and improved SWAT models

A2.1 Reductions of the original version of SWAT at depths of 200 and 600 mm

CTD_{200}	Flow (%)	Sediment (%)	Org-N (%)	Org-P (%)	NO_3^--N (%)	NH_4^+-N (%)	NO_2^--N (%)	Min-P (%)	TN (%)	TP (%)
1981	-7.2	-6.6	12.3	12.1	18.5	16.4	20.1	20.4	17.9	18.3
1982	-2.7	-1.5	5.6	6.5	0.6	7.7	9.3	12.8	3.5	11.2
1983	-9.0	-11.1	7.5	5.9	-19.6	10.8	13.1	13.1	-7.9	10.9
1984	-7.6	-7.1	9.2	6.8	7.9	13.5	15.4	15.1	10.1	12.7
1985	-5.3	-8.2	4.6	6.2	-16.9	6.8	8.6	14.0	-7.8	11.5
1986	-3.5	-2.5	7.8	6.5	8.9	10.0	13.9	17.0	9.3	14.0
1987	1.9	5.9	3.5	4.5	-3.3	3.9	5.1	9.2	-0.4	7.9
1988	-0.3	0.6	2.0	4.0	0.0	3.1	5.6	9.9	1.2	8.4
1989	-1.3	-1.3	6.7	4.0	-5.2	9.0	11.1	12.1	-0.7	9.9
1990	-3.0	0.6	4.7	6.2	-12.2	6.2	6.8	11.7	-5.5	10.1
1991	1.3	4.0	1.7	2.6	-2.6	1.9	2.1	4.7	-0.5	4.0
1992	-0.8	-0.6	0.9	-0.1	0.7	0.9	1.2	1.5	0.8	1.0
1993	-0.3	1.9	2.0	1.6	-0.7	2.0	1.8	2.6	0.1	2.3
1994	0.1	0.5	2.5	2.8	-0.6	2.4	1.7	4.2	0.5	3.8
1995	-0.9	0.4	1.6	1.5	-8.0	1.9	2.3	3.2	-6.6	2.7
1996	-0.6	-2.9	2.3	2.4	-3.7	2.2	2.1	4.9	-1.9	4.3
1997	2.8	3.1	3.8	5.2	2.9	3.2	2.7	5.4	3.0	5.4
1998	1.5	2.0	1.2	2.4	-3.1	0.9	0.4	3.8	-2.1	3.4
1999	8.7	7.3	5.8	8.0	-4.0	4.3	2.7	7.7	-1.9	7.8
2000	2.7	5.2	6.1	12.5	1.3	5.2	4.3	13.7	2.2	13.4
2001	8.6	13.3	4.8	5.9	-4.6	3.8	2.6	6.8	-2.1	6.5
2002	2.6	4.3	2.8	6.9	-5.1	2.7	2.0	11.2	-4.0	9.8
2003	3.3	6.7	4.9	10.5	-4.7	4.7	4.0	12.7	-2.9	12.0
2004	5.0	5.7	4.0	3.1	-6.9	3.7	3.8	5.5	-3.2	4.9
2005	1.6	3.1	11.1	14.1	-7.2	11.3	12.3	26.6	-4.0	23.5
Total	**-0.5**	**0.4**	**5.2**	**6.3**	**-1.9**	**6.2**	**7.0**	**11.2**	**0.4**	**9.8**
CTD_{600}										
1981	-1.5	-0.7	1.7	2.4	20.9	1.7	2.2	4.3	16.1	3.8
1982	-1.2	-0.9	1.2	1.5	6.5	1.5	2.0	4.0	4.5	3.3
1983	-2.2	0.1	0.8	0.2	13.3	1.1	2.0	2.6	8.6	1.9
1984	-2.8	-7.0	2.7	2.1	7.5	3.4	4.0	4.4	5.5	3.7
1985	-2.3	-4.0	2.0	2.3	34.7	2.7	3.4	5.3	22.2	4.4
1986	-0.6	-0.6	1.0	1.3	6.7	1.2	1.8	4.2	5.4	3.3
1987	-0.1	0.1	1.7	1.6	18.9	2.1	2.5	3.2	12.2	2.7
1988	-0.2	-1.7	0.7	1.3	23.6	0.9	1.8	3.5	15.6	3.0
1989	-0.3	-1.4	1.4	1.2	39.2	1.9	2.2	2.7	27.4	2.3
1990	-0.5	-0.2	1.2	1.3	24.8	1.3	1.5	3.3	16.1	2.7
1991	-0.9	-0.7	1.5	1.0	21.7	1.8	1.9	2.1	12.3	1.8
1992	0.0	-0.1	0.5	0.6	4.2	0.4	0.3	1.0	2.6	0.9
1993	-0.1	-1.6	0.9	0.3	3.0	0.9	0.9	0.5	2.4	0.5
1994	0.0	-0.1	0.7	0.7	0.2	0.8	0.5	1.2	0.4	1.1
1995	-0.1	1.8	0.0	0.1	1.4	0.0	0.0	0.6	1.2	0.5
1996	-0.2	-1.6	0.5	0.3	3.5	0.5	0.5	1.1	2.6	0.9
1997	0.0	-0.2	0.6	1.4	14.2	0.6	0.6	1.5	8.6	1.5
1998	0.5	0.8	0.3	0.7	3.0	0.1	0.0	1.1	2.2	1.0
1999	3.3	0.0	2.0	2.2	5.0	1.5	1.1	1.9	4.1	2.0
2000	1.0	2.6	1.5	4.3	4.0	1.1	0.6	4.0	3.3	4.1
2001	2.6	4.4	1.7	2.8	10.3	1.4	0.9	2.6	7.6	2.6
2002	1.1	-0.2	1.1	2.3	3.4	1.0	1.1	3.6	3.0	3.2
2003	1.4	2.9	1.6	3.4	3.7	1.7	1.5	4.6	3.3	4.2
2004	1.6	1.3	2.1	1.6	8.0	1.9	1.7	2.5	5.9	2.2
2005	1.3	3.6	2.3	3.8	3.2	2.2	2.5	6.7	3.0	6.0
Total	**0.0**	**-0.1**	**1.3**	**1.8**	**9.7**	**1.4**	**1.6**	**3.1**	**7.4**	**2.7**

ii. A2.2 Reductions by the improved version of swat at depths of 200 and 600 mm

CTD_{200}	Flow (%)	Sediment (%)	Org-N (%)	Org-P (%)	NO_3^--N (%)	NH_4^+-N (%)	NO_2^--N (%)	Min-P (%)	TN (%)	TP (%)
1981	-7.2	-6.6	12.3	12.1	-31.8	16.3	20.1	20.4	-19.7	18.3
1982	-2.7	-1.5	5.6	6.5	-0.7	7.6	9.3	12.8	2.8	11.2
1983	-9.0	-11.1	7.5	5.9	-25.4	10.8	13.1	13.0	-11.6	10.9
1984	-7.6	-7.1	9.2	6.8	0.0	13.5	15.4	15.1	5.9	12.6
1985	-5.3	-8.2	4.6	6.2	-20.1	6.8	8.6	14.0	-9.7	11.5
1986	-3.5	-2.5	7.8	6.5	-25.5	10.0	13.9	17.0	-17.1	14.0
1987	1.8	5.9	3.5	4.5	-8.5	3.9	5.1	9.1	-3.5	7.8
1988	-0.3	0.6	2.0	4.0	-14.1	3.1	5.6	9.9	-7.9	8.4
1989	-1.3	-1.3	6.6	4.0	-12.4	9.0	11.0	12.0	-5.7	9.8
1990	-3.0	0.6	4.7	6.2	-20.2	6.2	6.8	11.7	-10.6	10.0
1991	1.3	4.0	1.7	2.6	-4.5	1.9	2.1	4.7	-1.5	4.0
1992	-0.8	-0.6	0.9	-0.1	-1.5	0.9	1.2	1.5	-0.5	1.0
1993	-0.3	1.9	2.0	1.6	-5.7	2.0	1.8	2.6	-3.5	2.3
1994	0.1	0.5	2.5	2.8	-2.2	2.4	1.7	4.2	-0.6	3.8
1995	-0.9	0.4	1.6	1.5	-10.3	1.8	2.2	3.1	-8.6	2.6
1996	-0.6	-2.9	2.3	2.4	-8.0	2.2	2.1	4.8	-4.8	4.2
1997	2.8	3.1	3.8	5.2	0.9	3.2	2.7	5.4	1.9	5.3
1998	1.4	2.0	1.2	2.4	-5.5	0.9	0.4	3.7	-3.8	3.4
1999	8.7	7.3	5.8	8.1	-8.9	4.3	2.7	7.7	-5.6	7.8
2000	2.7	5.2	6.1	12.4	-10.9	5.2	4.3	13.6	-7.4	13.3
2001	8.6	13.3	4.8	5.9	-8.6	3.8	2.6	6.8	-4.9	6.5
2002	2.6	4.3	2.8	7.0	-12.6	2.7	2.0	11.2	-10.3	9.8
2003	3.3	6.7	4.9	10.5	-10.2	4.7	3.9	12.7	-7.4	12.0
2004	5.0	5.7	4.0	3.1	-8.6	3.7	3.8	5.5	-4.3	4.8
2005	1.6	3.1	11.1	14.2	-12.7	11.3	12.3	26.6	-8.6	23.5
Total	**-0.5**	**0.4**	**5.2**	**6.3**	**-13.0**	**6.2**	**7.0**	**11.1**	**-7.6**	**9.8**
CTD_{600}										
1981	-1.5	-0.7	1.7	2.4	-14.0	1.7	2.2	4.2	-10.0	3.8
1982	-1.2	-0.9	1.2	1.5	-2.3	1.5	2.0	3.9	-0.7	3.3
1983	-2.2	0.1	0.8	0.2	-7.6	1.1	2.0	2.6	-4.1	1.9
1984	-2.8	-7.0	2.7	2.1	0.5	3.4	4.0	4.4	1.8	3.7
1985	-2.3	-4.0	2.0	2.3	-11.0	2.7	3.4	5.3	-5.7	4.4
1986	-0.6	-0.6	1.0	1.3	-15.1	1.2	1.8	4.1	-11.3	3.3
1987	-0.1	0.1	1.7	1.6	-4.2	2.1	2.5	3.2	-1.7	2.7
1988	-0.2	-1.8	0.7	1.3	-9.3	0.9	1.8	3.5	-5.6	2.9
1989	-0.3	-1.4	1.4	1.2	-7.1	1.8	2.1	2.6	-4.3	2.2
1990	-0.5	-0.2	1.2	1.3	-7.3	1.3	1.5	3.2	-4.1	2.7
1991	-0.9	-0.7	1.5	1.0	-2.8	1.8	1.9	2.1	-0.7	1.7
1992	0.0	-0.1	0.5	0.6	-1.2	0.4	0.3	1.0	-0.5	0.9
1993	-0.2	-1.6	0.9	0.3	-2.1	0.9	0.9	0.5	-1.2	0.4
1994	0.0	-0.1	0.7	0.7	-1.3	0.8	0.5	1.2	-0.6	1.1
1995	-0.1	1.8	0.0	0.1	-3.3	0.0	0.0	0.5	-2.8	0.4
1996	-0.2	-1.6	0.5	0.3	-2.4	0.5	0.5	1.0	-1.5	0.8
1997	0.0	-0.2	0.6	1.4	-0.8	0.6	0.6	1.5	-0.2	1.4
1998	0.5	0.8	0.3	0.7	-3.2	0.1	0.0	1.1	-2.3	1.0
1999	3.3	0.1	2.0	2.2	-4.2	1.4	1.1	1.9	-2.7	2.0
2000	1.0	2.6	1.5	4.2	-4.5	1.1	0.6	4.0	-3.3	4.0
2001	2.6	4.4	1.7	2.8	-4.6	1.4	0.9	2.5	-2.9	2.6
2002	1.1	-0.2	1.1	2.4	-5.2	1.0	1.1	3.6	-4.2	3.2
2003	1.4	2.9	1.6	3.4	-4.2	1.7	1.5	4.5	-3.0	4.2
2004	1.6	1.3	2.1	1.6	-5.5	1.9	1.7	2.4	-2.9	2.2
2005	1.3	3.6	2.3	3.8	-6.1	2.2	2.5	6.7	-4.7	6.0
Total	**0.0**	**-0.1**	**1.3**	**1.7**	**-6.0**	**1.4**	**1.6**	**3.1**	**-3.9**	**2.7**

Appendix 3 Parameters of the SWAT model for the SNRW

No.	Parameter	Starting value	Final value	Unit	Name
1	r__CN2.mgt	-0.1~0.1	-0.043048		SCS runoff curve number
2	v__TDRAIN.mgt	0~48	35.106438	hour	Time to drain soil to field capacity
3	v__GDRAIN.mgt	0~30	20.008259	hour	Drain tile lag time
4	v__ALPHA_BF.gw	0~1	0.691866	1/days	Base flow factor
5	v__GW_DELAY.gw	0~500	229.675888	day	The delay time
6	v__GWQMN.gw	0~5000	2816.03125	mm H_2O	Treshold depth of water in the shallow aquifer required for return flow to occur
7	v__RCHRG_DP.gw	0~1	0.605321		Deep aquifer percolation fraction
8	v__REVAPMN.gw	0~500	107.826782	mm H_2O	Threshold depth of water in the shallow aquifer for "revap" to occur (mm)
9	v__GW_REVAP.gw	0.02~0.2	0.093265		Groundwater "revap" coefficient
10	r__SOL_AWC().sol	-0.1~0.1	-0.076302		Available water capacity of the soil layer
11	r__SOL_K().sol	-0.1~0.2	0.19277		Saturated hydraulic conductivity
12	r__SOL_BD().sol	-0.1~0.2	0.18851		Moist bulk density
13	v__ESCO.hru	0~1	0.57879		Soil evaporation compensation factor
14	v__EPCO.hru	0~1	0.336837		Plant uptake compensation factor
15	r__OV_N.hru	-0.3~0.3	-0.25095		Manning's "n" value for overland flow
16	v__SURLAG.bsn	0.5-10	6.790113		Surface runoff lag time
17	v__SNOCOVMX.bsn	0~500	288.504272	mm H_2O	Minimum snow water content that corresponds to 100% snow cover
18	v__SNO50COV.bsn	0~1	0.268921		Snow water equivalent that corresponds to 50% snow cover
19	v__TIMP.bsn	0~1	0.414115		Snow pack temperature lag factor
20	v__SFTMP.bsn	-5~5	-2.392653	°C	Snowfall temperature
21	v__SMTMP.bsn	-5~5	4.558773	°C	Snow melt base temperature
22	v__SMFMX.bsn	0~10	7.781702	mm H_2O/°C-day	Minimum melt rate for snow during the year (occurs on winter solstice)
23	v__SMFMN.bsn	0~10	9.977348	mm H_2O/°C-day	Melt factor for snow on December 21
24	v__CH_N2.rte	-0.01~0.3	0.099838		Manning's "n" value for the main channel
25	v__CH_K2.rte	0~100	41.019154		Effective hydraulic conductivity in main channel alluvium
26	v__PRF_BSN.bsn	0~2	0.855813		Peak rate adjustment factor for sediment routing in the main channel.

No.	Parameter	Starting value	Final value	Unit	Name
27	v__SPEXP.bsn	1~1.5	1.487642		Exponent parameter for calculating sediment reentrained in channel sediment routing
28	v__SPCON.bsn	0.0001~0.01	0.004318		Linear parameter for calculating the maximum amount of sediment that can be reentrained during channel sediment routing
29	v__ADJ_PKR.bsn	0.5~2	0.741114		Peak rate adjustment factor for sediment routing in the subbasin
30	r__CH_ERODMO().rte	0~1	0.220732		Channel erodibility factor
31	v__CH_COV1.rte	0~0.6	0.409625		Channel erodibility factor
32	v__CH_COV2.rte	0~1	0.341298		Channel cover factor
33	v__CH_BNK_BD.rte	1.1~1.9	1.688361	g/cc	Bulk density of channel bank sediment
34	v__CH_BED_BD.rte	1.1~1.9	1.357708	g/cc	Bulk density of channel bed sediment
35	v__CH_BNK_KD.rte	0.001~3.75	1.735133	$cm^3/N\text{-}s$	Erodibility of channel bank sediment by jet test
36	v__CH_BED_KD.rte	0.001~3.75	0.681571	$cm^3/N\text{-}s$	Erodibility of channel bed sediment by jet test
37	v__CH_BNK_D50.rte	1~10000	5268.851074	μm	D50 Median particle size diameter of channel bank sediment
38	v__CH_BED_D50.rte	1~10000	4540.993164	μm	D50 Median particle size diameter of channel bed sediment
39	v__CH_BNK_TC.rte	0~400	181.069687	N/m^2	Critical shear stress of channel bank
40	v__CH_BED_TC.rte	0~400	384.046539	N/m^2	Critical shear stress of channel bed
41	r__USLE_C{5}.plant.dat	-0.2~0.2	0.095463		Min value of USLE C factor applicable to the land cover/plant
42	r__USLE_C{6}.plant.dat	-0.2~0.2	-0.177423		Min value of USLE C factor applicable to the land cover/plant
43	r__USLE_C{9}.plant.dat	-0.2~0.2	0.013185		Min value of USLE C factor applicable to the land cover/plant
44	r__USLE_C{19}.plant.dat	-0.2~0.2	0.177856		Min value of USLE C factor applicable to the land cover/plant
45	r__USLE_C{27}.plant.dat	-0.2~0.2	0.025298		Min value of USLE C factor applicable to the land cover/plant
46	r__USLE_C{56}.plant.dat	-0.2~0.2	0.061992		Min value of USLE C factor applicable to the land cover/plant
47	r__USLE_P.mgt	-0.2~0.1	-0.116386		USLE equation support practice factor
48	r__USLE_K().sol	-0.4~0.4	-0.387948		USLE equation soil erodibility (K) factor.
49	v__LAT_SED.hru	0~5000	41.079483	mg/L	Sediment concentration in lateral flow and groundwater flow
50	v__SLSOIL.hru	0~150	123.835594	m	Slope length for lateral subsurface flow

No.	Parameter	Starting value	Final value	Unit	Name
51	v__SOL_SOLP().chm	0~100	2.333235	mg/kg	Initial P concentration in the soil layer
52	v__PPERCO_SUB().chm	10~17.5	16.828157		Phosphorus percolation coefficient
53	v__SOL_ORGP().chm	0~100	0.795955	mg/kg	Initial organic P concentration in surface soil laye
54	v__CH_OPCO.rte	0~100	8.002236	ppm	Organic phosphorus concentration in the channel
55	v__CH_OPCO_BSN.bsn	0~100	0.324459		Organic phosphorus concentration in the channel
56	v__P_UPDIS.bsn	0~100	20.883842		Phosphorus uptake distribution parameter
57	v__PPERCO.bsn	10~17.5	16.828157		Phosphorus percolation coefficient
58	v__PHOSKD.bsn	100~200	118.36953	m^3/Mg	Phosphorus soil partitioning coefficient
59	v__PSP.bsn	0.01~0.7	0.171872		Phosphorus sorption coefficient
60	v__GWSOLP.gw	0~1000	0.86165	mg/L	Concentration of soluble phosphorus in groundwater contribution to streamflow from subbasin
61	v__LAT_ORGP.gw	0~200	0.602048	mg/L	Organic P in baseflow
62	v__ERORGP.hru	0~5	4.681594		Organic P enrichment ratio
63	v__BC4_BSN.bsn	0.01~0.7	0.089554	1/day	Rate constant for decay of organic phosphorus to dissolved phosphorus
64	v__SOL_NO3().chm	0~100	14.921002	mg/kg	Initial NO3 concentration in the soil layer
65	v__SOL_ORGN().chm	0~100	59.391693	mg/kg	Initial organic N concentration in the soil layer
66	v__CH_ONCO.rte		6.013103		
67	v__BC1_BSN.bsn	0.1~1	0.703924	1/day	Rate constant for biological oxidation of NH3
68	v__BC2_BSN.bsn	0.2~2	0.275338	1/day	Rate constant for biological oxidation NO^2 to NO^3
69	v__BC3_BSN.bsn	0.02~0.4	0.106304	1/day	Rate constant for hydrolosis of organic nitrogen to ammonia
70	v__CH_ONCO_BSN.bsn	0~100	0.781747	ppm	Channel organic nitrogen concentration in basin
71	v__CMN.bsn	0.001~0.003	0.000899		Rate factor for humus mineralization of active organic nitrogen
72	v__SDNCO.bsn	0~1	0.917777		Denitrification threshold water content
73	v__RSDCO.bsn	0.02~0.1	0.064758		Residue decomposition coefficient
74	v__LAT_ORGN.gw	0~200	2.611476		Organic N in the baseflow
75	v__HLIFE_NGW.gw	0~200	60.574234	day	Half-life of nitrate in the shallow aquifer
76	v__ERORGN.hru	0~5	4.690934		Organic N enrichment ratio
77	v__CDN.bsn	0~3	0.967263		Denitrification exponential rate coefficient
78	v__DECR_MIN.bsn	0~0.05	0.034065		Minimum daily residue decay

No.	Parameter	Starting value	Final value	Unit	Name
79	v__N_UPDIS.bsn	0~100	54.750198		Nitrogen uptake distribution parameter
80	v__NPERCO.bsn	0~1	0.223891		Nitrogen percolation coefficient
81	v__RCN.bsn	0~15	10.49003		Concentration of nitrogen in rainfall
82	v__SHALLST_N.gw	0~1000	454.696289	mg/L	Concentration of nitrate in groundwater contribution to streamflow from subbasin
83	v__ANION_EXCL_BSN.bsn	0.01~1	8.435902		Fraction of porosity from which anions are excluded
84	v__RSDIN.hru	0~10000	3002.272461	kg/ha	Initial residue cover
85	r__SOL_CBN().sol	-0.4~0.4	-0.348576		Organic carbon content
86	v__FIXCO.bsn	0~1	0.954823		Nitrogen fixation coefficient
87	v__RSDCO_PL{5}.plant.dat	0.01~0.099	0.020979		Plant residue decomposition coefficient
88	v__RSDCO_PL{6}.plant.dat	0.01~0.099	0.037235		Plant residue decomposition coefficient
89	v__RSDCO_PL{9}.plant.dat	0.01~0.099	0.060175		Plant residue decomposition coefficient
90	v__RSDCO_PL{19}.plant.dat	0.01~0.099	0.058049		Plant residue decomposition coefficient
91	v__RSDCO_PL{27}.plant.dat	0.01~0.099	0.068602		Plant residue decomposition coefficient
92	v__RSDCO_PL{56}.plant.dat	0.01~0.099	0.053507		Plant residue decomposition coefficient

Note:

v__ means the existing parameter value is to be replaced by the given value and

r__ means the existing parameter value is multiplied by (1+ a given value).